A COMPARATIVE GEOCHEMICAL STUDY OF HUMIC COALS FROM CENOZOIC SARAWAK BASIN, MALAYSIA AND CRETACEOUS BENUE TROUGH, NIGERIA

ASIWAJU LANRE OLUWASEUN

FACULTY OF SCIENCE
UNIVERSITI MALAYA
KUALA LUMPUR

2023

A COMPARATIVE GEOCHEMICAL STUDY OF HUMIC COALS FROM CENOZOIC SARAWAK BASIN, MALAYSIA AND CRETACEOUS BENUE TROUGH, NIGERIA

ASIWAJU LANRE OLUWASEUN

**THESIS SUBMITTED IN
FULFILMENT OF THE
REQUIREMENTS FOR THE DEGREE
OF DOCTOR OF PHILOSOPHY**

**FACULTY OF SCIENCE
UNIVERSITI MALAYA
KUALA LUMPUR**

2023

UNIVERSITI MALAYA

ORIGINAL LITERARY WORK DECLARATION

Name of Candidate: **ASIWAJU LANRE OLUWASEUN**

Matric No: **SHC160004**

Name of Degree: **DOCTOR OF PHILOSOPHY**

Title of Thesis ("this Work"):

A COMPARATIVE GEOCHEMICAL STUDY OF HUMIC COALS FROM CENOZOIC SARAWAK BASIN, MALAYSIA AND CRETACEOUS BENUE TROUGH, NIGERIA

Field of Study:

PETROLEUM GEOLOGY

I do solemnly and sincerely declare that:

(1) I am the sole author/writer of this Work;
(2) This Work is original;
(3) Any use of any work in which copyright exists was done by way of fair dealing and for permitted purposes and any excerpt or extract from, or reference to or reproduction of any copyright work has been disclosed expressly and sufficiently and the title of the Work and its authorship have been acknowledged in this Work;
(4) I do not have any actual knowledge nor do I ought reasonably to know that the making of this work constitutes an infringement of any copyright work;
(5) I hereby assign all and every rights in the copyright to this Work to the University of Malaya ("UM"), who henceforth shall be owner of the copyright in this Work and that any reproduction or use in any form or by any means whatsoever is prohibited without the written consent of UM having been first had and obtained;
(6) I am fully aware that if in the course of making this Work I have infringed any copyright whether intentionally or otherwise, I may be subject to legal action or any other action as may be determined by UM.

Candidate's Signature Date 13th March 2023

Subscribed and solemnly declared before,

Witness's Signature Date 13th March 2023

Name:

Designation:

A COMPARATIVE GEOCHEMICAL STUDY OF HUMIC COALS FROM CENOZOIC SARAWAK BASIN, MALAYSIA AND CRETACEOUS BENUE TROUGH, NIGERIA

ABSTRACT

Although humic coal is generally described as a gas-prone source rock, a significant number of oil-prone coal-bearing sequences in Australasia and Southeast Asia have expelled commercial volumes of oil. Nevertheless, the mechanism of oil generation and expulsion from humic coals remains poorly understood. Therefore, this thesis seeks to provide new insights into the geochemical controls on the petroleum potential of humic coals. A total of sixty Tertiary and Upper Cretaceous coals from Sarawak Basin, Malaysia, and Benue Trough, Nigeria were investigated using bulk and molecular geochemical techniques such as standard proximate analysis, pyrolysis-gas chromatography (Py-GC), Rock-Eval pyrolysis, Fourier transform infrared spectroscopy (FTIR), gas chromatography-mass spectrometry (GC-MS), elemental analyser isotope ratio mass spectrometry (EA-IRMS), and inductively coupled plasma mass spectrometry (ICP-MS) to determine their thermal maturity, hydrocarbon generation potential, organic matter input, kerogen type, paleovegetation, paleoclimate, and environments of deposition. Furthermore, principal component analysis (PCA) of geochemical parameters was carried out to evaluate the probable controls on the hydrocarbon generation potential of the coals. First, vitrinite reflectance and T_{max} data, and maturity-related biomarker parameters all signify low thermal maturity for all studied coals except the Lamja Formation coals of the Benue Trough which are in the early maturity stage. Furthermore, hydrogen index (< 300 mg HC/g TOC), TOC (> 20 wt. %), *A*-factor (> 0.4) and extract yield (> 10000 ppm) data for most of the coals indicate excellent potential for gas and mixed oil and gas generation. Rock-Eval, Py-GC, and source-related aliphatic and

aromatic hydrocarbon parameters indicate that the coals are derived mainly from terrestrial organic matter but with a considerable proportion of marine algal organic matter in the Benue Trough coals. Additionally, $\delta^{13}C$ values and the abundance of terpenoids imply the predominant contribution of gymnosperms and angiosperms to the paleoflora of the Benue Trough and Sarawak Basin, respectively. Bimetal proxies (Sr/Ba, Sr/Cu, and C-value), and δD values are generally suggestive of a warm and humid climate during the accumulation of the paleopeats. However, the presence of ≥ 6-ring combustion-derived polycyclic aromatic hydrocarbons (PAHs) in the Gombe Formation coals of the Upper Benue Trough implies relatively drier conditions during the Maastrichtian. Additionally, *n*-alkane proxies (P_{wax}, P_{aq}, n-C_{23}/n-C_{29}, etc.) suggest that Liang Formation coals of the Sarawak Basin were deposited under relatively drier and strongly seasonal paleoclimate during the Late Pliocene. When compared with published global average abundances, the investigated coals are mostly depleted in major oxides and trace elements, suggesting peat accumulation in freshwater-influenced environments. Furthermore, the low to moderately high ash content of the Sarawak Basin coals indicates the presence of ombrotrophic and rheotrophic peat deposits, while the relatively higher ash content of the Benue Trough coals is indicative of prevalent rheotrophic conditions. PCA result of selected geochemical proxies suggests that thermal maturity, source input, peat hydrology, paleoflora, and marine incursions do not influence hydrocarbon generation potential. However, climatic, and depositional conditions both appear to slightly influence the hydrocarbon generation potential of the studied humic coals.

Keywords: Humic Coal, Sarawak Basin, Benue Trough, Hydrocarbon Potential, Geochemistry

KAJIAN GEOKIMIA PERBANDINGAN ARANG HUMIC DARI LEMBANGAN CENOZOIC SARAWAK, MALAYSIA DAN CRETACEOUS BENUE TROUGH, NIGERIA

ABSTRAK

Walaupun arang batu humik secara amnya dianggap sebagai batuan sumber yang terdedah kepada gas, sebilangan besar jujukan yang mengandungi arang batu terdedah kepada minyak di Australasia dan Asia Tenggara telah mengeluarkan isipadu minyak komersial. Namun begitu, mekanisme penjanaan minyak dan pengusiran daripada arang humik masih kurang difahami. Oleh itu, tesis ini bertujuan untuk memberikan pandangan baharu tentang kawalan geokimia terhadap potensi petroleum arang humik. Sebanyak enam puluh arang Tertiary dan Upper Cretaceous dari Lembangan Sarawak, Malaysia, dan Benue Trough, Nigeria telah disiasat menggunakan teknik geokimia pukal dan molekul seperti analisis proksimat standard, kromatografi gas pirolisis (Py-GC), pirolisis Rock-Eval, Fourier spektroskopi inframerah transformasi (FTIR), spektrometri jisim kromatografi gas (GC-MS), spektrometri jisim nisbah isotop penganalisis unsur (EA-IRMS), dan spektrometri jisim plasma (ICP-MS) yang digandingkan secara induktif untuk menentukan kematangan terma, potensi penjanaan hidrokarbon. , input bahan organik, jenis kerogen, paleovegetasi, paleoklimat, dan persekitaran pemendapan. Tambahan pula, analisis komponen utama (PCA) parameter geokimia telah dijalankan untuk menilai kemungkinan kawalan ke atas potensi penjanaan hidrokarbon arang batu. Pertama, pemantulan vitrinit dan data T_{max}, dan parameter biomarker berkaitan kematangan semuanya menandakan kematangan terma yang rendah untuk semua arang batu yang dikaji kecuali arang batu Formasi Lamja di Benue Trough yang berada di peringkat kematangan awal. Tambahan pula, data indeks hidrogen (< 300 mg HC/g

TOC), TOC (> 20 wt. %), A-faktor (> 0.4) dan hasil ekstrak (> 10000 ppm) untuk kebanyakan arang batu menunjukkan potensi yang sangat baik untuk gas dan penjanaan minyak dan gas campuran. Rock-Eval, Py-GC, dan parameter hidrokarbon alifatik dan aromatik berkaitan sumber menunjukkan bahawa arang batu berasal terutamanya daripada bahan organik daratan tetapi dengan sebahagian besar bahan organik alga marin dalam arang Benue Trough. Di samping itu, nilai δ13C dan kelimpahan terpenoid membayangkan sumbangan utama gimnosperma dan angiosperma kepada paleoflora Benue Trough dan Lembangan Sarawak, masing-masing. Proksi dwilogam (nilai Sr/Ba, Sr/Cu dan C-value), dan nilai δD secara amnya menunjukkan iklim panas dan lembap semasa pengumpulan paleopeat. Walau bagaimanapun, kehadiran ≥ 6-cincin hidrokarbon aromatik polisiklik (PAH) yang berasal dari pembakaran dalam arang batu Formasi Gombe di Upper Benue Trough membayangkan keadaan yang agak kering semasa Maastrichtian. Selain itu, proksi n-alkana (P_{wax}, P_{aq}, n-C_{23}/n-C_{29}, dsb.) mencadangkan bahawa arang batu Formasi Liang di Lembangan Sarawak telah dimendapkan di bawah paleoklimat yang agak kering dan bermusim kuat semasa Pliosen Akhir. Jika dibandingkan dengan kelimpahan purata global yang diterbitkan, arang batu yang disiasat kebanyakannya habis dalam oksida utama dan unsur surih, mencadangkan pengumpulan gambut dalam persekitaran yang dipengaruhi air tawar. Tambahan pula, kandungan abu yang rendah hingga sederhana tinggi arang Lembangan Sarawak menunjukkan kehadiran mendapan gambut ombrotropik dan rheotropik, manakala kandungan abu yang agak tinggi bagi arang Benue Trough menunjukkan keadaan rheotropik yang lazim. Keputusan PCA proksi geokimia terpilih menunjukkan bahawa kematangan terma, input sumber, hidrologi gambut, paleoflora, dan pencerobohan marin tidak mempengaruhi potensi penjanaan hidrokarbon. Walau bagaimanapun, keadaan iklim dan pemendapan kelihatan sedikit mempengaruhi potensi penjanaan hidrokarbon arang humik yang dikaji.

Kata kunci: Arang Batu Humic, Lembangan Sarawak, Palung Benue, Potensi Hidrokarbon, Geokimia

ACKNOWLEDGEMENTS

First, this research work was carried out with the financial support, in part, of the Petroleum Technology Development Fund, Nigeria through its Overseas Scholarship Scheme. I am indeed grateful to the Fund for helping me achieve my academic goals. Second, my immense gratitude to my supervisors, Professor Wan Hasiah Abdullah and Dr Khairul Azlan Bin Mustapha. I am most grateful for their guidance and support, both financial and moral, over the last few years. In particular, I am appreciative of the helpful discussions and patience in reading this thesis and manuscripts for journal publication.

I am also grateful to senior geochemists, Drs Hail Hakimi, Yousif Makeen, Habeeb Ayinla, Segun Akinyemi, and Say-See Gia, for providing coal samples, sharing ideas, and reviewing manuscripts. Furthermore, I appreciate the help provided by the technical staff, Mr Mohamad Zamri Rashid, Ms Zaleha Abdullah, Mr Aliff Zhafri and Mr Mohamad Shahrizad, of the organic geochemistry laboratory at the Department of Geology, University of Malaya. My gratitude is also extended to Teng King Kuen, whose earlier unpublished work provided much-needed geological information on the Merit-Pila coals. In addition, I appreciate friends at the Department of Geology, Asia DCO headquarters of the Redeemed Christian Church of God, and the Nigerian community, University of Malaya. Thank you all for the support and prayers.

Finally, I am grateful and indebted to my family for their love, support, patience and prayers. A very big thank you to my wife, Esther, for the care and encouragement during those long nights writing up this thesis.

To the almighty God, the giver and redeemer of life; thank you for your love, saving grace, favour and tender mercies, and daily benefits. To you, Lord, be all the glory.

TABLE OF CONTENTS

LIST OF FIGURES

LIST OF TABLES

LIST OF SYMBOLS AND ABBREVIATIONS

δ	:	Lower delta; variation in isotopic ratio of an element
A_F	:	A-factor
C_F	:	C-factor
DAC	:	degree of aromatic ring condensation
I_{AL}	:	aliphaticity index
I_{HG}	:	index for hydrocarbon generation
P_{aq}	:	proxy aqueous
P_{wax}	:	proxy wax
R_o	:	vitrinite reflectance
S1	:	free hydrocarbons
S2	:	pyrolysable hydrocarbons
S3	:	organic CO_2
T_{max}	:	temperature at maximum *S2*
A	:	anthracene
ACL	:	average chain length
AGI	:	angiosperm-gymnosperm index
al-AGI’	:	aliphatic angiosperm-gymnosperm index
Al_phen	:	alkylation index of phenols
Ali	:	aliphatic hydrocarbons
Aro	:	aromatic hydrocarbons
ASTM	:	American Society for Testing and Materials Standards
BaA	:	benzo[*a*]anthracene
BaPy	:	benzo[*a*]pyrene
BbFl	:	benzo[*b*]fluoranthene
BePy	:	benzo[*e*]pyrene

BgPer	:	benzo[*ghi*]pyrelene
BkFl	:	benzo[*k*]fluoranthene
BI	:	bitumen index
C	:	carbon
cad	:	cadalene
Ch	:	chrysene
CL	:	chain length
Cor	:	coronene
CPI	:	carbon preference index
DBF	:	dibenzofuran
DBT	:	dibenzothiophene
DCM	:	dichloromethane
DHI-2	:	dehydroxylation index
DMN	:	dimethylnaphthalene
DMP	:	dimethylphenanthrene
EOM	:	extractable organic matter
F	:	fluorene
FAME	:	fatty acid methyl ester
Fl	:	fluoranthene
GC-MS	:	gas chromatography-mass spectrometry
GI	:	gelification index
GP	:	genetic potential
H	:	hydrogen
HC	:	hydrocarbon
HFSTE	:	high field strength trace elements
HI	:	hydrogen index

HPI	:	higher plant input
HPP	:	higher plant parameter
ICCP	:	International Committee for Coal and Organic Petrology
InPy	:	indeno[*1,2,3-cd*]pyrene
ip-iHMN	:	6-isopropyl-1-isohexyl-2-methylnaphthalene
MA	:	methylanthracene
MDBF	:	methyldibenzofuran
MDBT	:	methyldibenzothiophene
mHPI	:	modified higher plant input
MMCO	:	Middle Miocene Climate Optimum
MN	:	methylnaphthalene
MP	:	methylphenanthrene
N	:	nitrogen
Np	:	naphthalene
NGS	:	Norwegian geochemical standard
NIST	:	National Institute of Standards and Technology
OEP	:	odd-even predominance
OM	:	organic matter
PFI	:	pristane formation index
Ph	:	phytane
PHE	:	phenanthrene
PI	:	production index
POI	:	phytane oxidation index
Polar	:	polar compounds
Pr	:	pristane
Py	:	pyrene

Py-GC	:	pyrolysis-gas chromatography-mass spectrometry
Ret	:	retene
S_T	:	total sulfur
TAR	:	terrigenous aquatic ratio
TeMN	:	tetramethylnaphthalene
THM	:	thermally assisted hydrolysis and methylation
TMAH	:	tetramethylammonium hydroxide
TMN	:	trimethylnaphthalene
TMP	:	trimethylphenanthrene
TOC	:	total organic carbon
Tph	:	triphenylene
TPI	:	tissue preservation index
TQPA	:	total quantified peak area
TTE	:	transition trace elements
QI	:	quality index
WI	:	wax index
xy	:	m(+p)-xylene

LIST OF APPENDICES

CHAPTER ONE: INTRODUCTION

1.1 Background and Problem Statement

Coal is a black or brownish-black combustible sedimentary rock formed by the degradation, compaction, and induration of accumulated remains of plant debris, usually in a mire environment (McCabe, 1984). With burial, plant remains are subjected to increasing temperature and pressure, transforming them over time, first into peat and successively into lignite, sub-bituminous coal, bituminous coal, and finally anthracite. The biochemical transformation of plant materials into peat is called peatification, while the subsequent progressive physiochemical transformation from peat through lignite to anthracite, and approaching graphite is referred to as coalification (Diessel, 1992; Orem & Finkelman, 2003; O'Keefe et al., 2013). Coal is the most abundant fossil fuel and cheapest energy source, and its use has evolved over the years from transportation fuel to power generation to steel production and industrial manufacturing.

Coal typically contains more than 50 wt. % organic carbon and in varying quantities of other elements such as hydrogen, oxygen, and sulfur. Hence, coals can be classified based on the percentage composition of elemental carbon, hydrogen, and oxygen. Before deposition and subsequent incorporation into peat, plant remains differ in morphological and chemical nature (Scott, 2002). During diagenesis, oxygen-containing functional groups are removed from peat until the oxygen/carbon ratio decreases to about 0.1 (Orem & Finkelman, 2003). With increasing burial, bacteria activity decreases due to increasing temperature and pressure, and catagenesis begins. While removal of oxygen continues during catagenesis, the main reactions are decarboxylation and aromatization of alkyl side chains occurs. During catagenesis, the hydrogen/carbon ratio reduces until it becomes graphite, which is pure carbon (Orem & Finkelman, 2003). Thus, the physical properties

of coal such as colour, hardness, and gravity are dependent on the composition of the original peat, the amount of impurities, and thermal maturity (McCabe, 1984).

Coals are composed of optically homogenous aggregates of organic substances with distinct physical and chemical properties termed macerals (Spackman, 1958). The major maceral groups are huminite/vitrinite, derived mainly from woody material; liptinite, primarily derived from spores and cuticles; and inertinite, sourced from oxidized biomass (McCabe, 1984). The term huminite is used for lignite and sub-bituminous coals (<0.5% R_o), while vitrinite is used for bituminous coals (≥ 0.5% R_o). The International Committee for Coal and Organic Petrology (ICCP) System 1994 classification of coal organic compounds are used to identify and classify the macerals in coals (ICCP, 2001; Sýkorová et al., 2005; Pickel et al., 2017). The distribution of maceral groups in coals is dependent on the composition of organic matter at burial, which in turn primarily depends on plant type in peat-mire and the depositional environment (Hunt, 1991). For instance, the absence or low abundance of inertinite macerals in coals is generally regarded as an indicator of steady precipitation and constantly high water-table levels during peat accumulation, while the abundance of inertinite macerals is suggestive of frequent dry episodes (McCabe 1984; Diessel, 1992).

There are two types of coals: sapropelic and humic coals. Sapropelic coals are formed from spores, pollen, and algae deposited in sub-oxic to anoxic conditions that are common in lakes (McCabe, 1984). Sapropelic coals are rich in resins and waxes and consequently have higher hydrogen content than humic coals. In addition, sapropelic coals are thin, lenticular, and non-banded, and often occur as single bands or at the top of humic coals. However, sapropelic coals are relatively uncommon and volumetrically insignificant. Conversely, humic coals constitute over 80% of the world's coal resources and are formed by the deposition of plant cell and wall materials in anoxic-suboxic conditions found in

peat mires (McCabe 1984; Orem & Finkelman, 2003). Humic coals are often dominated by huminite/vitrinite maceral with heterogeneous organic matter structures (Petersen, 2006). In addition, humic coals are banded and tend to form cleats.

Given the low hydrogen content of humic coal, it is conventionally regarded as a gas-prone source rock, while shale and carbonates which have generated commercial quantities of oil are known to be oil-prone source rocks. However, Tertiary coals in Taranaki Basin, New Zealand, and Late Cretaceous coals in Gippsland Basin, Australia, are known to have expelled commercial volume of oil. Therefore, several studies have investigated oil-prone humic coals (Clayton et al. 1991; Hunt, 1991; Fleet & Scott, 1994; Killops et al., 1998; Isaksen et al., 1998; Sykes, 2001; Wilkins & George, 2002; Abdullah, 2003; Petersen, 2006; Petersen & Nytoft, 2006). Nevertheless, the mechanism of oil generation in these coals is still not fully understood.

1.2 Aim and Objectives of Study

This thesis aims to provide new insights into the geochemical controls of the petroleum-generating potential of humic coals. This aim was achieved by investigating similarly ranked coals of different ages from Sarawak Basin, Malaysia, and Benue Trough, Nigeria using a novel combination of bulk and molecular geochemical techniques such as proximate analysis, pyrolysis-gas chromatography (Py-GC), Rock-Eval pyrolysis, attenuated total reflection-Fourier-transform infrared spectroscopy (ATR-FTIR), gas chromatography-mass spectrometry (GC-MS), elemental analyser isotope ratio mass spectrometry (EA-IRMS), and inductively coupled plasma mass spectrometry (ICP-MS). Furthermore, correlation and principal component analyses were carried out to evaluate the strength of relationships between petroleum-generating potential

indicators and source input-, paleovegetation-, paleoclimate-, and paleoenvironment-related proxies.

The objectives of this thesis are summarized as follows:

1. To evaluate the hydrocarbon generation potential of the coal samples,
2. To determine their organic matter source input,
3. To reconstruct the paleovegetation and paleoclimate of the study areas,
4. To determine the environmental conditions of peat accumulation,
5. To compare the elemental, isotopic, and hydrocarbon composition of the Sarawak Basin and Benue Trough coals,
6. To determine the geochemical controls on the hydrocarbon-generating potential of the studied Malaysian and Nigerian coals.

1.3 Research Hypotheses

The research hypotheses developed in this thesis align with the sixth research objective in section 1.2 above, and are as follows:

H_1: The hydrocarbon generation potential of the studied coals is influenced by organic matter source input.

H_2: The hydrocarbon generation potential of the studied coals is influenced by paleovegetation.

H_3: The hydrocarbon generation potential of the studied coals is influenced by past hydrological and climatic conditions.

H_4: The hydrocarbon generation potential of the studied coals is influenced by the environmental conditions of the paleopeats.

These hypotheses were tested by undertaking principal component analysis (PCA) of selected geochemical proxies of organic matter input, paleoflora, paleohydrology, paleoclimate, and depositional environment to either accept or reject the above-stated propositions.

1.4 Thesis Organisation

The thesis is divided into seven chapters. Chapter 1 presents an introduction to the research and outlines the scope and objectives of the work, while Chapter 2 reviews published studies regarding oil-prone humic coals, marine-influenced coals, and geochemical proxies. Furthermore, Chapter 3 describes the geology of Sarawak Basin, Malaysia, and Benue Trough, Nigeria, and study areas within Sarawak Basin and Benue Trough. Chapter 4 outlines the analytical methods employed for this research work, while Chapter 5 presents the results and preliminary interpretations.

Chapter 6 discusses the results, broadly characterizing the coals and determining their thermal maturity, hydrocarbon generation potential, organic matter source input, and provenance of source areas. In addition, this chapter assesses the paleovegetation, paleoclimate, and paleodepositional conditions of the studied coals, and importantly, discusses the potential geochemical controls on the generation potential of the coals. Finally, chapter 7 summarises the overall findings of this research work, highlights the limitations, and outlines the scope of future work.

CHAPTER 2: LITERATURE REVIEW

2.1 Oil-prone Humic Coals

Due to the low hydrogen contents of humic coals, they are conventionally regarded as a gas-prone source rocks whereas shale and carbonates which have generated commercial quantities of oil are known to be oil-prone source rocks. Nevertheless, some early studies show liquid hydrocarbon generation could occur in coal seams (Young, 1967). Two theories were proposed for this observation. First, coals generate oil but not in significant quantity, and second that coals generate a significant volume of oil but the oil cannot be expelled. Durand & Paratte (1983) investigated coals of different ages and found that significant amounts of oil can be generated in most coals and that expulsion is likely to commence sooner after generation than in other source rocks. The authors, however, suggested that fracturing due to basin evolution and the poor capacity of coals to retain oil likely explain the loss of generated oil. Shibaoka et al. (1978) indicated that the oil in the Gippsland basin is derived mainly from the liptinite maceral group, while Durand & Paratte (1983) found no correlation between maceral composition and the potential to generate liquid hydrocarbon. Furthermore, Durand & Paratte (1983) emphasized that all coal types can generate liquid hydrocarbon.

Based on biomarker analysis, Shanmugam (1985) suggested that the 3 billion barrels of recoverable oil in the Gippsland Basin Australia could be sourced from the coaly succession of the Upper Cretaceous-Tertiary Latrobe Group. The high wax content, presence of long-chain *n*-alkanes, high pristane/phytane ratio, and dominant C_{29} sterane in the oil indicated a possible terrestrial source of organic matter. Furthermore, the depletion of liptinites in the offshore Latrobe coals proved that oil was generated from liptinites. In addition, Shanmugam (1985) suggested that extensive fracturing and the

observed decrease in the proportion of coals in the Latrobe Group from onshore to offshore areas facilitated oil expulsion. Hunt (1991) evaluated the importance of hydrogen in the generation of petroleum and concluded that as the percentage of liptinites in sedimentary organic matter increases, its hydrogen content increases and consequently, its oil generation potential. Whilst the oil potential of Latrobe Group coals of the Gippsland Basin was attributed to high liptinite content (Shibaoka et al. 1978; Shanmugam, 1985), the coals of the Taranaki Basin contain little liptinite. Mukhopadhyay et al. (1991) attributed the oil-generative potential of the Taranaki Basin coals to desmocollinite, a part of the vitrinite maceral group. Furthermore, Hunt (1991) postulated that coals with hydrogen/carbon (H/C) ratios > 0.9, hydrogen index (HI) values > 200 mgHC/gTOC and liptinite contents > 15% are capable of liquid hydrocarbon generation. However, this postulation was rejected by Powell & Boreham (1994). The authors concluded that the overall maceral composition of coal is a poor indicator of its petroleum potential as vitrinitic and inertinitic macerals also contribute to petroleum potential.

Killops et al. (1994) evaluated oils from Taranaki Basin, New Zealand, and characterized the oils as waxy with high hopane/sterane ratios and dominant C_{29} steranes. Based on this characterization, the authors pointed out that most of the oils in the basin were sourced from terrestrial organic matter and accordingly suggested that the Pakawau and Kapuni Group coals as the most probable source rocks with varying contributions from marine shales. Powell & Boreham (1994) noted that the terrestrial oils are sourced from higher plants that became widespread post-Carboniferous, and, therefore, there is no clear evidence of a floral or depositional control on terrestrial organic matter.

According to Killops et al. (1994), New Zealand coals began significant oil generation and expulsion at approximately 0.7% R_o and 1.0 % R_o, respectively. The expulsion of

hydrocarbons from source rocks is seemingly controlled by two consecutive processes: the release of hydrocarbons from kerogen and movements within the source rocks. However, there are opposing theories on which of the processes is the important limiting factor (Pepper & Corvi, 1995b). Furthermore, parameters like organic matter type and hydrogen richness, which vary with depositional environment and thermal maturity, are also considered factors. Inan et al. (1998) investigated oil expulsion efficiencies of seven different lithologies and found that source rocks containing hydrogen-rich kerogen efficiently expel oil as neither of the two consecutive processes is the major limiting factor. Hydrogen-poor kerogen-like humic coals do not expel large volumes of liquid hydrocarbon because both the release from kerogen and movements within rocks are limiting factors. However, Inan et al. (1998) found that oil is expelled from liptinite-rich humic coal once the amount of generated oil surpasses the sorption capacity of the coals. The author's finding suggests that oil expulsion from humic coal is largely controlled by the release of hydrocarbons from kerogen, which in turn is controlled by the hydrogen richness of the kerogen.

Comparing Middle Jurassic gas-prone North Sea coals and Cretaceous and Tertiary oil-prone coals from New Zealand, Australia, and Indonesia, Isaksen et al. (1998) sought to determine the key geochemical controls on hydrocarbon generation and expulsion from humic coals. The workers established that the North Sea coals had elevated HI values that suggested the capability to generate non-volatile oil (C_{15+}) but the pyrolysis-gas chromatograms showed that the coals were depleted in non-volatile oil and enriched in aromatic moieties when compared to Taranaki basin coals of similar maturity. Hence, Isaksen et al. (1998) proposed that oil-prone coals are formed by the incorporation of highly aliphatic biopolymers into coals and that the amount of aliphatic long-chains in coal structures is the most significant control on petroleum generation potential. Furthermore, the authors noted that maceral distribution and elemental ratios and

parameters are not accurate indicators of oil generative potential in coals and terrigenous organic matter as they can lead to overestimation of non-volatile liquid hydrocarbon generation potential. This finding contradicts the earlier research by Hunt (1991) which had postulated the minimum attributes for oil generation in coals. However, Isaksen et al. (1998) concurred that the adsorptive capacity of coals is a key factor in the timing and composition of expelled petroleum.

Various researchers have established that geochemical parameters like vitrinite reflectance and Rock Eval's hydrogen index (HI) and T_{max} are not linear indices to measure the maturity and petroleum generation potential of source rocks. Vitrinite reflectance measurements can vary greatly with different operators and reflectance of vitrinite can be suppressed (Mukhopadhyay, 1994), while HI can anomalously vary with rank and changes in maceral composition (Peters, 1986). Hence, in appraising New Zealand coals from Taranaki Basin, Killops et al. (1998) employed the rank scheme (S_r) developed for New Zealand coals by Suggate (1959) as the tool to measure maturity. Killops et al. (1998) noted that coal-generated oils are characteristically very paraffinic and thus, the paraffinic component (polymethylene) would be a more accurate measure of coal's petroleum generation potential. However, the suggested linear relationship between petroleum potential and polymethylene required a zero polymethylene baseline that the authors noted corresponded to lignin and its diagenetic products. The authors, therefore, assumed that it was possible to determine the contribution of polymethylene (HI_{PM}) to petroleum potential if the lignin contribution (HI_{lignin}) is known, using Equations 2.1 and 2.2:

$$HI = HI_{PM} + HI_{lignin} \quad (2.1)$$

$$HI_{PM} = 1167 * (HI_{max} - 165) / 1002 \quad (2.2)$$

Commercial oil accumulations in the Danish North Sea are sourced from marine shales, except in Harald and Lulita fields, where the oils were derived from terrestrial organic matter (Petersen et al., 1996). Hence, Petersen et al. (2000) investigated Harald and Lulita fields, and based on biomarker and stable carbon isotope analyses, the authors concluded that the oil in Lulita was sourced from Middle Jurassic coals which are dominated by vitrinite macerals with a high proportion of inertinites and subordinate proportion of liptinites. The Middle Jurassic coals also contributed to the gas and condensate-dominated petroleum in the Harald field. Additionally, Petersen et al. (2000) noted that the absence of commercial oil accumulation in the Harald field can be explained by the uneven distribution of generation potential and the high thickness of the coals as both factors may have prevented oil saturation from reaching the expulsion threshold.

The Cooper Basin in Australia is another example of petroleum sourced from terrestrial organic matter. Using geochemical and petrographic analyses, Kramer et al. (2001) evaluated the source rock potential and petroleum expulsion efficiency of the Permian Patchawarra Formation coals. Samples from two cores, comprising thin and thick coal beds each, were analysed and in agreement with the finding by Petersen et al. (2000), the thinner coal beds more efficiently expelled their hydrocarbons. Similarly, Boreham et al. (2003) investigated the source of petroleum in Australia's Bass Basin and based on the results of the oil-source correlation study, the authors suggested that oils in the Bass Basin are generated from terrestrial sources. Furthermore, Boreham et al. (2003) concluded that the Tertiary coals and claystones possess sufficient organic richness to generate petroleum.

Given the difference in the organic matter characteristic of coals and marine/lacustrine source rocks, Sykes & Snowdon (2002) argued that a distinct approach was required to

evaluate the thermal maturity and petroleum potential of coaly source rocks. The authors, therefore, developed a maturity pathway based on the Rock-Eval data of New Zealand coals and the modified rank scale of Suggate (2000). The modified S_r is independent of variations in coal type and lateral and vertical changes in coal rank. The maturation scheme by Sykes & Snowdon (2002) indicated that oil generation and expulsion thresholds are typified by an increase in the bitumen index (BI) and a decrease in the quality index (QI), respectively. Furthermore, the authors concluded that the HI values of immature coals underestimate the generative potential and that the HI values near the expulsion threshold, termed effective HI (HI'), more accurately indicate potential.

Petersen (2006) created a global dataset of 509 humic coals to estimate the oil expulsion window. The author concluded that the peaking of the bitumen index (BI) and decline in the quality index (QI) indicates the start of the effective oil window, which was defined as the maturity at which efficient oil expulsion commences. Petersen (2006) therefore proposed 0.85-1.7% R_o or 440-490 °C as the oil window for humic coals instead of the conventional 0.5-1.3% R_o recognized in marine source rocks. In addition, Petersen (2006) suggested that the oil-generation capacity of coals is influenced by floral and depositional conditions. The author established a link between marine influence and the formation of vitrinite macerals with higher than normal hydrogen content, which mostly accumulated in the Cenozoic when angiosperm flora dominated. Furthermore, the vitrinitic composition of coals was directly associated with the effective oil window. Cenozoic coals which possess a comparably higher proportion of long-chain aliphatic are possibly able to attain the expulsion threshold at lower maturity levels (Table 2.1).

Table 2.1: Maximum hydrogen index (HI_{max}) and effective oil window for humic coals of different ages (Petersen, 2006)

Age	HI_{max} (mg HC/g TOC)	Effective oil window (R_o and T_{max})
Carboniferous	120 to 320	0.90-1.05% to 1.50-1.75% 445-455 °C to 480-500 °C
Permian	120 to 290	0.90-1.05% to 1.50-1.80% 445-455 °C to 470-500 °C
Jurassic	105 to 290	0.85-0.95% to 1.70-1.90% 440-450 °C to 485-510 °C
Cenozoic	250 to 370	0.65-0.95% to 1.70-2.00% 430-450 °C to 490-510 °C

Based on the global dataset of HI, vitrinite reflectance and T_{max}, Petersen (2006) observed that minimum and maximum HI were attained at the reflectance of 1.0 %R_o and 0.6 %R_o or T_{max} of 455 °C and 430 °C, respectively. Hence, the author proposed that the maximum HI (HI_{max}) line ranged from 0.60 to 0.95 %R_o. Whilst Pepper & Corvi (1995a) and Hunt (1996) suggested a minimum HI value of > 200 mg HC/g TOC for oil expulsion from coal to occur, Petersen (2006) specified that coals with HI_{max} values ≤ 150 mg HC/g TOC are mainly gas-prone.

Petersen & Nytoft (2006) examined the impact of floral evolution on the petroleum generation potential of coals from four major coal-forming periods and found that the amount of longer chain aliphatic hydrocarbon increases from Palaeozoic to Cenozoic coals, which conforms with the evolution from primitive Carboniferous plants towards more complex higher plants in the Cenozoic. This finding is in agreement with the conclusion by Isaksen et al. (1998) that plant evolution is a key control of the occurrence of oil-prone coals (Figure 2.1). Furthermore, Petersen & Nytoft (2006) argued that aromatic hydrocarbons contribute to the hydrogen index, establishing it is not a reliable measure of the paraffinic content of coals and thus, its oil generation potential.

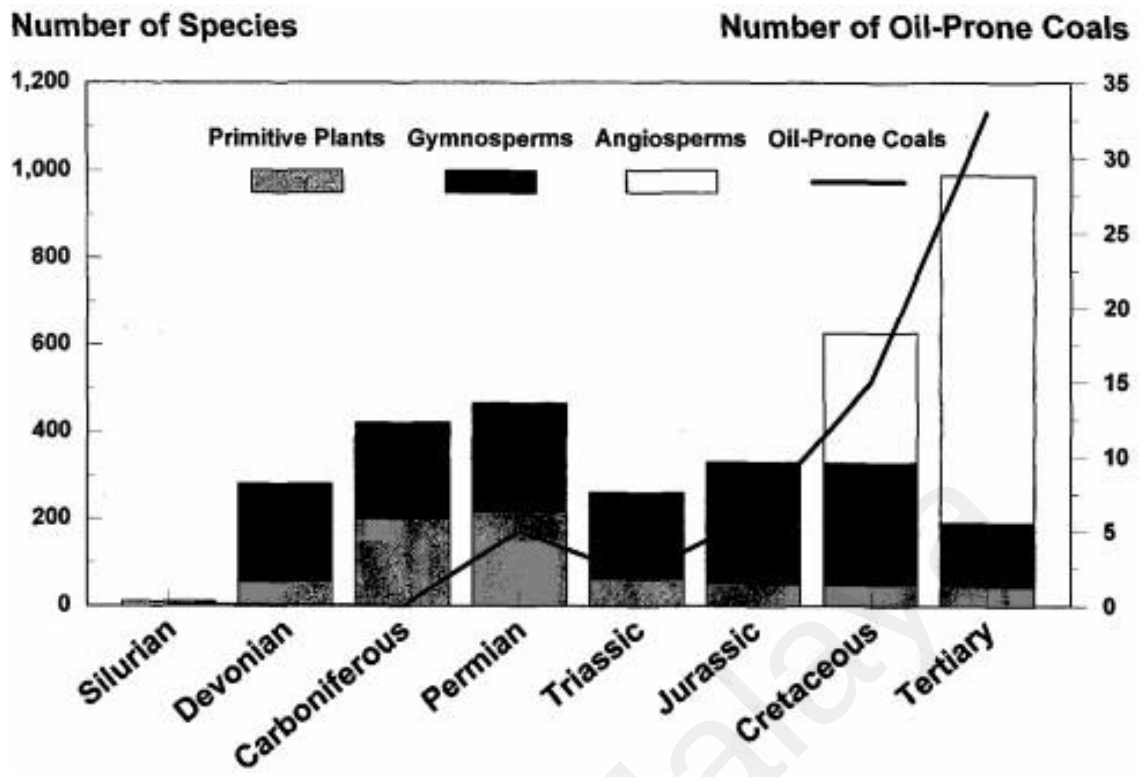

Figure 2.1: Relationship between plant evolution and prevalence of oil-prone coals (Killops et al., 1998).

Following this finding by Petersen & Nytoft (2006) and others (e.g. Isaksen et al., 1998; Killops et al., 1998) and based on source rock analysis of samples from Turpan Basin, China, Zhao et al. (2009) proposed the use of absolute concentration of aliphatic and aromatic hydrocarbons as parameters to distinguish between oil and gas-prone source rocks. *n*-alkanes/aromatics ratio > 8.0, *n*-alkanes concentration > 110 μg/mg, and total aromatics concentration < 15 μg/mg suggest an oil-prone source rock, while *n*-alkanes/aromatics < 1.5, *n*-alkanes concentration < 82 μg/mg and total aromatics concentration > 40 μg/mg suggest a gas-prone source rock.

Murchison (1987), Fleet & Scott (1994), and Wilkins & George (2002) presented summaries of the state of knowledge on oil-prone coals. Fleet & Scott (1994) concluded that oil-prone coals mostly occur as low latitude tertiary deposits or late Jurassic-Palaeogene sequences, and that liquid hydrocarbons derived solely from coals and other

terrestrial sources have pristane/phytane ratios greater than 3-4, while Wilkins & George (2002) noted that bulk techniques like elemental analysis and ^{13}C NMR spectroscopy that allows for the measurement of coal's PM component offer a more accurate estimate of petroleum potential. Based on the current understanding as summarized in this sub-section, it is apparent that the main factors governing the capacity of coals to generate oil include the botanical origin of organic matter input, depositional environment, and early diagenetic effects.

2.2 Marine Influence

The sulfur content of coals is often a useful indicator of marine influence (Casagrande, 1987). Coals with sulfur contents < 1% and > 3% could be regarded as low-S and high-S coals, respectively, while coals with intermediate values (1-3%) are regarded as medium-S coals. According to Chou (2012), sulfur is derived primarily from parent plant material in low-S coals while in medium-S and high-S coals, it is sourced from both parent plant material and sulfate-rich seawater during peat accumulation and diagenesis. However, Sykes et al. (2014) assumed a maximum sulfur content of 0.5% for coals deposited under freshwater conditions and consequently, values > 0.5% indicate some degree of marine influence. Nonetheless, Oskay et al. (2016) showed that sulfate-rich karstic aquifer contribution to freshwater paleomire water supply could elevate total sulfur content.

Marine influence in coals has been documented during early burial (syngenetic) and coalification (epigenetic). Dai et al. (2002) studied high sulfur coals from the Wuda coalfield, China and concluded that the No. 9 seam was influenced by seawater during peat accumulation. Similarly, Gayer et al. (1999) investigated the origin of sulfur in coals from the Bute seams in South Wales. The seams were without a marine roof but with a

relatively high abundance of sulfur (0.73-2.0 wt.%) in the lower plies. The authors attributed this to initial peat accumulation under the brackish-water influence. In addition, Sykes et al. (2014) concluded that the coaly source rocks from Mangahewa seams, New Zealand were inundated by brackish water during early burial while peatification was ongoing. Whilst sulfur content is no useful indicator of the type of marine influence, forms of pyrite in coals are effective indicators of the type/timing of marine influence as syngenetic and epigenetic pyrites are incorporated into coals during accumulation/early burial and after compaction/partial consolidation, respectively (Widodo et al., 2010). The formation of pyrite is governed by the availability of a reducing environment and ferrous ion (Casagrande, 1987).

Cretaceous and Tertiary oil-prone coaly source rocks in Australasia and southeast Asia are known to have been deposited in coastal plain settings but the marine influence on oil potential and generation kinetic is not well established. Using organic geochemical and petrographic tools, Sykes et al. (2014) investigated the effects of early diagenetic marine influence on the oil generation potential of Eocene humic coals of Taranaki Basin, New Zealand. According to the authors, the presence of pyrites and elevated sulfur content in the coals indicated marine influence. In addition, suppressed vitrinite reflectance and elevated vitrinite fluorescence affirmed some degree of marine influence on the coals. Sykes et al. (2014) concluded that marine-influenced Cenozoic coals are typified by abundant hydrogen-rich perhydrous vitrinite as the increase in anaerobic bacteria activity due to low acidic conditions in brackish environments results in hydrogen enrichment. Additionally, the authors concluded that whilst early diagenetic marine influence does not increase inherent bitumen and capacity to generate non-volatile paraffinic oil, it significantly enhances the bio-resistance of peat biomass by sulfurization, reducing its biodegradation and thus preserving organic richness.

2.3 Conditions for Peat Accumulation

The physical properties and chemical composition of coals are considerably influenced by the environmental conditions under which the paleopeats accumulated. Based on studies of modern peat-forming environments, a few factors have been documented to govern peat accumulation and quality. A recent comprehensive overview of peat depositional environments is provided by Dai et al. (2020), and references therein.

McCabe (1984) summarized the conditions for peat accumulation as primarily the balance between plant production and organic matter degradation. Increasing temperature and moisture enhance plant growth and higher production of plant biomass (Diessel, 1992). However, it also enhances the post-depositional microbial reworking of organic matter and peat destruction as microbial alteration is a temperature-sensitive process that is slower under cold and dry climatic conditions (McCabe et al., 1984). Hence, despite the relatively lower precipitation in the mid-latitudes, peat is currently accumulating mostly under cool climates (McCabe, 1984). Similarly, Hobday (1987) identified that peat formation and accumulation are governed by a combination of local, regional, and global factors such as depositional environment, climate and tectonics, and sea-level changes, respectively.

For peat to accumulate, the rate of biomass production must be higher than the rate of bacterial decomposition (Fulton, 1987). The rate of peat accumulation is however dependent on climatic conditions, water-table levels, and surface topography (Cameron et al., 1989). Whereas peat can accumulate in different environments, varying vegetation types and depositional conditions impact seam structure and coal properties (McCabe, 1987; Powell & Boreham, 1991). The two main types of mires or peat-forming systems are ombrotrophic mire and minerotrophic or rheotrophic mire which depend mainly on precipitation and groundwater, respectively, for moisture. Therefore, in peatlands,

vegetation type depends mainly on the availability of moisture and nutrient while peat composition depends primarily on contributing plant species and their mode of decomposition (Cameron et al., 1989). Orem & Finkelman (2003) noted that the principal factors for peat accumulation are vegetation type and redox conditions. Nevertheless, peat only forms in environments where organic accumulation exceeds organic decay, while accumulated peat only transforms to coal beds in environments with a minimal influx of clastic sediments (O'Keefe et al., 2013).

Coal facies are also closely associated with groundwater fluctuation. Hence, the groundwater level is critical for peat accumulation and preservation. Groundwater levels are governed by climatic conditions, basin subsidence, eustasy, and rate of plant growth (Anderson, 1964; Moore, 1987; Diessel, 1992). Constantly high water-table levels due to relative sea-level rise and increased precipitation result in the waterlogging of plant biomass, which creates anaerobic conditions that support peatification. Consequently, when peat accumulation exceeds inorganic sediment accumulation, deposits assume a domed shape (Cameron et al., 1989). Furthermore, for thick peat to accumulate, the rates of subsidence and peat accumulation must proceed at similar rates (Courel, 1989). Rapid subsidence and the consequent rise in the water table can lead to the drowning of mires if the peat accumulation rate does not keep pace (McCabe, 1984). Nevertheless, plant biomass is presumably better preserved in rheotrophic mires due to its higher groundwater level which ensures a limited degree of organic matter biodegradation. However, as peat accumulates and the mire becomes more elevated, the degree of groundwater influence progressively decreases and the mire increasingly depends on precipitation for water and nutrient (Shotyk, 1988). Additionally, the peat-forming vegetation becomes less diverse as nutrient-poor rainfall increasingly provides moisture (McCabe, 1987).

The ash content of coals supposedly reflects its mineral sediment input (Love & Bustin, 1985). According to McCabe (1984), minerals in coals can originate from three sources: transportation by air or groundwater into peatlands; inorganic materials in plants; and introduction during or after peat accumulation or during coalification. Hence, low (< 10%) mineral content in coals indicates the absence of a clastic source, typical of ombrotrophic mires that are largely dependent largely on precipitation. Conversely, low-lying, rheotrophic mires which get water and nutrient mostly from groundwater results in clastic partings with medium to high (> 25%) ash content (Love & Bustin, 1985). The ash content of peat has also been found to correlate with its sulfur content and the pH of peatland water (Esterle & Fern, 1994). In lower pH environments such as the Baram River area, in Malaysia, microbial activity is limited, and this results in the reduced degradation and sulfurization of organic matter, thereby yielding low ash and sulfur peat (Anderson, 1964; Cameron et al., 1989).

In summary, the preconditions for coal formation include interrelated and interdependent factors such as tectonics, climate, and vegetation (Friederich et al., 2016).

2.4 Biomarker and isotopic proxies

The molecular and isotopic compositions of *n*-alkanes from peat-forming plants and peat sequences are widely employed techniques for reconstructing past environmental conditions (Ficken et al., 2000; Nott et al., 2000; Pancost et al., 2002; Nichols et al., 2006; Zheng et al. 2007; Bingham et al. 2010; Andersson et al., 2011; López-Días et al., 2013**;** Zhao et al., 2018; He et al., 2019; Naafs et al., 2019).

Over the last 20 years, several studies have developed and applied proxies for reconstructing past climate and vegetation. In a study of plants from Lake Qinghai, China,

and its surrounding areas, Duan & Xu (2012) found that the mean δD values of *n*-alkanes from aquatic plants (-143‰) are relatively lower than from terrestrial plants (-113‰). The authors attributed this to the greater isotopic fractionation, relative to environmental water, in aquatic plants. Similarly, Duan et al. (2014) found a distinction in the δD values of *n*-alkanes from different plant types in the order: of woody plants > aquatic plants > herbaceous plants. Also, the authors noted that hydrogen isotopic (δD) values of *n*-alkanes generally decrease with increasing average chain length (ACL) values. This is corroborated by Hou et al. (2007), which established that the δD values of seven plant types show variation up to 70‰.

According to Dawson et al. (2004), sediments deposited in high latitudes and under glacial climates show more negative hydrogen isotopic (δD) values than sediments deposited in low latitudes with tropical climatic conditions. Furthermore, Dawson et al. (2004) observed that the δD values become more negative with increasing distance from the ocean. The authors ascribed this trend to the δD values of meteoric waters in the different paleoenvironments as the isotopic composition is mainly related to temperature and thus latitude. Duan & He (2011) also studied the relationship between latitude and temperature, and the influence on the isotopic composition of *n*-alkanes in plants across five Chinese locations, spanning latitudes 22º to 39º. The authors observed lower ACL values for the same plant type as latitude increases from south to north. Also, the isotopic composition of plants is relatively lighter at high latitudes and altitudes as precipitation is relatively depleted in deuterium (Duan & He, 2011).

Vegetation type and environmental factors such as temperature and aridity have been found to impact the *n*-alkane chain length. Hoffmann et al. (2013) observed that while ACL values are influenced by hydroclimatic conditions, additional information is needed to validate findings as both vegetational and hydrological changes affect the isotopic

composition. The authors, however, suggested that ACL be employed as a paleoclimate proxy under stable vegetational cover. In contrast, Bush & McInerney (2015) studied leaf and soil samples from across the United States and concluded that ACL values are influenced by temperature and not vegetation type (i.e. C_3 or C_4 plants).

Ortiz et al. (2013) applied the relative proportion of C_{27}, C_{29}, and C_{31} *n*-alkanes to distinguish varying OM inputs in response to changing environmental conditions. According to the authors, deciduous tree forests and grasses expanded during wetter and drier periods, respectively. This finding was corroborated by López-Días et al (2013), which employed the n-C_{27}/n-C_{31} ratio to estimate the contribution of arboreal vegetation relative to herbaceous vegetation.

CHAPTER 3: GEOLOGY OF STUDY AREAS

3.1 Sarawak Basin, Malaysia

The Sarawak Basin (Figure 3.1) is one of Malaysia's prolific hydrocarbon-producing basins, accounting for 80 per cent of coal resources, 23 per cent of known oil reserves, and 51 per cent of its proven natural gas reserves (Madon, 1999b). The Basin forms the southern margin of the Oligocene-Recent South China Sea Basin, initiating as a foreland basin due to the collision of rifted South China continental fragment with Sarawak and thereafter developed into a passive continental margin (Madon, 1999a; Madon, 1999b). The development of the Sarawak Basin started in the Late Oligocene and has undergone phases of rifting and sea-floor spreading, evolving from deep foreland basin phase pre-Oligocene to shallow marine shelf progradation phase from post-Oligocene to the present day (Mat-Zin & Swarbrick, 1997; Madon et al., 2013).

According to Ho (1978), the entire sedimentary succession in Sarawak Basin from Early Eocene to the Pleistocene consists of eight sedimentary cycles that are separated by regressive sequences. Lunt & Madon (2017) provides a historical overview of the sedimentary cycles identified in the Sarawak Basin. Based on tectonostratigraphic history, the onshore Sarawak Basin can be classified into three zones: Miri, Sibu and, Kuching Zones (Madon, 1999b). The Kuching Zone reportedly comprises Carboniferous to Triassic marine limestones which are overlain by Jurassic-Cretaceous sediments while the Miri Zone is comprised of thick Paleogene to Neogene sedimentary successions (Madon, 1999b; Hennig-Breitfeld et al., 2019). The Sibu Zone is underlain mainly by the low-grade metamorphosed Late Cretaceous to Eocene sediments of the Rajang Group (Madon, 1999b). Additionally, seven structural-stratigraphic provinces have been identified in the Sarawak Basin, namely SW Sarawak, Tatau, Balingian, Tinjar, Central Luconia, West Luconia, and North Luconia (Madon, 1999a; Figure 3.2).

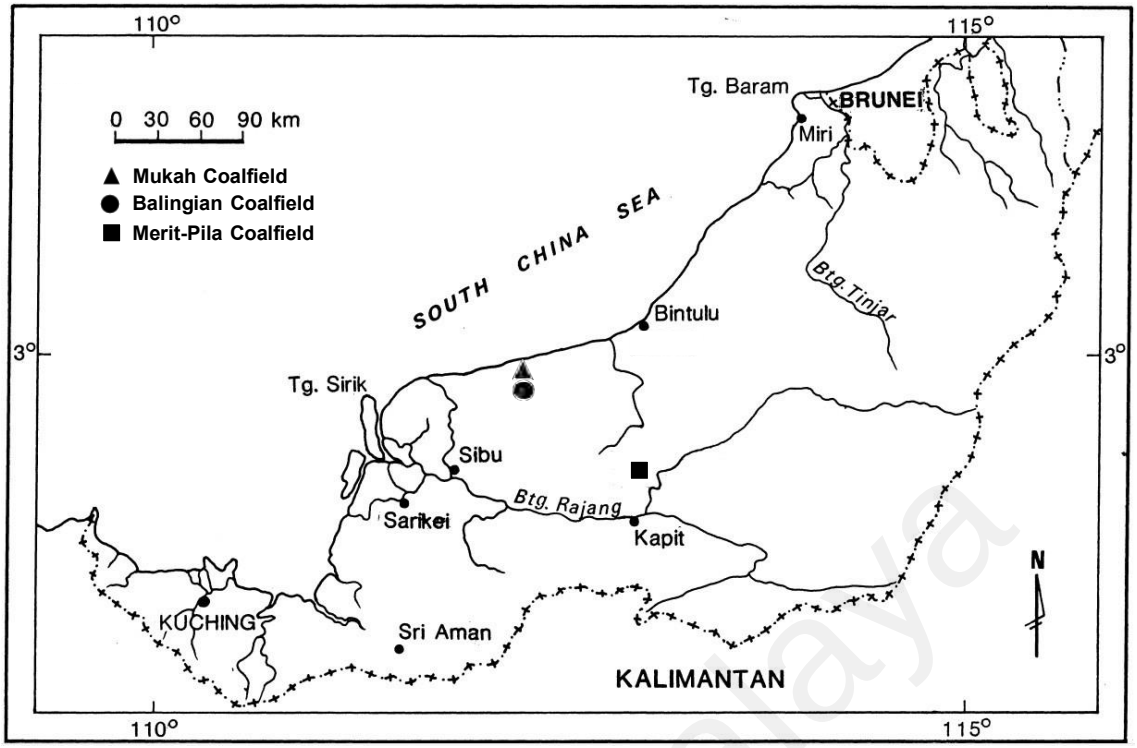

Figure 3.1: Regional map showing the location of study areas in onshore Sarawak Basin (modified from Wan Hasiah, 1999).

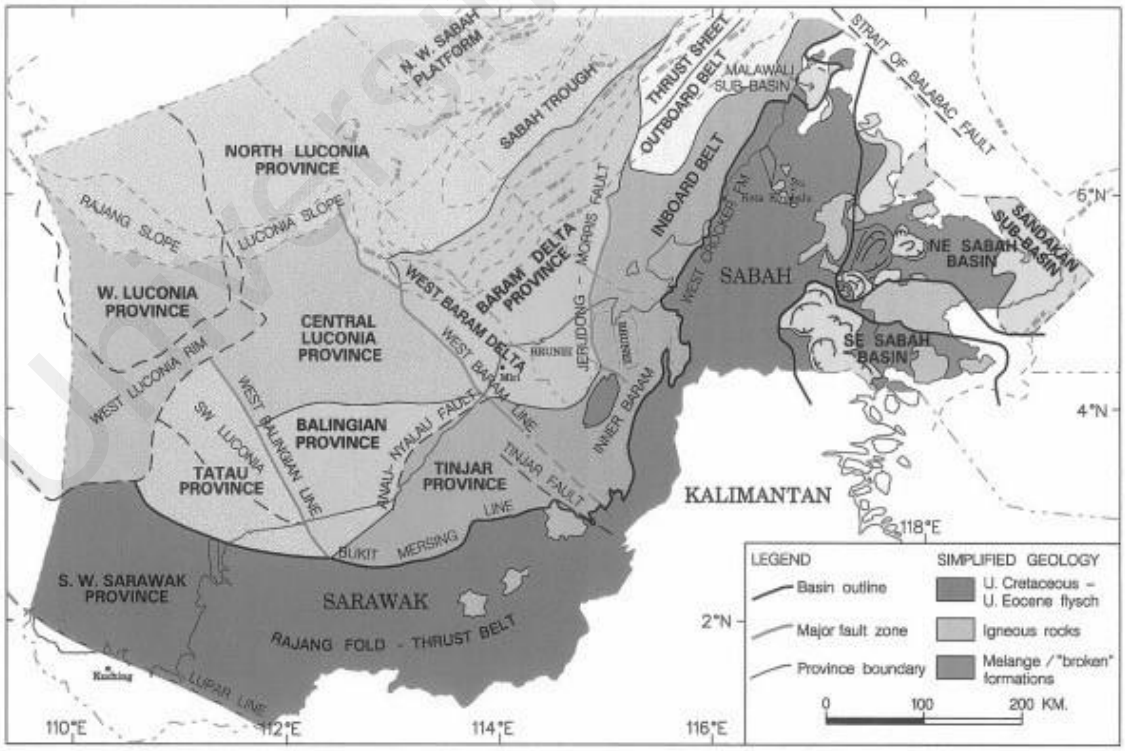

Figure 3.2: Regional map showing Basins and Provinces of northern and eastern continental margins of Sarawak and Sabah (from Madon, 1999a).

The study areas considered in this research are in the onshore part of the Balingian Province, which lies between the West Balingian and West Baram lines and are bounded to the north and south by the Central Luconia and Tinjar Provinces, respectively (Figure 3.2). The onshore Sarawak Basin coals have generally been mined for energy and industry uses. The dominant coal seams occur in four main Tertiary coalfields: Bintulu, Merit-Pila, Mukah-Balingian, and Silantek coalfields (Kiat et al., 1987; Johari et al., 1994). Currently, the coal mined at the Merit-Pila, Mukah, and Balingian coalfields are used as feeding coals of the Sejingkat, Mukah, and Balingian coal-fired power stations, respectively, while the coal mined at the Silantek coalfield is exported. Sia & Abdullah (2012) documents the history of coal exploration and mining in the Basin. This research investigated the Balingian Formation and Liang Formation coals from the Mukah-Balingian coalfield and the Nyalau Formation coals from the Merit-Pila coalfield. The Balingian Formation, Liang Formation, and Nyalau Formation coals are commonly referred to as Mukah, Balingian, and Merit-Pila coals, respectively. Abdullah (2002) classified the Mukah-Balingian and Merit-Pila coals as autochthonous and hypautochthonous deposits, respectively.

Although no commercial accumulation of petroleum has been discovered onshore, petroleum is currently produced in the offshore areas of the Sarawak Basin and the source sediments consist of coals, fluvial and estuarine channel sands, and clays of tidal and coastal plain deposits (Madon & Abolins, 1999; Amir Hassan et al., 2017). The Nyalau Formation from the Bintulu area is an onshore extension of the offshore Balingian Province that is known to possess coaly source rocks from Cycles I and II (Du Bois, 1985). Petrographic study and source rock evaluation of the coals and carbargillites from the Bintulu area indicate good oil-generating potential for the coals and carbargillites (Wan Hasiah, 1999; Abdullah, 2001; Hakimi et al., 2013). Furthermore, geochemical analysis of crude oils from offshore Sabah and Sarawak has established that the oils were

derived from mature terrigenous source rocks that were deposited in the peatlands environment (Awang Jamil et al., 1991).

Important earlier studies of foraminifera assemblages prompted Wolfenden (1960) and Liechti et al. (1960) to assign probable ages of Late Oligocene to Miocene, Late Miocene, and Late Pliocene to Pleistocene to the Nyalau, Balingian and Liang Formations, respectively. However, based on new data, recent studies have reviewed the stratigraphy of the Sarawak Basin and reassigned ages to the formations (Abdullah, 2001; Sia et al., 2014; Murtaza et al., 2018; Ramkumar et al., 2018; Hennig-Breitfeld et al., 2019; Breitfeld et al., 2020; Lunt, 2020). For example, based on the results of palynology studies of the Balingian Formation, Sia et al. (2014) and Murtaza et al. (2018) have both revised the earlier ascribed Late Miocene age to Early Miocene and Early to Middle Miocene ages, respectively.

Similarly, based on a stratigraphy and paleogeography study of north-western Borneo using Zr and U-Pb dating and biostratigraphy, Hennig-Breitfeld et al. (2019) assigned an Oligocene to Early Miocene, uppermost Early to Middle Miocene, and latest Middle Miocene age to the Nyalau, Balingian and Liang Formations, respectively. Hennig-Breitfeld et al. (2019) identified the Nyalau Unconformity, a main event at c. 17 Ma, that is characterised by a change in the provenance of the Nyalau and Balingian Formations and change of the coastline to NE-SW orientation. Consequently, the researchers concluded that the top of the Liang Formation is approximately c. 11 Ma. Additionally, Hennig-Breitfeld et al. (2019) posited that their conclusion is corroborated by the Ramkumar et al. (2018) study which associated the presence of an extensive tephra layer interbedded within thick coal beds in the Balingian coalfield with an explosive volcanic event that occurred between 11.44 and 11.76 Ma in the Middle Miocene. However, the latest Middle Miocene age assigned to Liang Formation by Hennig-Breitfeld et al. (2019)

contradicts the Late Pliocene to Pleistocene age assigned by other workers (Wolfenden, 1960; Liechti et al., 1960; de Silva, 1986; Madon, 1999b, Sia & Abdullah, 2012). Hence, discussions by workers on the stratigraphy in Figure 3.3, and in particular the appropriate age, of the clastic formations of the Sarawak region are still ongoing (Hennig-Breitfeld et al., 2020; Lunt, 2020).

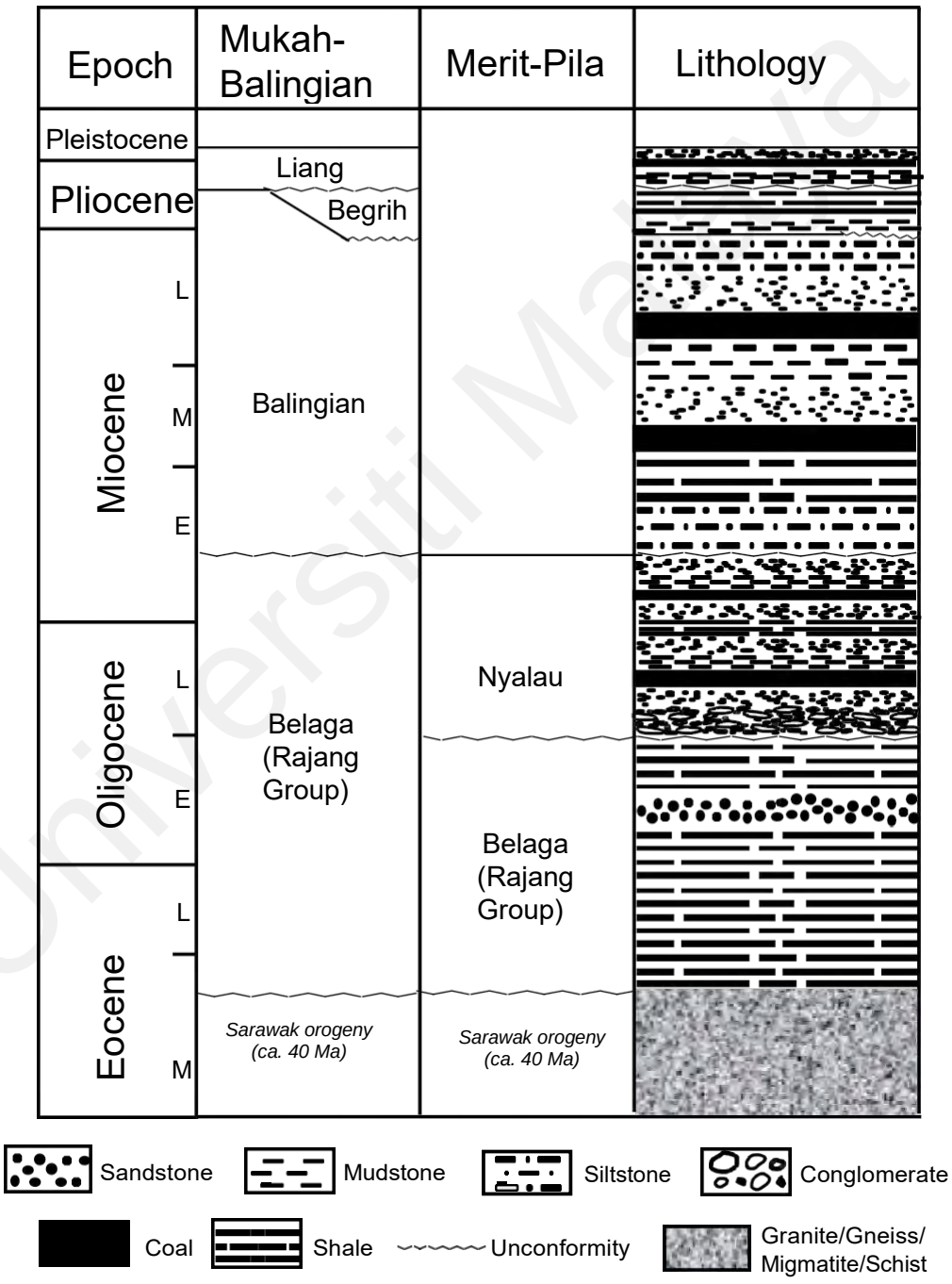

Figure 3.3: Generalised stratigraphy column of the study areas in the Sarawak Basin.

3.1.1 Nyalau Formation coals in Merit-Pila coalfield

The Merit-Pila coalfield covers an area of about 260 km^2 and is elongated in an E-W direction (Hutchison, 2005). The deposits are hosted in the Nyalau Formation, a Miocene outlier of the older Eocene Belaga Formation and located in the upper reaches of the Rajang River, about 50 km south of Bintulu and 75 km upstream of Kapit Division. The coal seam in its eastern and western boundaries are split into separate wedges by the uplifted and intensely folded Belaga Formation, which consists predominantly of dark shales that have been metamorphosed into argillite and phyllite (Chen, 1993; Hutchison, 2005). The main deposits of the Merit-Pila coal seam are found within the Nanga Merit and Iran River beds, which underlie the central and western parts, respectively, of the coalfield. The Nanga Merit beds, however, contain the most important deposits and consist of a homicidally dipping succession of conglomerate, sandstone, mudstone, and coal while the Iran River beds are made up of a slightly deformed succession of conglomerate, sandstone, shale, and coal (Chen, 1986).

The Nyalau Formation at Merit-Pila coalfield is approximately 1000 m thick and divided into five stratigraphic units, consisting of upper sandstone, upper coal zone, middle shale sandstone, lower coal zone, and lower sandstone units, with the thickness of the units varying from 100 m to 300 m. The coalfield is underlain by the Belaga Formation which forms the basement rock and it is overlain by the lower sandstone unit (Kiat et al., 1987). The lower coal zone, which overlies the lower sandstone unit, consists of a sandstone-mudstone sequence that hosts 18 coal seams. The middle shale sandstone unit overlies the lower coal zone but no coals are found within the unit. The upper coal zone overlies the middle shale sandstone unit, consisting mainly of a sandstone-siltstone sequence that hosts four coal seams. The upper and lower coal zones are exposed at Belawie Mujan and Tebulan Block mining sites. Samples MP1L to MP2U are from the

lower coal zone in the Tebulan Block outcrops exposed at latitude 2°18'667" N and longitude 113°02'687" E. Samples MP3L to MP7U are from the upper coal zone exposed in the Belawie Mujan area at latitude 2°17'N and longitude 113°05'E. The Nyalau Formation coals are dominated by huminites but contain a significant amount of liptinite macerals (Abdullah, 1997; Wan Hasiah, 1999).

3.1.2 Liang Formation and Balingian Formation coals in Mukah-Balingian Coalfields

The Liang Formation and Balingian Formation coals and coaly sediments occur in the Mukah-Balingian coalfields which are in the low-lying coastal plain between Mukah and Balingian rivers and about 260 km northeast of Kuching (Chen, 1986; Sia & Abdullah, 2012). Coal seams in the Mukah and Balingian coalfields are underlain by the Lower Miocene Balingian Formation and Upper Pliocene Liang Formation, respectively, and are separated by the Lower Pliocene Begrih Formation. The Mukah-Balingian area is flat in the north and gently undulating in the south, where the Balingian Formation is separated from the Begrih Formation by an unconformity (Sia & Abdullah, 2012; Sia et al. 2014). Based on sedimentological and palynological data, Murtaza et al. (2018) described seven facies association observed in the Miocene-Pleistocene Formations in the Mukah-Balingian area.

The Lower Miocene Balingian Formation consists of sandstone, clay, shale, and coal, and is estimated to be 3000-3600 m thick but only approximately 1900 m of the topmost section is exposed in the study area. The Formation which unconformably underlies the Begrih Formation was deposited in coastal and inland peat mires (Hutchison, 2005; Sia et al, 2014). The coals contain varying amounts of ash, high amounts of argillaceous mineral matter, low abundance of pyrites, and are dominated by huminite macerals with

varying amounts of liptinitic macerals and minor amounts of inertinites (Sia et al, 2014; Zainal Abidin et al., 2022).

The Upper Pliocene Liang Formation is ca. 950 m thick and made up of clay, sand, and intercalations of coal. The Formation overlies the Eocene Belaga Formation in the south and Lower Pliocene Begrih Formation in the North (Hutchison, 2005). According to Sia et al. (2012), the coals are dominated by huminite maceral and are characterised by low sulfur, low ash, and high moisture content.

3.2 Benue Trough, Nigeria

Coal is Nigeria's earliest fossil fuel and was used to power the economy until the discovery of oil in the late 1950s. Nigeria is reported to have coal reserves of 190 million tonnes, most of which are deposited within the Benue Trough (Figure 3.4). The Benue Trough constitutes a part of the West and Central African rift system of Niger, Chad, Cameroon, and Sudan (Genik, 1993), and consists of a series of rift basins that trend SSW-NNE for about 1,000 km (Figure 3.5). The Trough is bounded in the north and south by the Chad and Niger Delta Basins, respectively, and its depth increases south-westward and decreases north-eastward (Nwachukwu, 1985).

The opening of the South Atlantic Ocean due to the continental separation of Africa and South America led to the accumulation of up to 6000 m of Cretaceous-Tertiary sedimentary rocks in the Trough (Nwachukwu, 1985; Abubakar et al., 2008; Obaje et al., 2004b). The deposition of the mostly marine Albian-Santonian sediments was terminated by a deformation episode in the Middle Santonian (Fitton, 1980; Obaje et al., 2004b). Hence, the pre-Middle Santonian sediments are folded, faulted, and uplifted in several locations (Jauro et al., 2007; Edegbai et al., 2019a). These eroded marine sediments were

overlain by deltaic sediments. The accumulation of deltaic sediments persisted until a transient but widespread marine transgression in the Maastrichtian. The origin, evolution, and stratigraphy of the Benue Trough are described by Olade (1975), Fitton (1980), Petters & Ekweozor (1982), Ofoegbu (1985), Benkhelil (1989), Obaje et al. (2004b) and Edegbai et al. (2019a) among others.

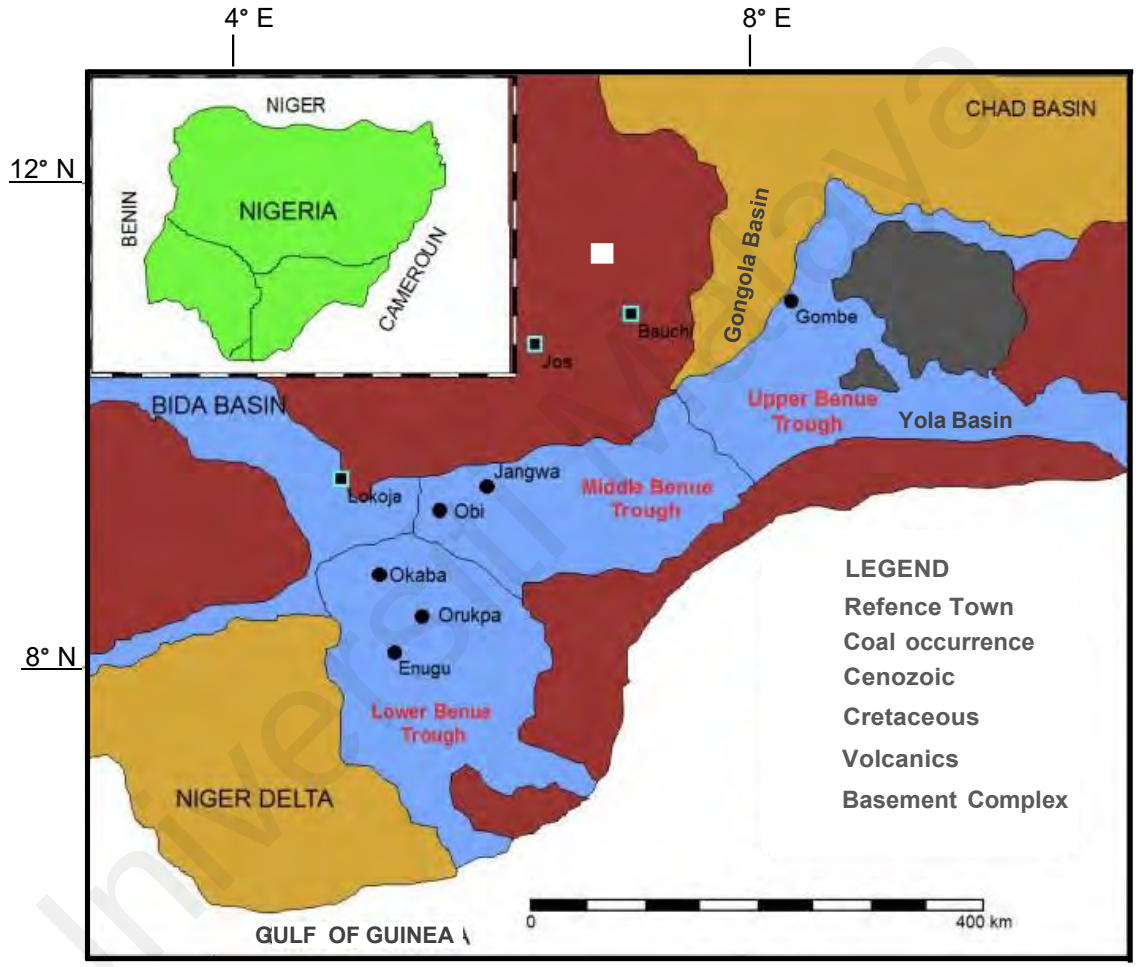

Figure 3.4: Geological map of Nigeria showing inland basins and coal sites. Inset: geographical Map showing Nigeria and bordering countries (modified from Fatoye & Gideon, 2013).

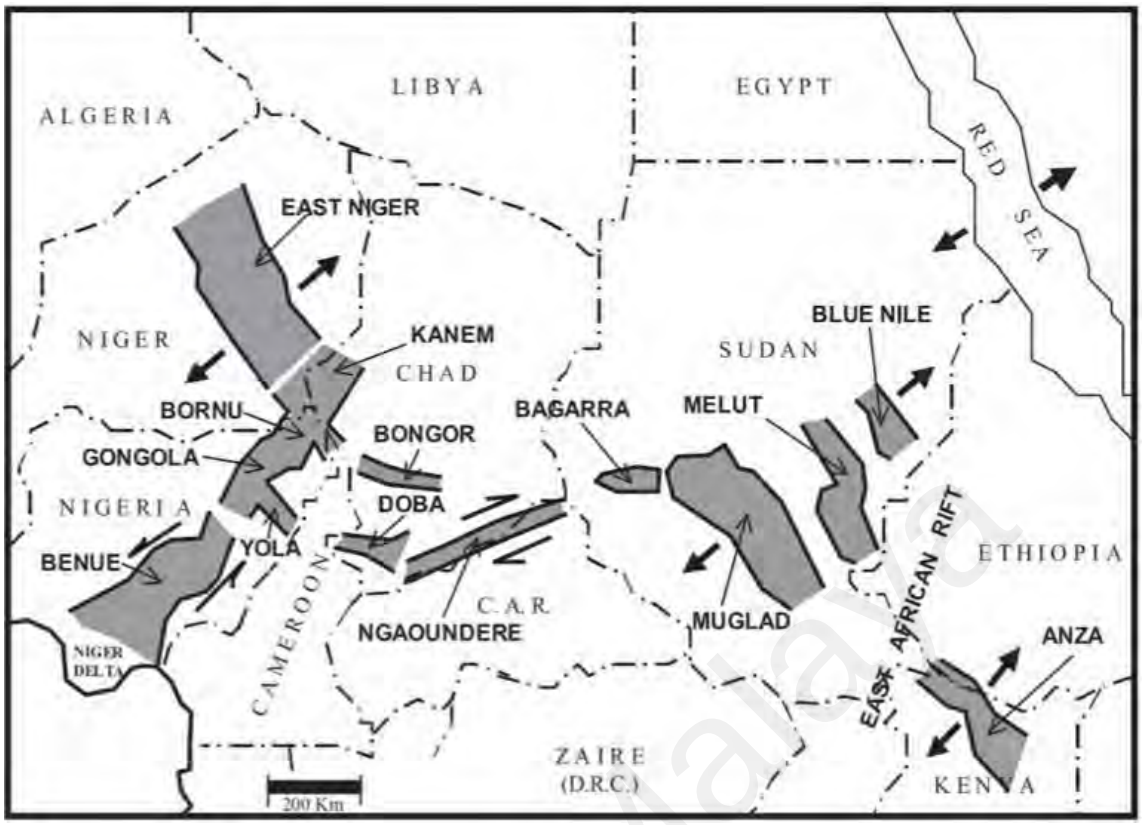

Figure 3.5: Regional tectonic map of West and Central African rift basins (from Obaje et al., 2004b).

Based on lithostratigraphic and geographical differences, the Trough can be divided into three sub-divisions: Upper, Middle, and Lower Benue Trough (Figure 3.4). The Lower Benue Trough consists of the Anambra and Abakaliki Basins while Gongola and Yola Basins make up the Upper Benue Trough. The Middle Benue Trough occupies the area north of the Gboko regional fracture system (Obaje et al., 2004b). Lignite and bituminous coals are found in Mamu and Gombe Formations, respectively, of the Lower and Upper Benue Trough while bituminous coals are found within the Agwu Formation in the Middle Benue Trough (Obaje et al., 2004b; Fatoye and Gideon, 2013). Samples were collected from the Maiganga coal mine in Gongola Basin, Upper Benue Trough, and coal sites across the Trough. The detail of the studied samples in this research are presented in Table 4.1.

3.2.1 Gombe and Lamja Formations in Upper Benue Trough

The Upper Benue Trough, which is divided into the north-south trending Gongola Basin and the east-west trending Yola Basin, is underlain by Precambrian basement rocks and the overlying Albian Bima and Cenomanian Yolde Formations (Abubakar et al, 2008). According to Jauro et al. (2007), the Yolde Formation represents the onset of marine transgression into the Upper Benue Trough. In the Gongola Basin, the Yolde Formation is overlain by the Pindiga, Gongila, and Fika Formations, whilst it underlies the Dukul, Jessu, Sekuliye, Numanha, and Lamja Formations in the Yola Basin (Abubakar et al., 2008). Post-Santonian sediments are only limited to the Gongola Basin with the Maastrichtian Gombe Formation and the Paleogene Kerri-Kerri Formation. The Stratigraphy of the Upper Benue Trough is shown in Figure 3.6 and further described by Jauro et al. (2007) and Abubakar et al. (2008).

Research interests have recently increased in sediments of the Upper Benue Trough following the discovery of commercial oil reserves in the Doba Basin, Chad, and Logome-Birni Basin, Cameroon. These basins and the Upper Benue Trough share similar structures and are a part of the West and Central African rift system (Genik, 1993). Hence, three exploration wells have thus been drilled in the Upper Benue Trough. Well *Kolmani River-I*, drilled by Shell Nigeria Exploration and Production Company (SNEPCo) in 1999, encountered gas and little oil while two other wells (*Kuzari-I* and *Nasara-I)* were dry (Obaje et al., 2004a). Following ongoing exploratory work on the Kolmani River blocks in the Gongola Basin, the Nigerian National Petroleum Corporation (NNPC) announced in 2019 the discovery of gas, condensate, and oil in the *Kolmani River-II* well.

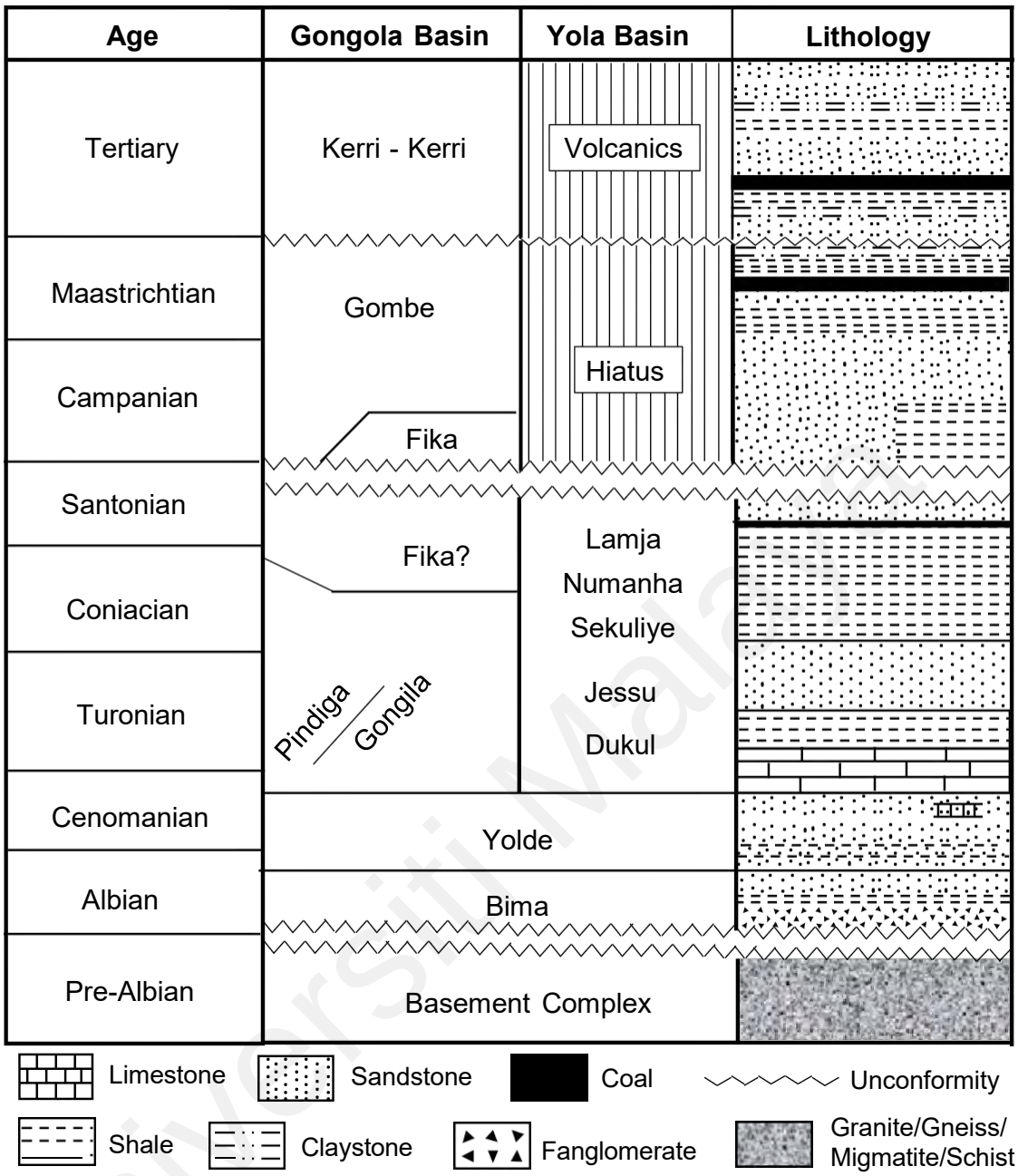

Figure 3.6: Stratigraphy of the Upper Benue Trough (modified after Obaje et al., 2004b).

Earlier studies of the Upper Benue Trough sediments include Pearson & Obaje, (1999), Obaje et al. (2004a), Obaje et al. (2004b), Jauro et al. (2007), and Abubakar et al. (2008). According to Pearson & Obaje (1999), the similar levels of thermal maturity between the pre-Santonian Pindiga Formation and post-Santonian Gombe Formation indicate little erosion following the Middle Santonian deformation. Shaly sediments of the Bima, Yolde, Pindiga, and Gombe Formations in the Gongola Basin were analysed

by Abubakar et al. (2008). Rock-Eval pyrolysis data implies that the Gombe and Pindinga Formations are immature for hydrocarbon generation while the Yolde Formation is marginally mature and Bima Formation is at a peak maturity stage (Abubakar et al., 2008). Furthermore, the pyrolysis data suggests the presence of both terrigenous and marine/algal organic matter in the Upper Benue Trough samples.

3.2.1.1 Gombe Formation

The Gombe Formation is made up of siltstones, claystones, mudstones, sandstones, and shales in the Maiganga coalfield, which is located in the Gongola Basin of the Upper Benue Trough and covers an area of 48 km^2 (Ayinla et al. 2017a). Four seams were observed in the coalfield with a total estimate of 4.5 million tons of coal (Ayinla et al., 2017a). The Gombe Formation is approximately 35 m thick in the Maiganga area and a Maastrichtian age has been assigned (Obaje et al., 2004b; Jauro et al., 2007). The Formation is reportedly a continental deposit that resulted from the extensional uplift in the Maastrichtian (Pearson & Obaje, 1999).

Previous geochemical, petrographic, and stratigraphic studies have concluded that the Maiganga coals possess good to excellent generating potential, are thermally immature, and deposited in a transitional deltaic environment (Jimoh & Ojo, 2016; Ayinla et al., 2017a; Ayinla et al. 2017b). Maceral analysis by Ayinla et al. (2017b) indicates that the coals are dominated by huminites but contain subordinate abundances of liptinite and inertinite macerals.

3.2.1.2 Lamja Formation

The Lamja Formation is the youngest sedimentary unit and coal-bearing layer in the Yola Basin. The Formation consists of sandstones, mudstones, limestones, and thin coal interbeds deposited in a brackish-water environment (Edegbai et al., 2019a). The Lamja Formation coals are in the peak oil generation window and dominated by Type-III kerogen, suggesting potential for gas generation (Obaje et al., 2004b; Sarki Yandoka et al., 2015b).

3.2.2 Agwu Formation in Middle Benue Trough

The Agwu Formation coals occur in the Middle Benue Trough and a Turonian-Coniacian age has been assigned to the Formation (Akande et al., 20212). The Middle Benue Trough is underlain by the Precambrian to Lower Palaeozoic basement rocks and the Asu River Group, which consists of Uomba Arufu, and Awe Formations that unconformably overlies the basement rocks (Figure 3.7). The Asu River Group is overlain unconformably by Keana, Makurdi, and Agwu Formations. The Agwu Formation is unconformably overlain by the Lafia Formation (Ehinola et al., 2002; Akande et al., 2012 Adedosu et al., 2012). Ehinola et al. (2002) recognised six periods within the Middle Benue Trough sediments. The periods include Albian, Cenomanian, Turonian, Coniacian, Campanian-Maastrichtian and Paleocene. In contrast, Akande et al. (2012) categorized the sediments in the Lower and Middle parts of the Benue Trough into three unconformity-bounded cycles: Aptian/Albian-Cenomanian, Turonian-Coniacian, and Campanian-Maastrichtian.

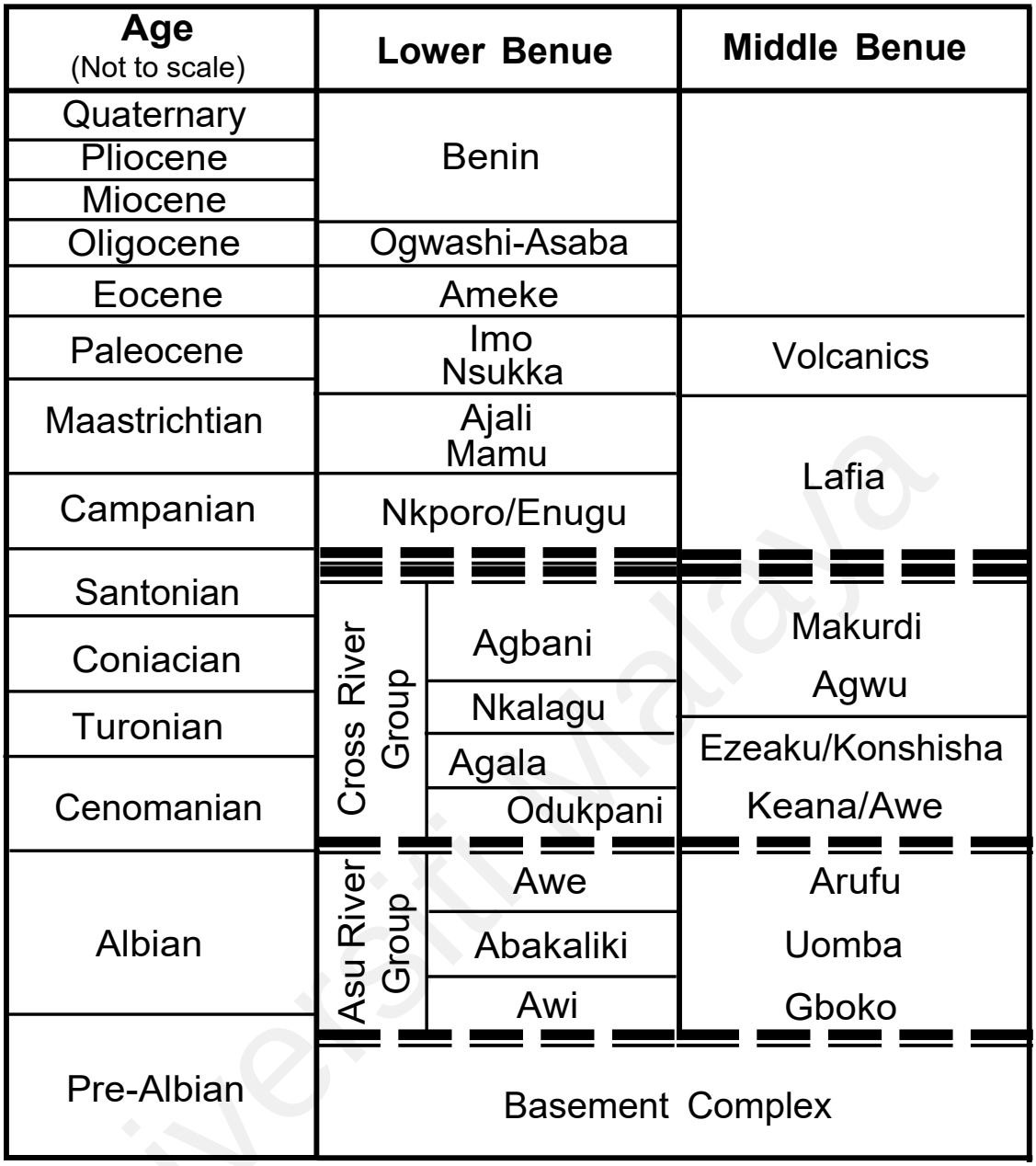

Figure 3.7: Stratigraphy of the Lower and Middle Benue Trough (modified after Petters & Ekweozor, 1982; Obaje et al., 2004b).

The Agwu Formation consists of shales, limestones, and sandstones interbedded with coal seams (Ehinola et al., 2002). Geochemical and isotopic studies of the Formation by Ehinola et al. (2002), Obaje et al. (2004b), and Adedosu et al. (2012) indicate high thermal maturity in the oil generation window range, a mixed terrestrial and marine organic matter input, and fluvial/deltaic depositional environment. However, recent review work by Edegbai et al. (2019a) reports a marine environment.

3.2.3 Mamu Formation in Lower Benue Trough

The Mamu Formation in the Anambra Basin, Lower Benue Trough is characterised by the intercalation of shale and sandstone facies with coal beds (Ogala et al., 2009; Akande et al., 2012). The Mamu Formation coals in the Basin outcrops mainly in Enugu, Okaba, and Orukpa areas. The Anambra Basin is bounded in the south by the Tertiary Niger Delta Basin. The Basin contains post-Santonian deformation sedimentary strata beginning with the marine Nkporo and Enugu Formations which are overlain by the deltaic Mamu Formation whilst the marginal marine Ajali Formation overlies the Mamu Formation (Figure 3.7). Source rock evaluation study by Akande et al. (2012) and Obaje et al. (2004b) concluded that the Sub-Bituminous Mamu Formation coals are immature to marginally mature for hydrocarbon generation but with the capacity to generate oil and gas at higher maturity.

CHAPTER 4: SAMPLES AND METHODS

4.1. Samples

A total of sixty coal samples comprising forty Tertiary Sarawak Basin coals and twenty Late Cretaceous Benue Trough coals were analysed for this study. The coals were collected from mine faces and outcrops and sufficient care was taken to avoid weathered outcrop samples. The sample identification as well as their age and location are provided in Table 4.1.

Table 4.1: List of analysed samples

S/N	Sample	Basin	Location/Coalfield	Formation	Age
1	B01-1*	Sarawak	Balingian	Liang	Pliocene
2	B01-4	Sarawak	Balingian	Liang	Pliocene
3	B01-5	Sarawak	Balingian	Liang	Pliocene
4	B02-4	Sarawak	Balingian	Liang	Pliocene
5	B03-2*	Sarawak	Balingian	Liang	Pliocene
6	B03-3	Sarawak	Balingian	Liang	Pliocene
7	B03-6*	Sarawak	Balingian	Liang	Pliocene
8	E55-2*	Sarawak	Balingian	Liang	Pliocene
9	L04A-1*	Sarawak	Balingian	Liang	Pliocene
10	L04B-1	Sarawak	Balingian	Liang	Pliocene
11	ML46A-6	Sarawak	Balingian	Liang	Pliocene
12	ML46A-7*	Sarawak	Balingian	Liang	Pliocene
13	BG1*	Sarawak	Balingian	Liang	Pliocene
14	BG2*	Sarawak	Balingian	Liang	Pliocene
15	0464A*	Sarawak	Mukah	Balingian	Miocene
16	M03-2*	Sarawak	Mukah	Balingian	Miocene
17	MK1*	Sarawak	Mukah	Balingian	Miocene
18	MK2*	Sarawak	Mukah	Balingian	Miocene
19	MK3A*	Sarawak	Mukah	Balingian	Miocene
20	MK3B	Sarawak	Mukah	Balingian	Miocene
21	MP1L*	Sarawak	Merit-Pila	Nyalau	Miocene
22	MP1M*	Sarawak	Merit-Pila	Nyalau	Miocene
23	MP1U*	Sarawak	Merit-Pila	Nyalau	Miocene
24	MP2L*	Sarawak	Merit-Pila	Nyalau	Miocene
25	MP2U*	Sarawak	Merit-Pila	Nyalau	Miocene
26	MP3L	Sarawak	Merit-Pila	Nyalau	Miocene

*selected for principal component analysis

Table 4.1, continued.

S/N	Sample	Basin	Location/Coalfield	Formation	Age
27	MP3M*	Sarawak	Merit-Pila	Nyalau	Miocene
28	MP3U	Sarawak	Merit-Pila	Nyalau	Miocene
29	MP4L*	Sarawak	Merit-Pila	Nyalau	Miocene
30	MP4M	Sarawak	Merit-Pila	Nyalau	Miocene
31	MP4U*	Sarawak	Merit-Pila	Nyalau	Miocene
32	MP5L	Sarawak	Merit-Pila	Nyalau	Miocene
33	MP5M*	Sarawak	Merit-Pila	Nyalau	Miocene
34	MP5U	Sarawak	Merit-Pila	Nyalau	Miocene
35	MP6L*	Sarawak	Merit-Pila	Nyalau	Miocene
36	MP6M*	Sarawak	Merit-Pila	Nyalau	Miocene
37	MP6U	Sarawak	Merit-Pila	Nyalau	Miocene
38	MP7L*	Sarawak	Merit-Pila	Nyalau	Miocene
39	MP7M	Sarawak	Merit-Pila	Nyalau	Miocene
40	MP7U	Sarawak	Merit-Pila	Nyalau	Miocene
41	MGL3A	Benue Trough	Maiganga	Gombe	Late Cretaceous
42	MGL4A*	Benue Trough	Maiganga	Gombe	Late Cretaceous
43	MGL1C*	Benue Trough	Maiganga	Gombe	Late Cretaceous
44	MGL2A	Benue Trough	Maiganga	Gombe	Late Cretaceous
45	MGL2B*	Benue Trough	Maiganga	Gombe	Late Cretaceous
46	MGL2H	Benue Trough	Maiganga	Gombe	Late Cretaceous
47	MGL2I*	Benue Trough	Maiganga	Gombe	Late Cretaceous
48	MGL2O*	Benue Trough	Maiganga	Gombe	Late Cretaceous
49	MGL2P	Benue Trough	Maiganga	Gombe	Late Cretaceous
50	MGL2T*	Benue Trough	Maiganga	Gombe	Late Cretaceous
51	AFZ*	Benue Trough	Afuze	Mamu	Late Cretaceous
52	ENG*	Benue Trough	Enugu	Mamu	Late Cretaceous
53	IMG*	Benue Trough	Imeagba	Mamu	Late Cretaceous
54	OGB*	Benue Trough	Ogboligbo	Mamu	Late Cretaceous
55	OKB*	Benue Trough	Okaba	Mamu	Late Cretaceous
56	WKP*	Benue Trough	Owukpa	Mamu	Late Cretaceous
57	CKL*	Benue Trough	Chikila	Lamja	Late Cretaceous
58	LMZ1*	Benue Trough	Lamza	Lamja	Late Cretaceous
59	LFO*	Benue Trough	Lafia-Obi	Agwu	Late Cretaceous
60	SKJ*	Benue Trough	Shankodi-Jangwa	Agwu	Late Cretaceous

4.2 Sample Preparation

The coal samples were brushed to remove surface dirt and thereafter separated into three portions where possible. The first portion, about 60-100 g of each sample, was ground to powder (< 150 µm) using a rotary mill at the Geology Department of the University of Malaya. The second portion about 10-20 g of each sample was crushed into fragments (~ 2 mm), while the third portion was stored in a cool and dry environment.

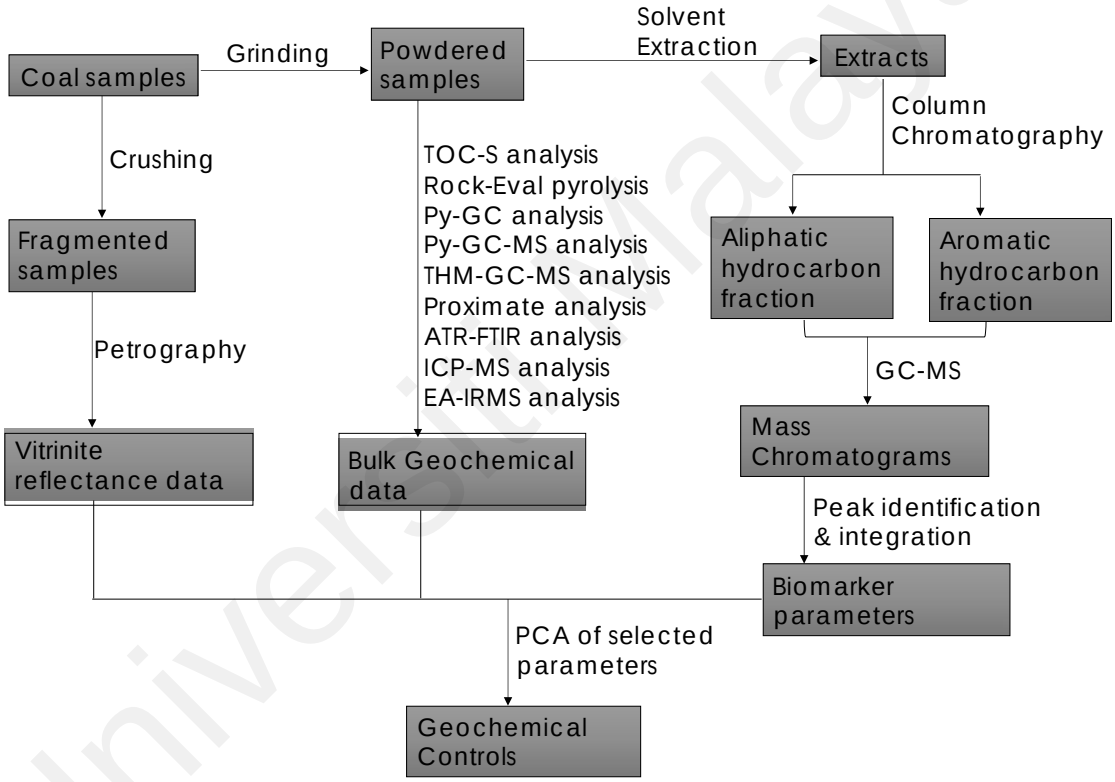

Figure 4.1: A schematic of employed analytical techniques. Abbreviations are defined in Table 4.2

Table 4.2: Partial list of utilized analytical techniques.

Abbreviation	Definition
TOC-S	Total organic carbon and sulfur
Py-GC	Pyrolysis-gas chromatography
GC-MS	Gas chromatography-mass spectrometry
Py-GC-MS	Pyrolysis-gas chromatography mass spectrometry
THM-GC-MS	Thermally assisted hydrolysis and methylation-gas chromatography mass spectrometry
EA-IRMS	Elemental analysis-isotope ratio mass spectrometry
ATR-FTIR	Attenuated total reflection-Fourier transform infrared spectroscopy
ICP-MS	Inductively coupled plasma mass spectrometry
PCA	Principal component analysis

4.3 Vitrinite Reflectance Analysis

The coal samples were crushed into fragments (~ 2 mm), mounted in epoxy resin mixed with hardener (methyl ethyl ketone peroxide), and allowed to harden overnight. The hardened coal blocks were thereafter grinded on a wet diamond lap to produce a flat surface. The coal blocks were subsequently polished using silicon carbide papers (grades 320, 800, and 1200), and colloidal alumina suspension.

The vitrinite reflectance (%Ro) of the samples was measured on a LEICA CTR 6000 Orthoplan microscope using x50 oil immersion objectives with a refractive index of 1.518 at 23 °C. The measurements were carried out under reflected white light and calibrated using a sapphire glass standard with a refractive value of 0.589%. Huminite/vitrinite reflectance values were determined in random mode on ulminite maceral at a wavelength of 546 nm and the mean values were calculated after 100 measurements.

4.4 Total Organic Carbon and Sulfur Analysis

Prior to total organic carbon (TOC) and total sulfur (S_T) content determination, the powdered coal samples were treated with sufficient 4M hydrochloric acid to remove carbonates, rinsed with deionized water to remove residual acid, oven-dried at temperature of 65 °C, and subsequently analysed using a Leco CS832 Carbon - Sulfur analyser at organic geochemistry laboratory of the Department of Geology, University of Malaya, Kuala-Lumpur, Malaysia.

4.5 Attenuated Total Reflection-Fourier Transform Infrared Spectroscopy

Attenuated Total Reflection-Fourier Transform Infrared Spectroscopy (ATR-FTIR) analysis, which is a commonly used non-destructive technique to determine the distribution of functional groups in coal samples (Ganz & Kalkreuth, 1991; Mastalerz et al., 2013), was performed on a PerkinElmer Spotlight 300 FT-IR microscope system at the organic geochemistry laboratory of the Department of Geology, University of Malaya, Kuala-Lumpur, Malaysia. 5 mg of the powdered samples were placed on the Diamond/ZnSe crystal plate of the PerkinElmer Universal ATR accessory unit. The infrared spectra were measured in both transmittance and absorbance modes at 4000 cm^{-1} to 650 cm^{-1} wavelength frequency and the peaks were assigned based on published spectra (Ganz & Kalkreuth, 1987; Ganz & Kalkreuth, 1991; Mastalerz et al., 2013; Wang et al., 2013; Patricia et al., 2020).

4.6 Pyrolysis-Gas Chromatography

Pyrolysis-gas chromatography (Py-GC) analysis was carried out on all the coal samples to determine their petroleum-generating potential, the probable composition of generated hydrocarbons, and kerogen type. 4 mg of each sample was pyrolyzed using a double-shot Frontier Lab Pyrolyzer (PY-2020iD) connected to an Agilent Technologies 5975 gas chromatograph fitted with an ultra-alloy capillary column (30 m x 0.32 mm I.D. x 0.25 μm) and flame ionisation detector (FID). The open system pyrolysis was programmed to start at 330 ℃, increased to 600 °C at the rate of 25 °C/min, and held for 3 minutes at 600 °C (Weiss et al., 2000). The pyrolysate corresponds to the Rock Eval's *S*2 peak. The major compounds and components of the chromatograms were identified by comparing their relative retention times with standard samples and published spectra (Horsfield, 1989; Wan Hasiah, 1999; Weiss et al., 2000; Sykes, 2004).

4.7 Rock-Eval Pyrolysis

Rock-Eval pyrolysis is a geochemical technique employed to estimate the petroleum potential of source rocks by heating under non-isothermal conditions (Behar et al., 2001). The coal samples were pyrolyzed using the Rock-Eval 6 equipment at Core Laboratories offices in Shah Alam, Selangor, Malaysia, and Houston, Texas, USA. About 10-20 mg of the powdered coal samples were initially heated at 300 °C for three minutes in an inert atmosphere to release the thermovapourised free hydrocarbons. The temperature was thereafter steadily increased to 650 °C at 25 °C/min to release accumulated hydrocarbons (Figure 4.2). For further detail on the instrumentation of the Rock-Eval 6, refer to Behar et al. (2001) and Carvajal-Ortiz & Gentzis (2015).

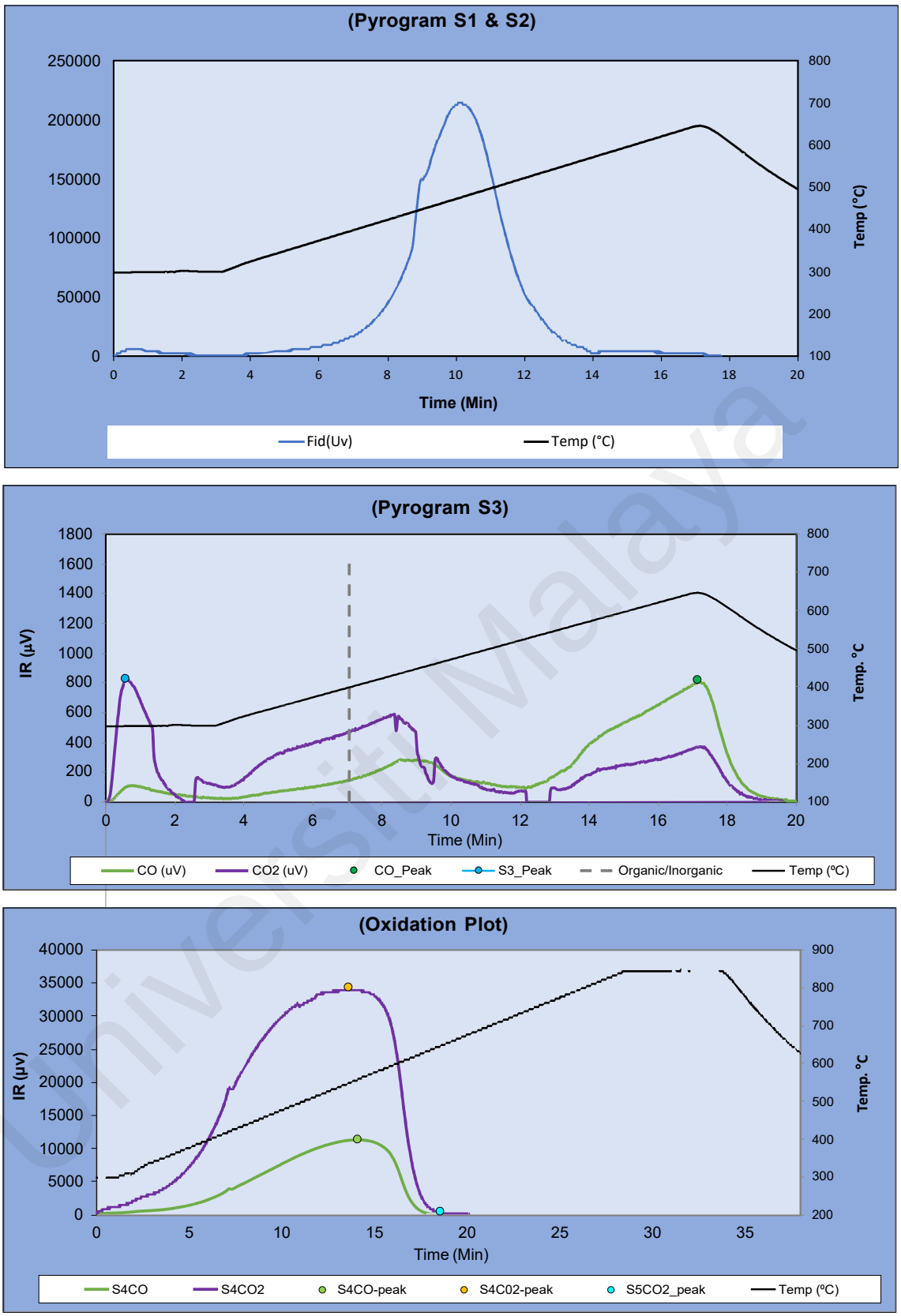

Figure 4.2: Rock-Eval pyrolysis temperature profile of a representative sample.

Geochemical data obtained by Rock-Eval pyrolysis includes: the amount of free hydrocarbons in the rocks (*S1*), amount of hydrocarbons generated from thermal cracking of sedimentary organic matter (*S2*), amount of organic CO_2 released during pyrolysis (*S3*) and the temperature at which maximum amount of hydrocarbons was produced during pyrolysis (T_{max}; Behar et al., 2001). Additionally, geochemical parameters calculated from Rock-Eval pyrolysis data include: genetic potential (GP), production index (PI), hydrogen index (HI), oxygen index (OI), bitumen index (BI), and quality index (QI). The parameters are defined in Table 4.3.

Table 4.3: Calculated Rock-Eval parameters.

Parameter	Definition	Formula	Unit
Production index (PI)	Indicates level of thermal evolution of organic matter	$\frac{S1}{S1+S2}$	
Bitumen index (BI)	Amount of free hydrocarbon relative to organic carbon	$\frac{S1 \text{ x } 100}{\text{TOC}}$	mg HC/g TOC
Hydrogen index (HI)	Relative amount of hydrogen to organic carbon	$\frac{S2 \text{ x } 100}{\text{TOC}}$	mg HC/g TOC
Oxygen index (OI)	Relative amount of oxygen to organic carbon	$\frac{S3 \text{ x } 100}{\text{TOC}}$	mg CO_2/g TOC
Genetic potential (GP)	Amount of free and generated hydrocarbons	$S1+S2$	mg HC/g rock
Quality index (QI)	Total genetic potential per unit of organic carbon	$\frac{(S1+S2) \text{ x } 100}{\text{TOC}}$	mg HC/g TOC

TOC: total organic carbon

4.8 Proximate Analysis

Proximate analysis was carried out on the studied coals to determine their moisture, volatile matter, fixed carbon, and ash contents using a PerkinElmer Diamond Thermogravimetric/Differential Thermal Analyzer (TG/DTA) at the organic geochemistry laboratory of the Department of Geology, University of Malaya, Kuala-Lumpur, Malaysia. 5-10 mg of the coal samples were heated to 900 °C in presence of

nitrogen. The analytical procedure is described by Donahue & Rais (2009). The temperature was programmed to start at 25 °C, increased to 110 °C at the rate of 85 °C/min, and then held at 110 °C for 6 min. Successively, the temperature was increased from 110 °C to 900 °C at the rate of 80 °C/min and then held for 5 min at 900 °C. Following Donahue & Rais (2009), the instrument software was employed to determine the percentages of moisture, volatile matter and fixed carbon whilst the ash content was obtained by subtracting the sum percentages of moisture, volatile matter, and fixed carbon from 100 percent.

4.9 Inductively Coupled Plasma Mass Spectrometry

Thirty-five coal samples were analysed for major and trace element concentrations at the Mineral Laboratories of Bureau Veritas (AcmeLabs), Vancouver, Canada. For trace element analysis, 0.5g of the powdered samples were digested with a modified aqua regia mixture of HCl, HNO_3, and H_2O (1:1:1 v/v/v) and thereafter analysed for 37 elements using inductively coupled plasma mass spectrometry (ICP-MS). To measure the abundances of major element oxides, 5g of the pulverized samples were dissolved with the lithium borate fusion technique and subsequently investigated with ICP-MS analysis. Analysis of reference materials (DS11 and OREAS262) and duplicate samples were carried out to ensure optimal working conditions and accurate results.

4.10 Bitumen Extraction and Hydrocarbon Fractionation

About 8-10 g of each powdered sample was extracted with 250 ml of an azeotropic mixture of dichloromethane (DCM) and methanol (93:7, v/v) in a Soxhlet apparatus for

a minimum of 72 hours or until the solvent became colourless. Activated copper and anti-bumping granules were however added to the azeotropic mixture before extraction to remove elemental sulfur and prevent violent releases of vapour, respectively. The extracts were rotatory evaporated to about 1 ml and consequently decanted into clean weighed vials. The total extractable organic matter (EOM) concentrations of the coal samples were determined via gravimetric measurements.

Liquid column chromatography was thereafter used to separate aliquots of the coal extracts into aliphatic, aromatic, and polar fractions by using solvents of increasing polarity; petroleum ether (100 mL), DCM (100 mL), and methanol (50 mL), respectively. The ca. 10 m column was made with a slurry of silica in petroleum ether. About 70 to 100 mg of the coal extracts were added to alumina and then subsequently introduced into the column. The three fractions were evaporated under reduced pressure on the rotatory evaporator and with a stream of nitrogen gas to remove excess solvent until constant weights were obtained. Fractions of aliphatic and aromatic hydrocarbons were thereafter concentrated with DCM for gas chromatography-mass spectrometry (GC-MS) analysis.

4.11 Gas Chromatography Mass Spectrometry

The aliphatic and aromatic hydrocarbons were analysed using an Agilent 5890 gas chromatograph coupled to an Agilent 5975B mass selective detector set at electron ionisation energy of 70 eV, 100 mA filament emission current, and 230 °C source temperature. The gas chromatograph (GC) was equipped with flexible silica capillary columns (30 m x 0.32 mm I.D. x 0.25 µm) using helium as carrier gas. The GC temperature, which was programmed to start at 40 ℃, increased to 310 °C at the rate of 4 °C/min and was then held at 310 °C for 30 min. For aliphatic biomarker analysis, mass

chromatograms for *n*-alkanes and isoprenoids (*m/z* 85) and terpenoids (*m/z* 123 and *m/z* 191) were recorded. Aromatic biomarker data were acquired via mass chromatograms for phenanthrene and anthracene (*m/z* 178), methylphenanthrenes (*m/z* 192), dimethylphenanthrenes (*m/z* 206), fluorene (*m/z* 166), methylfluorenes (m/z 180), dibenzofuran (*m/z* 168), methyldibenzofurans (*m/z* 182), naphthalene (*m/z* 128), methylnaphthalenes (*m/z* 142), dimethylnaphthalenes (*m/z* 156), trimethylnaphthalenes (*m/z* 170), tetramethylnaphthalenes and dibenzothiophene (*m/z* 184), methyldibenzothiophenes (*m/z* 198), cadalene (*m/z* 183), 6-*iso*propyl-1-*iso*hexyl-2-methylnaphthalene (*ip*-iHMN; m/z 197), and retene (*m/z* 219). Compounds in mass chromatograms were identified by comparing their relative retention times with Norwegian geochemical standard (NGS) samples and published mass spectra (Noble et al., 1986; Weston et al., 1989; Killops et al., 1995; van Aarssen et al., 1999, 2000; Radke et al., 2000; Weiss et al., 2000; Ahmed et al., 2009; Nakamura et al., 2010; Romero-Sarmiento et al., 2011; Marynowski et al., 2013; Stojanović & Životić, 2013; Escobar et al., 2016; Jiang & George, 2018; Jiang & George 2019; Cesar & Grice, 2019; Yan et al., 2019; Zakrzewski et al., 2020).

4.12 Thermochemolysis- and Pyrolysis-Gas Chromatography Mass Spectrometry

Thermochemolysis, or thermally assisted hydrolysis and methylation (THM) is an analytical technique that combines pyrolysis and derivatization in presence of derivatizing agents such as tetramethylammonium hydroxide (TMAH), producing less polar and lower molecular weight compounds more suitable for GC-MS analysis. The THM-GC-MS analysis of coals reportedly yields *n*-alkanes, *n*-alkenes, alkenes, fatty acid methyl esters (FAMEs), and polycyclic aromatic compounds (PAHs). A comparative study by Kaal et al. (2017) established that Py-GC-MS and THM-GC-MS techniques

provide an improved understanding of the chemistry of resin-derived materials and about polymethylene compounds, respectively. Challinor (2001) and He et al. (2020) summarizes the historical applications of THM-GC-MS analysis and its complementarity with other analytical techniques such as Py-GC-MS.

1-2 mg of fifteen powdered coals samples were introduced, with the aid of quartz wool, into quartz tubes and analysed using a CDS Analytical Pyroprobe AS5250 instrument. The temperature of the Pyroprobe was set at 325 °C and increased to 750 °C at 10 °C ms^{-1}. For THM-GC-MS analysis, aliquots of 25% aqueous TMAH were added to the coal samples in the quartz tubes and thereafter allowed to react for a minimum of 30 min before pyrolysis. For both Py-GC-MS and THM-GC-MS, the pyrolysates were moved under helium flow into an Agilent 6890 GC instrument in 1:50 split mode and equipped with a non-polar HP-5MS capillary column (30 m x 0.25 mm I.D. x 0.25 μm). The separated compounds were thereafter detected by the connected Agilent 5977 mass spectrometer. The operating conditions and procedures for Py-GC-MS and THM-GC-MS analyses are further described in detail by Kaal et al. (2017).

Similarly, compounds were identified by comparing their retention times and mass fragments with published literature and the NIST 05 library. The identified compounds were semi-quantified based on the relative proportions of the peak areas of dominant and characteristic m/z fragments. For both Py-GC-MS and THM-GC-MS analytical techniques, the relative proportions of identified compounds are expressed as a percentage of the total quantified peak area (TQPA).

4.13 Elemental Analyser Isotope Ratio Mass Spectrometry

The elemental analyser isotope ratio mass spectrometry (EA-IRMS) analysis was carried out on a flash Elemental Analyzer linked to a Sercon Geo 20-20 continuous flow mass spectrometer. Before analysis, the samples were oven-dried and thereafter stored in a desiccator. The dried samples were finally weighed and wrapped in tin capsules. The reference material, pure Graphite, with a carbon isotopic ($\delta^{13}C$) value of -15.99‰ on the Vienna Pee Dee Belemnite (VPDB) scale, was used to calibrate the system. The carbon isotopic ratios were measured in triplicates and the average $\delta^{13}C$ values were reported. For hydrogen isotope measurements, the samples were analysed in duplicates and the mean hydrogen isotopic (δD) values were recorded. A reference standard material, polyethylene with a δD value of 100.30‰, was used to calibrate the system. All bulk isotopic measurements were carried out at the Department of Chemistry, Malaysia. The standard deviation of replicate measurements is < 0.3‰ and ± 2‰ for $\delta^{13}C$ and δD values, respectively.

4.14 Statistical Analysis

Statistical analysis was carried out to identify the strength of relationships between geochemical parameters and to also identify the principal components. The analyses were performed on JASP 0.16 for macOS. For linear correlation analysis, Pearson's correlation coefficient was employed. Coefficients (r) > ± 0.7, ± 0.5 to 0.7, ± 0.3 to 0.5, and < ± 0.3 are accordingly regarded as strong, moderate, weak, and very weak correlations.

The above-listed geochemical analyses were not carried out on all sixty coal samples. Hence, forty-one samples were selected for principal component analysis (PCA). The selected samples are asterisked in Table 3.1. The number of components was auto-derived

based on the distribution of components, and up to six principal components were obtained for each PCA run. In addition, the rotation method applied was Promax, an oblique rotation method that allows factors to be correlated.

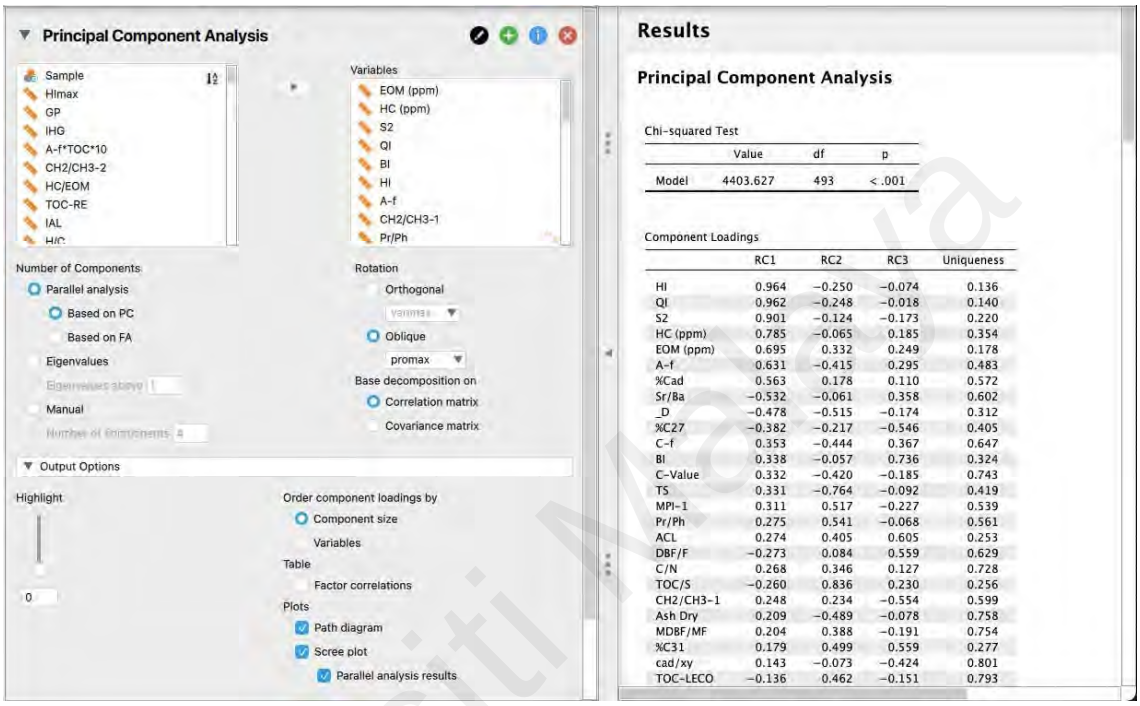

Figure 4.3: Screenshot of JASP software showing input features and outputs of the principal component analysis.

CHAPTER 5: RESULTS AND INTERPRETATIONS

5.1 Coal Rank and Chemical Properties

5.1.1 Proximate Analysis

The result of the proximate analysis, which indicates the moisture, fixed carbon, ash, and volatile matter contents of the studied Sarawak Basin and Benue Trough coals, is given in Table 5.1 and the average values for both groups of coals are compared in Figure 5.1.

The total moisture content (as received) of the Sarawak Basin coals varies widely between 3.3 and 42.3 wt.% with an average value of 15.0 wt.%. In contrast, the moisture content of the Benue Trough coals is relatively higher, varying widely from 2.3 to 60.2 wt.% with an average value of 21.0 wt%. Within the Sarawak Basin coals, the moisture content is relatively higher for the Liang Formation (avg. 22.4 wt.%) coals than for the Balingian Formation (avg. 7.0 wt.%) and Nyalau Formation (avg. 12.2 wt.%) coals whilst the Gombe Formation coals have the highest the moisture content (avg. 27.1 wt.%) of the Benue Trough coals (Table 5.1).

The ash content (on dry-basis) of the studied samples ranges widely in both groups of coals, varying from 0.8 to 37.5 (avg. 9.5 wt.%) and 6.3 to 34.9 (avg. 16.3 wt.%) in the Sarawak Basin and Benue Trough coals, respectively. The average ash content of the coals indicates generally low mineral matter content in the Sarawak Basin coals and low to medium mineral matter content in the Benue Trough coals. Correlation analysis of proximate and vitrinite reflectance data for all the studied coals indicates that the ash content moderately correlates (-0.619) with volatile matter content and strongly correlates (-0.780) with fixed carbon content (Table 5.2).

Table 5.1: Vitrinite Reflectance (R_o), Total organic carbon (TOC) and total sulfur (S_T) content and proximate analysis data of the studied Cenozoic Sarawak Basin and Upper Cretaceous Benue Trough coals.

Sample	Basin/ Formation	R_o (%)	S_T (%)	TOC (%)	TOC/ S_T	M_{ad}	A_d	V_d	C_d
B01-1	Sarawak/ Liang	0.30	0.29	61.0	210	7.9	6.3	54.2	39.5
B01-4		0.29	0.16	61.6	385	17.6	6.4	45.3	48.3
B01-5		0.32	0.17	60.3	355	12.2	6.9	44.2	48.9
B02-4		0.32	0.46	62.8	137	21.2	4.3	42.1	53.6
B03-2		0.30	0.17	61.4	361	21.0	5.0	49.7	45.2
B03-3		0.27	0.15	63.9	426	42.3	6.1	53.7	40.2
B03-6		0.28	0.13	61.5	473	25.3	14.9	46.1	39.0
E55-2		0.34	0.23	62.4	271	20.4	8.4	46.1	45.5
L04A-1		0.31	1.48	53.1	36	15.9	19.3	42.1	38.6
L04B-1		0.32	1.18	58.6	50	40.4	11.1	43.8	45.1
ML46A-6		0.36	0.18	61.0	339	40.0	5.5	49.5	45.0
ML46A-7		0.34	0.58	60.8	105	31.1	5.1	47.3	47.6
BG1		0.36	0.23	65.0	283	7.9	1.0	52.0	47.0
BG2		0.35	0.13	61.4	472	10.2	1.7	47.2	51.2
046A	Sarawak/ Balingian	0.40	0.85	65.2	77	-	-	-	-
M03-2		0.38	0.20	46.9	235	3.3	37.5	33.3	29.2
MK1		0.39	0.31	52.1	168	5.4	22.5	37.6	39.8
MK2		0.38	0.27	66.3	246	5.4	5.8	43.9	50.3
MK3A		0.39	0.34	68.0	200	4.1	0.8	46.5	52.8
MK3B		0.41	0.36	65.1	181	-	-	-	-
MP1L	Sarawak/ Nyalau	0.42	0.17	80.4	473	16.2	6.3	45.1	48.6
MP1M		0.41	0.12	66.0	550	14.4	0.9	48.1	51.0
MP1U		0.39	0.20	62.3	312	18.1	4.0	45.6	50.5
MP2L		0.39	0.15	66.5	443	13.3	6.6	52.0	41.4
MP2U		0.37	0.20	65.6	328	13.4	6.6	52.0	41.4
MP3L		0.40	0.21	67.3	320	10.6	27.3	43.4	29.3
MP3M		0.38	0.22	51.6	235	9.4	16.0	54.0	30.1
MP3U		0.41	0.21	62.0	295	10.3	23.9	42.6	33.5
MP4L		0.40	0.22	56.7	258	12.3	5.9	51.9	42.2
MP4M		0.38	0.30	63.3	211	10.3	14.5	46.2	39.3
MP4U		0.38	0.12	61.7	514	12.1	9.4	49.4	41.3
MP5L		0.37	0.27	61.4	228	13.9	9.4	48.6	42.1
MP5M		0.36	0.22	61.9	281	5.7	15.1	47.6	37.3
MP5U		0.41	0.19	67.8	357	13.8	8.7	48.1	43.2
MP6L		0.40	0.21	63.2	301	13.5	6.0	48.8	45.1
MP6M		0.43	0.17	63.2	372	13.4	4.9	46.0	49.1
MP6U		0.41	0.20	61.5	314	14.1	9.8	50.8	39.3
MP7L		0.39	0.12	66.7	556	7.7	4.7	51.1	44.3
MP7M		0.39	0.09	63.1	701	11.2	3.8	50.2	45.9
MP7U		0.37	0.23	65.1	283	10.6	8.5	47.1	44.4

Table 5.1, continued.

Sample	Basin/ Formation	R_o (%)	S_T (%)	TOC (%)	TOC/ S_T	M_{ad}	A_d	V_d	C_d
MGL3A	Benue Trough/ Gombe	0.35	0.53	67.8	128	9.6	16.7	35.2	48.1
MGL4A		0.36	0.34	71.8	211	19.4	11.0	32.9	56.0
MGL1C		0.32	0.90	65.6	73	60.2	12.6	53.6	33.8
MGL2A		0.35	0.43	67.3	157	25.4	11.0	44.4	44.5
MGL2B		0.28	0.32	67.0	209	25.9	13.3	44.8	41.9
MGL2H		0.33	0.51	65.2	128	36.9	7.7	47.4	44.9
MGL2I		0.32	0.29	64.8	223	19.7	15.4	40.6	43.9
MGL2O		0.30	0.46	60.6	132	19.7	14.5	42.7	42.8
MGL2P		0.35	0.42	52.7	125	27.3	34.2	39.5	26.3
MGL2T		0.32	0.55	50.2	91	26.7	34.9	42.3	22.8
AFZ	Benue Trough/ Mamu	-	1.29	78.7	61	-	-	-	-
ENG		0.36	1.36	56.7	42	7.3	9.8	44.6	45.6
IMG		0.43	2.50	25.3	10	-	-	-	-
OGB		-	2.48	34.7	14	-	-	-	-
OKB		0.32	2.20	59.6	27	7.6	10.5	44.2	45.3
WKP		-	0.52	69.0	133	-	-	-	-
CKL	Benue Trough/ Lamja	0.57	0.58	58.7	101	2.3	29.5	29.4	41.0
LMZ1		0.61	0.60	63.7	106	-	-	-	-
LFO	Benue Trough/ Agwu	0.33	1.94	68.6	35	6.5	6.3	53.5	40.2
SKJ		-	2.21	72.8	33	-	-	-	-

M_{ad}: moisture, as received (% wt.); A_d: ash, dried basis (% wt); V_d: volatile matter, dried basis (% wt); C_d: fixed carbon, dried basis (% wt).

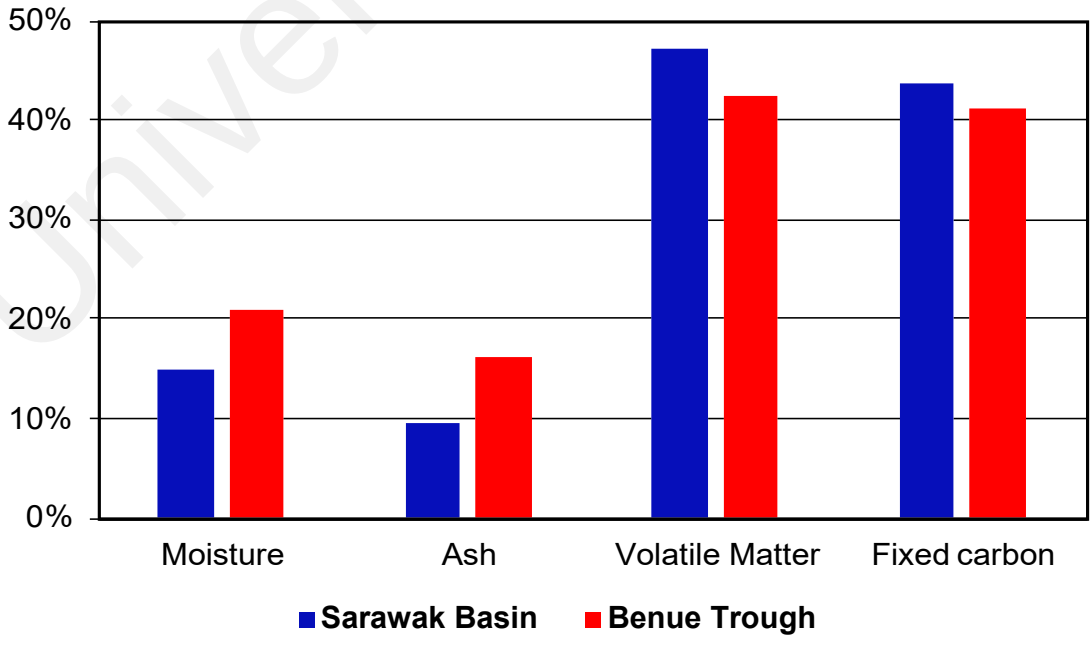

Figure 5.1: The average content of moisture, ash, volatile matter, and carbon in the studied coals

Table 5.2: Correlation coefficients of vitrinite reflectance, and proximate analysis data

Variable	R_o	M_{ad}	A_d	V_d	C_d
R_o	1.000				
M_{ad}	-0.482	1.000			
A_d	0.130	-0.045	1.000		
V_d	-0.216	0.179	-0.619	1.000	
C_d	-0.063	-0.111	-0.780	0.012	1.000

R_o: vitrinite reflectance; M_{ad}: moisture, as received; A_d: ash, dried basis; V_d: volatile matter, dried basis; C_d: fixed carbon, dried basis.

Volatile matter in coals consists of methane, carbon monoxide and other incombustible gases. Therefore, the volatile matter content is a measure of the gaseous fuels present in coals and high values indicate rapid ignition. Measured values of volatile matter (dried basis) are similar for both groups of coals, varying from 33.3 to 54.2 (avg. 47.3 wt.%) and 29.4 to 53.6 (42.5 wt.%) in the Sarawak Basin and Benue Trough coals, respectively (Table 5.1). The fixed carbon content is an imprecise estimate of coal's heating value. The fixed carbon content varies from 29.2 to 53.6 wt.% and 22.8 to 56.0 wt.% with average values of 43.7 wt.% and 41.2 wt.% for the Sarawak Basin and Benue Trough coals, respectively. The slightly higher average volatile matter and fixed carbon contents for the Sarawak Basin coals suggest better combustion properties than the Benue Trough coals.

5.1.2 Huminite/Vitrinite Reflectance

Huminite/vitrinite reflectance in coals reflect its level of coalification. The measured reflectance values of the coal samples are recorded in Table 5.1 and Appendix A. The Benue Trough (0.28-0.61%) coals have relatively higher $\%R_o$ values than the Sarawak Basin (0.27-0.43%) coals (Figure 5.2). According to the ASTM standard classification of coals by rank, the reflectance values show the Sarawak Basin coals are Lignite to

sub-bituminous B while the Benue Trough coals are Lignite to high volatile bituminous C (Orem & Finkelman, 2003).

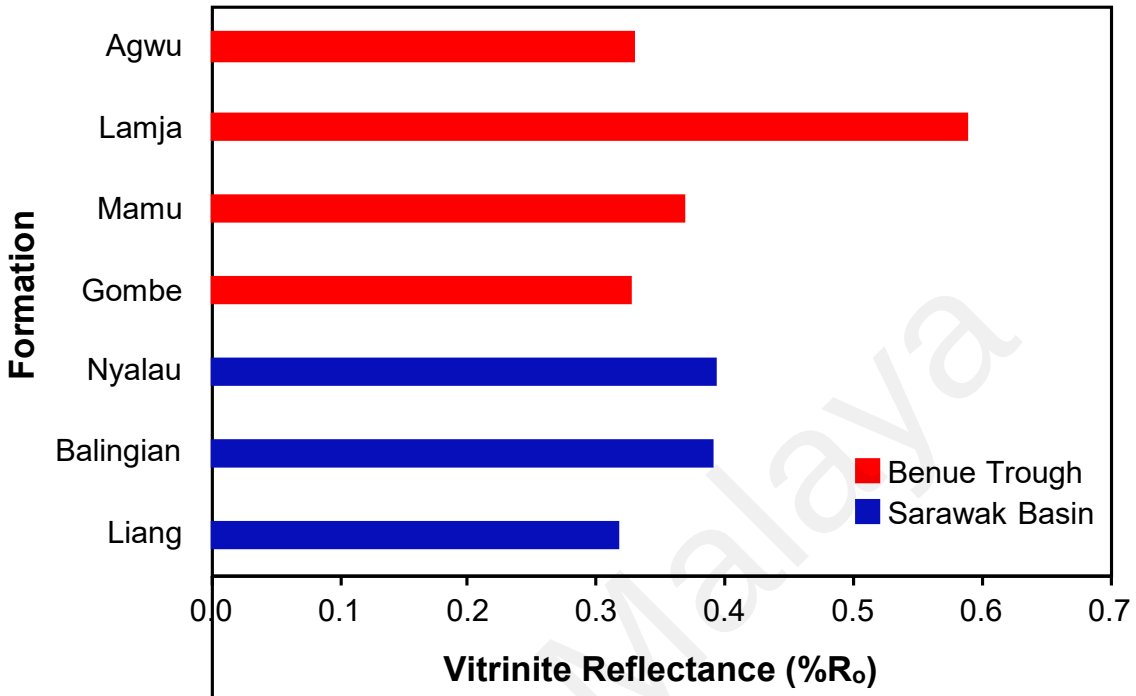

Figure 5.2: Bar plot of the average vitrinite reflectance value of analysed coal formations.

5.2 Total Organic Matter (TOC) and Total Sulfur (S_T) contents

The total organic matter (TOC) content of sedimentary rocks is a measure of organic richness (Peters & Cassa, 1994). TOC values for the analysed Sarawak Basin coals range between 46.9 and 80.4 wt.% with an average value of 62.4 wt.%. Similarly, the TOC values for the Benue Trough coals range between 25.3 and 78.7 wt.% with aan average value of 61.0 wt.%. Generally, the TOC values show that the Sarawak Basin coals are marginally richer than the Benue Trough coals. Within the Sarawak Basin, TOC values are generally slightly higher for the Nyalau Formation (avg. 63.9 wt.%) than for the Liang Formation (avg. 61.1 wt.%) and Balingian Formation (avg. 60.6 wt.%) coals.

Measured total sulfur (S_T) values range between 0.09 and 1.48% and 0.29 and 2.50%, respectively, for the Sarawak Basin and Benue Trough coals. TOC and S_T values are plotted in Figure 5.3, showing mostly low (< 0.5%) S_T values for Sarawak Basin coals that are typical for coals, in which the precursor peat was deposited in a freshwater environment (Chou 2012). The relatively higher (avg. 1.02%) S_T values recorded for the Benue Trough coals could possibly signify marine influence during/after the accumulation of the precursor peat in the Late Cretaceous (Sykes et al., 2014). The TOC/S_T ratio is a proxy for paleoredox conditions and higher values indicate oxidizing conditions (Algeo & Liu, 2020). Ratios for coals are quite higher for the Sarawak Basin coals (avg. 308) than the Benue Trough coals (avg. 102), which signifies relatively less oxidizing depositional conditions for the Benue Trough coals.

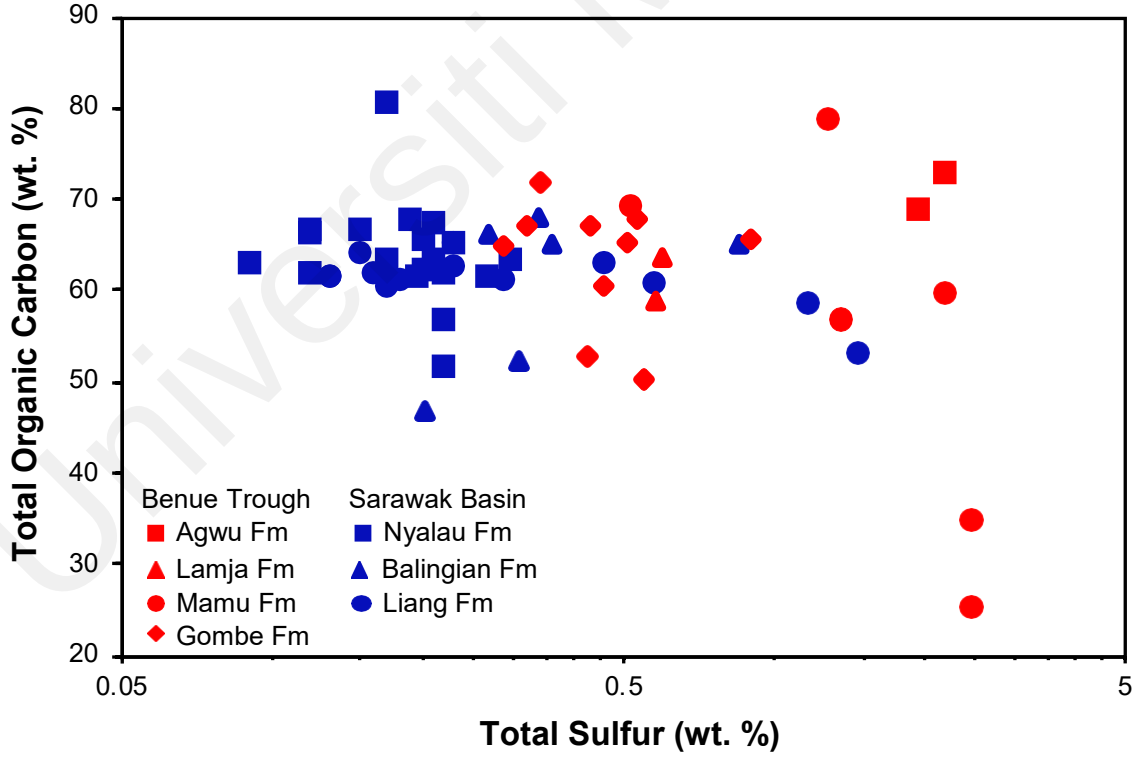

Figure 5.3: Cross-plot of total sulfur and total organic carbon contents for the studied coals.

5.3 Rock-Eval Pyrolysis

Bulk organic parameters obtained from the Rock-Eval pyrolysis of the Sarawak Basin and Benue Trough coals are given in Tables 5.3 and 5.4, respectively. The quality of the organic matter as shown by the TOC values is marginally higher in the Benue Trough coals with values between 23.0 and 74.5 (avg. 59.1 wt.%) than in the Sarawak Basin coals with values varying from 27.0 to 63.1 (avg. 54.7 wt.%). The TOC values by the Rock-Eval 6 equipment are mostly slightly lower than the values measured by Leco CS832, particularly for the Sarawak Basin coals (Figure 5.4). Nevertheless, the Rock-Eval 6 TOC values were used for calculating the other Rock-Eval parameters.

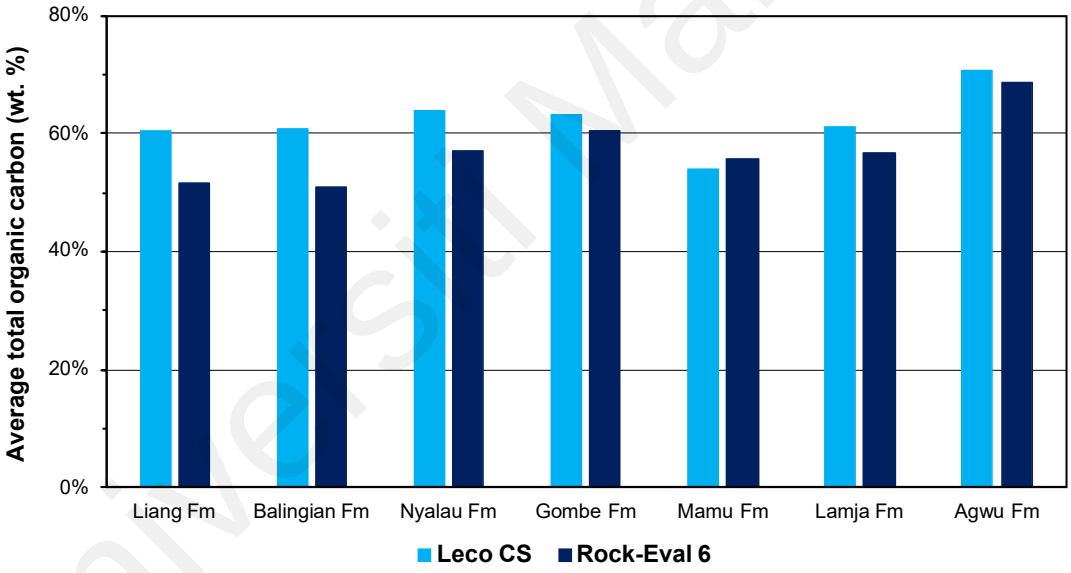

Figure 5.4: Average total organic carbon (TOC) values obtained from Leco CS832 and Rock-Eval 6 equipment for the studied coal formations.

The quantity of free hydrocarbons in the coals, as indicated by *S1* values, varies between 0.9 to 18.7 (avg. 4.7 mg HC/g rock) in the Sarawak coals and is considerably higher than in the Benue Trough coals with values ranging from 1.3 to 7.6 (avg. 3.1 mg HC/g rock). Conversely, the potential hydrocarbon content (*S2*) is relatively higher in the Benue Trough coals with values in the 32.1 to 331.6 (avg. 136.7 mg HC/g rock)

range. The Sarawak Basin coals show lower *S2* values that vary between 37.0 and 259.2 (avg. 111.4 mg HC/g rock). Resultantly, the genetic potential (*S1* + *S2*) of the coals varies widely from 40.2 to 277.9 and 33.4. to 337.4 mg HC/g rock in the Sarawak Basin and Benue Trough coals, respectively. Furthermore, the hydrogen index (HI) range is generally similar with values varying broadly from 68 to 456 (avg. 202 mg HC/g TOC) and 50 to 445 (avg. 231 mg HC/g TOC) in the coals from Sarawak Basin and Benue Trough, respectively. The T_{max} values of the Benue Trough coals (avg. 424 °C) are higher than the values for the Sarawak Basin coals (avg. 411 °C). Additionally, production index (PI) values for all the studied coals are < 0.1, varying from 0.01 to 0.09 and thus indicative of generally low thermal maturity (Peters & Cassa, 1994).

Evaluation of the Sarawak Basin coals shows that TOC values generally increase from Liang Formation (avg. 51.5 wt.%) and Balingian Formation (avg. 50.9 wt.%) to Nyalau Formation (avg. 56.9 wt.%) coals. Similarly, S_2 values increase from Liang Formation (avg. 68.0 mgHC/g rock) to Balingian Formation (avg. 103.3 mgHC/g rock) and to Nyalau Formation (avg. 129.0 mgHC/g rock). Expectedly, the HI values are higher for the Nyalau Formation (avg. 226 mg HC/g TOC) than for the Liang Formation (avg. 131 mg HC/g TOC) and Balingian Formation (avg. 204 mg HC/g TOC) coals. The T_{max} values of the studied coals are similar and generally increase from Liang Formation (avg. 403 °C) to Nyalau Formation (avg. 412 °C) and to Balingian Formation (avg. 418 °C).

Table 5.3: Rock-Eval parameters of the studied Sarawak Basin coals.

Sample	Formation	T_{max} (°C)	TOC (wt. %)	*S1*	*S2*	GP	*S3*	BI	HI	HI'	QI	OI	PI	*S2*/ *S3*
				(mg HC/g rock)			(mg CO_2/g rock)		(mg HC/g TOC)			(mg CO_2/g TOC)		
E55-2	Liang	407	53.3	3.9	85.4	89.4	49.1	7.4	160	299	168	92	0.04	1.7
L04A-1	Liang	405	47.2	3.1	52.6	55.7	43.7	6.5	111	253	118	93	0.05	1.2
L04B-1	Liang	401	51.4	1.5	39.9	41.3	86.8	2.9	77	214	80	169	0.04	0.5
ML46A-6	Liang	401	53.4	3.5	87.9	91.4	54.4	6.5	165	276	171	102	0.04	1.6
ML46A-7	Liang	402	50.9	4.8	76.0	80.8	59.4	9.4	149	260	159	117	0.06	1.3
BG1	Liang	396	53.7	5.7	90.9	96.6	31.5	10.7	169	280	180	59	0.06	2.9
BG2	Liang	407	50.8	0.9	43.0	43.9	39.2	1.8	85	228	87	77	0.02	1.1
046A	Balingian	411	60.5	4.1	129.0	133.0	35.8	6.7	213	308	220	59	0.03	3.6
M03-2	Balingian	424	27.0	2.3	49.4	51.7	5.6	8.5	183	262	191	21	0.04	8.8
MK1	Balingian	411	39.7	1.6	102.4	104.0	15.1	4.1	258	350	262	38	0.02	6.8
MK2	Balingian	419	57.1	1.1	104.9	106.0	20.5	1.9	184	254	186	36	0.01	5.1
MK3A	Balingian	424	61.4	3.1	123.6	126.7	33.0	5.0	201	246	206	54	0.02	3.7
MK3B	Balingian	416	59.7	2.2	110.6	112.8	32.7	3.6	185	268	189	55	0.02	3.4
MP1L	Nyalau	420	61.8	5.4	152.2	157.6	47.5	8.7	246	295	255	77	0.03	3.2
MP1M	Nyalau	422	59.5	2.9	93.4	96.3	50.6	4.9	157	263	162	85	0.03	1.8
MP1U	Nyalau	414	54.7	3.2	37.0	40.2	56.6	5.9	68	209	73	104	0.08	0.7
MP2L	Nyalau	410	62.6	5.8	196.4	202.2	39.5	9.2	314	404	323	63	0.03	5.0
MP2U	Nyalau	403	57.7	7.6	137.6	145.2	43.4	13.2	239	348	252	75	0.05	3.2

TOC: Total Organic Carbon
S1: Free Hydrocarbons
S2: Remaining Hydrocarbon generative potential
S3: Organic CO_2

T_{max}: Temperature at Maximum *S2*
GP: Genetic Potential = *S1* + *S2*
BI: Bitumen Index = (*S1*/TOC) x 100
QI: Quality Index = [(*S1* + *S2*)/TOC] x 100

PI: Production Index = *S1*/(S1 + *S2*)
HI: Hydrogen Index = (*S2*/TOC) x 100
OI: Oxygen Index = (*S3*/TOC) x 100
HI': Effective HI

Table 5.3, continued.

Sample	Formation	T_{max} (°C)	TOC (wt. %)	*S1*	*S2*	GP	*S3*	BI	HI	HI'	QI	OI (mg CO_2/g TOC)	PI	*S2*/ *S3*
				(mg HC/g rock)			(mg CO_2/g rock)		(mg HC/g TOC)					
MP3L	Nyalau	420	47.6	3.3	155.3	158.6	29.2	6.8	327	365	333	61	0.02	5.3
MP3M	Nyalau	383	56.8	18.7	259.2	277.9	37.1	32.9	456	523	489	65	0.07	7.0
MP3U	Nyalau	422	46.9	2.8	111.3	114.1	35.4	5.9	237	281	243	76	0.02	3.1
MP4L	Nyalau	415	59.7	5.2	175.8	181.0	42.9	8.7	295	365	303	72	0.03	4.1
MP4M	Nyalau	410	57.2	4.2	126.3	130.5	45.0	7.4	221	321	228	79	0.03	2.8
MP4U	Nyalau	408	53.8	8.8	90.5	99.4	47.0	16.4	168	307	185	87	0.09	1.9
MP5L	Nyalau	417	63.1	6.7	148.8	155.5	45.0	10.5	236	300	246	71	0.04	3.3
MP5M	Nyalau	415	56.3	7.2	183.5	190.7	37.5	12.7	326	396	339	67	0.04	4.9
MP5U	Nyalau	414	56.6	6.4	114.5	120.9	46.1	11.2	202	289	213	81	0.05	2.5
MP6L	Nyalau	428	57.2	5.0	115.0	119.9	49.4	8.7	201	262	210	86	0.04	2.3
MP6M	Nyalau	417	58.0	3.0	80.1	83.1	50.4	5.1	138	280	143	87	0.04	1.6
MP6U	Nyalau	414	53.7	2.9	71.0	73.9	49.3	5.4	132	272	137	92	0.04	1.4
MP7L	Nyalau	403	58.6	5.3	113.1	118.4	53.1	9.1	193	304	202	91	0.05	2.1
MP7M	Nyalau	413	60.6	6.8	151.7	158.5	44.7	11.3	250	334	262	74	0.04	3.4
MP7U	Nyalau	390	55.8	5.1	66.5	71.6	60.0	9.2	119	261	128	107	0.07	1.1

Table 5.4: Rock-Eval parameters of the studied Benue Trough coals.

Sample	Formation	T_{max} (°C)	TOC (wt. %)	*S1*	*S2*	GP	*S3*	BI	HI	HI'	QI	OI (mg CO_2/g TOC)	PI	*S2*/*S3*
				(mg HC/g rock)			(mg CO_2/g rock)		(mg HC/g TOC)					
MGL3A	Gombe	420	61.2	1.9	73.1	75.0	32.9	3.1	120	237	123	54	0.03	2.2
MGL4A	Gombe	420	64.0	1.3	32.1	33.4	22.0	2.0	50	193	52	34	0.04	1.5
MGL1C	Gombe	427	57.8	1.6	101.6	103.2	32.6	2.8	176	241	179	56	0.02	3.1
MGL2I	Gombe	424	58.7	2.7	104.6	107.2	28.9	4.5	178	259	183	49	0.02	3.6
AFZ	Mamu	431	74.5	5.8	331.6	337.4	7.4	7.8	445	435	453	10	0.02	44.9
ENG	Mamu	419	58.0	3.8	163.2	166.9	28.2	6.5	282	337	288	49	0.02	5.8
IMG	Mamu	429	23.0	2.3	63.7	66.0	2.1	10.0	277	295	287	9	0.03	30.5
OGB	Mamu	422	43.4	2.2	104.4	106.5	11.2	5.0	241	300	246	26	0.02	9.4
OKB	Mamu	420	68.6	3.4	119.8	123.2	27.6	5.0	175	269	180	40	0.03	4.3
WKP	Mamu	424	67.7	2.8	183.6	186.3	14.5	4.1	271	312	275	21	0.01	12.7
CKL	Lamja	438	59.5	5.4	216.7	222.1	4.1	9.1	364	374	374	7	0.02	52.3
LMZ1	Lamja	435	53.7	1.3	51.9	53.2	31.3	2.4	97	151	99	58	0.02	1.7
LFO	Agwu	422	63.0	7.6	277.3	284.8	20.0	12.0	440	453	452	32	0.03	13.9
SKJ	Agwu	409	74.3	2.1	90.3	92.4	16.6	2.8	122	303	124	22	0.02	5.4

TOC: Total Organic Carbon
S1: Free Hydrocarbons
S2: Remaining Hydrocarbon generative potential
S3: Organic CO_2

T_{max}: Temperature at Maximum *S2*
GP: Genetic Potential = *S1* + *S2*
BI: Bitumen Index = (*S1*/TOC) x 100
QI: Quality Index = [(*S1* + *S2*)/TOC] x 100

PI: Production Index = *S1*/(S1 + *S2*)
HI: Hydrogen Index = (*S2*/TOC) x 100
OI: Oxygen Index = (*S3*/TOC) x 100
HI': Effective HI

5.4 Distribution of Functional Groups

The spectra of representative samples (Figure 5.5) show distinct bands in the aliphatic stretching, aromatic C-H stretching, and aromatic bending regions at 3000 to 2800 cm^{-1}, 3100 to 3000 cm^{-1}, and 1460 to 1350 cm^{-1}, respectively. In addition, the three distinct peaks in the 900-1100 cm^{-1} spectral region can be assigned to minerals in the coals (Wang et al., 2013). The absorbance of the peaks in the region is highest for sample CKL from Lamja Formation, Upper Benue Trough (Figure 5.5a). Furthermore, the peaks near 2920 cm^{-1} and 2850 cm^{-1} were assigned to methylene (CH_2) groups while the peaks near 1590 cm^{-1} were assigned to aromatic C=C stretching groups. The spectra also display the asymmetric CH_3 stretching peak at 2955 cm^{-1} and the carboxy/carboyl group peak at 1710 cm^{-1}. Peaks at 1375 cm^{-1} and 1450 cm^{-1} were assigned to symmetric methyl bending and aliphatic chain CH_3 deformation vibration, respectively, while the 3750-3600 cm^{-1} region is assigned to H_2O in clay minerals (Geng et al., 2009; Patricia et al., 2020).

According to Ganz & Kalkreuth (1987), Ganz & Kalkreuth (1991), and Misra et al. (2018), FTIR parameters such as the A-factor (A_F), C-factor (C_F), aliphaticity index (I_{AL}), aromaticity index (I_{AR}), and hydrocarbon generation index (I_{HG}) are useful for evaluating hydrocarbon generation potential and classifying kerogen type. The A_F is a ratio of the abundance of aliphatic over aromatic bands while C_F is a measure of the relative abundance of carboxyl over carboxyl and aromatic bands. The I_{AL} and I_{AR}, respectively, quantify the relative intensities of aliphatics and aromatics to total aliphatics and aromatics in the coals (Ganz & Kalkreuth, 1991; Biswas et al., 2020). In addition, Misra et al. (2018) proposed the index for hydrocarbon generation (I_{HG}) to estimate the aliphatic proportion of the remaining hydrocarbon in the samples.

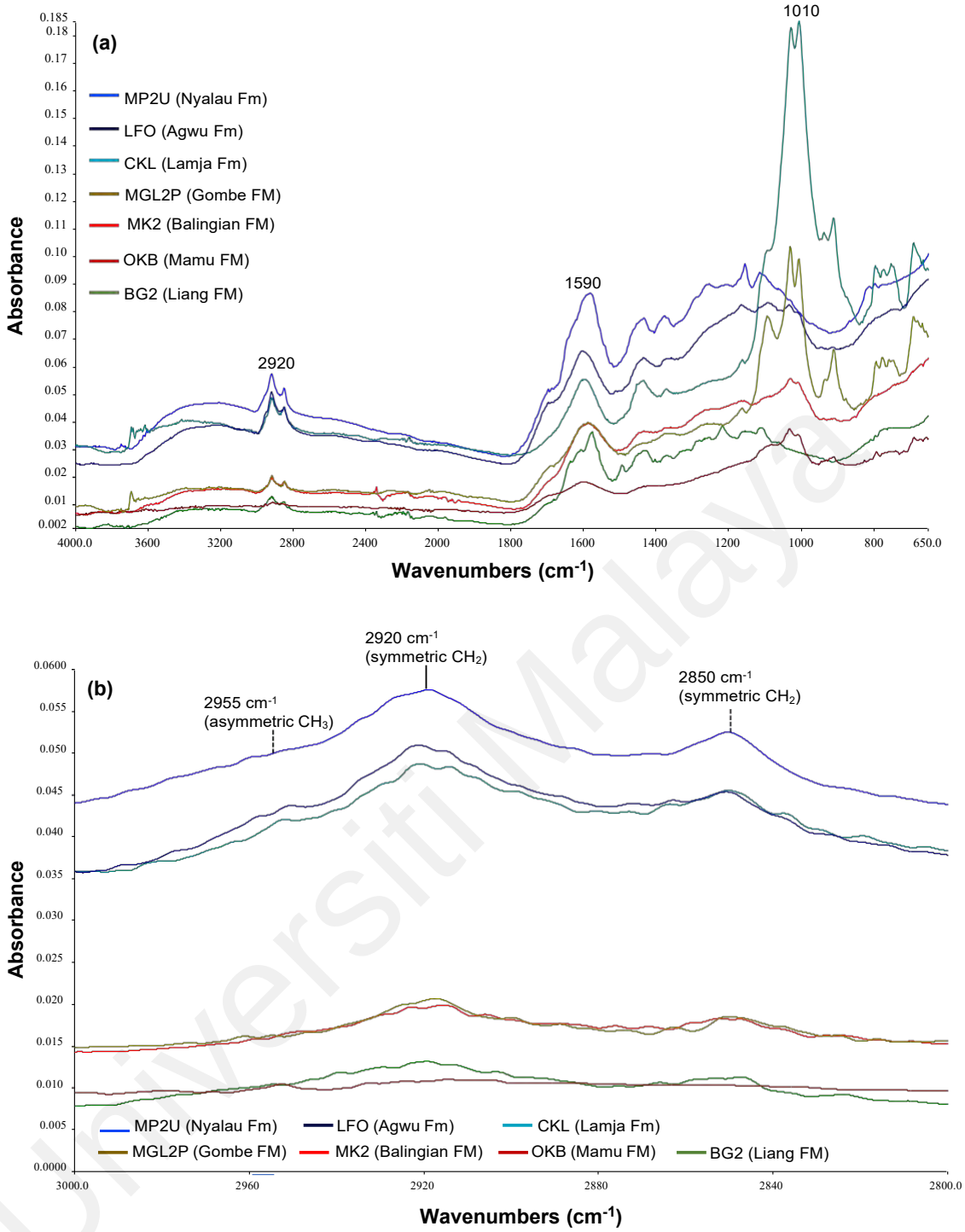

Figure 5.5. FTIR spectra of the representative coals from Sarawak Basin and Benue Trough.

The FTIR parameters (Table 5.5) were calculated using the equations below:

$$A_F = [(2930 + 2860)\ cm^{-1}] / [(2930 + 2860 + 1630)\ cm^{-1}] \quad (5.1)$$

$$C_F = [1710 / (1710 + 1630)\ cm^{-1}] \quad (5.2)$$

$$I_{AL} = [(2950 + 2920 + 2850)] / [(2950 + 2920 + 2850 + 3030 + 1600)\ cm^{-1}] \quad (5.3)$$

$$I_{HG} = IAL \times HI \quad (5.4)$$

The A_F vary considerably in the Benue Trough coals (0.29-0.65) but over a narrower range in the Sarawak Basin coals (0.39-0.65). The C_F ranges from 0.28 to 0.48 with average values of 0.41 for both groups coals.

Table 5.5: FTIR parameters for the studied coal samples.

Sample	A_F	C_F	CL_1	CL_2	DAC	I_{AL}	A_F x TOC x 10	I_{HG}
B01-1	-	-	0.88	0.82	1.86	-	-	-
B01-4	0.48	0.35	0.96	1.11	1.47	0.48	295	79
B01-5	0.61	0.43	0.97	1.02	1.11	0.57	370	105
B02-4	0.54	0.41	0.97	1.05	1.08	0.51	337	87
B03-2	0.62	0.46	0.96	1.04	1.11	0.58	381	101
B03-3	0.61	0.46	0.96	1.00	1.09	0.57	390	92
B03-6	0.58	0.44	1.00	1.10	1.26	0.55	357	103
E55-2	0.59	0.41	0.96	1.05	1.18	0.55	368	89
L04A-1	0.58	0.43	0.99	1.05	1.47	0.54	310	61
L04B-1	0.60	0.48	0.95	1.00	0.99	0.56	353	43
ML46A-6	0.61	0.47	0.95	1.00	1.18	0.56	372	92
ML46A-7	0.59	0.47	0.94	1.02	1.16	0.56	360	83
BG1	0.47	0.28	1.07	1.25	1.28	0.48	307	81
BG2	0.46	0.30	1.00	1.11	1.34	0.45	281	38
0464A	0.58	0.42	1.09	1.13	1.18	0.55	380	117
M03-2	-	-	0.95	0.84	4.08	-	-	-
MK1	0.58	0.38	1.12	1.17	1.71	0.56	304	143
MK2	0.52	0.34	1.14	1.17	1.41	0.50	347	93
MK3A	0.53	0.36	1.01	1.05	1.30	0.51	358	102
MK3B	0.58	0.38	1.00	1.05	1.13	0.54	377	99
MP1L	0.39	0.43	1.18	1.26	1.28	0.44	317	108
MP1M	0.45	0.40	1.11	1.20	1.26	0.46	294	73
MP1U	0.50	0.45	1.03	1.12	1.34	0.47	309	32
MP2L	0.67	0.41	1.01	1.06	1.18	0.60	443	187
MP2U	0.59	0.39	1.05	1.14	1.09	0.56	384	132
MP3L	0.65	0.42	1.04	1.10	1.29	0.59	435	193
MP3M	0.64	0.44	0.99	1.12	1.35	0.61	333	280
MP3U	0.58	0.42	1.08	1.18	1.41	0.56	359	132
MP4L	0.59	0.42	1.06	1.13	1.21	0.56	334	164
MP4M	0.59	0.42	1.06	1.15	1.20	0.56	373	124
MP4U	0.58	0.42	1.03	1.10	1.17	0.55	357	92
MP5L	0.58	0.41	1.08	1.16	1.15	0.55	357	130
MP5M	0.65	0.43	1.06	1.14	1.14	0.60	403	195
MP5U	0.67	0.44	1.02	1.07	1.19	0.60	452	122
MP6L	0.55	0.42	1.05	1.11	1.47	0.54	350	108
MP6M	0.55	0.36	1.02	1.07	1.27	0.52	351	72
MP6U	0.65	0.43	0.99	1.03	1.36	0.58	399	76
MP7L	0.55	0.41	1.03	1.14	1.19	0.53	368	102
MP7M	0.49	0.38	0.94	1.11	1.25	0.49	307	122
MP7U	0.57	0.44	1.02	1.11	1.42	0.54	371	65

A_F: *A*-factor = (2930 + 2860)/(2930 + 2860 + 1630) cm^{-1}

C_F: *C*-factor = [1710/(1710+1630) cm^{-1}]

CL: Chain Length. CL_1 = 2850/2955 cm^{-1}. CL_2 = 2920/2950 cm^{-1}

DAC: Degree of Aromatic Ring Condensation = 720/1600 cm^{-1}

I_{AL}: Aliphaticity Index = [(2950 + 2920 + 2850) cm-1] / [(2950 + 2920 + 2850 + 3030 + 1600) cm^{-1}]

I_{HG}: Index for Hydrocarbon Generation = I_{AL} x Hyde3rogen Index (HI)

Table 5.5, continued.

Sample	A_F	C_F	CL_1	CL_2	DAC	I_{AL}	A_F x TOC x 10	I_{HG}
MGL3A	0.57	0.42	1.03	1.07	1.17	0.52	387	63
MGL4A	0.54	0.45	1.03	1.03	1.93	0.51	386	26
MGL1C	-	-	0.92	0.95	3.34	-	-	-
MGL2A	0.57	0.40	0.99	1.04	1.15	0.52	382	-
MGL2B	0.57	0.40	1.09	1.18	1.18	0.54	371	-
MGL2H	0.41	0.38	1.03	1.14	1.52	0.42	268	75
MGL2I	0.29	0.33	1.32	1.43	1.73	0.33	177	-
MGL2O	0.52	0.39	1.13	1.25	1.48	0.50	272	-
MGL2P	-	-	0.96	0.91	3.17	-	-	-
MGL2T	0.57	0.40	0.99	1.04	1.15	0.52	382	-
AFZ	0.62	0.41	1.14	1.21	1.29	0.58	486	259
ENG	0.57	0.43	1.06	1.12	1.27	0.55	326	154
IMG	0.65	0.41	0.97	1.08	3.21	0.60	163	166
OGB	0.61	0.42	1.05	1.13	1.90	0.57	210	138
OKB	0.55	0.43	1.02	1.06	1.62	0.53	330	92
WKP	0.61	0.42	1.07	1.11	1.19	0.56	422	152
CKL	0.65	0.40	1.10	1.16	1.47	0.60	381	217
LMZ1	0.50	0.39	0.95	1.01	1.67	0.48	319	46
LFO	0.61	0.43	1.07	1.17	1.25	0.58	418	255
SKJ	0.55	0.43	1.12	1.16	1.83	0.54	400	65

5.5 Elemental Composition

The concentrations of major and trace elements have been widely applied as proxies for past redox, climatic and depositional conditions in coals (Goodarzi & Swaine, 1993; Goodarzi & Swaine, 1994; Spears & Tewalt, 2009; Spears, 2017; Krzeszowska, 2019; Li et al., 2019; Lv et al., 2019; Liu et al., 2021; Zhou et al., 2021), marine sediments (Jones & Manning, 1994; Algeo & Maynard, 2004; Tribovillard et al., 2006; Kombrink et al., 2008; Cao et al., 2012; Roy & Roser, 2013; Adegoke et al., 2014; Tao et al., 2017; Algeo & Liu, 2020; Bennett & Canfield, 2020; Han et al., 2020; Samad et al., 2020), and crude oils (Galarraga et al., 2008).

Given that coals are only formed in non-marine environments with comparably low detrital inputs, the concentrations of elements in the studied coals are normalized to their global average concentrations, following the method by Kombrink et al. (2008):

$$CC = \frac{\blacksquare^{+} \; {}^{"}\frac{!"\#\$\%\&"'}{!"\$(')\$*'}\$}{\%} \tag{5.5}$$

The concentration coefficient (*CC)* is defined as the ratio of abundance of a particular element in a coal sample relative to the reported global average abundance. The concentrations of the major element oxides in studied coals were compared with their reported abundances in Chinese coals by Dai et al. (2012) while the trace elements were compared with global average concentrations reported by Ketris & Yudovich (2009). The *CC*s of major element oxides and trace elements in the coals were calculated, and coefficients < 0.5 and > 5 indicate that the elements are depleted and significantly enriched, respectively. Furthermore, *CC*s over the 0.5-2.0 and 2.0-5.0 range indicate normal and slightly enriched abundance, respectively.

5.5.1 Major Element Geochemistry

The loss on ignition (LOI) and abundances of major element oxides in the analysed coals are shown in Table 5.6. The abundances of the major oxides in both the Malaysian and Nigerian coals are either relatively depleted or comparable to the values reported for Chinese coals by Dai et al. (2012), which suggests low quartz content in the studied coals (Liu et al., 2021). In addition, the average concentrations of the major oxides are relatively higher in the Benue Trough coals than in the Sarawak Basin coals as the Sarawak Basin coals are depleted in all the major oxides except K_2O, MgO and MnO

(Figure 5.6). The relatively higher concentration of major oxides in the Benue Trough coals indicates a higher input of terrestrial detrital materials during peat accumulation.

Table 5.6: Concentration of major oxides (% on ash), and ash yield (A_d), and total sulfur (S_T) content (% whole coal basis) for the studied coals.

Major Oxides	Sarawak Basin			Benue Trough		
	Min.	Max.	Mean (n=23)	Min.	Max.	Mean (n=12)
A_d	0.8	22.5	7.38	6.3	29.4	14.39
S_T	0.05	0.99	0.17	0.11	1.81	0.75
Al_2O_3	0.05	5.99	1.01	0.47	6.21	1.79
CaO	0.03	1.46	0.44	0.05	1.54	0.55
Fe_2O_3	0.12	1.19	0.67	0.30	3.98	1.54
K_2O	0.01	0.87	0.21	0.06	0.43	0.25
MgO	0.03	0.72	0.26	0.01	0.83	0.23
MnO	0.01	0.02	0.02	0.01	0.04	0.03
Na_2O	0.02	0.14	0.05	0.06	0.12	0.09
P_2O_5	0.01	0.05	0.03	0.01	0.18	0.04
SiO_2	0.04	10.80	1.96	0.83	38.02	7.29
TiO_2	0.03	0.22	0.09	0.04	2.43	0.34
LOI	80.5	99.3	95.5	51.2	95.7	88.2

LOI = loss on ignition

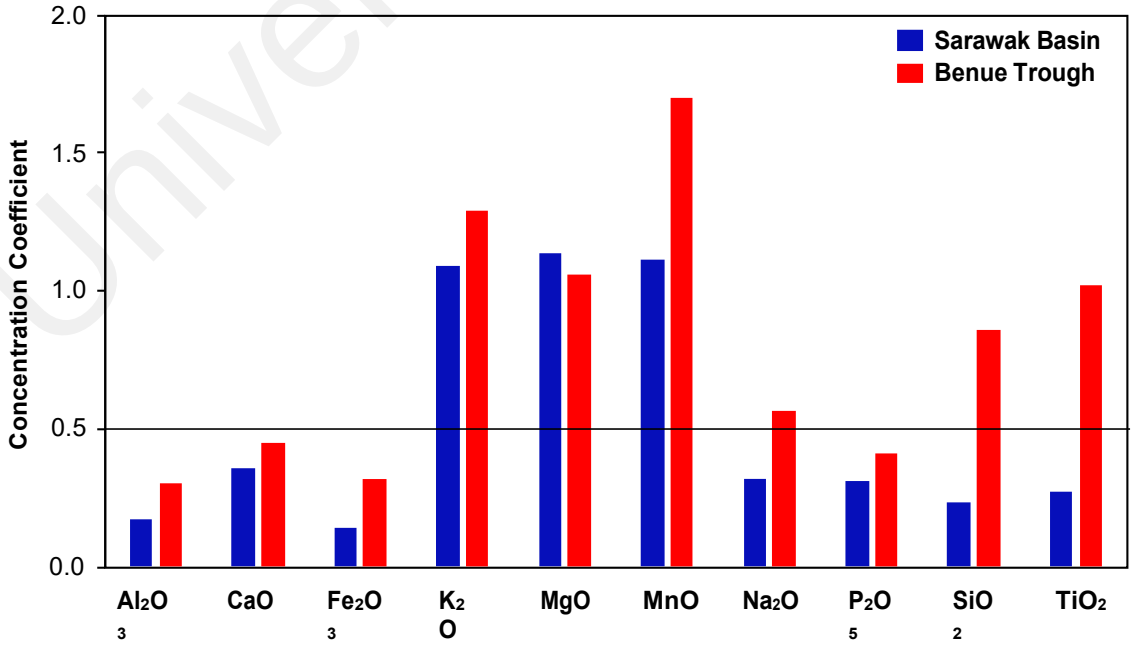

Figure 5.6: Correlation coefficients of major oxides in the studied Sarawak Basin and Benue Trough coals, normalized to the Chinese averages reported by Dai et al. (2012).

The distribution of major element oxides in both groups of coal is dominated by SiO_2, Al_2O_3 and Fe_2O_3 with subordinate abundances of CaO, MgO, and K_2O and low abundances of TiO_2, Na_2O, MnO and Cr_2O_3. The abundance of SiO_2 in the studied coals ranges from 0.04 to 38.02% with average values of 1.96% and 7.29% in the Sarawak Basin and Benue Trough samples, respectively. The abundances of Al_2O_3 are relatively lower, ranging from 0.05 to 6.21%, respectively, with average values of 1.01% and 1.79% in the Sarawak Basin and Benue Trough samples, respectively. Consequently, the SiO_2/Al_2O_3 ratios in the studied Sarawak Basin and Benue Trough vary from 0.18 to 7.30 and 1.32 to 9.36, respectively. The average SiO_2/Al_2O_3 ratios of 2.09 and 3.42 for the Malaysian and Nigerian coals are higher than those of Chinese coals (1.42; Dai et al., 2012) and the theoretical value of kaolinite (1.18; Zhou et al., 2021). For the Malaysian coals, the average SiO_2/Al_2O_3 ratios are relatively higher in the Liang Formation (2.84) than in the Nyalau Formation (1.96) and Balingian Formation (1.18). The relatively lower SiO_2/Al_2O_3 ratios of the Sarawak Basin coals, particularly the Miocene Balingian and Nyalau Formations, are probably due to a higher abundance of al-rich clay minerals such as kaolinite and illite (Figure 5.7). Conversely, the higher SiO_2/Al_2O_3 ratios of the Benue Trough coals suggest the presence of quartz in high abundance relative to other minerals (Cullers, 2000). Furthermore, Fe_2O_3/Al_2O_3 ratios are higher in the Sarawak coals, varying widely between 0.07 and 15.60 (avg. 4.39), and lower in the Benue trough Coals with ratios ranging narrowly from 0.18 to 3.41 (avg. 1.20).

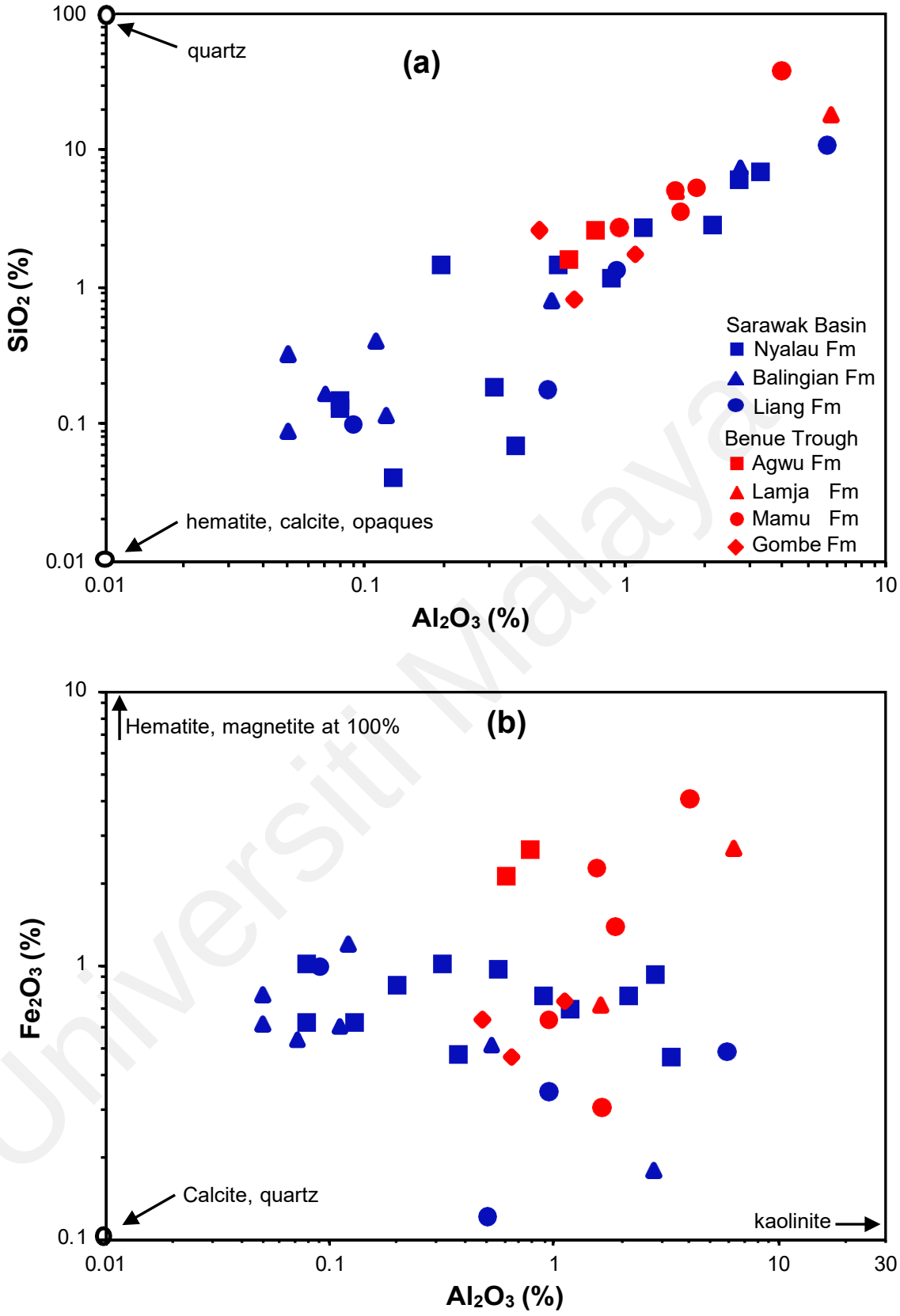

Figure 5.7: Cross-plots of (a) – Al_2O_3 vs. SiO_2, and (b) – Al_2O_3 vs. Fe_2O_3 in the studied coal samples (after Cullers, 2000).

Elements in coals are associated with the organic or mineral parts (Vejahati et al., 2010; Spears, 2017). In general, lithophile elements such as Si, Al, K, and Ti are associated with the mineral factions. Several studies have employed different statistical analytical techniques to determine elemental associations in coals (Spears & Tewalt, 2009; Bai et al., 2015; Spears 2017; Ameh, 2019). Results of the correlation analysis of the concentrations of major element oxides and organic carbon and sulfur contents for the Malaysian and Nigerian coals are presented in Tables 5.7 and 5.8. Significant correlations were observed between elements in both groups of coals. The ash content in the Sarawak Basin is positively correlated with SiO_2 (0.949), Al_2O_3 (0.912), K_2O (0.848), and TiO_2 (0.829), and negatively correlated with TOC (-0.418). Similarly, the ash content in the Benue Trough coals is positively correlated with SiO_2 (0.804), Al_2O $(0.809)_3$, and TiO_2 (0.431), and negatively correlated with TOC (-0.293). The strong, positive correlations imply that Si, Al, K and Ti originate from clay minerals. However, the relatively weaker coefficients for the Benue Trough coals suggest the Si, and Al are derived from a mixed clay assemblage (Bai et al., 2015).

Furthermore, the no correlation (0.063) and strong correlation (0.856) between the ash content and MgO concentration in the Malaysian and Nigerian coals, respectively, are suggestive of mineralogical controls as Mg is present in illite and mixed-layer clays (Spears & Tewalt, 2009). In addition, the weak relationships of LOI with CaO and MgO in both groups of coals suggest the absence of carbonate minerals (Tao et al., 2017). The positive correlation (0.698) between S and Fe_2O_3 in the Benue Trough coals suggests the presence of pyrites. In contrast, S and Fe_2O_3 are negatively correlated (-0.410) in the Sarawak Basin coals, which implies the absence of pyrites in the coals. This is corroborated by the mostly low S_T values (< 0.5 wt.%) in the Sarawak coals which implies the predominance of organic sulfur that is derived mostly from parent plant materials (Casagrande, 1987; Chou, 2012).

Table 5.7: Pearson's correlation coefficients of major element oxides, loss on ignition (LOI), ash content (A_d), sulfur (S), and total organic carbon (TOC) contents in the studied Sarawak Basin coals.

Variable	TOC	S	A_d	SiO_2	Al_2O_3	Fe_2O_3	CaO	MgO	K_2O	TiO_2	MnO	P_2O_5	LOI
TOC	1.000												
S	-0.264	1.000											
A_d	-0.418	0.448	1.000										
SiO_2	-0.400	0.337	0.949	1.000									
Al_2O_3	-0.411	0.219	0.912	0.969	1.000								
Fe_2O_3	0.208	-0.410	-0.369	-0.293	-0.290	1.000							
CaO	-0.483	-0.271	-0.064	-0.107	-0.086	-0.069	1.000						
MgO	-0.458	-0.188	0.063	0.048	0.088	-0.304	0.896	1.000					
K_2O	-0.835	0.070	0.848	0.891	0.951	-0.385	0.213	0.637	1.000				
TiO_2	-0.365	0.719	0.829	0.817	0.645	-0.405	-0.489	-0.257	0.572	1.000			
MnO	0.527	-0.385	-0.139	-0.177	-0.118	0.322	-0.080	-0.261	-0.459	-0.524	1.000		
P_2O_5	0.135	0.072	0.254	0.234	0.236	-0.427	-0.171	0.054	-0.230	-0.033	-0.730	1.000	
LOI	0.464	-0.232	-0.939	-0.984	-0.977	0.252	-0.035	-0.184	-0.945	-0.715	0.148	-0.202	1.000

Table 5.8: Pearson's correlation coefficients of major element oxides, loss on ignition (LOI), ash content (A_d), sulfur (S), and total organic carbon (TOC) contents in the studied Benue Trough coals.

Variable	TOC	S	A_d	SiO_2	Al_2O_3	Fe_2O_3	CaO	MgO	TiO_2	MnO	P_2O_5	LOI
TOC	1.000											
S	-0.051	1.000										
A_d	-0.293	-0.715	1.000									
SiO_2	-0.662	0.360	0.804	1.000								
Al_2O_3	-0.428	-0.014	0.809	0.765	1.000							
Fe_2O_3	-0.298	0.698	0.217	0.760	0.588	1.000						
CaO	-0.173	-0.405	-0.076	-0.396	-0.463	-0.402	1.000					
MgO	-0.281	-0.562	0.856	-0.074	0.130	-0.170	0.770	1.000				
TiO_2	-0.638	0.515	0.431	0.942	0.517	0.712	-0.358	-0.237	1.000			
MnO	0.497	0.561	-0.741	-0.28	-0.382	0.180	-0.290	-0.696	-0.139	1.000		
P_2O_5	0.005	-0.018	-0.091	-0.146	-0.277	-0.165	0.387	0.075	-0.042	-0.470	1.000	
LOI	0.655	-0.338	-0.825	-0.994	-0.805	-0.786	0.360	0.002	-0.910	0.301	0.131	1.000

In addition, the negative and positive correlations of S_T and Fe_2O_3 for the Sarawak Basin (-0.410) and Benue Trough (0.698) coals, respectively, are suggestive of pyritic sulfur abundance in the Benue Trough coals (Spears & Tewalt, 2009). This is corroborated by the moderate to strong, positive correlations of Fe_2O_3 with SiO_2 (0.760), Al_2O_3 (0.588) and TiO_2 (0.712) in the Benue Trough coals and the weak, negative correlations of Fe_2O_3 with SiO_2 (-0.293), Al_2O_3 (-0.290) and TiO_2 (-0.415) in the Malaysian coals.

Calcium is present in the coal ashes in minor abundances and no significant correlations were observed between CaO and the aluminosilicate-affiliated elements for both groups of coals. However, CaO and MgO are strongly correlated in the Malaysian (0.896) and Nigerian (0.770) coals.

5.5.2 Trace Element Geochemistry

The abundance of trace elements in the studied coals is tabulated in Appendix B. Based on the CC ratios, the Sarawak Basin coals are depleted in all monitored trace elements except Au, B, Ba, Mn and Pt (Figure 5.8). Whilst the Malaysian coals are slightly enriched in Pt, the abundances of Au, B, Ba and Mn are comparable to the average global concentrations reported by Ketris & Yudovich (2009) as shown in Figure 5.8. Similarly based on the *CC* ratios, the studied Benue Trough coals are relatively depleted in elements such as As, Au, Bi, Cd, Ce, Cs, Hf, La, Li, Mo, Nb, Rb, Sb, Ta, Tl, U, W, Zn and Zr whilst the abundances of Ag, B, Ba, Be, Co, Cr, Cu, Ga, Ge, Hg, Mn, Ni, Pb, Sc, Sr, Sn, Th, Ti, V and Y are normal when compared with the average global concentrations. Furthermore, the Nigerian coals are slightly and significantly enriched in Se and Pt, respectively (Figure 5.9).

The abundances of major oxides and trace elements across the Sarawak Basin coal formations were also compared (Figure 5.10). Again, the coals are relatively depleted in elements. The Liang Formation, however, coals show enrichment for B which is suggestive of relatively saline depositional conditions due to mild brackish-water influence (Dai et al., 2020). It is important to however note that B enrichment is not only related to paleosalinity. Coals from the Waikato region, New Zealand have elevated B concentrations, up to 7000 ppm, which Moore et al. (2005) attributed to a hydrothermal source. However, the significantly lower concentration (47-248 ppm) of B in the Balingian Formation coals is possibly due to saline paleoconditions. In general, the observed relative depletion of trace elements in the studied coals is indicative of low detrital input during mire development. According to Shotyk (1988), elemental abundance reflects the composition of precipitation and dust in ombrotrophic peats, and the composition of source area rocks and sediments in minerotrophic peats.

Elemental ratios are often employed as proxies to estimate depositional conditions within paleomires (Dai et al., 2020). Hence, ratios of elemental abundance in the studied coals are given in Table 5.10.

Table 5.9: Concentrations (ppm) of selected minor and trace elements in the studied coals.

Elements	Sarawak Basin			Benue Trough		
	Min.	Max.	Average (n = 23)	Min.	Max.	Average (n = 12)
Ag*	5	140	25	8	1136	161
As	0.1	3.9	0.8	0.1	4.1	1.5
Au*	0.3	9.3	3.3	0.4	3.0	1.4
B	24	248	94	22	72	49
Ba	9.4	326.1	108.1	11.0	277.8	89.5
Be	0.1	2.6	0.6	0.4	6.1	3.1
Bi	0.02	0.94	0.29	0.02	1.01	0.34
Cd	0.01	0.17	0.08	0.02	0.07	0.04
Ce	0.1	74.2	5.3	0.8	26.6	9.4
Co	0.4	12.8	5.0	1.0	15.2	5.2
Cr	1.4	13.1	5.0	2.6	27.5	9.0
Cs	0.03	1.10	0.32	0.02	0.56	0.12
Cu	0.6	11.7	3.8	2.2	22.8	11.4
Ga	0.1	2.9	1.1	0.6	6.9	3.2
Ge	0.1	0.1	0.1	0.3	15.7	2.8
Hf	0.02	0.19	0.04	0.03	0.79	0.20
Hg*	5	31	16	6	443	158
La	0.5	20.7	5.3	1.0	9.6	4.5
Li	0.1	4.8	0.7	0.1	7.1	1.3
Mo	0.01	0.94	0.17	0.11	0.88	0.41
Nb	0.03	1.32	0.24	0.07	6.92	1.56
Ni	0.1	11.6	4.7	1.6	17.4	8.2
Pb	0.19	9.83	1.83	1.00	10.85	4.44
Pt*	2	303	110	182	3468	807
Rb	0.1	6.0	0.8	0.2	3.2	0.6
Sb	0.02	0.12	0.08	0.02	0.07	0.04
Se	0.1	0.6	0.2	0.3	12.0	3.3
Sc	0.2	3.0	1.2	0.6	6.2	2.3
Sr	4.0	129.3	43.2	5.1	292.4	58.2
Sn	0.1	1.0	0.3	0.1	1.1	0.6
Te	0.02	0.03	0.02	0.02	0.05	0.03
Th	0.1	2.4	0.6	0.6	5.5	2.5
TI	0.02	0.07	0.03	0.02	0.55	0.18
U	0.1	0.2	0.2	0.1	5.6	1.0
V	1	17	8	3	41	13
W	0.1	0.4	0.3	0.1	0.9	0.3
Y	0.05	40.70	3.80	0.89	18.81	5.67
Zn	0.7	88.1	10.0	0.4	34.7	11.4
Zr	0.1	5.4	0.7	1.0	31.7	7.2

*in pp

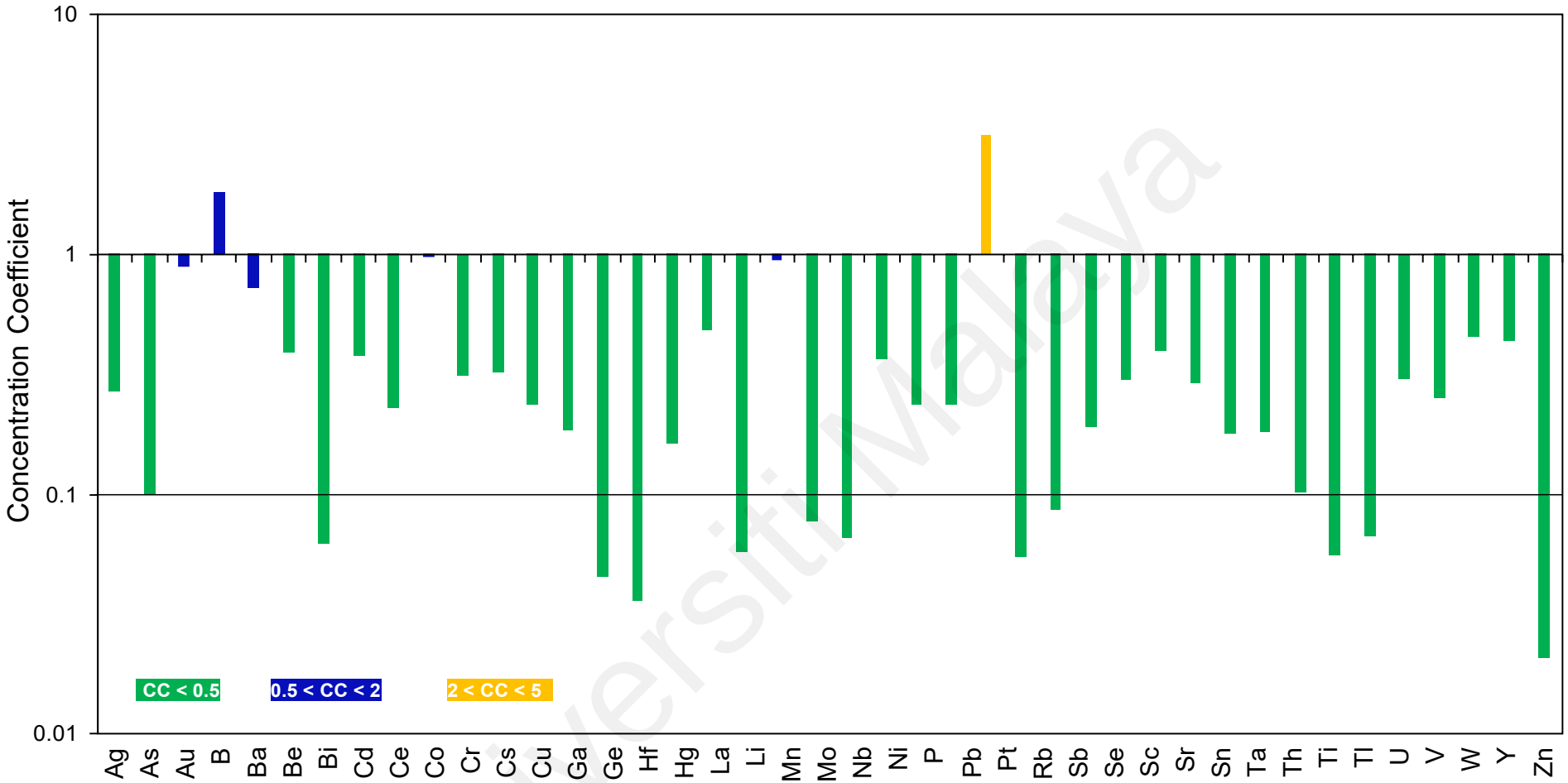

Figure 5.8: Correlation coefficients of trace elements in the studied Sarawak Basin coals, normalized to the global averages reported by Ketris & Yudovich (2009).

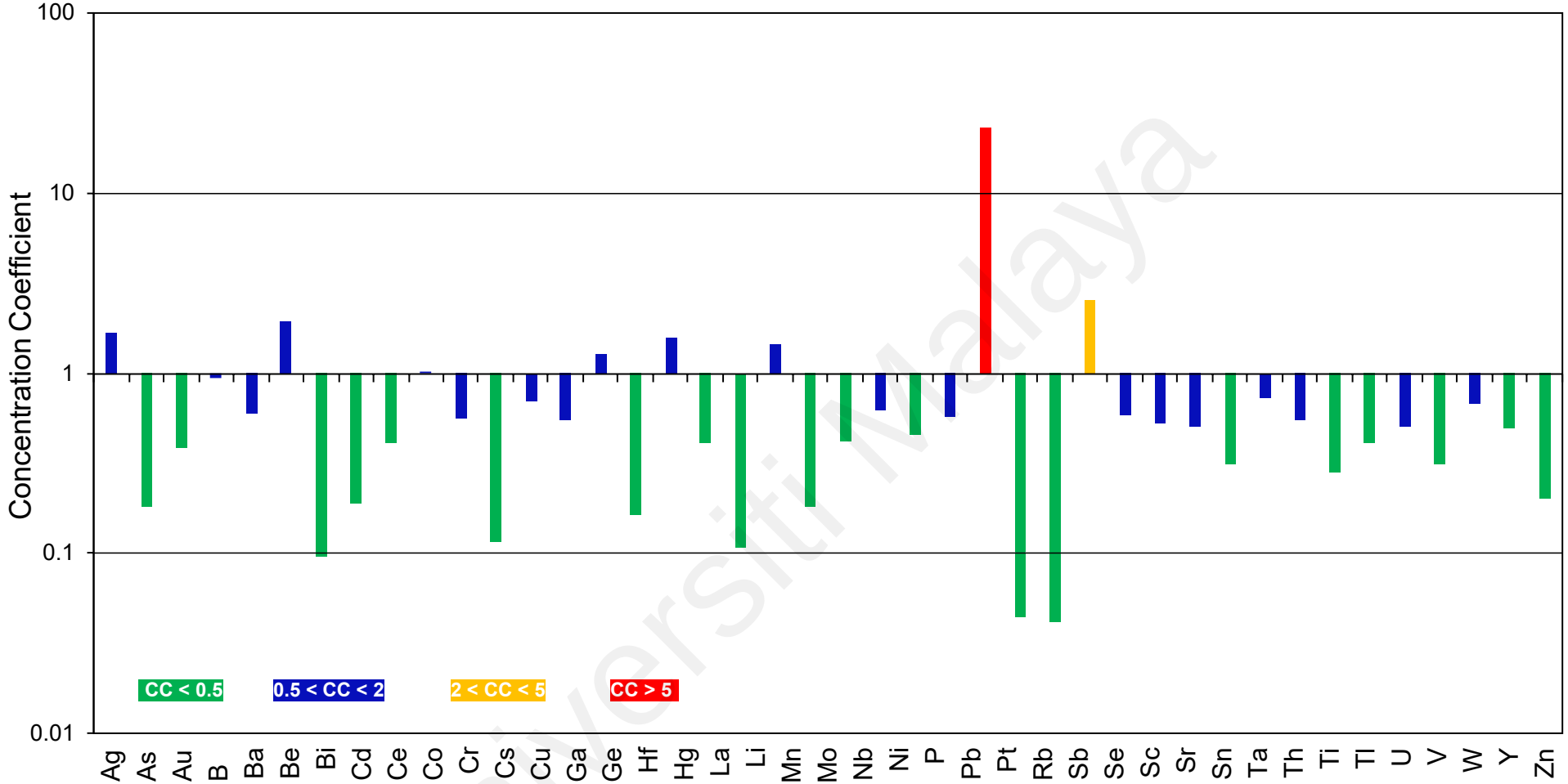

Figure 5.9: Correlation coefficients of trace elements in the studied Benue Trough coals, normalized to the global averages reported by Ketris & Yudovich (2009).

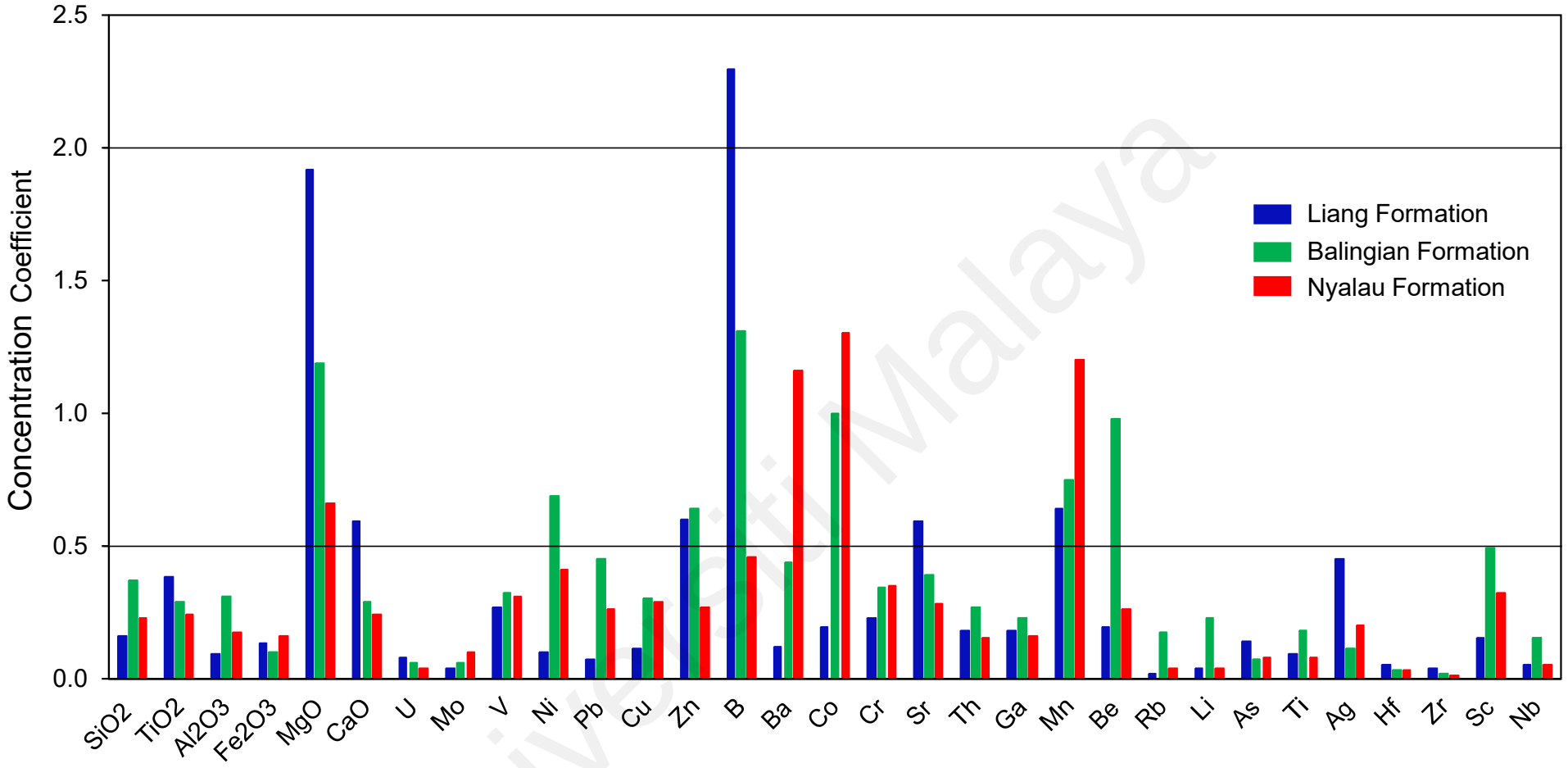

Figure 5.10: Correlation coefficients of major oxides and trace elements in the studied Sarawak coal formations, normalized to their Chinese and global averages reported by Dai et al. (2012) and Ketris & Yudovich (2009), respectively.

Table 5.10: Selected elemental parameters for the studied coals.

Sample	SiO_2/ Al_2O_3	(Fe_2O_3 + CaO + MgO)/ (SiO_2 + Al_2O_3)	Al_2O_3/ TiO_2	TiO_2/ Zr	Sr/ Ba	Th/ U	Fe/S
B01-1	1.58	1.91	17.3	55.6	13.76	6.0	1.72
B03-2	6.60	4.03	-	-	1.24	-	6.22
E55-2	3.73	4.79	-	-	5.27	-	2.50
L04A-1	2.78	0.03	12.5	1294.1	2.13	6.5	0.09
ML46A-7	1.00	6.92	-	-	1.41	-	2.16
BG1	2.43	8.42	-	-	4.28	-	4.13
BG2	1.80	13.57	-	-	3.99	-	4.78
046A	0.35	0.30	-	-	0.40	-	0.24
MK1	1.80	0.09	37.4	1600.0	0.64	12.0	1.21
MK2	1.45	0.66	31.3	750.0	0.74	6.0	2.30
MK3A	1.11	5.95	-	-	0.35	-	3.88
MP1L	0.31	4.53	-	-	0.09	-	7.17
MP1M	1.63	3.67	-	-	0.09		7.83
MP1U	0.18	1.40	-	-	0.13	-	2.67
MP2L	7.30	0.70	3.3	857.1	0.12	-	6.56
MP2U	2.57	0.64	5.6	1666.7	0.10	-	6.09
MP3M	2.06	0.12	30.1	1833.3	0.19	11.0	2.27
MP4L	2.29	0.25	13.2	1800.0	0.13	-	4.18
MP4U	1.29	0.19	43.6	714.3	0.07	-	3.19
MP5M	2.15	0.18	28.0	2000.0	0.20	-	6.56
MP6L	1.28	0.78	22.5	1333.3	0.24	-	5.30
MP6M	1.88	8.57	-	-	0.28	-	9.86
MP7L	0.59	2.96	-	-	0.20	-	13.00
MGL3A	1.32	1.45	15.8	111.1	1.05	18.0	1.04
MGL1C	1.61	0.61	21.8	277.8	0.31	6.0	1.04
MGL2I	5.57	0.65	6.7	388.9	0.68	12.0	2.73
AFZ	2.88	0.13	7.3	464.3	0.39	0.2	0.45
ENG	2.81	0.46	8.2	187.0	0.21	4.7	1.15
OGB	9.36	1.23	1.7	1021.0	0.21	3.2	1.18
OKB	3.18	1.11	5.6	88.3	0.20	4.2	0.87
WKP	2.21	0.19	9.2	600.0	0.16	5.3	0.90
CKL	2.95	0.22	18.8	2750.0	0.77	11.8	11.00
LMZ1	3.22	0.10	14.4	458.3	8.40	5.0	3.08
LFO	2.61	0.37	10.2	428.6	0.46	10.0	0.82
SKJ	3.29	0.07	6.5	1200.0	0.28	-	1.33

Table 5.10, Continued.

Sample	Ni/ Co	V/ Ni	V/ Cr	Sr/ Cu	Ga/ Rb	C-Value	Fe/ Mn	Ca/ Mg	Ba/ Ti
B01-1	2.20	3.64	1.48	99.0	10.0	0.24	64.6	2.94	0.09
B03-2	0.17	-	-	79.2	-	1.06	69.1	2.71	3.78
E55-2	2.25	-	-	108.1	2.0	0.29	59.3	1.95	0.80
L04A-1	2.03	2.30	1.07	11.1	2.9	2.72	128.6	-	0.06
ML46A-7	1.25	4.00	0.56	27.5	0.5	2.68	106.5	1.73	1.58
BG1	-	-	-	24.0	-	0.37	55.9	1.50	-
BG2	-	-	-	21.8	-	0.48	78.2	1.55	-
046A	2.57	0.18	0.36	1.5	-	1.67	250.0	-	0.99
MK1	1.10	3.70	1.72	7.7	0.4	0.27	37.0	1.75	0.28
MK2	1.47	0.43	1.28	31.9	1.4	0.28	32.4	1.89	2.04
MK3A	2.18	-	-	2.2	2.0	6.94	48.2	2.00	-
MP1L	0.67	-	-	2.1	-	4.00	102.4	4.00	-
MP1M	2.44	-	-	7.0	-	4.03	95.9	2.67	-
MP1U	1.58	0.49	0.71	1.1	-	2.78	118.5	4.50	-
MP2L	0.74	0.17	0.43	4.3	2.0	2.53	44.4	2.14	2.32
MP2U	1.22	1.13	0.63	4.3	16.0	2.85	45.9	2.67	2.97
MP3M	0.83	4.67	1.57	4.2	0.7	0.50	30.1	1.81	2.17
MP4L	0.59	0.92	1.04	7.5	3.3	2.16	47.9	3.00	1.99
MP4U	0.77	2.71	2.03	1.6	4.0	3.38	40.2	1.80	1.73
MP5M	0.90	3.18	1.54	5.3	1.6	1.32	49.6	3.20	3.48
MP6L	0.53	1.02	0.98	30.9	3.3	0.89	37.6	2.80	10.87
MP6M	10.00	-	-	29.0	-	1.09	40.8	2.26	-
MP7L	0.45	0.35	0.48	20.3	3.0	1.97	60.2	2.88	9.96
MGL3A	1.60	1.88	1.03	132.9	7.0	0.27	41.8	3.81	1.74
MGL1C	1.89	1.47	1.14	10.0	23.0	0.78	27.8	3.92	0.72
MGL2I	3.65	0.32	0.91	20.9	3.0	0.46	37.3	3.50	0.34
AFZ	2.05	2.22	1.96	0.2	19.5	12.74	272.7	-	0.04
ENG	2.28	2.42	1.44	2.2	15.3	5.73	29.0	6.50	0.11
OGB	1.14	2.36	1.49	0.9	9.7	28.27	295.8	5.00	0.04
OKB	2.00	2.23	1.56	1.6	17.7	10.12	51.0	6.00	0.10
WKP	2.96	1.56	1.15	0.5	-	4.05	41.9	-	0.05
CKL	1.58	2.56	1.68	0.4	0.6	3.75	183.3	0.29	0.12
LMZ1	2.03	0.61	1.34	15.3	1.4	0.26	153.8	2.30	0.07
LFO	0.73	0.61	0.68	3.7	9.0	3.17	68.5	5.00	0.41
SKJ	0.88	0.48	1.15	2.5	7.0	4.06	116.5	3.43	0.75

Table 5.10, Continued.

Sample	Th/ Sc	Zr/ Sc	Th/ Co	Th/ Cr	La/ Sc	La/ Th	Zr/ Hf	Y/ Ni	Cr/ V	Cr/ Ni
B01-1	1.50	6.75	2.40	0.44	1.25	0.83	28.4	1.58	0.68	2.45
B03-2	1.33	1.67	0.67	0.24	-	-	16.7	0.70	-	17.00
E55-2	1.33	2.00	1.00	0.21	-	-	30.0	0.31	-	2.11
L04A-1	0.93	1.21	0.43	0.10	9.64	10.38	21.3	0.65	0.94	2.15
ML46A-7	0.57	1.43	1.00	0.11	-	-	33.3	1.90	1.80	7.20
BG1	0.67	1.00	-	0.14	-	-	-	0.40	-	7.00
BG2	1.00	1.50	-	0.11	-	-	15.0	0.25	-	9.50
046A	0.21	0.32	0.09	0.07	10.89	51.75	30.0	3.60	2.80	0.50
MK1	0.80	0.33	0.57	0.24	1.13	1.42	20.0	0.89	0.58	2.15
MK2	0.25	0.17	0.08	0.15	0.67	2.67	20.0	0.54	0.78	0.34
MK3A	0.67	0.67	0.05	0.09	-	-	-	0.04	-	0.27
MP1L	0.33	0.67	0.01	0.05	-	-	-	0.04	-	0.38
MP1M	0.50	1.50	0.06	0.03	-	-	-	0.03	-	0.90
MP1U	0.33	0.33	0.08	0.07	-	-	-	0.22	1.40	0.68
MP2L	0.60	1.40	0.04	0.13	-	-	17.5	0.11	2.30	0.40
MP2U	0.23	0.23	0.10	0.05	-	-	15.0	1.10	1.59	1.79
MP3M	0.50	0.27	0.31	0.12	0.41	0.82	20.0	0.43	0.64	2.97
MP4L	0.50	0.36	0.05	0.10	0.36	0.71	12.5	0.39	0.96	0.88
MP4U	0.42	0.29	0.13	0.13	0.42	1.00	17.5	0.80	0.49	1.34
MP5M	0.40	0.20	0.20	0.11	-	-	25.0	0.18	0.65	2.07
MP6L	0.36	0.21	0.05	0.08	-	-	-	1.48	1.02	1.03
MP6M	0.33	0.33	0.20	0.06	-	-	-	0.03	-	0.32
MP7L	0.67	0.67	0.03	0.10	-	-	20.0	0.08	2.10	0.74
MGL3A	2.57	5.14	1.80	0.62	4.71	1.83	21.2	1.79	0.97	1.81
MGL1C	1.33	2.00	0.67	0.27	1.11	0.83	20.0	1.23	0.88	1.29
MGL2I	2.00	3.00	0.46	0.36	6.83	3.42	20.0	0.09	1.10	0.35
AFZ	0.41	0.88	0.59	0.25	3.00	7.38	31.1	2.35	0.51	1.13
ENG	1.08	4.73	0.97	0.25	2.65	2.46	35.1	1.17	0.69	1.68
OGB	0.89	3.84	0.36	0.20	0.65	0.73	50.6	0.41	0.67	1.58
OKB	0.81	6.10	0.75	0.26	1.12	1.38	40.1	1.68	0.64	1.43
WKP	1.17	1.67	0.81	0.20	-	-	30.0	0.22	0.87	1.35
CKL	1.68	0.43	0.90	0.38	3.21	1.91	20.0	0.31	0.60	1.52
LMZ1	2.14	1.71	0.41	0.45	2.50	1.17	30.0	0.30	0.74	0.45
LFO	0.77	1.08	0.11	0.17	0.92	1.20	35.0	0.67	1.48	0.89
SKJ	0.86	1.43	0.08	0.23	1.43	1.67	33.3	0.44	0.87	0.41

5.6 Atomic and Bulk Isotopic Composition

5.6.1 Atomic Abundances and Ratios

The hydrogen content of the Sarawak Basin and Benue Trough coals varies widely from 4.7 to 7.1 (avg. 5.5 wt.%) and 4.0 to 7.2 (avg. 5.1 wt.%), respectively (Table 5.11).

The average hydrogen content suggests the studied coals are generally orthohydrous (Diessel, 1992).

The atomic C/N ratios for the Sarawak Basin coals vary widely between 33.0 and 57.4 while ratios for the Benue Trough coals vary between 35.4 and 51.4 (Table 5.11). The wider variation in C/N ratio for the Sarawak Basin coals is suggestive of greater heterogeneity, probably due to differing paleoflora and environmental factors. In contrast, the atomic H/C ratios for the analysed coals range from 0.10 to 0.19 and 0.11 to 0.28, respectively, for the samples from Sarawak Basin and Benue Trough (Table 5.11). The H/C ratio is a reliable proxy for organic matter type as lignin-rich vascular plants have greater C contents than lipid-rich materials (Lopez-Dias et al., 2013). Hence, the generally similar H/C ratios (Figure 5.11) for all the coals are indicative of the predominant contribution of vascular plants to peat formation.

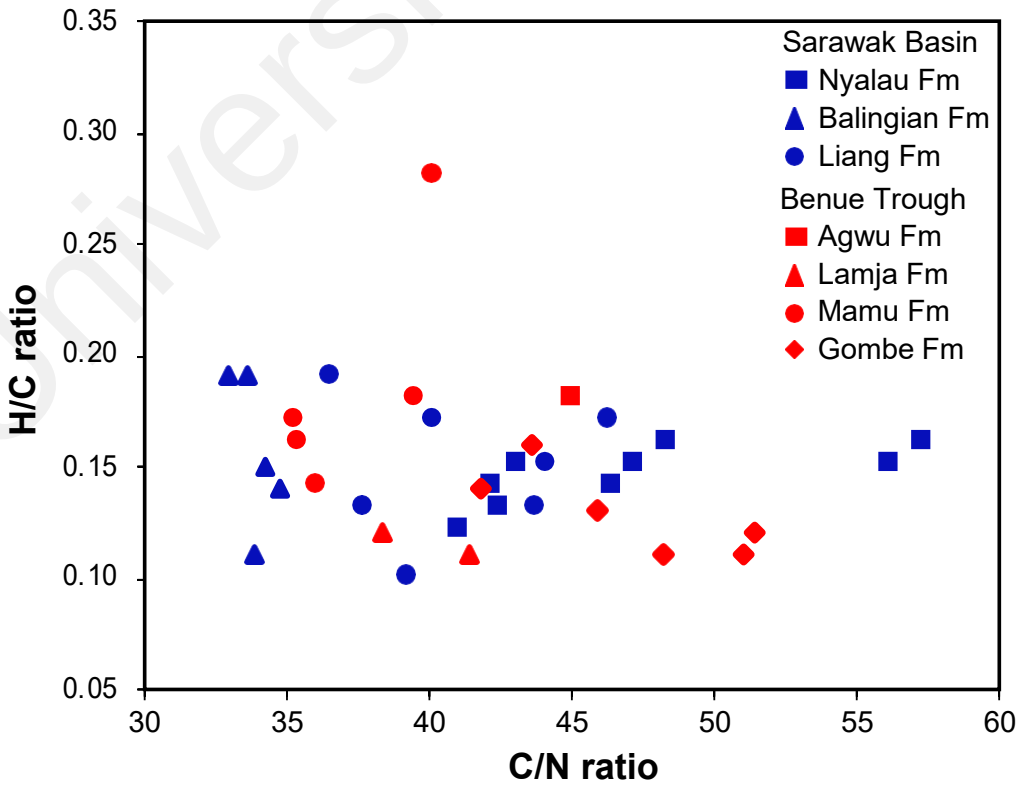

Figure 5.11: Cross-plot of atomic ratios for the studied coals.

Table 5.11: Atomic and isotopic composition of the studied coals.

Sample	$\delta^{13}C$ (‰)	$\delta^{2}H$ (‰)	%C	%H	%N	%O	C/N	H/C
B01-1	-28.7	-104.7	34.5	6.4	0.9	57.9	42.8	2.22
B03-6	-27.7	-107.8	35.0	6.0	0.9	58.0	46.8	2.05
E55-2	-28.7	-104.3	53.6	7.1	1.4	37.6	44.0	1.58
L04A-1	-27.9	-103.1	32.0	5.5	0.7	60.3	54.2	2.06
ML46A-7	-27.3	-125.3	46.7	4.7	1.2	46.9	46.0	1.20
BG1	-28.0	-133.6	37.9	4.8	0.9	56.2	51.1	1.50
BG2	-27.4	-123.8	31.5	4.7	0.7	63.0	51.6	1.77
0464A	-27.6	-130.0	34.4	5.1	1.0	58.6	40.0	1.77
M03-2	-26.8	-91.0	24.4	4.8	0.7	69.9	38.8	2.32
MK1	-27.6	-110.3	31.3	5.8	0.9	61.6	39.2	2.23
MK2	-24.2	-128.5	40.2	5.6	1.2	52.7	40.6	1.67
MK3A	-27.4	-129.9	44.0	4.7	1.3	49.7	39.5	1.28
MP1L	-26.7	-128.7	39.3	5.6	0.9	54.0	49.3	1.70
MP1U	-28.0	-122.4	37.7	4.8	0.9	56.3	49.6	1.53
MP2L	-28.6	-145.2	36.7	5.4	0.8	56.9	55.2	1.75
MP2U	-29.4	-153.2	33.8	5.5	0.7	59.8	56.6	1.95
MP3M	-28.0	-173.5	38.9	5.8	0.7	54.4	65.6	1.78
MP4L	-28.2	-154.7	39.6	5.8	0.9	53.5	50.4	1.74
MP5M	-29.3	-144.4	37.8	5.3	0.8	55.9	54.2	1.67
MP6M	-28.3	-139.0	40.1	5.0	1.0	53.8	48.0	1.49
MP7L	-28.0	-129.6	37.9	6.1	0.7	55.2	66.9	1.93
MGL1C	-25.9	-115.5	32.5	5.2	0.7	60.7	50.8	1.89
MGL2B	-25.0	-112.1	42.3	4.7	0.9	51.8	56.4	1.33
MGL2I	-25.8	-117.0	40.2	4.9	0.8	53.8	59.9	1.45
MGL2O	-25.7	-116.8	36.8	4.8	0.8	57.1	53.7	1.55
MGL2T	-25.8	-116.9	31.2	4.3	0.7	63.1	48.7	1.65
MGL3A	-25.2	-113.8	38.8	4.5	0.8	55.4	59.6	1.37
ENG	-25.2	-101.4	36.8	6.3	1.0	54.5	41.3	2.03
IMG	-24.7	-102.7	15.7	4.4	0.4	77.0	47.0	3.30
OGB	-26.8	-114.6	21.8	4.0	0.6	71.2	46.2	2.20
OKB	-25.2	-102.5	37.7	5.9	1.1	53.2	41.4	1.87
WKP	-25.3	-98.8	40.5	5.7	1.1	52.1	42.2	1.69
CKL	-24.7	-94.1	36.4	4.4	1.0	57.6	45.0	1.45
LMZ1	-24.8	-66.4	45.5	5.2	1.1	47.6	48.5	1.35
LFO	-26.1	-124.1	41.1	7.2	0.9	48.8	52.6	2.10

C: carbon; H: hydrogen; O: oxygen; N: nitrogen. $\%O = 100 - (C + H + N + S_T)$

5.6.2 Bulk Carbon Isotopes

The bulk stable carbon isotopic ($\delta^{13}C$) values for the coals vary between -29.4 and -24.2‰, with mean values of -27.8‰ and -25.4‰ for the Sarawak Basin and Benue Trough coals, respectively (Table 5.11). These values show that the Benue Trough coals are isotopically heavier than the Sarawak Basin coals and thus indicative of different paleoflora and/or environmental conditions. Furthermore, within the Sarawak Basin, coal samples from Mukah coalfield have more positive $\delta^{13}C$ values that suggest slightly different vegetation.

5.6.3 Bulk Hydrogen Isotopes

The hydrogen isotopic ($\delta\Delta$) values of the analysed samples vary widely between a maximum -66.4‰ and minima -173.5‰. The Sarawak Basin coals are relatively depleted in deuterium with $\delta\Delta$ values ranging from -173.5‰ to -91.0‰. In contrast, the Benue Trough coals are relatively enriched in deuterium and show more positive $\delta\Delta$ values, fluctuating between -117.0‰ and 66.4‰ (Table 5.11). Both groups of coals show wide variation in $\delta\Delta$ values, which are suggestive of fluctuating environmental conditions. However, the marked difference in $\delta\Delta$ values of the Sarawak Basin (mean -127.8‰) and Benue Trough (mean -106.9‰) implies relatively distinct conditions.

5.7 Pyrolysis-Gas Chromatography

The representative pyrolysate gas chromatograms of the studied Sarawak Basin and Benue Trough coals are shown in Figure 5.12.

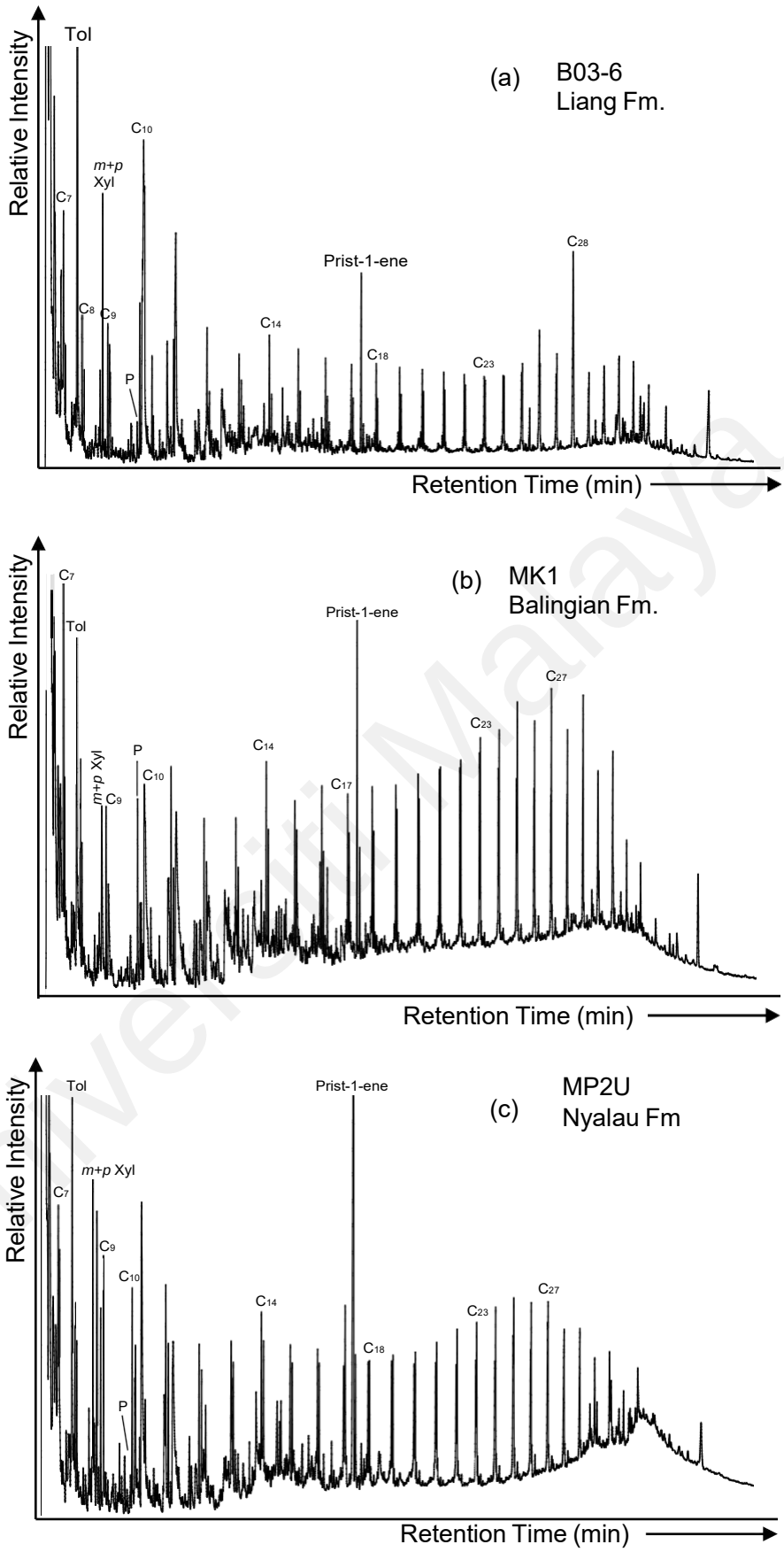

Figure 5.12: Representative pyrolysate gas chromatograms of the studied coals. C_x: *n*-alkane + *n*-alk-1-ene doublets; Tol: toluene P: phenol; *m*+*p* Xyl: meta- + para-xylene.

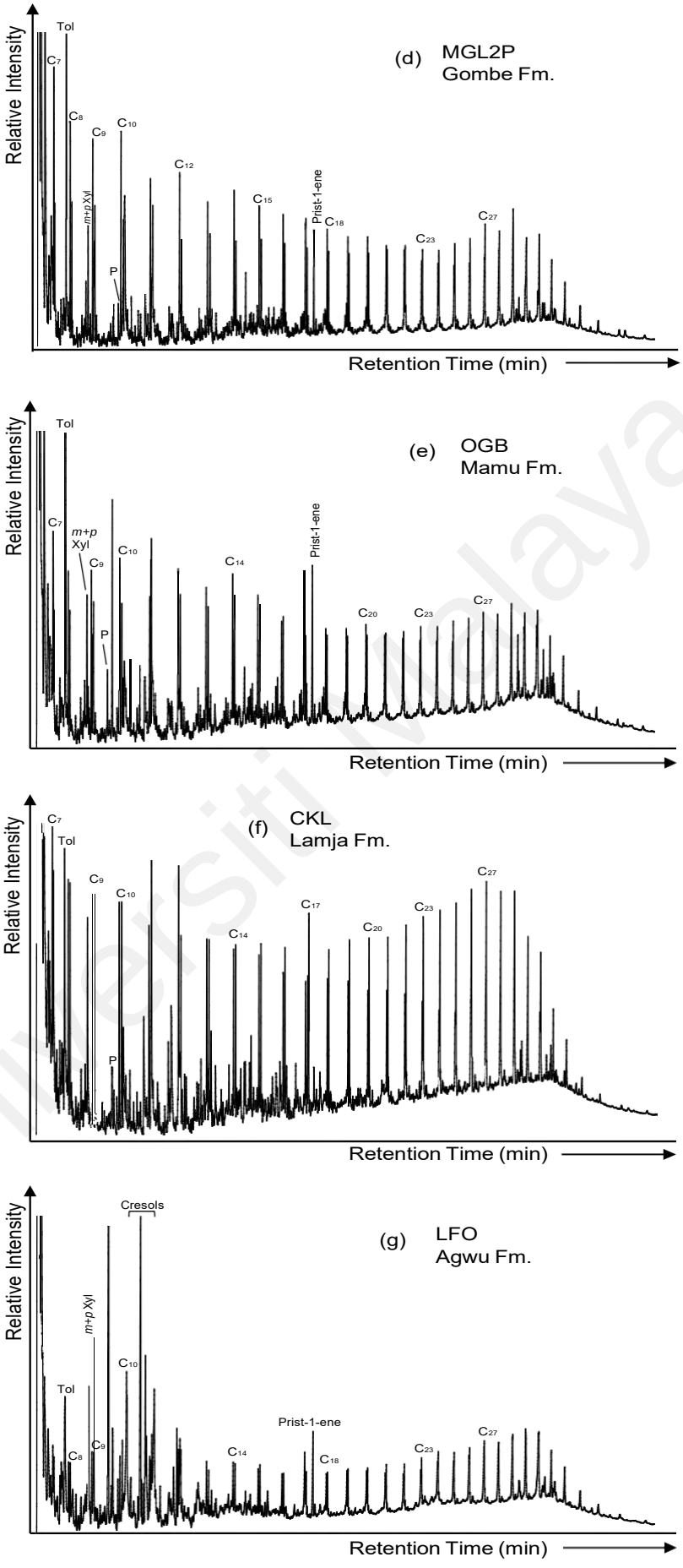

Figure 5.12, continued.

The pyrograms show that prist-1-ene is the most abundant hydrocarbon in most of the Sarawak Basin coals. However, its abundance is comparably lower in the Benue Trough coals. In addition, the pyrograms display abundant aromatic compounds such as toluene, xylene, phenol, and cresols. Geochemical parameters based on the relative abundances of identified compounds in the Py-GC pyrograms are presented in Table 5.12.

Table 5.12: Py-GC parameters for the studied coals.

Sample	Type Index	C_8/xy	cad/xy	C_8 (%)	xy (%)	Phenol (%)
B01-1	2.08	0.48	0.08	29.4	61.2	9.4
B01-4	2.17	0.46	0.08	28.6	61.9	9.5
B01-5	2.21	0.45	0.07	28.1	62.2	9.6
B02-4	2.80	0.36	0.07	23.7	66.3	10.1
B03-2	1.74	0.58	0.05	33.3	57.9	8.8
B03-3	1.68	0.60	0.05	34.2	57.5	8.2
B03-6	2.94	0.34	0.05	22.7	66.7	10.7
E55-2	2.13	0.47	0.05	28.8	61.3	9.9
L04A-1	1.79	0.56	0.07	32.2	57.5	10.3
L04B-1	1.77	0.57	0.03	33.3	59.0	7.7
ML46A-6	1.49	0.67	0.05	36.9	54.9	8.2
ML46A-7	1.91	0.52	0.03	31.2	59.6	9.2
BG1	1.38	0.73	0.09	37.2	51.2	11.6
BG2	-	-	-	-	-	-
0464A	1.88	0.53	0.11	31.1	58.5	10.4
M03-2	1.89	0.53	0.31	30.6	58.1	11.3
MK1	0.83	1.20	0.20	48.0	40.0	12.0
MK2	0.63	1.58	0.33	51.4	32.4	16.2
MK3A	0.92	1.09	0.35	43.1	39.7	17.2
MK3B	-	-	-	-	-	-
MP1L	1.70	0.59	0.06	31.7	53.8	14.5
MP1M	1.64	0.61	0.05	29.7	48.6	21.6
MP1U	-	-	-	-	-	-
MP2L	2.08	0.48	0.07	29.9	62.1	8.0
MP2U	1.49	0.67	0.16	36.2	54.0	9.8
MP3L	1.09	0.92	0.14	42.7	46.6	10.7
MP3M	-	-	-	-	-	-
MP3U	0.79	1.27	0.13	50.0	39.3	10.7
MP4L	1.42	0.71	0.14	36.6	51.9	11.5
MP4M	1.49	0.67	0.15	35.6	52.9	11.5
MP4U	1.71	0.58	0.10	32.8	56.3	10.9

C_8: *n*-1-octene; xy: m(+p)-xylene; cad: cadalene; Type Index = m(+p)-xylene/*n*-1-octene; C_8 (%) = [C_8/(C_8 + xy + Phenol) x 100]; xy (%) = [xy/(C_8 + xy + Phenol) x 100]; Phenol (%) = [Phenol/(C_8 + xy + Phenol) x 100].

Table 5.12, continued.

Sample	Type Index	C_8/xy	cad/xy	C_8 (%)	xy (%)	Phenol (%)
MP5L	1.55	0.65	0.13	34.4	53.3	12.2
MP5M	1.22	0.82	0.12	39.8	48.4	11.8
MP5U	1.96	0.51	0.09	29.4	57.8	12.8
MP6L	1.50	0.67	0.04	35.8	53.8	10.4
MP6M	1.94	0.51	0.07	30.5	59.3	10.2
MP6U	1.87	0.53	0.05	31.1	58.1	10.8
MP7L	1.91	0.52	0.06	30.9	59.0	10.1
MP7M	1.52	0.66	0.09	35.5	54.1	10.5
MP7U	1.57	0.64	0.10	34.6	54.2	11.2
MGL3A	1.33	0.75	0.10	38.3	51.1	10.6
MGL4A	0.83	1.21	0.07	49.2	40.7	10.2
MGL1C	1.21	0.83	0.09	40.6	48.9	10.6
MGL2A	0.79	1.27	0.13	50.9	40.0	9.1
MGL2B	1.20	0.83	0.11	41.7	50.0	8.3
MGL2H	0.94	1.06	0.06	47.3	44.6	8.0
MGL2I	0.77	1.30	0.05	52.2	40.3	7.5
MGL2O	0.94	1.06	0.06	47.1	44.3	8.6
MGL2P	0.55	1.81	0.09	57.6	31.8	10.6
MGL2T	0.97	1.03	0.09	43.6	42.3	14.1
AFZ	0.90	1.11	0.14	34.2	30.9	34.9
ENG	1.19	0.84	0.11	38.1	45.2	16.7
IMG	0.82	1.23	0.18	46.3	37.8	15.9
OGB	0.86	1.16	0.16	30.5	26.3	43.1
OKB	0.85	1.18	0.11	48.6	41.3	10.1
WKP	0.74	1.36	0.17	50.9	37.4	11.7
CKL	0.87	1.15	0.24	47.0	40.9	12.1
LMZ1	1.86	0.54	0.10	30.6	56.9	12.5
LFO	3.00	0.33	0.07	11.4	34.2	54.4
SKJ	2.70	0.37	0.04	12.7	34.2	53.2

5.8 Pyrolysis- and Thermochemolysis-GC-MS Products

5.8.1 Pyrolysis-GC-MS

Over 230 compounds were identified in the Py-GC-MS-derived products of the analysed coals. The proportions of the compounds relative to the total quantified peak areas (TQPA) are listed in Appendix C while the average proportions of the main groups of products and maturity ratios are presented in Table 5.13.

Table 5.13: Average proportion (% TQPA) of major groups and maturity ratios of the products derived from Py-GC-Ms and THM-GC-MS analyses.

Analysis	Compound Groups and Ratios	Sarawak Basin	Benue Trough
Pyrolysis-gas chromatography-mass spectrometry (Py-GC-MS)	*n*-Alkanes (%)	21.36	33.62
	n-Alkenes (%)	12.31	17.01
	Isoprenoid Alkanes (%)	1.71	3.48
	Isoprenoid Alkenes (%)	4.08	1.17
	Monocyclic aromatic hydrocarbons (%)	13.54	15.99
	Lignin (%)	0.81	0.07
	Phenols (%)	19.81	9.14
	Catechols (%)	3.05	0.13
	Sesquiterpanes (%)	5.21	1.86
	Alkyl-substituted PAHs (%)	6.89	7.60
	Oxygen-substituted PAHs (%)	1.78	0.92
	non-substituted PAHs (%)	1.02	1.69
	Total O-aromatics (%)	12.80	9.88
	Total resin-aromatics (%)	23.67	9.34
	Total methylene chain compounds (%)	39.57	55.28
	Pristane Formation Index (PFI)	0.04	0.47
	Alkylation index of phenols (AI_phen)	0.20	0.38
	Dehydroxylation index (DHI-2)	0.21	0.25
	Cadinene aromatization index (CAI)	0.41	0.64
Thermochemolysis-gas chromatography-mass spectrometry (THM-GC-MS)	Alkenes and alkanes (%)	22.02	49.29
	Isoprenoids (%)	4.77	5.92
	Benzenecarboxylic acid methyl esters (%)	7.67	13.08
	$< C_{20}$ Fatty acid methyl esters (%)	4.50	10.97
	$\geq C_{20}$ Fatty acid methyl esters (%)	36.55	7.62
	Polycyclic aromatic hydrocarbons (%)	5.16	6.81
	Methoxybenzenes (%)	12.42	3.57
	Sesquiterpanes (%)	2.65	1.62
	Total fatty acid methyl esters (%)	41.05	18.59
	Total methylene chain compounds (%)	67.84	73.81
	Pristane Formation Index (PFI)	0.03	0.47
	Phytane Oxidation Index (POI)	0.54	0.13

TQPA: total quantified peak areas; PAHs: polycyclic aromatic hydrocarbons; AI_phen: alkylation index of the phenols = C_2–C_4/C_0–C_4 alkylphenols; DHI-2: dehydroxylation index = alkylphenols/alkyl-MAHs; Pristane Formation Index = pristane/(pristane + pristenes); Phytane Oxidation Index = homophytanic acid/phytane.

The products derived from the Py-GC-MS analysis of the Sarawak Basin and Benue Trough coals are dominated by C_9 to C_{35} *n*-alkanes, C_{10} to C_{33} *n*-alkenes, and isoprenoid alkanes and alkenes (Figure 5.13). However, aromatic moieties also constitute a significant proportion of the pyrolysates. The relative proportions of *n*-alkanes and *n*-alkenes are higher in the Benue Trough coals (avg. 50.64%) than in the Sarawak Basin coals (avg. 37.77%), whilst the proportions of total aromatic hydrocarbons are relatively higher in the Py-GC-MS-derived products of the Sarawak coals.

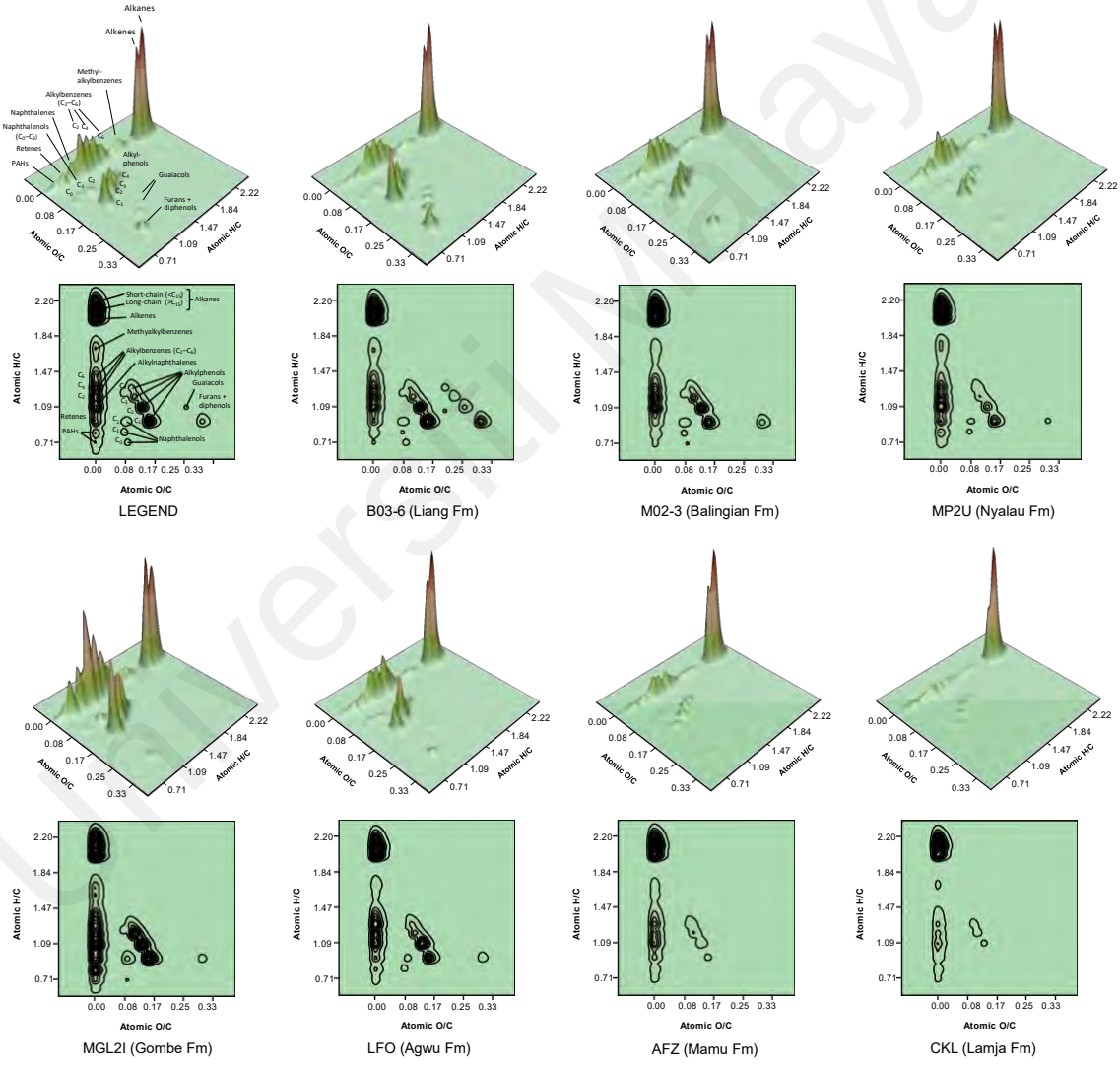

Figure 5.13: Surface density plots showing relative proportions of Py-GC–MS products of representative samples.

Monocyclic aromatic hydrocarbons (MAHs) with up to 5-carbon atoms in methyl groups account accordingly for an average of 13.54% and 15.99% of the TQPA of the Sarawak Basin and Benue Trough coal pyrolysates. Other identified compounds are phenols and sesquiterpenes, which were observed in relatively higher proportions in the coals from Sarawak Basin (avg. 19.81% and 5.21%) than from Benue Trough (avg. 9.14% and 1.86%). Additionally, long-chain alkylbenzenes, alkyl-substituted PAHs, O-substituted PAHs, non-substituted PAHs, methoxyphenols, catechols, and S-containing compounds were observed in lower proportions (Appendix C). Although most of the alkyl-PAHs and sesquiterpenes can be attributed to polymerized resin derivatives, phenols, catechols, and perhaps O-substituted PAHs are mostly derived from the lignin-containing tissues of vascular plants (Kaal et al., 2017).

5.8.2 THM-GC-MS

The THM-derived products of the studied Sarawak Basin and Benue Trough coals are generally dominated by *n*-alkanes, *n*-alkenes and fatty acid methyl esters (FAMEs). Other major groups of compounds observed include isoprenoids, sesquiterpanes, diterpanes, methoxybenzenes, benzenecarboxylic acid methyl esters (BCAs), polycyclic aromatic hydrocarbons (PAHs) and terpenoids (Appendix D). Of note, carbohydrate products were below the detection limit in all the analysed coal samples. The relative proportions of these major groups are shown in Figure 5.14.

The summed proportion of C_{11} to C_{35} *n*-alkanes and *n*-alkenes relative to the total quantified peak area (TQPA) for the analysed Sarawak Basin and Benue Trough coals. The relatively higher proportion of *n*-alkanes and *n*-alkenes in the Benue Trough samples is possibly due to their relatively higher thermal maturity. In contrast, the

proportion of isoprenoid hydrocarbons for both groups of coals is similar, ranging accordingly from 1.06 to 7.54 (avg. 4.77%) and 1.87 to 11.04 (avg. 5.92%) for the Malaysian and Nigerian coals. The isoprenoid hydrocarbons include 4,8,12,16-tetramethylheptadecan-4-olide, an isoprenoid fatty acid derivative and phytane oxidation product that is observed in low-rank coals (Kaal et al., 2017). Furthermore, the abundances of short-chain (< C_{20}) FAMEs are comparably higher in coals from Benue Trough (1.94-20.13%) than in Sarawak Basin (1.86-9.57%) whilst the abundances of long-chain (≥ C_{20}) FAMEs are relatively higher in the Sarawak Basin (10.56-59.27%) than the Benue Trough (0.17-35.37%).

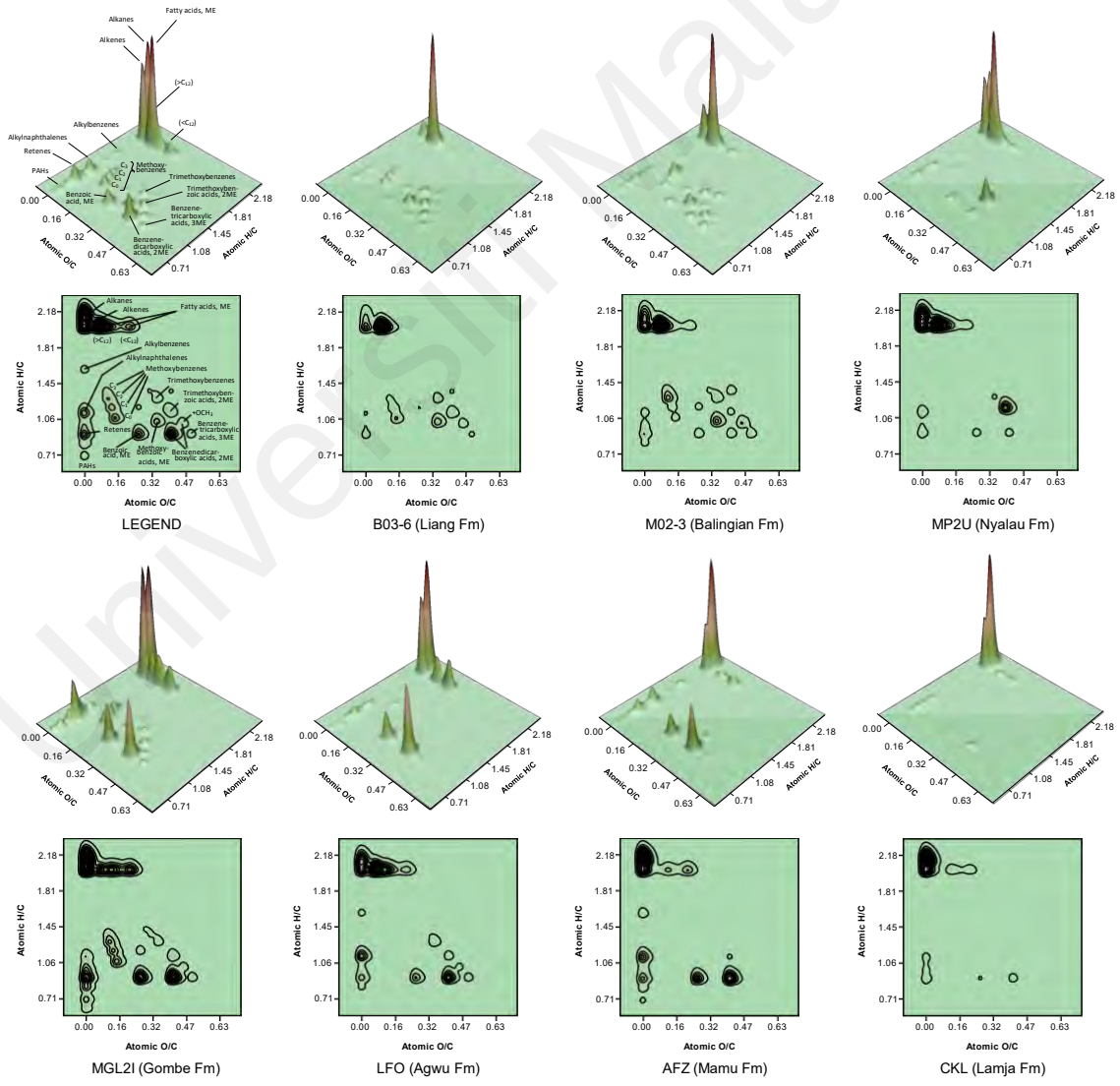

Figure 5.14: Surface density plots showing relative proportions of THM-GC–MS products of representative samples.

The relative abundance of FAMEs is vastly higher in the Sarawak Basin coals (avg. 41.05%) than in the Benue Trough coals (avg. 18.59%), possibly indicating the relative proportion of plant epicuticular waxes. However, the summed abundances of methylene chain compounds (MCC) relative to the TQPA are slightly higher in coals from Benue Trough (avg. 73.81%) than in Sarawak Basin (avg. 67.84%; Figure 5.15). The proportion of PAHs in the coals shows similar trends with average relative abundances of 5.16% and 6.81% for the Sarawak Basin and Benue Trough samples, respectively.

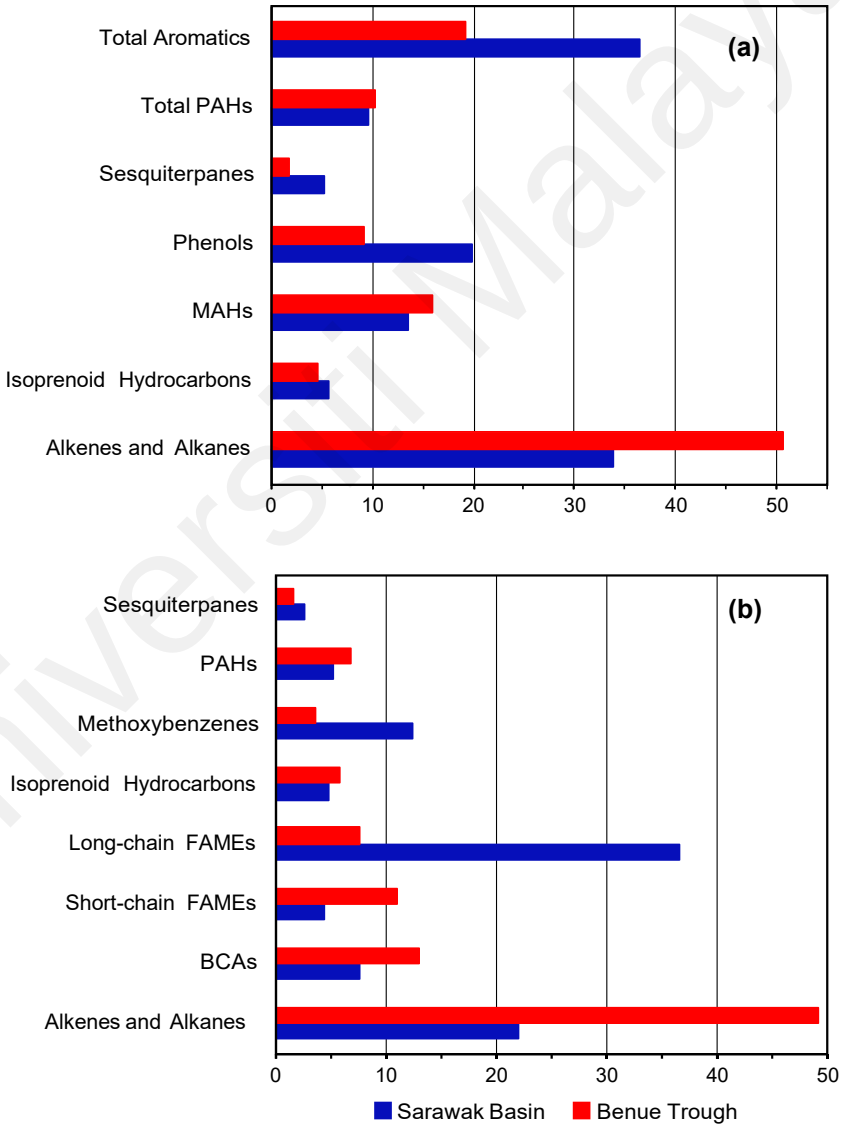

Figure 5.15: Bar graphs of the average relative proportion of major compounds in products obtained from (a) – Py-GC-MS and (b) – THM-GC-MS analysis of the analysed coals. MAHs: monocyclic aromatic hydrocarbons; PAHs: polycyclic aromatic hydrocarbons; FAMEs: fatty acid methyl esters; BCAs: Benzenecarboxylic acid methyl esters.

Additionally, the BCAs which possibly reflect the oxidized aromatic kerogen fractions in the analysed coals are observed in relatively similar abundances, varying widely from 2.19 to 26.96% and 1.98 to 23.47%. Furthermore, for both Py-GC-MS and THM-GC-MS products, the Nyalau Formation coals show the highest proportions of sesquiterpenoid derivatives (12–15% of TQOA) when compared with other samples (< 4% of TQPA), which mostly reflects the abundance of resinite maceral. This finding is supported by the petrographic study of the Merit-Pila coals by Abdullah (1997) which concluded that the coals are rich in liptinitic macerals. Additionally, sample IMG (Mamu Formation of Benue Trough) contains the highest proportion of organosulfur compounds (1.0 % of TQPA), producing a significant peak of elemental sulfur upon pyrolysis. This generally indicates high abundances of pyritic and organic sulfur in the coal.

The diagenetic effect on coals often varies for different constituents, and therefore, principal component analysis (PCA) is an improved technique to evaluate the overall maturity or rank effects on molecular composition (Kaal et al., 2017). PCA results of the distribution of Py-GC-MS and THM-GC-MS products are presented in Appendix E. The RC1 scores are mostly positive and negative for the Benue Trough and Sarawak Basin coals, respectively, and are thus indicative of a narrow range of coal rank and relatively distinct organic matter source inputs (Figure 5.16; Kaal et al., 2017). This is possibly due to the greater input of terrigenous organic matter in the Sarawak coals as some of the compounds with negative loadings on RC1 include plant-derived compounds such as methoxyphenols, catechols, phenols, and terpenoids. Conversely, the Benue Trough coals are positively loaded possibly due to the predominant inputs of short-chain alkanes and alkenes, isoprenoid alkanes and alkyl-PAHs that suggest a substantial algal organic matter contribution.

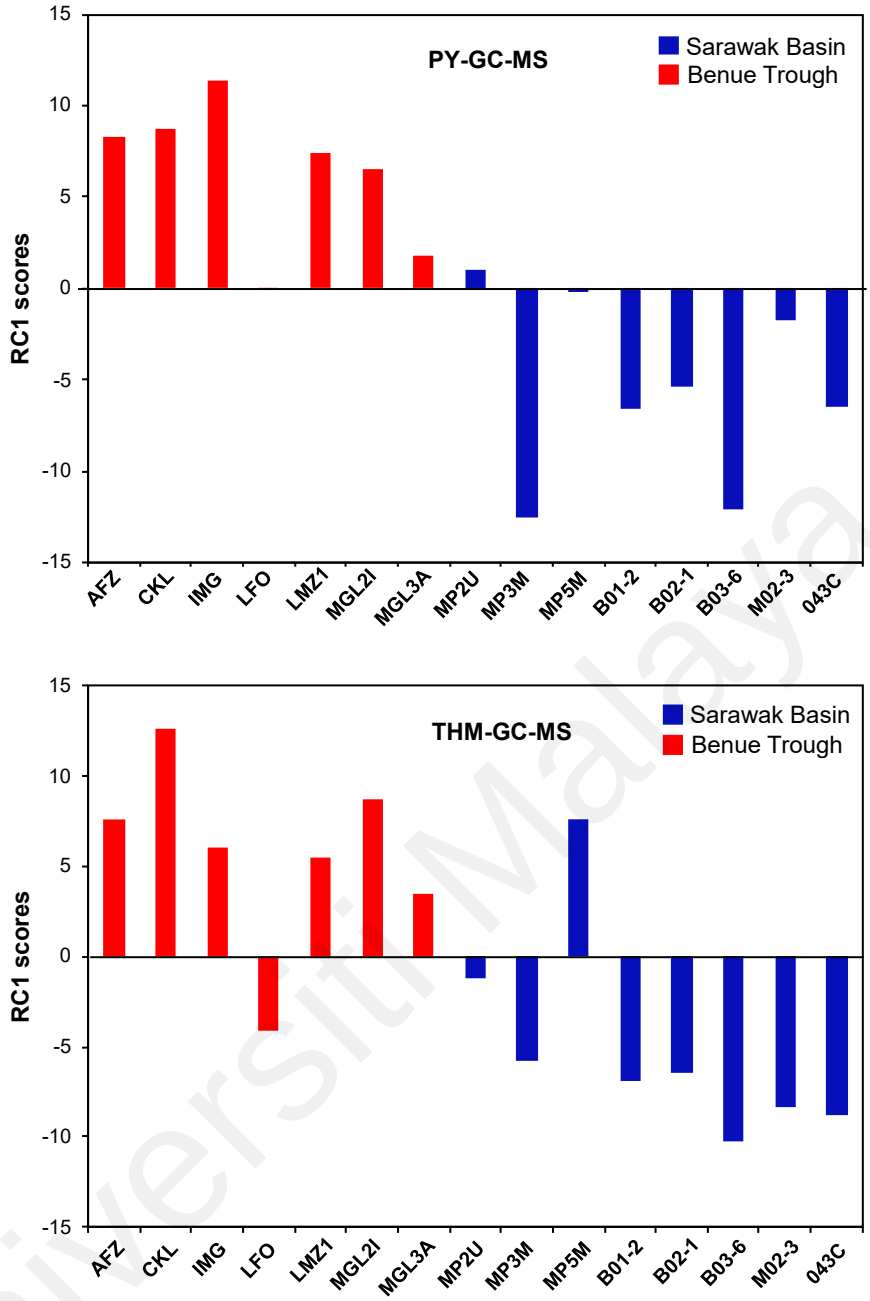

Figure 5.16: RC1 scores of Py-GC-MS and THM-GC-MS products.

Maturity parameters based on the abundance of specific compounds such as the alkylation index of phenols (Al_phen), pristane formation index (PFI) and phytane oxidation index (POI) were calculated for the coals and the ratios presented in Table 5.13. Al_phen ratios of Py-GC-MS products for the studied coals are relatively higher for the Benue Trough coals (0.11-0.65) than the Sarawak Basin coals (0.07-0.31), indicating relatively higher diagenetic impact (Kaal et al., 2017). The PFI is based on

the preferential increase in pristane abundance and the accompanying loss of pristenes with burial whilst the POI is based on the relative loss of homophytanic acid (methyl ester) gamma-lactone over phytane during early diagenesis (Goossens et al. 1988; Kaal et al., 2017). As expected from R_o values, the relatively lower PFI and higher POI and CAI ratios for the Sarawak Basin coals reflect relatively lower thermal maturity. Additionally, the cadinene aromatization index (CAI), which reflects the degree of resin condensation shows the highest values (>0.7) for the Mamu Formation coals and lowest values for Nyalau Formation coals.

5.9 Molecular Composition

The extractable organic matter (EOM) yield and relative proportions of aliphatic hydrocarbons, aromatic hydrocarbons and NSO compounds are recorded in Table 5.14. The EOM yield for the Sarawak coals (avg. 63532 ppm) is considerably higher than the yield for Benue (avg. 37352 ppm) coals. For the Sarawak Basin samples, the EOM yield for the Nyalau Formation coals (30643 to 224779 ppm) is considerably higher than the yield for Balingian Formation (21596 to 54551 ppm) and Liang Formation (26312 to 49695 ppm) coals. Additionally, the fractionated extracts are composed mainly of NSO compounds with a low proportion of hydrocarbons, typical of samples with generally low thermal maturity (Miles, 1994; Peters et al., 2005). The proportion of hydrocarbons in the extracts varies between 6.4 and 36.8% and with average values of 12.8% and 17.6% in the Sarawak Basin and Benue Trough coals, respectively. Aromatic hydrocarbons predominate over aliphatic hydrocarbons in all the coal samples. However, the average proportion of aliphatic hydrocarbons in the Benue Trough (15.7% of EOM) coals is relatively higher than in the Sarawak Basin (8.0% of EOM) coals (Figure 5.17).

Table 5.14: Group compositional data for the studied coals.

Sample	EOM (ppm)	HC (ppm)	%Sat[a]	%Aro[a]	%Polar[a]	%HC[a]	Sat/ Aro	HC/ Polar
B01-1	28889	4690	8.9	35.4	55.7	44.3	0.25	0.80
B01-4	43946	5630	9.8	28.2	62.0	38.0	0.35	0.61
B01-5	36988	4521	9.0	31.8	59.2	40.8	0.28	0.69
B02-4	48590	3871	6.6	25.7	67.6	32.4	0.26	0.48
B03-2	34500	4556	7.8	38.5	53.7	46.3	0.20	0.86
B03-3	41740	4479	7.2	30.8	62.0	38.0	0.23	0.61
B03-6	45537	5374	9.7	30.8	59.5	40.5	0.31	0.68
E55-2	36992	3541	8.2	21.5	70.4	29.6	0.38	0.42
L04A-1	26312	4334	16.9	31.5	51.6	48.4	0.54	0.94
L04B-1	35313	3685	11.2	30.2	58.7	41.3	0.37	0.70
ML46A-6	30628	3962	7.1	33.2	59.8	40.2	0.21	0.67
ML46A-7	43353	4066	6.7	30.0	63.2	36.8	0.22	0.58
BG1	49695	5919	6.3	15.2	78.5	21.5	0.41	0.27
BG2	26634	2763	4.5	11.1	84.4	15.6	0.41	0.19
0464A	54551	5126	7.8	24.1	68.1	31.9	0.32	0.47
M03-2	21596	4964	10.7	35.7	53.6	46.4	0.30	0.86
MK1	26066	5480	21.0	10.5	68.5	31.5	2.00	0.46
MK2	32255	5315	17.5	20.2	62.3	37.7	0.86	0.61
MK3A	48867	6312	10.2	42.2	47.6	52.4	0.24	1.10
MK3B	47364	4834	7.2	27.2	65.6	34.4	0.26	0.52
MP1L	71612	6015	7.7	12.9	79.4	20.6	0.60	0.26
MP1M	43708	4513	8.9	19.8	71.3	28.7	0.45	0.40
MP1U	30643	3699	12.4	15.3	72.4	27.6	0.81	0.38
MP2L	142516	9848	3.0	7.0	90.0	10.0	0.43	0.11
MP2U	148241	9506	3.8	8.7	87.5	12.5	0.43	0.14
MP3L	70296	11180	6.1	15.2	78.7	21.3	0.40	0.27
MP3M	224779	58922	9.8	31.7	58.5	41.5	0.31	0.71
MP3U	40421	6569	13.9	29.1	57.1	42.9	0.48	0.75
MP4L	107776	11891	4.0	11.0	85.0	15.0	0.36	0.18
MP4M	94824	11408	3.2	11.5	85.3	14.7	0.28	0.17
MP4U	81734	11651	10.0	21.9	68.1	31.9	0.45	0.47
MP5L	84252	9298	5.5	9.9	84.7	15.3	0.55	0.18
MP5M	78705	10955	5.3	12.6	82.1	17.9	0.42	0.22
MP5U	102254	14661	5.2	16.3	78.4	21.6	0.32	0.28
MP6L	56064	11823	4.5	22.0	73.5	26.5	0.20	0.36
MP6M	85058	5973	1.9	6.2	91.9	8.1	0.31	0.09
MP6U	47027	5675	7.4	20.6	72.0	28.0	0.36	0.39
MP7L	97668	9216	3.1	9.9	87.0	13.0	0.31	0.15
MP7M	110059	10546	3.4	9.2	87.5	12.5	0.37	0.14
MP7U	63820	9903	7.1	34.0	58.9	41.1	0.21	0.70

EOM: Extractable organic matter; HC: Hydrocarbons; Sat: Saturated Hydrocarbons; Aro: Aromatic Hydrocarbons; Polar: Polar Compounds. [a]normalised without asphaltenes

Table 5.14, continued.

Sample	EOM (ppm)	HC (ppm)	%Sat[a]	%Aro[a]	%Polar[a]	%HC[a]	Sat/ Aro	HC/ Polar
MGL3A	18576	3058	12.5	27.8	59.7	40.3	0.45	0.68
MGL4A	13296	1794	12.7	21.8	65.6	34.4	0.58	0.53
MGL1C	27977	3041	6.2	21.5	72.3	27.7	0.29	0.38
MGL2A	37025	4886	15.2	26.8	58.0	42.0	0.56	0.72
MGL2B	17112	2184	10.8	19.1	70.1	29.9	0.56	0.43
MGL2H	40994	3271	6.5	19.0	74.5	25.5	0.34	0.34
MGL2I	21240	4182	14.4	26.2	59.4	40.6	0.55	0.68
MGL2O	23374	4209	11.4	29.3	59.3	40.7	0.39	0.69
MGL2P	28280	3439	9.5	26.7	63.7	36.3	0.36	0.57
MGL2T	18974	2241	12.2	19.5	68.3	31.7	0.63	0.46
AFZ	60014	15366	18.5	39.8	41.8	58.2	0.46	1.39
ENG	46062	5635	13.8	25.3	60.9	39.1	0.55	0.64
IMG	24443	8901	29.6	35.0	35.4	64.6	0.85	1.83
OGB	29377	5958	16.5	30.8	52.7	47.3	0.54	0.90
OKB	46222	8701	23.3	29.0	47.7	52.3	0.80	1.10
WKP	26526	4961	14.9	35.4	49.7	50.3	0.42	1.01
CKL	52204	19210	15.9	50.2	33.9	66.1	0.32	1.95
LMZ1	28621	5534	18.7	28.7	52.6	47.4	0.65	0.90
LFO	125596	23650	41.7	11.1	47.2	52.8	3.75	1.12
SKJ	61121	5491	10.2	20.3	69.5	30.5	0.50	0.44

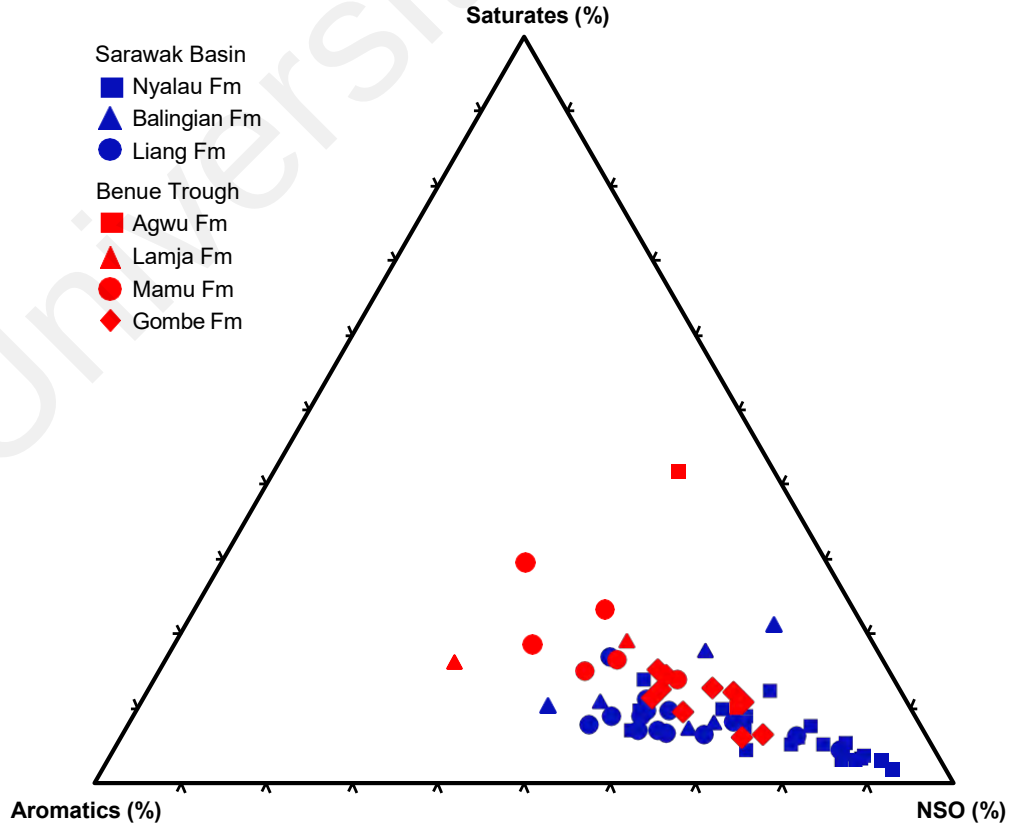

Figure 5.17: Ternary diagram of the molecular composition of the studied coals.

5.10 Aliphatic Hydrocarbons

5.10.1 *n*-Alkane Distribution

The *n*-alkane distribution for all the coals generally ranges from *n*-C_{15} to *n*-C_{35}. Representative *m/z* 85 chromatograms are shown in Figure 5.18. The coals are dominated by high molecular weight (MW) alkanes (≥ *n*-C_{27}) with strong odd-even predominance (except in samples CKL and LMZ1), indicating the dominant contribution of vascular plants to paleovegetation (Peters et al., 2005). Whilst *n*-C_{29} is the most abundant alkane in the Nigerian coals, the alkane distribution in the Malaysian coals is mostly dominated by *n*-C_{31}, thus, suggesting varying paleovegetation and paleoclimate (Schwark et al., 2002). Medium MW n-alkanes (*n*-C_{21} to *n*-C_{26}) are present in subordinate abundance in the samples while low MW alkanes (≤ *n*-C_{20}) are only present in low concentrations (Figure 5.19).

n-alkane ratios have been widely used to determine the maturity and organic matter input in sediments (Marzi et al., 1993; Bourbonniere & Meyers, 1996; Zheng et al., 2007). The carbon preference index (CPI) and odd-over-even predominance (OEP) values of all studied coals are ≥ 1, ranging from 1.1 to 5.9 and 1.0 to 6.9, respectively (Tables 5.15-5.16). The CPI values are, however, relatively higher in the coals from Sarawak Basin (avg. 2.9) than from Benue Trough (avg. 2.3). Similarly, the OEP values for the Sarawak Basin coals (avg. 3.2) are generally higher than the Benue Trough coals (avg. 2.9). The values of the terrigenous aquatic ratio (TAR), a relative measure of organic matter input from land and lake flora, range from 2.5 to 32.4 and 2.2 to 20.9, with average values of 15.8 and 7.4 in the studied Sarawak Basin and Benue Trough samples, respectively.

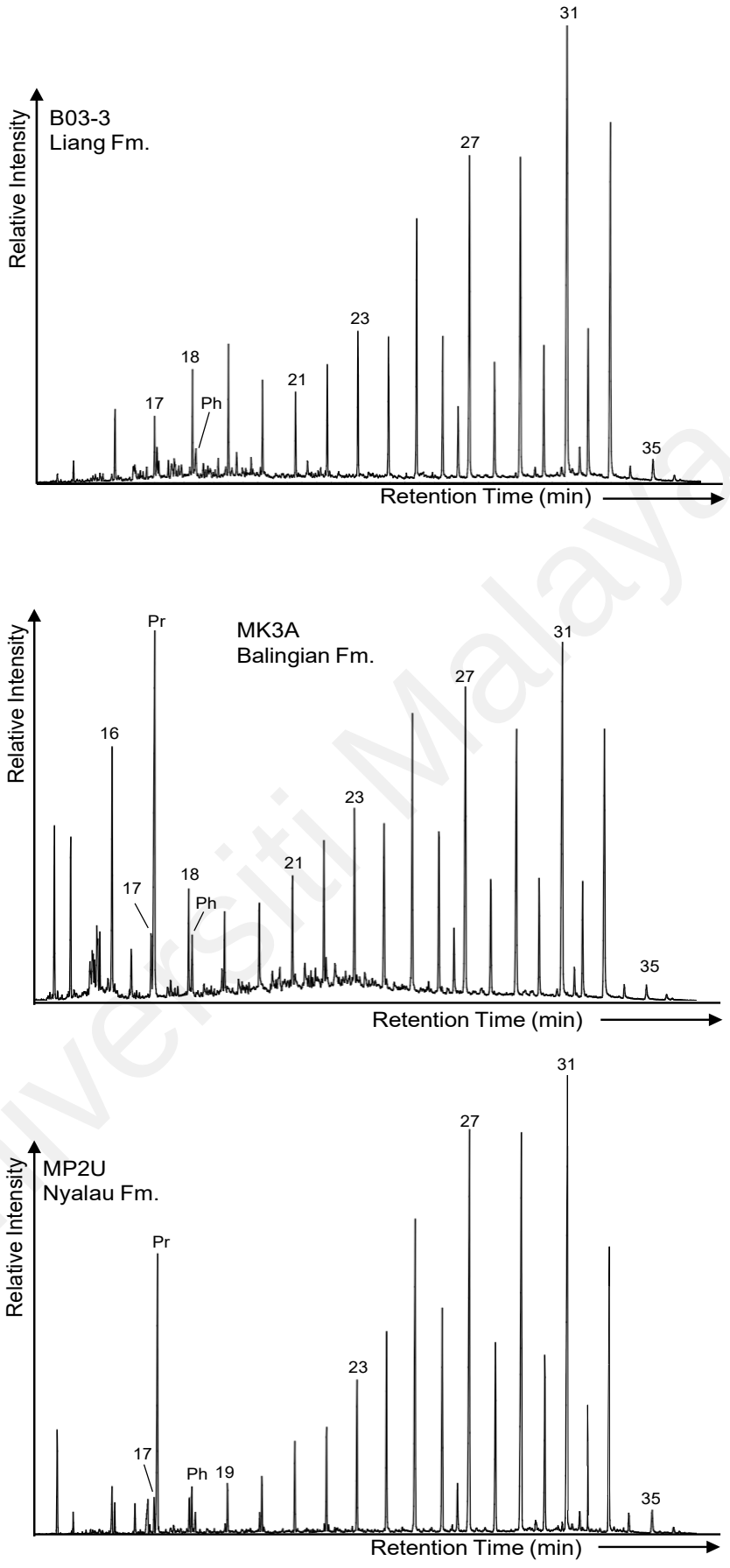

Figure 5.18: *m/z* 85 chromatograms of saturated hydrocarbon fractions of selected samples showing the *n*-alkane and isoprenoid distribution.
Numbers indicate carbon number. Pr = Pristane and Ph = Phytane.

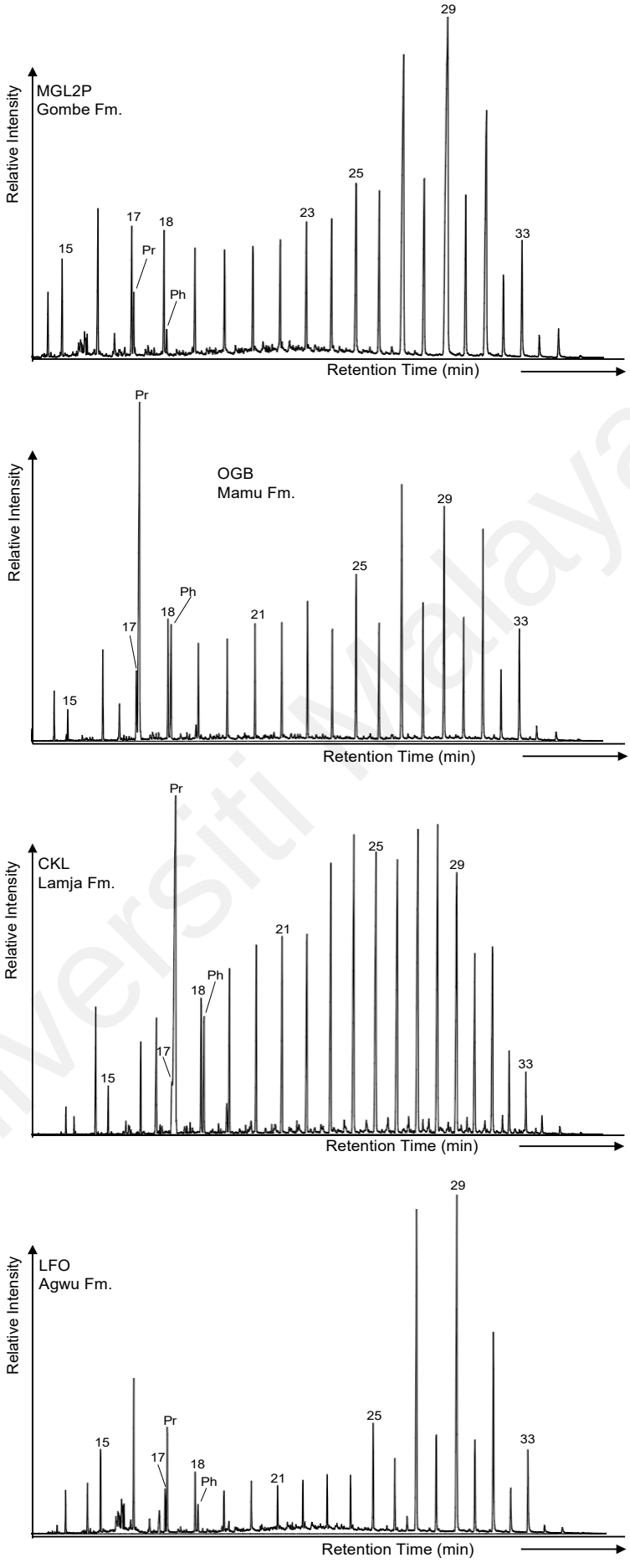

Figure 5.18, continued.

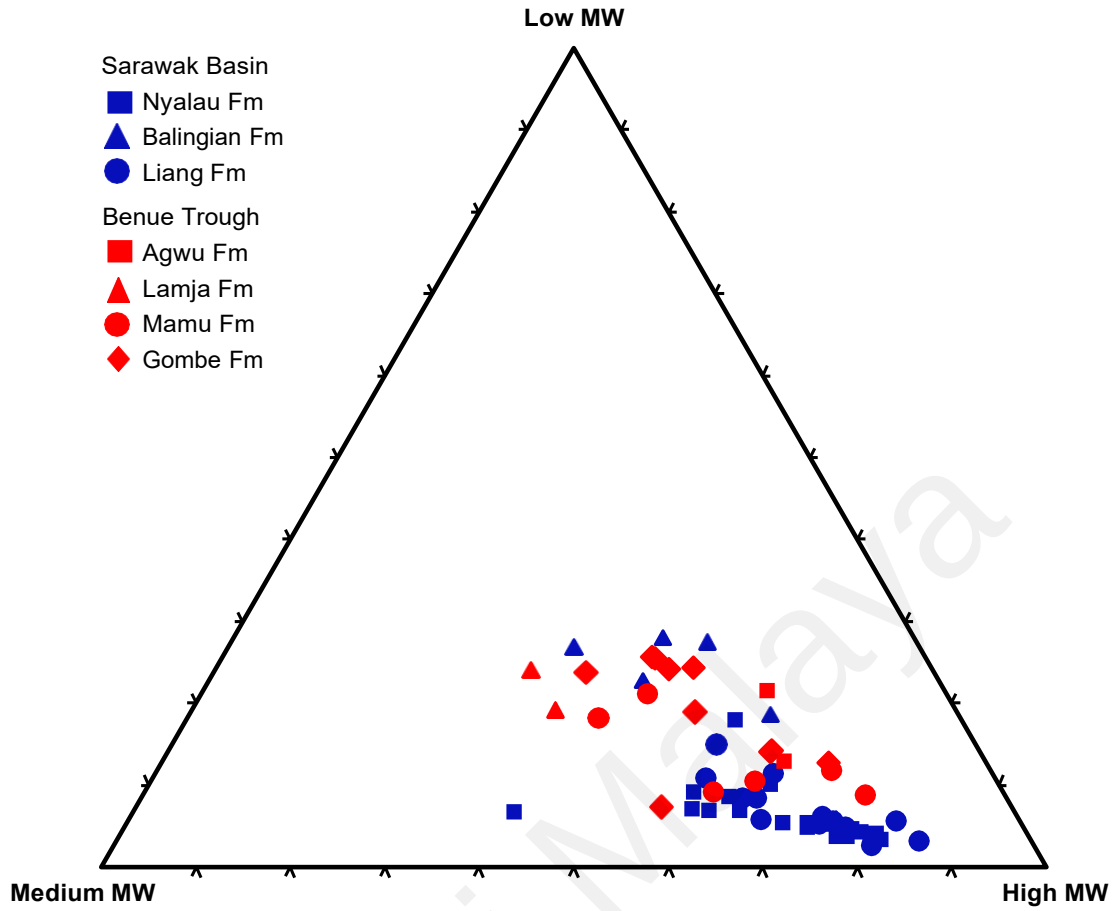

Figure 5.19: Ternary plot of *n*-alkane distribution in the studied coals showing proportion of high (C_{27-33}), medium (C_{21-26}) and low (C_{15-20}) molecular weight (MW) homologues.

The relative abundance of acyclic isoprenoids pristane (Pr) and Phytane (Ph) is widely used to infer redox conditions during sedimentation and diagenesis (Didyk, 1978). Although the Pr/Ph parameter is affected by thermal maturity (Peters et al., 2005), such effect is negligible since the studied coals are generally of low rank. Pr and Ph are observed in all the studied samples, and Pr/Ph ratios are relatively higher in the Sarawak Basin coals, varying from 0.6 to 14.0 (avg. 4.8). The Benue Trough coals show relatively lower Pr/Ph ratios, ranging from 1.5 to 4.8 and with an average of 3.0. In addition, *n*-C_{18} predominates over Ph in most of the samples (except BG1, AFZ and IMG), while Pr generally predominates over *n*-C_{17} except in some Liang and Gombe Formation coals (Tables 5.15-5.16).

Table 5.15: *n*-Alkane parameters for coals from Sarawak Basin, Malaysia.

Sample	C_{max}	CPI	OEP	TAR	WI	ACL	P_{aq}	P_{wax}	Pr/ Ph	Pr/ C_{17}
B01-1	C_{31}	3.3	4.0	22.6	12.9	29.2	0.21	0.84	3.7	1.4
B01-4	C_{27}	3.0	3.7	8.6	6.8	29.0	0.41	0.71	4.0	0.9
B01-5	C_{31}	3.5	3.8	29.3	14.4	29.2	0.30	0.77	2.0	0.8
B02-4	C_{31}	2.4	2.7	10.5	6.5	29.0	0.25	0.82	1.8	0.6
B03-2	C_{31}	3.5	3.6	22.7	13.2	29.4	0.21	0.83	1.0	0.5
B03-3	C_{31}	2.3	2.8	5.3	4.6	29.3	0.34	0.73	1.0	0.5
B03-6	C_{31}	3.3	3.5	32.4	16.0	29.4	0.21	0.84	0.7	0.2
E55-2	C_{31}	2.6	3.1	13.3	9.3	29.1	0.28	0.79	2.8	0.7
L04A-1	C_{31}	5.0	4.9	30.0	13.8	29.3	0.15	0.89	2.0	0.7
L04B-1	C_{31}	3.4	3.6	-	-	29.4	0.19	0.85	-	-
ML46A-6	C_{31}	2.6	3.1	13.0	9.3	29.1	0.30	0.77	2.0	0.7
ML46A-7	C_{27}	2.5	2.6	11.9	9.2	29.0	0.32	0.77	5.0	2.5
BG1	C_{31}	5.9	6.6	31.7	24.8	29.4	0.12	0.91	0.9	0.6
BG2	C_{27}	3.7	4.2	17.1	14.9	28.8	0.28	0.81	2.7	0.7
0464A	C_{27}	1.3	1.8	2.7	2.5	28.8	0.49	0.63	1.2	1.1
M03-2	C_{31}	3.5	4.6	3.4	2.4	29.0	0.32	0.77	2.3	1.8
MK1	C_{27}	3.9	4.2	19.9	14.0	28.9	0.27	0.81	4.7	4.7
MK2	C_{31}	2.9	3.6	4.7	3.4	29.2	0.26	0.81	4.2	3.1
MK3A	C_{31}	2.0	2.4	3.0	2.9	29.1	0.43	0.67	6.3	6.3
MK3B	C_{31}	2.1	2.9	2.5	2.2	29.2	0.35	0.73	7.7	4.8
MP1L	C_{31}	3.3	3.2	3.6	3.9	29.0	0.32	0.77	3.7	1.0
MP1M	C_{29}	4.7	6.9	9.4	8.2	28.7	0.27	0.81	4.0	1.7
MP1U	C_{25}	1.6	1.3	13.2	13.2	28.3	0.69	0.52	0.6	1.5
MP2L	C_{29}	2.1	2.7	11.3	11.2	29.2	0.31	0.75	12.5	9.4
MP2U	C_{31}	1.9	2.2	12.4	11.6	29.1	0.35	0.73	14.0	8.3
MP3L	C_{31}	2.4	2.4	16.6	14.5	29.4	0.23	0.81	5.7	4.7
MP3M	C_{31}	3.9	3.7	22.3	17.6	29.9	0.17	0.85	3.0	2.6
MP3U	C_{31}	2.3	2.1	26.0	21.4	29.4	0.22	0.83	4.4	2.7
MP4L	C_{31}	1.8	1.8	8.1	9.0	29.3	0.32	0.74	8.8	3.5
MP4M	C_{31}	1.8	1.9	8.4	8.5	29.3	0.36	0.72	4.6	4.3
MP4U	C_{31}	2.6	2.7	23.2	18.7	29.6	0.22	0.81	7.1	3.6
MP5L	C_{31}	3.0	2.9	22.9	19.6	29.7	0.17	0.86	9.4	6.0
MP5M	C_{31}	2.3	2.2	14.6	13.6	29.4	0.26	0.80	4.1	3.5
MP5U	C_{31}	2.4	2.5	24.0	20.5	29.5	0.21	0.83	5.3	3.3
MP6L	C_{31}	2.8	3.1	19.5	16.5	29.5	0.19	0.84	5.0	2.5
MP6M	C_{31}	2.3	2.5	10.8	10.8	29.2	0.41	0.68	7.1	7.1
MP6U	C_{31}	2.8	2.9	20.4	16.3	29.4	0.24	0.81	6.5	3.3
MP7L	C_{31}	2.9	2.6	23.6	16.9	30.0	0.16	0.86	6.4	3.8
MP7M	C_{31}	2.8	3.2	17.1	14.5	29.5	0.26	0.79	11.0	4.4
MP7U	C_{31}	3.2	3.1	23.9	21.7	29.9	0.14	0.88	7.3	4.8

C_{max}: *n*-alkane maxima; Pr: Pristane; Ph: Phytane; CPI: Carbon Preference Index = $1/2[((C_{23} + C_{25} + C_{27} + C_{29} + C_{31})/(C_{24} + C_{26} + C_{28} + C_{30} + C_{32})) + ((C_{25} + C_{27} + C_{29} + C_{31} + C_{33})/(C_{24} + C_{26} + C_{28} + C_{30} + C_{32}))]$; OEP: Odd Even Predominance = $[C_{29} + 6C_{29} + C_{31}]/[4C_{28} + 4C_{30}]$; TAR: Terrigenous Aquatic Ratio = $[C_{27} + C_{29} + C_{31}] / [C_{15} + C_{17} + C_{19}]$; WI: Wax Index = $\Sigma C_{21\text{-}31}/\Sigma C_{15\text{-}20}$; ACL: Average Chain Length = $[(27 * C_{27}) + (29 * C_{29}) + (31 * C_{31})]/[C_{27} + C_{29} + C_{31}]$; P_{aq}: Proxy Aqueous = $[C_{23} + C_{25}] / [C_{23} + C_{25} + C_{29} + C_{31}]$; P_{wax}: Proxy Wax = $[C_{27} + C_{29} + C_{31}] / [C_{23} + C_{25} + C_{27} + C_{29} + C_{31}]$.

Table 5.15, continued.

Sample	Ph/ C_{18}	$C_{17}/(C_{17} + C_{27})$	$C_{23}/(C_{27} + C_{31})$	C_{23}/C_{25}	C_{23}/C_{29}	C_{23}/C_{31}	C_{27}/C_{31}	C_{29}/C_{31}	C_{33}/C_{29}	C_{33}/C_{31}
B01-1	0.2	0.04	0.08	0.42	0.19	0.14	0.79	0.72	0.71	0.51
B01-4	0.1	0.08	0.13	0.35	0.53	0.27	1.01	0.50	1.55	0.78
B01-5	0.1	0.03	0.12	0.43	0.36	0.20	0.74	0.56	0.70	0.40
B02-4	0.2	0.10	0.09	0.46	0.26	0.18	0.96	0.71	0.94	0.67
B03-2	0.2	0.05	0.09	0.48	0.24	0.14	0.53	0.57	1.18	0.68
B03-3	0.3	0.16	0.19	0.57	0.46	0.31	0.67	0.67	1.11	0.74
B03-6	0.2	0.05	0.08	0.42	0.20	0.13	0.60	0.63	0.98	0.62
E55-2	0.1	0.07	0.13	0.47	0.26	0.24	0.90	0.91	0.57	0.52
L04A-1	0.2	0.05	0.03	0.23	0.09	0.05	0.67	0.59	0.82	0.48
L04B-1	-	-	0.07	0.39	0.17	0.10	0.55	0.59	1.25	0.74
ML46A-6	0.1	0.06	0.15	0.53	0.32	0.29	0.91	0.92	0.65	0.59
ML46A-7	0.3	0.06	0.15	0.52	0.35	0.29	1.02	0.85	0.86	0.74
BG1	1.7	0.04	0.04	0.34	0.09	0.06	0.59	0.69	0.76	0.53
BG2	0.3	0.05	0.09	0.35	0.21	0.20	1.24	0.93	0.93	0.86
0464A	0.4	0.29	0.39	0.82	0.83	0.91	1.35	1.10	0.73	0.81
M03-2	0.8	0.28	0.14	0.51	0.35	0.28	0.98	0.79	0.55	0.43
MK1	0.9	0.05	0.08	0.31	0.18	0.17	1.14	0.95	0.79	0.75
MK2	0.5	0.21	0.11	0.50	0.33	0.19	0.75	0.57	1.64	0.94
MK3A	0.6	0.17	0.27	0.64	0.68	0.51	0.88	0.76	1.01	0.77
MK3B	0.4	0.24	0.21	0.67	0.53	0.37	0.76	0.70	1.02	0.71
MP1L	0.4	0.17	0.15	0.57	0.43	0.30	0.99	0.69	0.89	0.61
MP1M	0.5	0.07	0.11	0.38	0.16	0.29	1.59	1.79	0.27	0.48
MP1U	0.2	0.01	0.31	0.39	1.52	1.08	2.47	0.71	0.73	0.52
MP2L	0.9	0.10	0.16	0.43	0.27	0.27	0.75	1.02	0.82	0.83
MP2U	0.4	0.08	0.18	0.49	0.38	0.33	0.88	0.87	0.72	0.63
MP3L	0.9	0.07	0.11	0.50	0.26	0.17	0.55	0.65	1.01	0.66
MP3M	0.8	0.08	0.05	0.30	0.19	0.06	0.25	0.33	1.83	0.60
MP3U	0.6	0.05	0.09	0.42	0.21	0.14	0.59	0.67	0.91	0.61
MP4L	0.5	0.13	0.16	0.51	0.42	0.26	0.63	0.62	0.94	0.59
MP4M	0.6	0.11	0.19	0.55	0.52	0.32	0.64	0.60	0.92	0.55
MP4U	0.5	0.07	0.09	0.40	0.22	0.13	0.37	0.58	0.89	0.52
MP5L	0.6	0.06	0.07	0.40	0.15	0.09	0.34	0.63	0.82	0.52
MP5M	0.9	0.06	0.12	0.53	0.35	0.19	0.58	0.54	1.44	0.78
MP5U	0.6	0.06	0.10	0.48	0.21	0.15	0.50	0.69	0.86	0.59
MP6L	0.5	0.07	0.08	0.38	0.16	0.11	0.46	0.70	0.99	0.69
MP6M	0.9	0.10	0.19	0.45	0.61	0.33	0.72	0.54	1.33	0.72
MP6U	0.4	0.06	0.10	0.43	0.24	0.16	0.60	0.67	0.78	0.52
MP7L	0.5	0.09	0.05	0.32	0.21	0.06	0.23	0.27	2.04	0.56
MP7M	0.5	0.09	0.10	0.37	0.26	0.15	0.48	0.58	0.90	0.53
MP7U	0.5	0.07	0.05	0.41	0.17	0.06	0.25	0.38	1.47	0.55

Table 5.15, continued.

Sample	$(C_{27} + C_{29})/(C_{23} + C_{25} + \ldots + C_{33})$	% C_{27}	% C_{29}	% C_{31}	% LMW	% MMW	% HMW
B01-1	0.43	31.6	28.6	39.8	6.2	20.6	73.2
B01-4	0.35	40.2	20.1	39.8	10.8	30.7	58.5
B01-5	0.39	32.1	24.5	43.4	5.8	27.3	66.9
B02-4	0.43	36.0	26.5	37.5	11.4	23.2	65.3
B03-2	0.34	25.1	27.3	47.6	5.7	19.7	74.6
B03-3	0.34	28.6	28.6	42.7	15.0	27.4	57.6
B03-6	0.37	26.9	28.2	44.9	4.8	18.8	76.4
E55-2	0.44	32.1	32.4	35.5	8.6	26.6	64.8
L04A-1	0.41	29.5	26.2	44.3	5.7	13.0	81.3
L04B-1	0.35	25.7	27.7	46.6	2.6	17.3	80.2
ML46A-6	0.43	32.1	32.4	35.5	8.5	27.9	63.5
ML46A-7	0.42	35.5	29.7	34.8	8.4	26.5	65.2
BG1	0.42	25.9	30.4	43.7	3.2	11.9	84.9
BG2	0.45	39.2	29.3	31.5	5.2	21.5	73.3
0464A	0.39	39.1	31.9	28.9	26.6	36.7	36.7
M03-2	0.44	35.5	28.4	36.1	27.1	22.3	50.6
MK1	0.46	37.0	30.6	32.4	5.6	19.5	74.9
MK2	0.35	32.3	24.7	43.0	18.4	20.0	61.6
MK3A	0.35	33.3	28.7	38.0	22.5	31.4	46.1
MK3B	0.36	31.1	28.3	40.6	27.6	26.8	45.5
MP1L	0.41	37.0	25.6	37.4	18.0	24.0	58.1
MP1M	0.57	36.3	40.8	22.9	10.1	24.2	65.7
MP1U	0.37	59.1	17.1	23.9	6.8	53.0	40.2
MP2L	0.39	27.0	36.9	36.2	7.0	29.0	64.0
MP2U	0.40	32.0	31.6	36.4	6.9	32.3	60.7
MP3L	0.36	24.9	29.5	45.6	5.3	20.8	73.9
MP3M	0.24	16.1	20.7	63.2	4.1	16.0	79.9
MP3U	0.38	26.1	29.6	44.2	3.7	19.3	77.0
MP4L	0.35	28.0	27.6	44.4	8.6	29.3	62.1
MP4M	0.34	28.6	26.9	44.5	9.2	32.7	58.1
MP4U	0.33	19.0	29.9	51.2	4.1	20.2	75.7
MP5L	0.35	17.4	31.9	50.7	4.0	16.7	79.3
MP5M	0.33	27.4	25.6	47.0	5.4	22.6	72.0
MP5U	0.37	22.6	31.7	45.7	3.8	20.4	75.8
MP6L	0.36	21.4	32.5	46.2	4.6	18.3	77.1
MP6M	0.31	31.9	23.9	44.2	7.2	34.0	58.9
MP6U	0.38	26.5	29.4	44.1	4.9	22.8	72.3
MP7L	0.22	15.3	18.2	66.4	4.3	17.5	78.2
MP7M	0.34	23.3	28.3	48.4	5.5	25.2	69.4
MP7U	0.26	15.2	23.2	61.6	3.4	15.8	80.8

$\%C_{27} = C_{27}/(C_{27} + C_{29} + C_{31})$ x 100; $\%C_{29} = C_{29}/(C_{27} + C_{29} + C_{31})$ x 100; $\%C_{31} = C_{31}/(C_{27} + C_{29} + C_{31})$ x 100; $\%LMW = (\Sigma C_{15\text{-}20} / \Sigma C_{15\text{-}33})$ x 100; $\%MMW = (\Sigma C_{21\text{-}26} / \Sigma C_{15\text{-}33})$ x 100; $\%HMW = (\Sigma C_{27\text{-}33} / \Sigma C_{15\text{-}33})$ x 100.

Table 5.16: *n*-Alkane parameters for coals from Benue Trough, Nigeria.

Sample	C_{max}	CPI	OEP	TAR	WI	ACL	P_{aq}	P_{wax}	Pr/ Ph	Pr/ C_{17}	Ph/ C_{18}	$C_{17}/(C_{17}+C_{27})$	$C_{23}/(C_{27}+C_{31})$	C_{23}/C_{25}	C_{23}/C_{29}	C_{23}/C_{31}
MGL3A	C_{25}	3.7	4.4	16.0	12.5	28.4	0.48	0.65	3.3	3.3	0.7	0.06	0.09	0.09	0.10	0.38
MGL4A	C_{29}	3.6	5.2	11.3	5.9	28.6	0.25	0.82	3.2	2.1	0.4	0.11	0.08	0.24	0.09	0.28
MGL1C	C_{29}	1.5	1.9	2.6	2.5	29.0	0.36	0.72	2.3	0.7	0.3	0.28	0.27	0.73	0.43	0.52
MGL2A	C_{29}	3.1	3.8	7.6	6.3	28.7	0.19	0.86	4.8	2.9	0.5	0.07	0.06	0.27	0.07	0.18
MGL2B	C_{29}	1.8	2.9	3.0	3.1	28.6	0.45	0.66	2.0	2.0	0.7	0.19	0.33	0.54	0.39	1.00
MGL2H	C_{29}	1.9	2.3	3.0	2.8	28.8	0.31	0.77	3.0	1.6	0.4	0.20	0.17	0.58	0.28	0.40
MGL2I	C_{29}	2.1	3.0	2.9	2.8	28.9	0.34	0.75	2.8	3.1	0.9	0.21	0.22	0.61	0.31	0.50
MGL2O	C_{29}	2.0	2.3	4.1	4.0	28.8	0.32	0.77	3.3	1.6	0.5	0.19	0.20	0.67	0.32	0.47
MGL2P	C_{29}	1.6	1.9	2.6	2.9	28.9	0.34	0.75	2.5	0.5	0.2	0.30	0.24	0.77	0.39	0.54
MGL2T	C_{27}	1.9	1.9	6.1	5.0	28.9	0.29	0.80	3.0	1.4	0.3	0.11	0.13	0.51	0.27	0.28
AFZ	C_{29}	1.2	1.3	11.4	9.0	29.1	0.32	0.75	3.1	27.4	2.8	0.06	0.23	0.76	0.38	0.43
ENG	C_{29}	3.6	4.8	13.8	7.1	28.7	0.16	0.89	3.4	5.4	0.7	0.08	0.09	0.50	0.08	0.26
IMG	C_{29}	1.1	1.2	3.5	4.1	28.9	0.46	0.64	1.5	13.4	2.2	0.09	0.41	0.86	0.73	0.88
OGB	C_{27}	1.7	1.8	3.6	3.4	28.9	0.41	0.70	3.0	5.2	1.0	0.21	0.30	0.83	0.59	0.66
OKB	C_{29}	4.3	6.2	20.9	10.0	28.7	0.12	0.91	3.4	5.7	0.6	0.05	0.07	0.46	0.06	0.21
WKP	C_{29}	2.5	2.9	12.2	8.1	28.7	0.28	0.80	3.5	4.0	0.6	0.07	0.14	0.46	0.19	0.36
CKL	C_{28}	1.1	1.0	2.8	4.0	28.7	0.55	0.57	3.1	6.9	0.9	0.14	0.56	0.97	1.05	1.47
LMZ1	C_{26}	1.1	1.1	2.2	3.1	28.7	0.56	0.56	2.4	9.2	0.8	0.12	0.59	0.95	1.05	1.56
LFO	C_{29}	2.9	3.5	5.3	3.4	28.7	0.23	0.85	3.8	2.5	0.5	0.12	0.10	0.47	0.15	0.26
SKJ	C_{29}	3.0	3.7	12.5	6.4	28.6	0.22	0.85	2.9	2.9	0.4	0.07	0.10	0.51	0.14	0.32

C_{max}: *n*-alkane maxima; Pr: Pristane; Ph: Phytane; CPI: Carbon Preference Index = $1/2[((C_{23}+C_{25}+C_{27}+C_{29}+C_{31})/(C_{24}+C_{26}+C_{28}+C_{30}+C_{32}))+((C_{25}+C_{27}+C_{29}+C_{31}+C_{33})/(C_{24}+C_{26}+C_{28}+C_{30}+C_{32}))]$; OEP: Odd Even Predominance = $[C_{29}+6C_{29}+C_{31}]/[4C_{28}+4C_{30}]$; TAR: Terrigenous Aquatic Ratio = $[C_{27}+C_{29}+C_{31}]/[C_{15}+C_{17}+C_{19}]$; WI: Wax Index = $\Sigma C_{21\text{-}31}/\Sigma C_{15\text{-}20}$; ACL: Average Chain Length = $[(27 * C_{27})+(29 * C_{29})+(31 * C_{31})]/[C_{27}+C_{29}+C_{31}]$; P_{aq}: Proxy Aqueous = $[C_{23}+C_{25}]/[C_{23}+C_{25}+C_{29}+C_{31}]$; P_{wax}: Proxy Wax = $[C_{27}+C_{29}+C_{31}]/[C_{23}+C_{25}+C_{27}+C_{29}+C_{31}]$; $\%C_{27} = C_{27}/(C_{27}+C_{29}+C_{31}) \times 100$; $\%C_{29} = C_{29}/(C_{27}+C_{29}+C_{31}) \times 100$; $\%C_{31} = C_{31}/(C_{27}+C_{29}+C_{31}) \times 100$; $\%LMW = (\Sigma C_{15\text{-}20} / \Sigma C_{15\text{-}33}) \times 100$; $\%MMW = (\Sigma C_{21\text{-}26} / \Sigma C_{15\text{-}33}) \times 100$; $\%HMW = (\Sigma C_{27\text{-}33} / \Sigma C_{15\text{-}33}) \times 100$.

Table 5.16, continued.

Sample	C_{27}/C_{31}	C_{29}/C_{31}	C_{33}/C_{29}	C_{33}/C_{31}	$(C_{27}+C_{29})/(C_{23}+C_{25}+\ldots+C_{33})$	$\%C_{27}$	$\%C_{29}$	$\%C_{31}$	%LMW	%MMW	%HMW
MGL3A	3.42	3.92	0.03	0.12	0.57	41.0	47.0	12.0	7.3	37.1	55.6
MGL4A	2.31	3.22	0.08	0.25	0.67	35.4	49.3	15.3	14.1	22.2	63.7
MGL1C	0.93	1.22	0.51	0.63	0.43	29.5	38.7	31.8	25.6	28.9	45.5
MGL2A	1.70	2.50	0.15	0.38	0.66	32.7	48.1	19.2	12.8	16.7	70.5
MGL2B	2.02	2.54	0.10	0.26	0.53	36.4	45.6	18.0	23.7	36.8	39.5
MGL2H	1.33	1.41	0.32	0.45	0.52	35.5	37.8	26.7	24.4	25.1	50.5
MGL2I	1.27	1.59	0.22	0.34	0.52	32.8	41.3	25.9	25.4	28.7	46.0
MGL2O	1.34	1.49	0.25	0.38	0.53	34.9	39.0	26.1	18.9	27.8	53.3
MGL2P	1.24	1.39	0.34	0.48	0.49	34.2	38.3	27.6	24.1	27.9	48.0
MGL2T	1.21	1.05	0.64	0.67	0.47	37.1	32.3	30.6	14.3	22.0	63.8
AFZ	0.91	1.14	0.33	0.38	0.46	29.9	37.3	32.8	9.1	30.7	60.2
ENG	1.97	3.19	0.08	0.26	0.72	31.9	51.8	16.2	11.8	16.9	71.3
IMG	1.14	1.21	0.39	0.47	0.41	34.1	36.0	29.9	18.1	38.4	43.5
OGB	1.21	1.11	0.49	0.54	0.44	36.5	33.5	30.0	21.1	31.7	47.2
OKB	1.89	3.82	0.06	0.21	0.75	28.2	56.9	14.9	8.8	14.8	76.4
WKP	1.64	1.91	0.16	0.30	0.59	36.1	41.9	22.0	10.4	25.6	63.9
CKL	1.64	1.40	0.23	0.33	0.41	40.6	34.6	24.8	19.0	42.4	38.6
LMZ1	1.65	1.49	0.23	0.35	0.41	39.9	36.0	24.1	23.7	42.7	33.6
LFO	1.62	1.76	0.23	0.41	0.60	37.0	40.2	22.8	21.5	18.9	59.7
SKJ	2.07	2.25	0.14	0.32	0.66	38.9	42.3	18.8	12.9	21.4	65.8

For the Sarawak Basin coal samples, the CPI values are generally similar for the Balingian (avg. 2.6) and Nyalau (avg. 2.6) formations but are relatively lower than the Liang Formation (avg. 3.4). Pristane/phytane ratios generally increase from Liang (avg. 2.3) to Balingian (avg. 4.4) and Nyalau Formation (avg. 6.5). In addition, TAR values are generally lowest in the Balingian Formation coals (avg. 6.0) and highest in the Liang Formation coals (avg. 19.1) while the Nyalau Formation coals have intermediate TAR values (avg. 16.6; Table 5.15).

5.10.2 Hopanoids and Steroids

5.10.2.1 Hopanoids

Hopanoids are abundant in the studied coals and representative *m/z* 191 chromatograms of the samples are shown in Figure 5.20. The hopanoids distribution for the studied coals is generally similar and characterized by the abundance of neohop-13(18)-enes, hop-17(21)-enes, ββ-hopanes and subordinate abundances of αβ-hopanes ranging from C_{27} to C_{31} without C_{28}. C_{27} β-trinorhopane was observed in most of the samples, while tricyclic terpanes, βα-moretanes and gammacerane were either absent or present in low abundance (except in the Lamja Formation samples). C_{29} neohop-13(18)-ene is the most abundant hopanoid in most of the coal samples, whereas C_{30} ββ-hopane and C_{31} αβ-homohopane (22R) predominates in a few samples (Figure 5.20). The relative abundances of hopanoids, which are widely employed as maturity and source input indicators (Peters et al., 2005), are presented in Table 5.17.

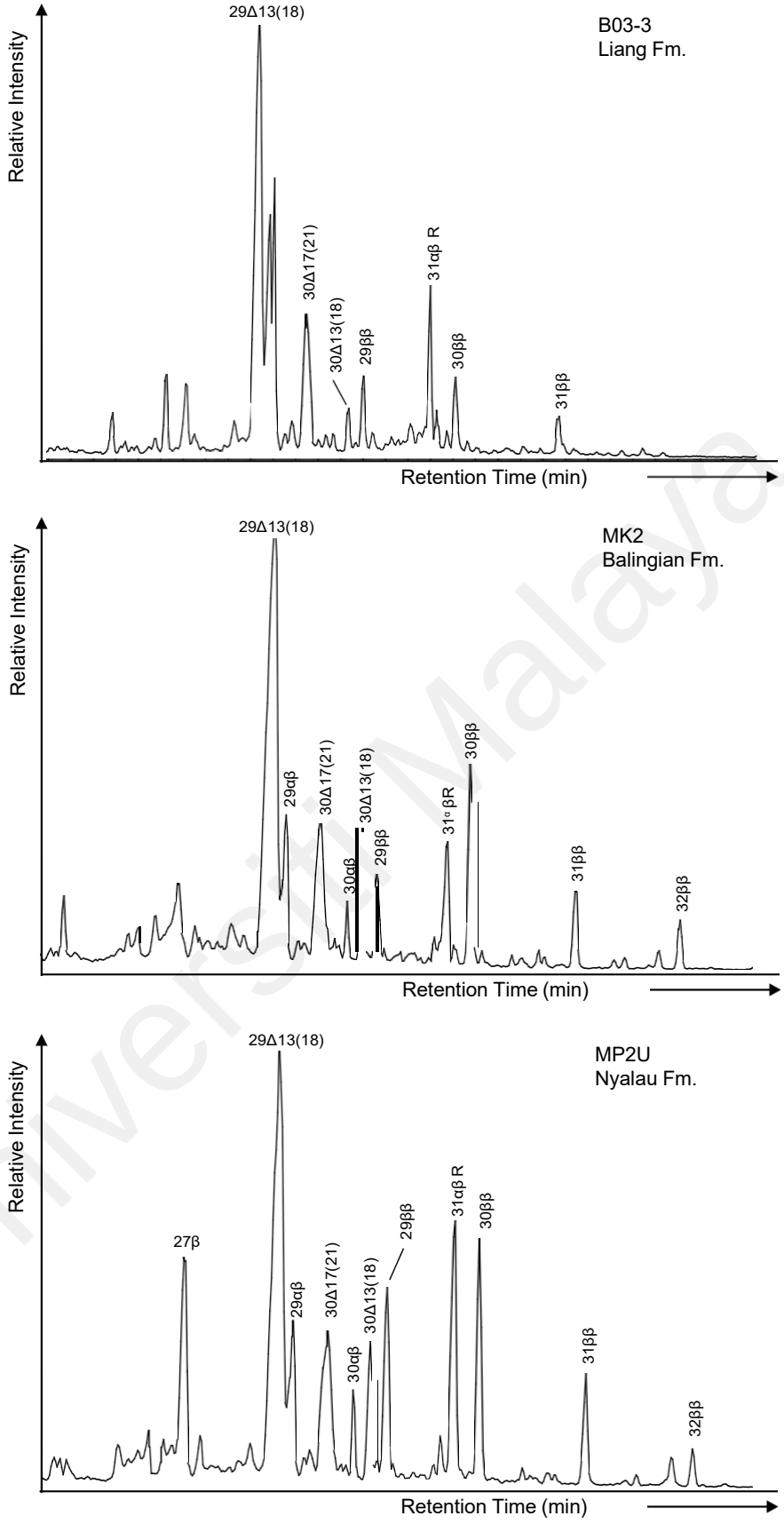

Figure 5.20: Partial chromatograms of *m/z* 191 of aliphatic fractions of the representative coal samples, showing the distribution of hopanoids. Selected peaks are labelled with their carbon number and stereochemistry. αβ = 17α(H),21β(H)-hopanes, ββ = 17β(H),21β(H)-norhopanes, Δ13(18) = neohop-13(18)-enes, and Δ17(21) = neohop-17(21)-enes.

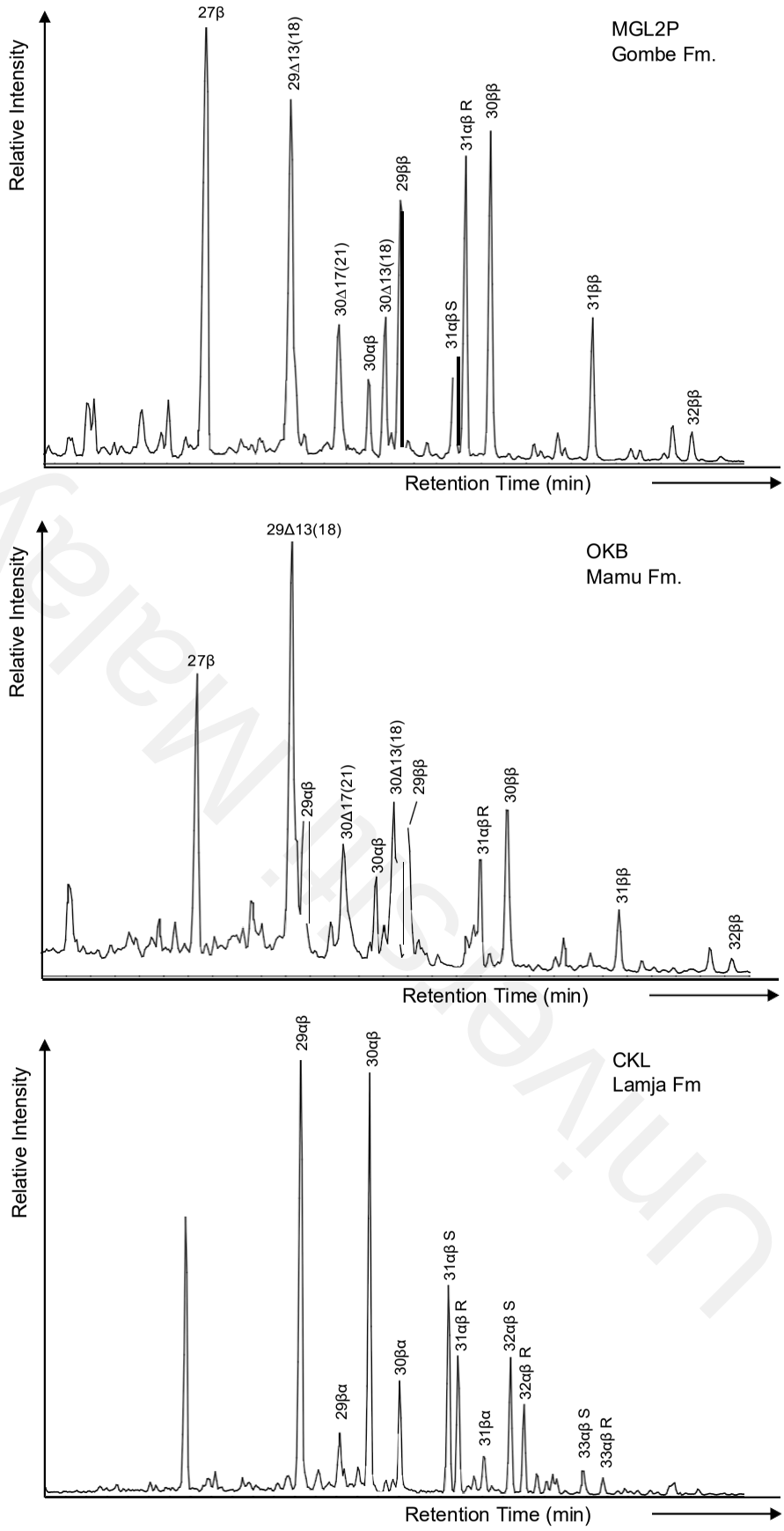

Figure 5.20, continued.

Table 5.17: Hopanoid parameters for the studied coals.

Sample	C_{29} αβ/ C_{30} αβ	(C_{29}+C_{31})/ C_{30} αβ	C_{31} R/ C_{30} αβ	C_{31} αβ S/(S+R)	C_{30} ββ/ (αβ+ββ)	C_{31} ββ/ (ββ+αβ)	pH
B01-1	-	-	-	0.16	-	0.12	3.7
B01-4	3.26	5.0	1.55	0.11	0.55	0.27	4.5
B01-5	-	-	-	-	-	0.17	4.0
B02-4	1.68	2.6	0.87	0.10	0.46	0.29	4.6
B03-2	5.26	7.4	1.85	0.15	0.45	0.21	4.2
B03-3	5.93	10.1	3.64	0.12	0.62	0.17	4.0
B03-6	-	-	-	0.16	-	0.14	3.9
E55-2	8.70	17.9	8.10	0.12	0.79	0.19	4.1
L04A-1	3.80	9.7	4.80	0.18	0.40	0.10	3.7
L04B-1	-	-	-	0.14	-	0.12	3.8
ML46A-6	9.61	20.3	9.26	0.14	0.79	0.17	4.0
ML46A-7	6.21	10.1	3.43	0.11	0.67	0.25	4.4
BG1	4.94	6.1	0.94	0.20	0.39	0.29	4.6
BG2	-	-	-	0.22	-	0.36	5.0
0464A	4.15	20.0	12.70	0.20	0.76	0.12	3.8
M03-2	5.50	7.9	1.92	0.19	0.56	0.17	4.0
MK1	4.46	7.3	2.85	-	0.73	0.27	4.5
MK2	2.40	4.8	1.95	0.19	0.76	0.33	4.9
MK3A	4.08	5.7	1.25	0.21	0.77	0.42	5.3
MK3B	1.71	3.4	1.17	0.29	0.72	0.38	5.1
MP1L	1.32	5.5	3.89	0.07	0.81	0.28	4.6
MP1M	2.45	5.8	3.30	-	0.81	0.35	5.0
MP1U	-	-	-	-	-	-	-
MP2L	1.47	5.9	4.11	0.08	0.81	0.34	4.9
MP2U	1.76	5.3	3.04	0.14	0.74	0.27	4.5
MP3L	3.47	8.2	3.85	0.19	0.73	0.24	4.3
MP3M	2.71	5.8	2.33	0.25	0.45	0.20	4.1
MP3U	7.13	13.6	5.06	0.21	0.84	0.32	4.8
MP4L	2.36	6.4	3.40	0.17	0.76	0.30	4.7
MP4M	2.08	7.7	4.81	0.14	0.77	0.24	4.3
MP4U	4.70	8.9	3.15	0.24	0.83	0.36	5.0
MP5L	2.93	11.3	6.93	0.17	0.78	0.23	4.3
MP5M	3.88	12.5	7.28	0.16	0.82	0.26	4.5
MP5U	4.91	15.8	8.27	0.24	0.83	0.21	4.2
MP6L	4.56	16.8	9.67	0.21	0.85	0.26	4.5
MP6M	7.86	11.6	2.71	0.27	0.84	0.41	5.2
MP6U	6.93	18.9	10.71	0.11	0.85	0.22	4.3
MP7L	2.18	10.2	7.00	0.13	0.80	0.19	4.1
MP7M	2.53	6.8	3.50	0.17	0.83	0.30	4.7
MP7U	6.44	23.7	13.11	0.24	0.83	0.18	4.1

αβ-Hopane = 17α(H),21β(H)-Hopane; ββ-Hopane = 17β(H),21β(H)-norhopane; R = 17α(H),21β(H)-22R-homohopane; S = 17α(H),21β(H)-22S-homohopane; pH = [5.22 x C_{31} ββ/(ββ + αβ)] + 3.11

Table 5.17, continued.

Sample	C_{29} αβ/ C_{30} αβ	(C_{29}+C_{31})/ C_{30} αβ	C_{31} R/ C_{30} αβ	C_{31} αβ S/(S + R)	C_{30} ββ/ (αβ + ββ)	C_{31} ββ/ (ββ + αβ)	pH
MGL3A	6.83	10.6	3.0	0.20	0.79	0.31	4.7
MGL4A	-	-	-	0.22	-	0.26	4.5
MGL1C	2.24	9.2	4.9	0.29	0.81	0.27	4.5
MGL2A	0.71	4.1	2.5	0.25	0.75	0.34	4.9
MGL2B	2.50	4.8	1.9	0.17	0.66	0.29	4.6
MGL2H	1.32	8.9	5.6	0.26	0.80	0.22	4.3
MGL2I	2.32	6.4	3.4	0.18	0.70	0.21	4.2
MGL2O	1.38	7.7	4.6	0.26	0.79	0.20	4.1
MGL2P	4.43	9.5	3.8	0.25	0.80	0.26	4.5
MGL2T	1.73	6.4	3.4	0.28	0.79	0.29	4.6
AFZ	0.86	2.0	0.5	0.53	-	-	-
ENG	1.41	3.7	1.8	0.21	0.66	0.29	4.6
IMG	0.72	1.4	0.3	0.59	-	-	-
OGB	0.27	1.5	0.9	0.25	0.22	-	-
OKB	1.75	3.5	1.4	0.21	0.66	0.31	4.7
WKP	0.48	2.0	1.1	0.23	0.40	0.11	3.7
CKL	1.07	1.9	0.3	0.60	-	-	-
LMZ1	0.91	1.8	0.4	0.59	-	-	-
LFO	5.33	14.8	7.3	0.23	0.79	0.18	4.0
SKJ	3.86	11.4	5.6	0.26	0.77	0.20	4.1

The values of the C_{31} αβ-homohopane 22S/(22S+22R) maturity parameter vary from 0.07 to 0.60 with averages of 0.17 and 0.30 for the Sarawak Basin and Benue Trough coals, respectively, indicating generally low thermal maturity but relatively higher maturity for the Nigerian coals (Farrimond et al., 1998). Additionally, the (C_{29}+C_{31})/C_{30} αβ-hopane parameter, which reflects the relative contributions of terrigenous and marine organic matter, ranges from 2.6 to 23.7 (avg. 10.0) and 1.4 to 14.8 (avg. 5.9) for the studied Sarawak Basin and Benue Trough coals, respectively. The lower values of the (C_{29}+C_{31})/C_{30} αβ-hopane parameter suggest greater marine algal OM input in the Benue Trough samples (Killops et al., 1994).

5.10.2.1 Steroids

Steroids with their concentrations above the detection limit were generally not observed in the *m/z* 217 mass chromatograms of the studied coals, except in the Lamja Formation coals (samples CKL and LMZ1) from the Upper Benue Trough (Figure 5.21). The dominating abundance of hopanes over steranes in the analysed samples is indicative of low biological productivity and the predominant abundance of terrigenous organic matter (Philp & Gilbert, 1986; Killops et al., 1994; Makeen et al., 2019). The sterane distribution of the Lamja Formation coals is dominated by regular C_{29} steranes with subordinate abundances of C_{27} and C_{28} steranes. In addition, rearranged steranes or diasteranes are present in the coals but generally in lower abundance when compared with the regular steranes. Ratios of the sterane C_{29} ααα 20S/(20S+20R) and C_{29} αββ/(αββ+ααα) maturity parameters for the two Lamja Formation coals are in the 0.45-0.54 and 0.34-0.35 range, respectively (Table 5.18). The ratios are slightly below the equilibrium end-point (0.55) of the C_{29} ααα 20S parameter, which implies an early thermal maturity threshold for the studied Lamja Formation coals (Farrimond et al., 1998; Peters et al., 2005).

Table 5.18: Steroid parameters for the Lamja Formation coals.

Parameters	CKL	LMZ1
C_{29} ααα 20S/(20S+20R)	0.45	0.54
C_{29} αββ/(αββ+ααα)	0.35	0.34
% C_{27} ααα 20R	15.2	16.8
%C_{28} ααα 20R	25.4	27.9
%C_{29} ααα 20R	59.4	55.3
C_{27} ααα 20R/C_{29} ααα 20R	0.26	0.30
C_{27} ααα 20R/C_{28} ααα 20R	0.60	0.60
C_{27} βα 20R/C_{27} ααα 20R	1.40	1.68
C_{29} βα 20R/C_{29} ααα 20R	0.36	0.30
C_{29} βα/(αββ+ααα+βα)	0.25	0.22

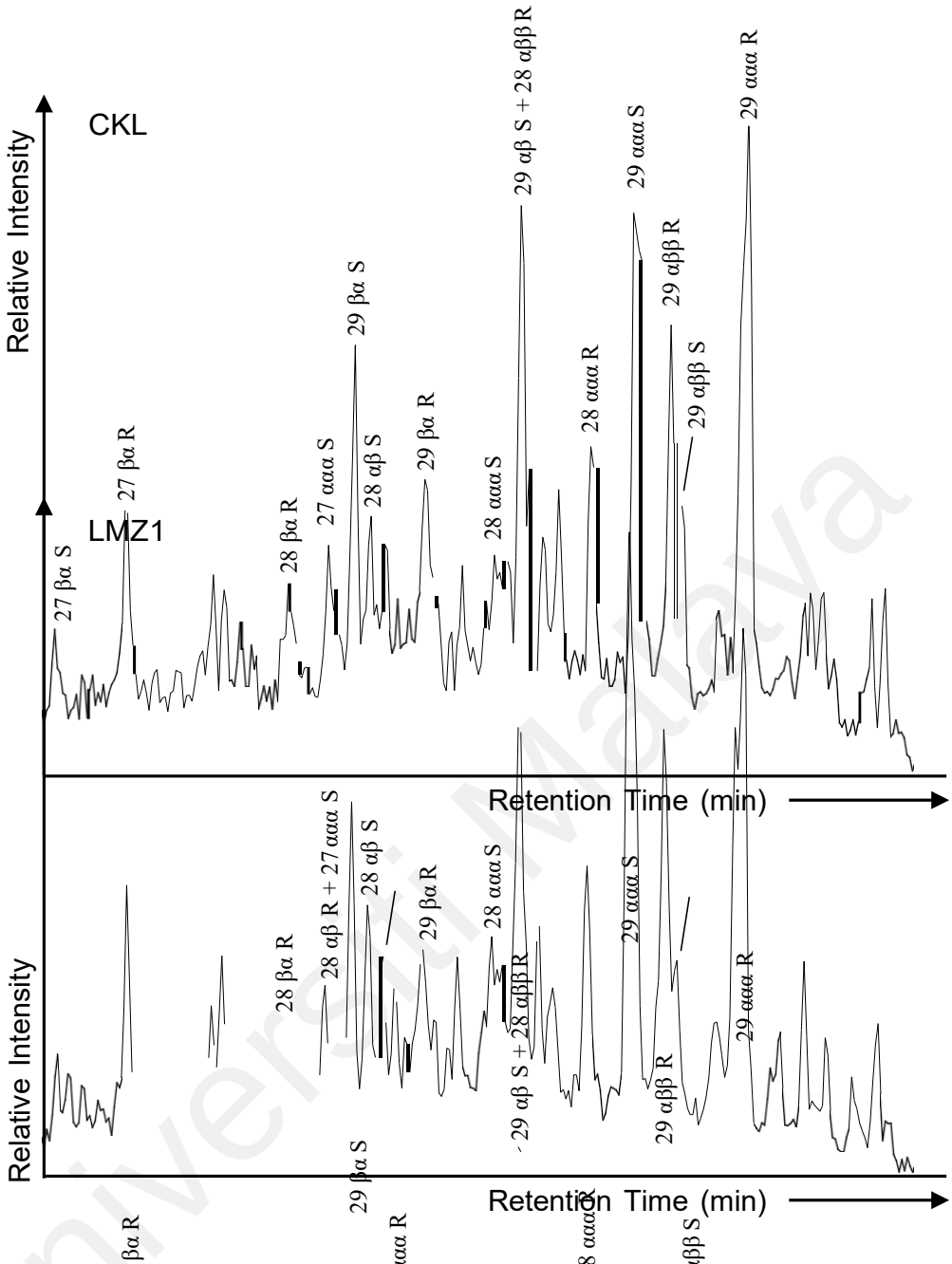

Figure 5.21: Partial chromatograms of *m/z* 217 of aliphatic fractions of the Lamja Formation coals, showing the distribution of steroids. βα = 13β(H),17α(H)-diasteranes; αβ = 13α(H),17β(H)-diasteranes; αββ = 5α(H),14β(H),17β(H)-steranes; ααα = 5α(H),14α(H),17α(H)-steranes.

5.10.3 Aliphatic Terpenoids

Terpenoids represent a vastly broad family of biomarkers. They are derived from higher plants and are well recognised in petroleum, sediments and coal as chemosystematic markers of palaeoflora and palaeoclimate (Killops et al., 1995; van Aarssen et al., 2000; Otto et al., 2002a; Otto et al., 2000b; Hautevelle et al., 2006; Nakamura et al., 2010; Jiang & George, 2018). Cretaceous sediments are typically characterized by a high concentration of diterpenes from gymnosperms, while Tertiary sediments are dominated by triterpenes derived from angiosperms (Bechtel et al., 2008; Widodo et al., 2009; Jiang & George et al., 2018; Radhwani et al., 2018). Although gymnosperm taxa declined rapidly during the Eocene, the evolution of angiospermous flora was irregular as there was a short resurgence of gymnosperm at the end of the Paleocene (Killops et al., 1995).

Partial chromatograms of aliphatic fractions of the studied coals showing the distributions of sesquiterpenoids and diterpenoids (*m/z* 123) are presented in Figure 5.22 whilst aliphatic triterpenoids (*m/z* 191) are shown in Figure 5.23. Diterpenoids mostly predominate sesquiterpenoids in the studied coals except in some Balingian, Nyalau and Lamja formation samples where sesquiterpenoids predominate, possibly due to their relatively higher thermal maturity (Jiang & George, 2018).

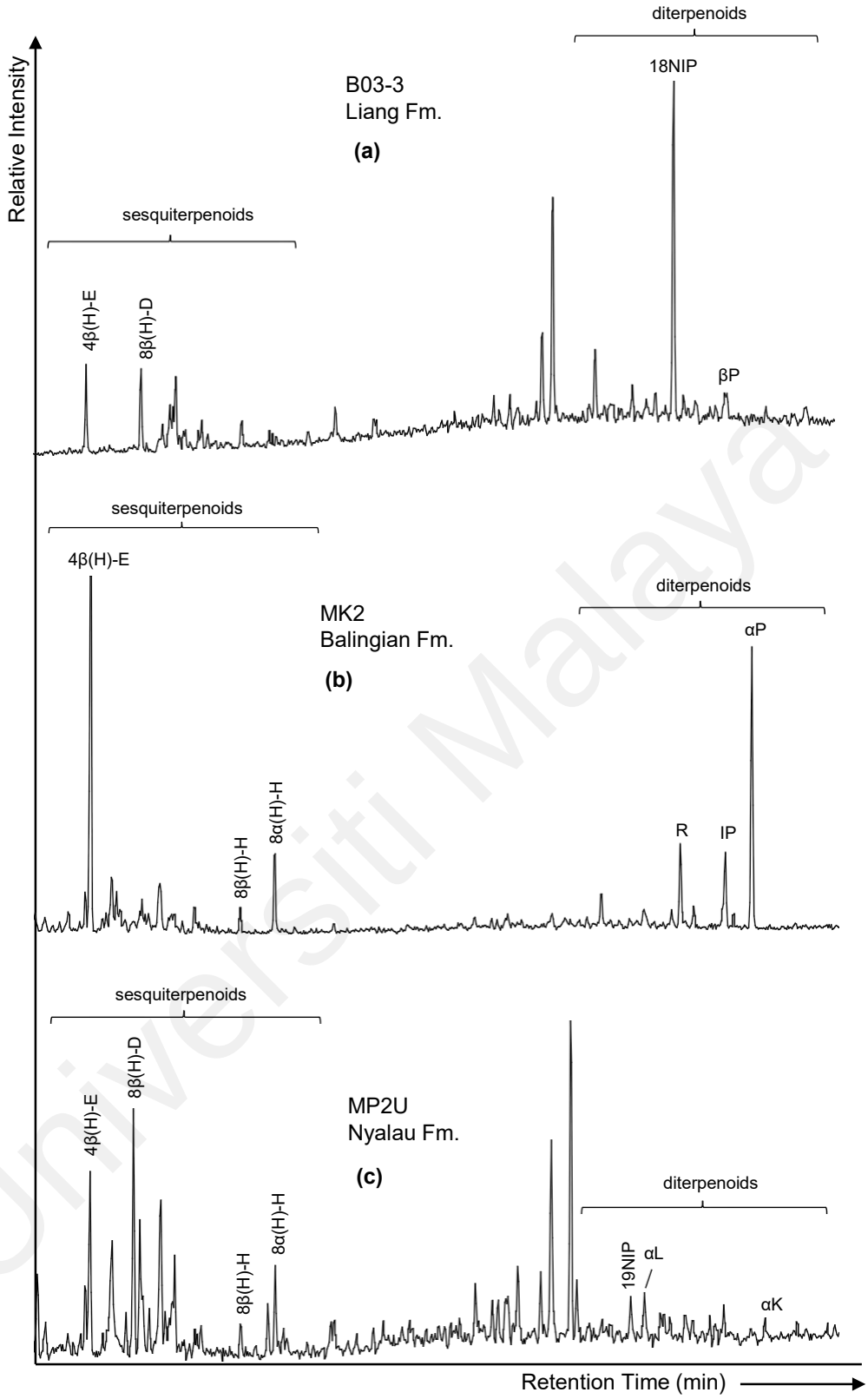

Figure 5.22: Partial *m/z* 123 chromatograms of the aliphatic hydrocarbon fractions showing the distributions of sesquiterpenoids and diterpenoids. 4β(H)-E – 4β(H)-Eudesmane; 8β(H)-D – 8β(H)-drimane; 8β(H)-D – 8β(H)-Homodrimane; 8α(H)-H – 8α(H)-Homodrimane; 18NIP – 4α-18-*nor*-isoprimaranes; 19NIP – 4α-19-*nor*-isoprimarane; R – rimuane; IP – sopimarane; αP – 16α(H)-phyllocladane; βP – 16β(H)-phyllocladane; αL – 8α-labdane; αK – *ent*-16α(H)-kaurane; NT – C_{19}-17-nortetracyclane.

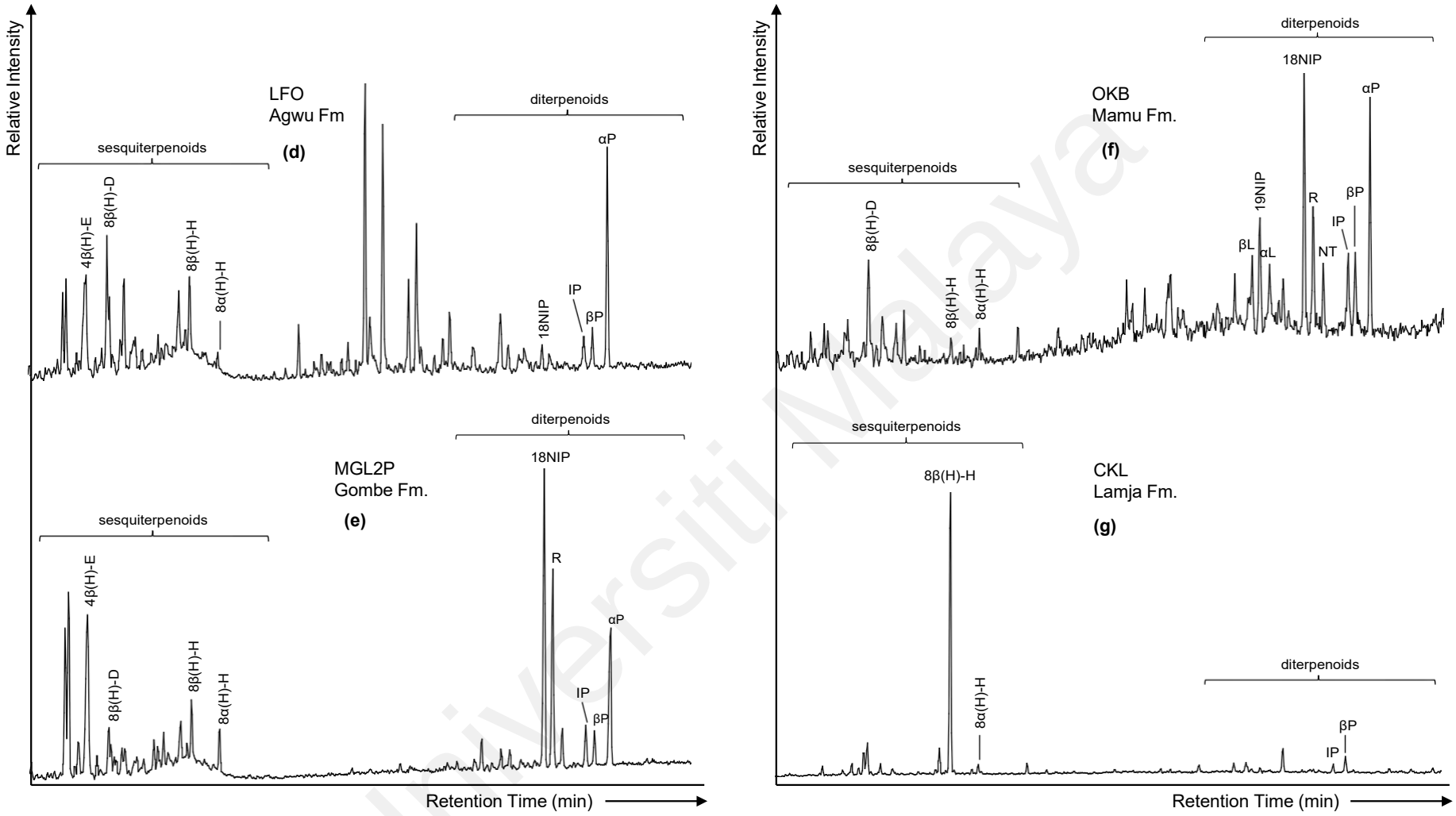

Figure 5.22, continued.

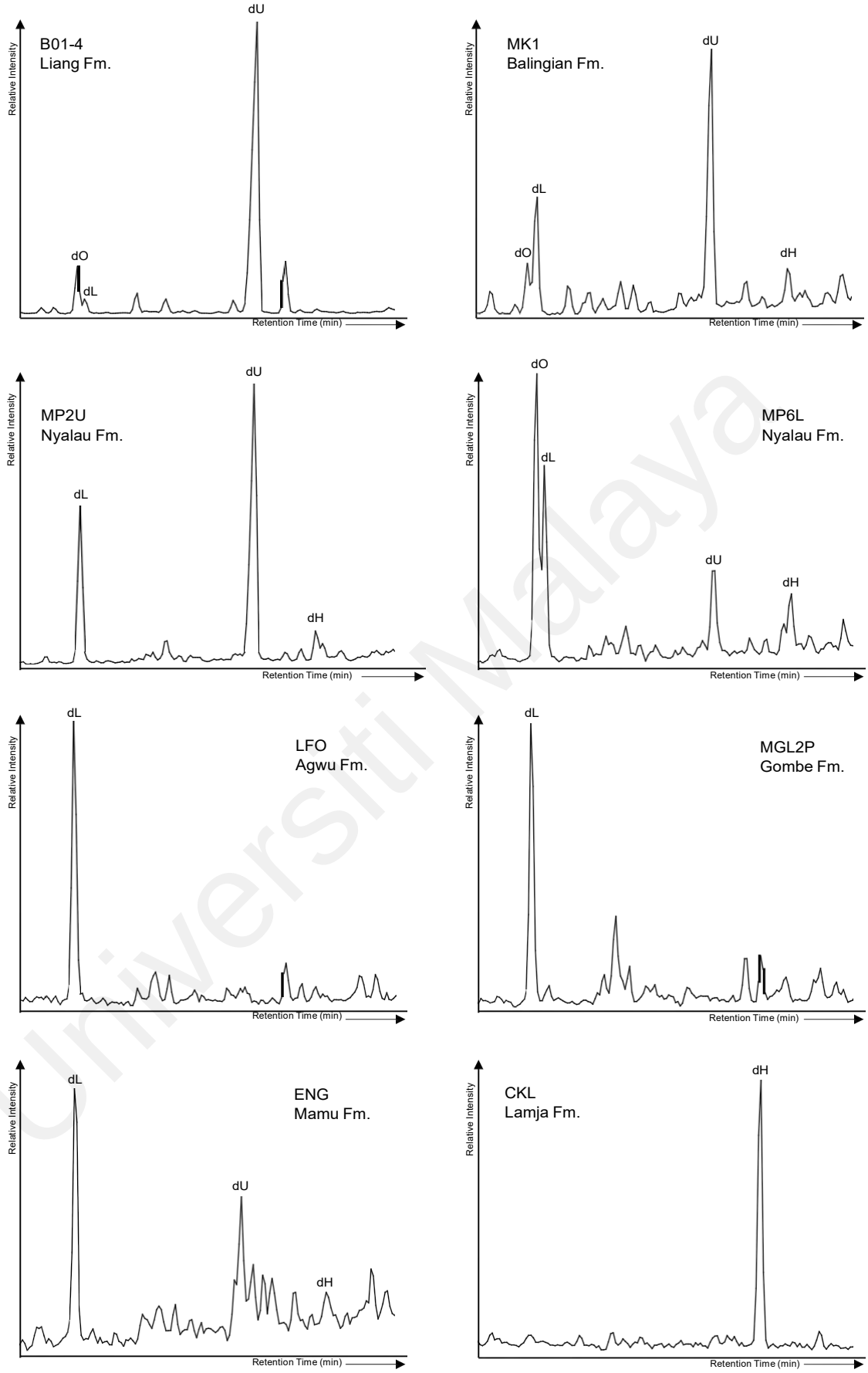

Figure 5.23: Partial mass chromatograms *(m/z* 191) of the aliphatic hydrocarbon fractions showing the distributions of triterpenoids. dO: 10β(H)-des-A-olenane; dL: 10β(H)-des-A-lupane; dU: 10β(H)-des-A-ursane; dH: 18β(H)-des-E-hopane.

5.10.3.1 Sesquiterpenoids

Bicyclic sesquiterpenoids are ubiquitous components of sediments, peats, coals and crude oils with a decahydronaphthalene skeleton substituted by alkyl side chains (Otto et al. 1997; Nytoft et al., 2009; Yin et al., 2020). Based on diagnostic fragment ions, published gas chromatographic elution orders, and comparison with published mass spectra (Böcker et al., 2013; Yan et al., 2019; Yin et al., 2020), C_{14} to C_{16} bicyclic sesquiterpenoids, 8β(H)-drimane, 8β(H)-homodrimane and 8α(H)-homodrimane were identified in the investigated coals (Figure 5.22). In addition, 4β(H)-eudesmane was observed in the Cretaceous Benue Trough and the Miocene Nyalau Formation coals while noticeably absent in the Pliocene Liang Formation coals. The compound is a diagnostic marker for plant input as it is formed from higher plant precursors β-eudesmol and γ-selinene (Alexander et al., 1983; Jiang & George, 2018). In contrast, a microbial origin has been established for 8β(H)-drimane as it is formed either directly from compounds with the bicyclic ring system or from the degradation of higher terpenes (Alexander et al., 1983). The presence of bicyclic alkanes in the coals is thus suggestive of a bacterial contribution to OM input (Romero-Sarmiento et al., 2011).

Following findings by earlier studies (Noble et al., 1987; Weston et al., 1989) establishing a correlation between thermal maturity and the relative abundance of rearranged to total drimanes, Yan et al. (2019) simulated the thermal evolution of bicyclic sesquiterpenes, and results of the pyrolysis experiments support the postulation that ratios of sesquiterpenoid compounds show upward trends with increasing temperature. Hence, based on the thermostability of 8β(H)-sesquiterpenoid compounds, Yan et al. (2019) proposed three sesquiterpenoid parameters as maturity indicators in low maturity samples (Table 5.19). Ratios of the 8β(H)-drimane/8α(H)-homodrimane, 8β(H)-drimane/8β(H)-homodrimane, and 8β(H)-homodrimane/8α(H)-homodrimane

parameters are mostly higher for the Benue Trough coals with mean values of 12.18, 2.14 and 11.90, respectively, and lower for the Sarawak Basin coals with corresponding mean values of 4.40, 4.37 and 1.93 (Table 5.19). The sesquiterpenoid parameters imply relatively higher thermal maturity for the Benue Trough samples (Noble et al., 1987; Yan et al., 2019).

Table 5.19: Sesquiterpenoid parameters for the studied coals.

Sample	8β(H)-D/ 8α(H)-HD	8β(H)-D/ 8β(H)-HD	8β(H)-HD/ 8α(H)-HD	8β(H)-HD/ [8β(H)-HD+8β(H)-D]
B01-1	2.38	2.62	0.91	0.28
B01-4	9.01	3.11	2.90	0.24
B01-5	3.10	6.72	0.46	0.13
B02-4	3.52	3.19	1.10	0.24
B03-2	1.94	0.84	2.32	0.54
B03-3	10.80	2.00	5.39	0.33
B03-6	5.54	3.42	1.62	0.23
E55-2	6.28	3.89	1.62	0.20
L04A-1	-	-	-	-
L04B-1	-	1.23	-	0.45
ML46A-6	5.34	2.82	1.90	0.26
ML46A-7	9.42	0.32	29.45	0.76
BG1	1.34	2.63	0.51	0.28
BG2	1.78	1.91	0.93	0.34
0464A	2.08	1.63	1.28	0.38
M03-2	1.73	1.80	0.96	0.36
MK1	1.57	3.91	0.40	0.20
MK2	0.62	1.93	0.32	0.34
MK3A	1.04	0.57	1.83	0.64
MK3B	0.77	0.31	2.47	0.76
MP1L	0.89	1.30	0.69	0.44
MP1M	0.80	1.53	0.52	0.40
MP1U	-	-	-	-
MP2L	3.27	5.23	0.63	0.16
MP2U	2.74	5.28	0.52	0.16
MP3L	3.44	5.38	0.64	0.16
MP3M	0.27	1.59	0.17	0.39
MP3U	23.44	40.95	0.57	0.02
MP4L	3.94	3.91	1.01	0.20
MP4M	9.21	8.87	1.04	0.10
MP4U	2.73	5.49	0.50	0.15
MP5L	2.93	2.65	1.11	0.27
MP5M	2.96	6.29	0.47	0.14
MP5U	4.40	6.61	0.67	0.13
MP6L	5.37	7.13	0.75	0.12

D: drimane; HD: homodrimane

Table 5.19, continued.

Sample	8β(H)-D/ 8α(H)-HD	8β(H)-D/ 8β(H)-HD	8β(H)-HD/ 8α(H)-HD	8β(H)-HD/ (8β(H)-HD+8β(H)-D
MP6M	0.97	1.27	0.77	0.44
MP6U	1.47	1.82	0.81	0.35
MP7L	1.80	3.77	0.48	0.21
MP7M	2.31	5.76	0.40	0.15
MP7U	21.53	6.36	3.39	0.14
MGL3A	3.37	4.37	0.77	0.19
MGL4A	5.12	1.58	3.25	0.39
MGL1C	6.35	5.42	1.17	0.16
MGL2A	2.14	3.85	0.56	0.21
MGL2B	153.21	1.38	111.09	0.42
MGL2H	3.13	0.68	4.57	0.59
MGL2I	5.50	0.82	6.67	0.55
MGL2O	8.21	1.20	6.86	0.46
MGL2P	1.74	0.60	2.90	0.63
MGL2T	2.98	8.02	0.37	0.11
AFZ	7.53	0.44	17.06	0.69
ENG	9.94	2.72	3.66	0.27
IMG	2.98	0.35	8.45	0.74
OGB	1.22	1.75	0.70	0.36
OKB	2.50	4.74	0.53	0.17
WKP	0.64	1.10	0.58	0.48
CKL	3.04	0.13	24.23	0.89
LMZ1	3.39	0.12	27.13	0.89
LFO	17.85	1.09	16.34	0.48
SKJ	2.74	2.33	1.17	0.30

5.10.3.2 Diterpenoids

Diterpenoids are generally regarded as conifer vegetation biomarkers since they are found primarily in gymnosperm species and only in a few angiosperms (Otto et al., 1997; Nakamura et al., 2010). Diterpenoids are a very diverse class of terpenoids with over 2000 compounds and 100 skeletal types identified and proven to belong to 17 structural classes in conifers (Otto & Wilde, 2001). Based on the number of rings in their skeletons, diterpenoids in conifers can be classified into three major classes, namely bicyclic, tricyclic, and tetracyclic diterpenoids (Table 5.20). Bicyclic terpenoids include the labdanes and clerodanes while tricyclic terpenoids comprise primaranes and

abietanes. Tetracyclic diterpenoids, which are derived from the cyclization of some tricyclic diterpenoids and their subsequent rearrangement, include phyllocladanes, beyeranes, kauranes, atisanes, and trachylobanes (Otto & Wilde, 2001).

Table 5.20: Classification of major diterpenoids in conifers (Otto & Wilde, 2001).

Groups	Structural class	Occurrence in conifer families
Bicyclic	Labdanes	All families
	Clerodanes	*Araucaria*
Tricyclic	Isopimaranes	All families
	Pimaranes	All families except Phyllocladaceae and Taxaceae
	Normal abietanes	All families except Phyllocladaceae
	Phenolic abietanes	Cupressaceae s.str., Taxodiaceae, Podocarpaceae, Cedrus, Pinus, *Araucaria*
	Totaranes	Cupressaceae s.str., Podocarpaceae
	Podocarpanes	Podocarpaceae, *Pinus*
	Rimuene	Cupressaceae s.str., Taxodiaceae, Podocarpaceae, Phyllocladaceae
Tetracyclic	Phyllocladanes	Cupressaceae s.str., Podocarpaceae, *Araucaria,* Taxodiaceae, *Phyllocladus, Picea*
	Beyeranes	Cupressaceae s.str., Podocarpaceae, *Araucaria*
	Kauranes	All families except Taxaceae

The varying abundance of these three major classes of naturally occurring diterpenoid hydrocarbons is presumably associated with the varying resin inputs from gymnosperms and/or certain angiosperms (Noble et al., 1985). According to Otto & Wilde (2001), diterpenoids occur in all conifer families (Pinaceae, Cupressaceae S. Str, Taxodiaceae, Sciadopityaceae, Podocarpaceae, Araucariaceae, Phyllocladaceae, and Taxaceae) except in Cephalotaxaceae. However, tetracyclic diterpanes, phenolic abietanes, totaranes and rimuene are wholly absent in the Pinaceae family while labdane acids are mostly absent. In addition, normal abietanes and primaric acid are absent in the Phyllocladaceae and Cupressaceae s.str families, respectively. Although labdane-type compounds are the most prevalent in conifers, isoprimaranes and pimaranes are

equally common constituents. As a result, labdanes, isopimaranes and pimaranes are generally regarded as non-specific conifer biomarkers (Otto & Wilde, 2001).

Aliphatic diterpenoids such as 8β-labdane (βL), 4α-19-*nor*-isoprimarane (19NIP), 8α-labdane (αL), 18-norabietane (NA), 4α-18-*nor*-isoprimarane (18NIP), rimuane (R), C_{19}-17-nortetracyclane (NT), *ent*-beyerane (B), isopimarane (IP), 16β(H)-phyllocladane (βP), abietane (A), and 16α(H)-phyllocladane (αP) were observed in varying abundances in the studied coals. In contrast, *ent*-16β(H)-kaurane (βK) and *ent*-16α(H)-kaurane (αK) were not present in detectable amounts. In addition, the abundance of the observed diterpanes is higher and varied in the Benue Trough samples than in the Sarawak Basin samples. Nevertheless, the aliphatic diterpenoid distributions are generally dominated by 14α-18-*nor*-isoprimarane and 16α(H)-phyllocladane, while 18-norabietane and abietane are only present in minor abundances. The absence of cuparane- and cedrane-class sesquiterpenoids, totarane, phenolic abietanes and most tetracyclic diterpenoids in the Tertiary Sarawak Basin coals suggests a predominantly Pinaceae family origin for the diterpenoids. In contrast, the presence of pimaranes and tetracyclic diterpanes in the Late Cretaceous Benue Trough coals is characteristic of contributions from Araucareacea and Podocarpaceae (Weston et al., 1989; Otto et al., 1997; Bastow et al., 2001; Otto & Wilde, 2001). Similarly, various studies have documented the predominant contribution of Araucareacea and Podocarpaceae groups to the higher plant communities during the Late Cretaceous and Paleogene in Australia and New Zealand coals (Killops et al., 1994; Killops et al., 1995; Jiang & George, 2018; Jiang et al., 2020).

Furthermore, the absence or presence in low abundances of 16β(H)-phyllocladane in the studied coals is indicative of low thermal maturity (Alexander et al., 1987). According to Noble et al. (1985), 16α(H)-phyllocladane predominates over 16β(H)-

phyllocladane in low-rank coals as the more geochemically stable 16β(H) isomer relatively increases with higher thermal maturity. βP/(βP+αP) ratios are slightly higher for the Benue Trough coals, ranging from 0.11 to 0.87 and slightly lower for the Sarawak Basin coals with values varying between 0.05 and 0.58 (Table 5.21). βP/(βP+αP) ratios for the studied coals are suggestive of relatively higher thermal maturity for the Benue Trough coals (Noble et al., 1985; Alexander et al., 1987).

5.10.3.3 Triterpenoids

As shown in Figure 5.23, the distributions of aliphatic triterpenoids in the studied coals are characterised by the presence in varying proportions of 10β(H)-des-A-oleanane (dO), 10β(H)-des-A-ursane (dU), 10β(H)-des-A-lupane (dL), and 18β(H)-des-E-hopane (dH), indicating the contribution of angiosperms to paleoflora of the study areas (Killops et al., 1994). Conversely, 18α(H)-oleanane (O), a broadly regarded diagnostic indicator of angiosperm contribution to paleoflora, was not detected in all the studied samples. The unique absence of 18α(H)-oleanane, particularly, in the Tertiary Sarawak Basin coals is in agreement with the finding by Murray et al. (1997) that Tertiary coals from Southeast Asia contain no oleananes or oleanoid triterpanes Similarly, low amount of oleanane was detected in the Early Eocene sediments from Northeast India (Chattopadhyay & Dutta, 2014), thus corroborating the conclusion by Murray et al. (1997) that the abundance of oleananes is no indicator of the degree of angiosperm land plant contribution to organic matter. According to the authors, the absence of saturated oleanoids is possibly due to the efficient aromatisation and or rearrangement of precursors lipids. In addition, Murray et al. (1997) concluded that the abundance of oleananes and rearranged oleananes is primarily influenced by the extent of early-diagenetic marine influence.

The varying abundances of aliphatic des-A-triterpenes have been employed to infer changes in paleovegetation; thus, this could be useful for estimating paleoenvironmental conditions (Killops et al., 1995; Jacob et al., 2007; Huang et al., 2008; Jiang & George, 2018; Jiang et al. 2020). The Sarawak Basin Formation coals are mostly dominated by the C_{24} ring-A degraded ursane derivative while the Benue Trough coals are generally dominated by the lupane derivative (Table 5.21). The predominance of 10β(H)-des-A-lupane in the Benue Trough coals is generally suggestive of relatively drier conditions (Jacob et al., 2007).

5.10.3.4 Angiosperm-gymnosperm ratios

The relative abundances of angiosperm-derived triterpenoid and gymnosperm-derived diterpenoid biomarkers have been widely utilized to reconstruct variation in past vegetation and climate. Killops et al. (1995) proposed the angiosperm/gymnosperm index (AGI) to evaluate flora changes in the Taranaki Basin, New Zealand during the Cretaceous and Paleogene. Similarly, based on the analysis of angiosperm fossils from Japan, Nakamura et al. (2010) proposed the aliphatic angiosperm/gymnosperm index (al-AGI') and aromatic angiosperm/gymnosperm index (ar-AGI'). In addition, Bechtel et al. (2001, 2008) proposed the Di-/Tri-terpenoids and Di-/(Di-+Tri-terpenoids) ratios. Furthermore, Haberer et al. (2006) proposed the use of angiosperm-gymnosperm aromatic ratio (AGAR) to determine the contribution of angiosperms and gymnosperms to paleovegetation.

The AGI, al-AGI' and Di-/Tri-terpenoids parameters are calculated for the studied Sarawak Basin and Benue Trough coals (Table 5.21). Di-/Tri-terpenoids ratios for the coals range from 0.12 to 3.49 with average values of 0.74 and 2.20 for the Sarawak

Basin and Benue Trough coals, respectively. Additionally, al-AGI' ratios range from 0.41 to 0.89 and 0.21 to 0.45 with average ratios of 0.60 and 0.33 for the Sarawak Basin and Benue Trough coals, respectively. These parameters are suggestive of a predominant contribution of angiosperms and gymnosperms, respectively, to the paleoflora of the Sarawak Basin and Benue Trough (Killops et al., 1995; Nakamura et al., 2010; Bechtel et al., 2008).

Table 5.21: Di- and tri-terpenoid parameters for the studied coals.

Sample	dL/(dL+dO)	βP/(βP+αP)	IP/TD	AGI	Al-AGI'	Di/Tri
B01-1	-	-	0.23	-	0.72	0.38
B01-4	0.25	-	-	8.44	0.89	0.12
B01-5	-	-	-	-	0.73	0.37
B02-4	0.40	-	-	1.32	0.57	0.76
B03-2	0.87	-	-	1.13	0.53	0.89
B03-3	0.84	-	-	1.21	0.55	0.82
B03-6	-	-	-	-	0.61	0.65
E55-2	0.78	-	-	2.34	0.70	0.43
L04A-1	0.71	-	-	2.79	0.74	0.36
L04B-1	-	-	-	-	0.43	1.35
ML46A-6	-	-	-	0.73	0.42	1.38
ML46A-7	0.84	-	-	0.94	0.48	1.06
BG1	0.80	-	0.13	1.01	0.50	0.99
BG2	0.67	-	0.25	-	0.56	0.77
0464A	0.76	0.28	0.08	1.24	0.55	0.80
M03-2	-	-	0.15	1.36	0.58	0.73
MK1	0.69	0.10	0.03	0.74	0.43	1.35
MK2	0.32	0.05	0.14	0.77	0.43	1.31
MK3A	0.33	-	0.40	1.11	0.53	0.90
MK3B	-	-	0.40	1.14	0.53	0.88
MP1L	0.61	-	0.23	1.95	0.66	0.51
MP1M	0.70	-	-	0.97	0.49	1.03
MP1U	-	-	-	-	-	-
MP2L	0.11	-	-	3.21	0.76	0.31
MP2U	-	-	-	3.67	0.79	0.27
MP3L	0.54	0.32	0.11	1.10	0.52	0.91
MP3M	0.48	-	-	-	-	-
MP3U	0.30	-	-	0.70	0.41	1.42
MP4L	0.32	-	0.27	1.92	0.66	0.52
MP4M	0.11	0.58	0.13	0.77	0.44	1.30
MP4U	0.38	-	-	2.61	0.72	0.38

dL: 10β(H)-des-A-lupane; dO: 10β(H)-des-A-oleanane; αP: 16α(H)- phyllocladane; βP: 16β(H)-phyllocladane; IP: isopimarane; TD: total diterpenoids; AGI: angiosperm/gymnosperm index (Killops et al., 1995); al-AGI': aliphatic angiosperm-gymnosperm index (Nakamura et al., 2010); Di/Tri: diterpenoids/triterpenoids (Bechtel et al., 2001).

Table 5.21, continued.

Sample	dL/(dL+dO)	βP/(βP+αP)	IP/TD	AGI	Al-AGI'	Di/Tri
MP5L	0.16	-	-	1.77	0.64	0.56
MP5M	0.07	-	-	1.57	0.61	0.64
MP5U	0.17	-	-	3.29	0.77	0.30
MP6L	0.40	-	-	1.25	0.56	0.80
MP6M	0.18	-	-	3.63	0.78	0.28
MP6U	-	-	0.22	1.53	0.60	0.66
MP7L	-	0.48	-	1.59	0.58	0.63
MP7M	0.37	-	-	1.71	0.63	0.59
MP7U	0.82	-	-	1.59	0.61	0.63
MGL3A	-	0.23	0.10	0.29	0.22	3.47
MGL4A	-	0.24	0.05	-	0.39	1.55
MGL1C	-	-	-	0.46	0.32	2.17
MGL2A	-	-	-	0.81	0.45	1.23
MGL2B	-	0.42	0.08	0.29	0.21	3.49
MGL2H	-	0.25	0.11	0.42	0.30	2.37
MGL2I	-	0.17	0.04	0.34	0.25	2.96
MGL2O	-	0.14	0.05	0.40	0.29	2.47
MGL2P	-	0.19	0.05	0.44	0.31	2.27
MGL2T	-	-	-	0.70	0.41	1.44
AFZ	0.43	-	-	0.64	0.39	1.57
ENG	-	0.30	0.06	0.62	0.38	1.62
IMG	0.39	0.11	-	0.62	0.38	1.61
OGB	0.41	-	-	0.41	0.29	2.43
OKB	-	0.26	0.07	0.46	0.32	2.16
WKP	0.57	0.19	0.11	0.38	0.27	2.65
CKL	-	0.85	0.11	0.36	0.26	2.78
LMZ1	-	0.87	0.09	0.31	0.24	3.18
LFO	-	0.15	0.07	0.83	0.45	1.21
SKJ	-	0.14	0.08	0.72	0.42	1.39

5.11 Aromatic Hydrocarbons

5.11.1 Total aromatic hydrocarbons

Aromatic compounds such as dibenzothiophene (DBT), dibenzofuran (DBF), phenanthrene (PHE), fluorene (F), naphthalene (Np) and their alkylated homologues were identified in the aromatic fractions of the investigated coal samples. The TICs of the aromatic fractions of the coals are, however, dominated by naphthalene, phenanthrene and their alkylated homologues (Figure 5.24).

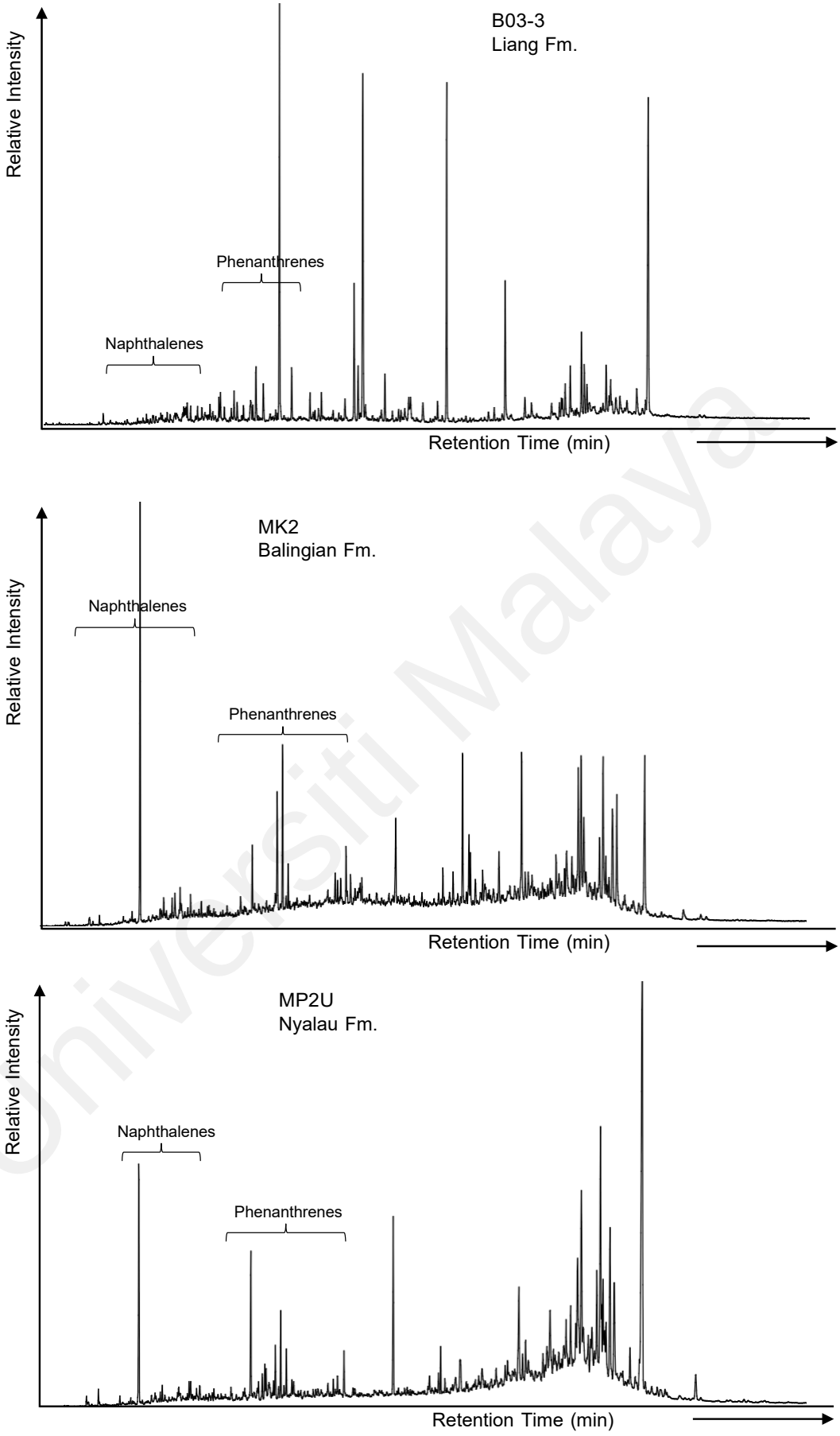

Figure 5.24: Total ion chromatograms (TICs) of the aromatic fractions of representative samples of the Sarawak coals.

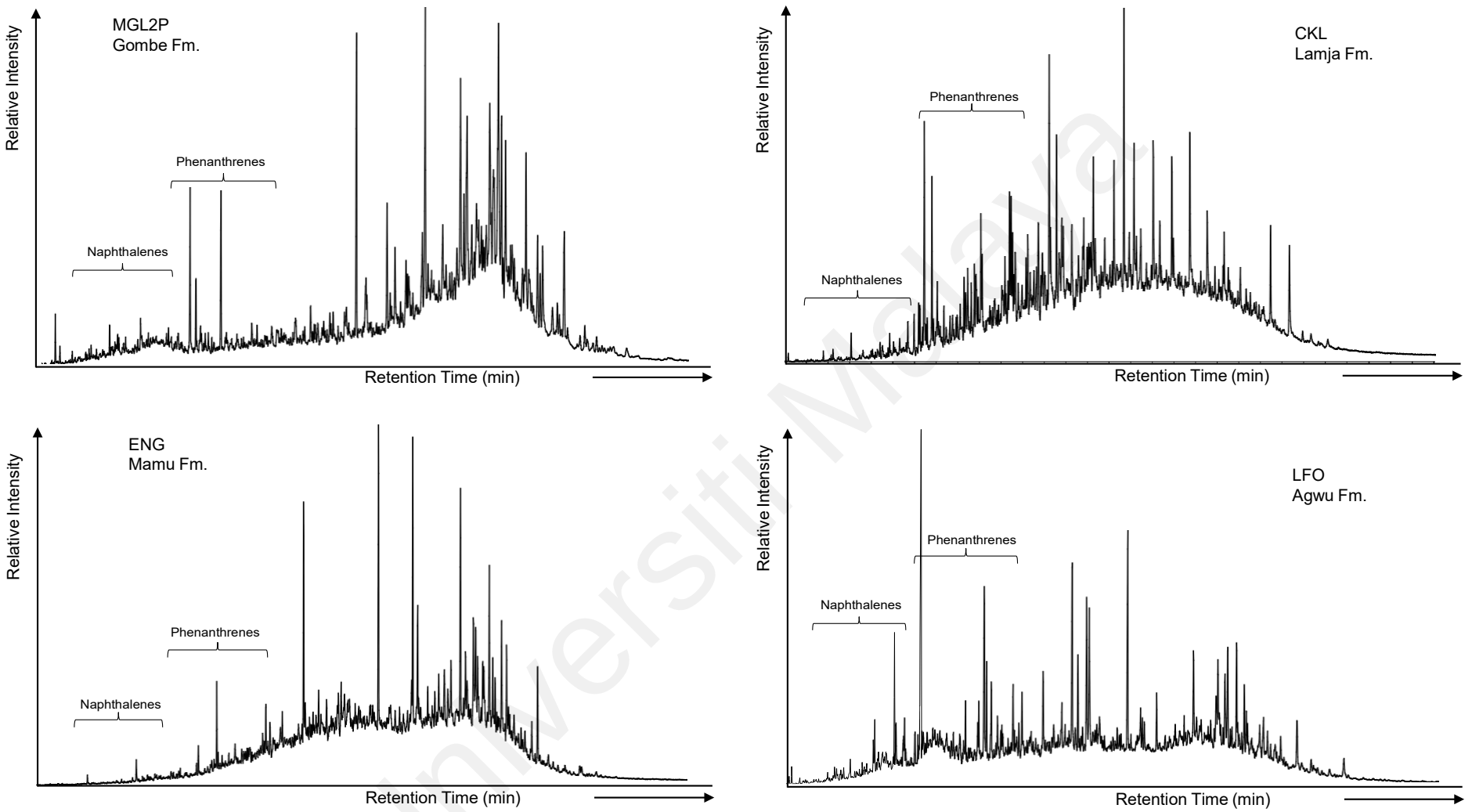

Figure 5.24, continued.

5.11.2 Alkylated Phenanthrenes and Naphthalenes

Alkylated homologues of aromatic compounds are abundant in the coals and their abundance are useful indicators of thermal maturity (Chakhmakhchev & Suzuki, 1995; Chakhmakhchev et al., 1997; Radke et al. 1986), depositional environment and lithologies (Pu et al., 1990; Hughes et al., 1995; Li et al., 2013) and source facies (Radke et al., 2000; Asif & Wenger, 2019).

5.11.2.1 Alkylated Phenanthrenes

The alkylphenanthrenes observed in the studied coals include methylphenanthrene (MP), ethylphenanthrene (EP), and dimethylphenanthrene (DMP) isomers (Figure 5.25). The Liang Formation coals from Sarawak Basin generally show a dominant abundance of 1-MP over other MP isomers, while the Nyalau Formation coals show a varying distribution of MPs with significant abundances of 1-MP, 2-MP, and 9-MP. The Balingian Formation coals are, however, dominated by 9-MP. Similarly, all the Benue Trough samples are dominated by 9-MP, indicating the presence of marine algal organic matter (Budzinski et al., 1995). The EPs are in very low abundance when compared to the DMPs in all the samples. The DMP are, however, dominated by 1,6 + 2,5 + 2,9-DMP and 1,7-DMP. Maturity- and source-related parameters based on the abundances of phenanthrene, and its alkylated homologues in the Sarawak Basin and Benue trough coals are given in Tables 5.21 and 5.22, respectively.

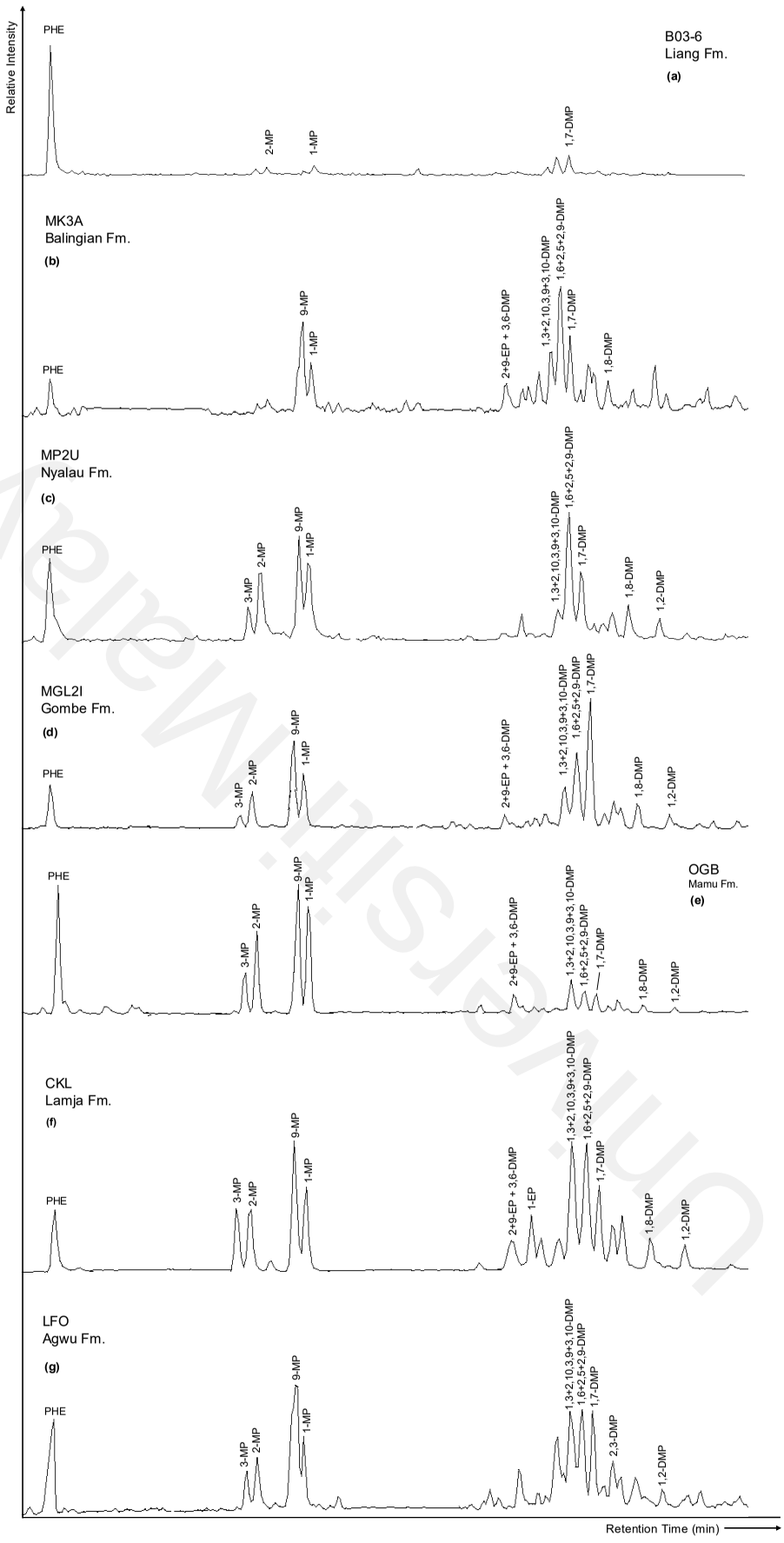

Figure 5.25: Partial *m/z* 178 + 192 + 206 mass chromatograms showing distribution of phenanthrene (PHE), methylphenanthrene (MP) and dimethylphenanthrene (DMP) isomers in the aromatic fractions of the studied coals

Table 5.22: Alkylated phenanthrene-based parameters for the Sarawak Basin coals.

Sample	MPDF	MPR	MPI-1	%R_c MPI-1	MPI-2	DPR	Log (1- / 9-MP)	Log (1,7-DMP/1-3-+3,9-+2,10-+3,10-DMP)	Log (Retene/ 9-MP)	MP/PHE
B01-1	0.37	0.46	0.15	0.49	0.19	0.12	0.56	0.18	1.41	0.34
B01-4	0.01	0.01	0.01	0.41	0.02	-	-	1.38	4.22	25.29
B01-5	0.34	0.35	0.13	0.48	0.15	-	0.80	0.66	1.45	0.30
B02-4	0.18	0.14	0.12	0.47	0.15	0.09	1.16	0.61	2.49	0.73
B03-2	0.55	0.91	0.12	0.47	0.14	0.17	0.52	0.25	1.02	0.16
B03-3	0.02	0.01	0.02	0.41	0.03	-	-	-	-	10.15
B03-6	0.49	0.74	0.16	0.50	0.20	-	0.59	0.40	0.95	0.25
E55-2	0.35	0.46	0.26	0.55	0.37	0.02	0.73	0.57	0.97	0.72
L04A-1	0.58	1.26	0.15	0.49	0.19	-	0.36	0.30	0.79	0.19
L04B-1	0.56	1.09	0.19	0.52	0.23	-	0.34	0.17	0.80	0.26
ML46A-6	0.19	0.17	0.11	0.47	0.15	0.07	1.18	0.47	1.33	0.57
ML46A-7	0.01	0.01	0.02	0.41	0.03	-	-	1.52	-	16.50
BG1	0.03	0.03	0.05	0.43	0.08	-	-	-	-	44.04
BG2	0.06	0.04	0.09	0.45	0.10	-	1.31	0.21	2.05	14.75
0464A	0.32	1.08	0.15	0.49	0.17	0.15	-0.49	-0.42	0.34	0.39
M03-2	0.22	0.53	0.16	0.49	0.19	-	-0.31	-	0.06	0.76
MK1	0.46	1.31	0.63	0.78	0.86	0.21	-0.12	0.07	0.05	1.85
MK2	0.10	0.10	0.12	0.47	0.06	-	-0.40	0.83	0.66	2.95
MK3A	0.16	0.40	0.22	0.53	0.32	-	-0.30	0.05	1.20	4.91
MK3B	0.13	0.68	0.18	0.51	0.19	0.10	-0.86	-0.24	1.15	4.16

PHE: Phenanthrene; MP: Methylphenanthrene; MPDF = (3-+2-MP)/(3-+2-+1-+9-MP); MPR = 2-MP/1-MP; MPI-1 = 1.5 x (2-+3-MP)/(PHE+1-MP+9-MP); %R_c: Calculated reflectance = (0.6 x MPI-1) + 0.4; MPI-2 = (3 x 2-MP)/(PHE+1-MP+9-MP) ; DPR = (3,5-+2,6-DMP+2,7-DMP)/(1-3-+3,9-+2,10-+3,10-DMP+1,6-+2,9-+2,5-DMP);

Table 5.22, continued.

Sample	MPDF	MPR	MPI-1	%R_c MPI-1	MPI-2	DPR	Log (1- / 9-MP)	Log (1,7-DMP/1-3-+3,9-+2,10-+3,10-DMP)	Log (Retene/ 9-MP)	MP/P
MP1L	0.41	0.76	0.74	0.84	1.21	0.01	0.48	0.72	2.12	4.13
MP1M	0.26	0.31	0.42	0.65	0.66	-	0.83	0.92	-	5.46
MP1U	0.17	0.17	0.20	0.52	0.29	-	0.75	0.41	1.92	2.49
MP2L	0.47	1.20	0.93	0.96	1.42	-	0.10	0.47	-	4.58
MP2U	0.40	1.03	0.65	0.79	1.00	-	0.01	-	-	2.97
MP3L	0.40	0.84	0.65	0.79	0.83	0.08	0.03	0.36	-	2.99
MP3M	0.35	0.68	0.39	0.64	0.57	-	0.10	0.52	-	1.50
MP3U	0.35	0.66	0.51	0.71	0.72	0.05	0.12	0.48	-	2.72
MP4L	0.39	1.12	0.47	0.68	0.68	0.06	-0.16	0.47	-	1.62
MP4M	0.41	0.74	0.79	0.87	1.21	-	0.43	-	-	5.04
MP4U	0.44	1.28	0.48	0.69	0.70	-	-0.08	0.37	-	1.21
MP5L	0.45	1.40	0.50	0.70	0.69	0.10	-0.16	0.39	-1.45	1.23
MP5M	0.39	1.39	0.51	0.71	0.76	0.05	-0.30	0.44	-1.25	1.93
MP5U	0.48	1.20	0.51	0.71	0.78	-	0.15	0.78	-	1.13
MP6L	0.53	1.28	1.10	1.06	1.48	-	0.15	0.75	-	4.10
MP6M	0.49	1.01	1.24	1.14	1.98	-	0.49	-	-	12.25
MP6U	0.48	1.09	0.91	0.95	1.44	-	0.32	0.61	-	3.60
MP7L	0.46	1.06	1.04	1.02	1.57	-	0.20	0.54	-	7.95
MP7M	0.53	1.43	1.51	1.31	2.41	-	0.23	-	-	17.31
MP7U	0.56	1.04	1.34	1.20	2.05	-	1.32	0.90	-	5.11

Table 5.23 Alkylated phenanthrene-based parameters for the Benue Trough coals.

Sample	MPDF	MPR	MPI-1	%R_c MPI-1	MPI-2	DPR	Log (1- / 9-MP)	Log (1,7-DMP/1-3-+3,9-+2,10-+3,10-DMP)	Log (Retene/ 9-MP)	MP/PHE
MGL3A	0.31	1.45	0.29	0.58	0.47	0.21	-0.48	0.32	-0.50	0.84
MGL4A	0.35	1.52	0.23	0.54	0.32	0.20	-0.51	0.10	-0.22	0.60
MGL1C	0.39	1.53	0.34	0.60	0.46	-	-0.41	0.13	-0.13	0.43
MGL2A	0.24	0.94	0.29	0.57	0.43	0.11	-0.48	0.31	-0.45	0.86
MGL2B	0.19	1.03	0.26	0.56	0.34	0.15	-0.75	0.40	-0.64	0.85
MGL2H	0.26	0.74	0.28	0.57	0.39	0.24	-0.32	0.23	-0.41	0.61
MGL2I	0.27	0.66	0.41	0.65	0.61	0.15	-0.16	0.42	-0.41	0.72
MGL2O	0.22	0.42	0.29	0.58	0.39	0.08	-0.10	0.14	-0.32	0.70
MGL2P	0.21	0.41	0.23	0.54	0.29	-	-0.14	0.23	-0.14	0.76
MGL2T	0.22	0.46	0.30	0.58	0.40	0.08	-0.17	0.03	-0.49	0.67
AFZ	0.32	0.97	0.48	0.69	0.55	0.12	-0.42	-0.16	0.32	3.31
ENG	0.29	0.92	0.21	0.52	0.26	-	-0.41	-0.13	0.29	0.73
IMG	0.35	1.01	0.47	0.68	0.59	0.09	-0.30	-0.23	0.35	2.21
OGB	0.32	0.67	0.47	0.68	0.61	0.07	-0.09	-0.30	0.32	2.94
OKB	0.29	0.80	0.16	0.50	0.20	-	-0.33	0.18	0.29	0.49
WKP	0.34	0.80	0.31	0.58	0.38	0.08	-0.18	0.13	0.34	1.00
CKL	0.38	0.81	0.71	0.83	0.76	0.10	-0.16	-0.27	-1.05	5.16
LMZ1	0.41	1.12	0.67	0.80	0.85	0.22	-0.20	0.00	-1.27	3.19
LFO	0.28	1.33	0.46	0.67	0.56	-	-0.65	-0.14	-1.11	4.62
SKJ	0.33	0.81	0.19	0.52	0.24	-	-0.24	0.03	0.00	0.54

PHE: Phenanthrene; MP: Methylphenanthrene; MPDF = (3-+2-MP)/(3-+2-+1-+9-MP); MPR = 2-MP/1-MP; MPI-1 = 1.5 x (2-+3-MP)/(PHE+1-MP+9-MP); %R_c: Calculated reflectance = (0.6 x MPI-1) + 0.4; MPI-2 = (3 x 2-MP)/(PHE+1-MP+9-MP) ; DPR = (3,5-+2,6-DMP+2,7-DMP)/(1-3-+3,9-+2,10-+3,10-DMP+1,6-+2,9-+2,5-DMP).

5.11.2.2 Alkylated Naphthalenes

The alkylnaphthalenes are mainly composed of methylnaphthalene (MN), dimethylnaphthalene (DMN) and trimethylnaphthalene (TMN) and tetramethylnaphthalene (TeMN) isomers. (Figure 5.26; Table 5.23). The most abundant DMN in the samples is generally 1,6-DMN, while 2,6 + 2,7-DMN predominates in a few samples. The distribution of TMNs in most samples is dominated by 1,6,7-TMN but with significant abundances of 1,2,5-TMN and 1,3,6-TMN in the Sarawak Basin and Benue Trough samples, respectively. The studied coals show a varying distribution of MNs, with the methylnaphthalene ratio (MNR; 2-MN/1-MN) ranging from 0.38 to 7.32 (avg. 1.29) and 0.72 to 2.00 (avg. 1.21) in the Malaysian and Nigerian coals, respectively. Other thermal maturity- and source-related alkylated naphthalene parameters are accordingly presented in Tables 5.24 and 5.25.

Table 5.24: Alkylnaphthalenes identified in studied coals (Figure 5.26).

Peak	Compounds
a	2,6- + 2,7-dimethylnaphthalene
b	1,3- + 1,7-dimethylnaphthalene
c	1,6-dimethylnaphthalene
d	1,4- + 2,3-dimethylnaphthalene
e	1,5-dimethylnaphthalene
f	1,2-dimethylnaphthalene
g	1,3,7-trimethylnaphthalene
h	1,3,6-trimethylnaphthalene
i	1,3,5- + 1,4,6-trimethylnaphthalene
j	2,3,6-trimethylnaphthalene
k	1,6,7-trimethylnaphthalene
l	1,2,6-trimethylnaphthalene
m	1,2,4-trimethylnaphthalene
n	1,2,5-trimethylnaphthalene
o	1,3,5,7-tetramethylnaphthalene
p	1,3,6,7-tetramethylnaphthalene
q	1,2,4,6- + 1,2,4,7- + 1,4,6,7-tetramethylnaphthalene
r	1,2,5,7-tetramethylnaphthalene
s	2,3,6,7-tetramethylnaphthalene
t	1,2,6,7-tetramethylnaphthalene
u	1,2,3,7-tetramethylnaphthalene
v	1,2,3,6-tetramethylnaphthalene
w	1,2,5,6- + 1,2,3,5-tetramethylnaphthalene

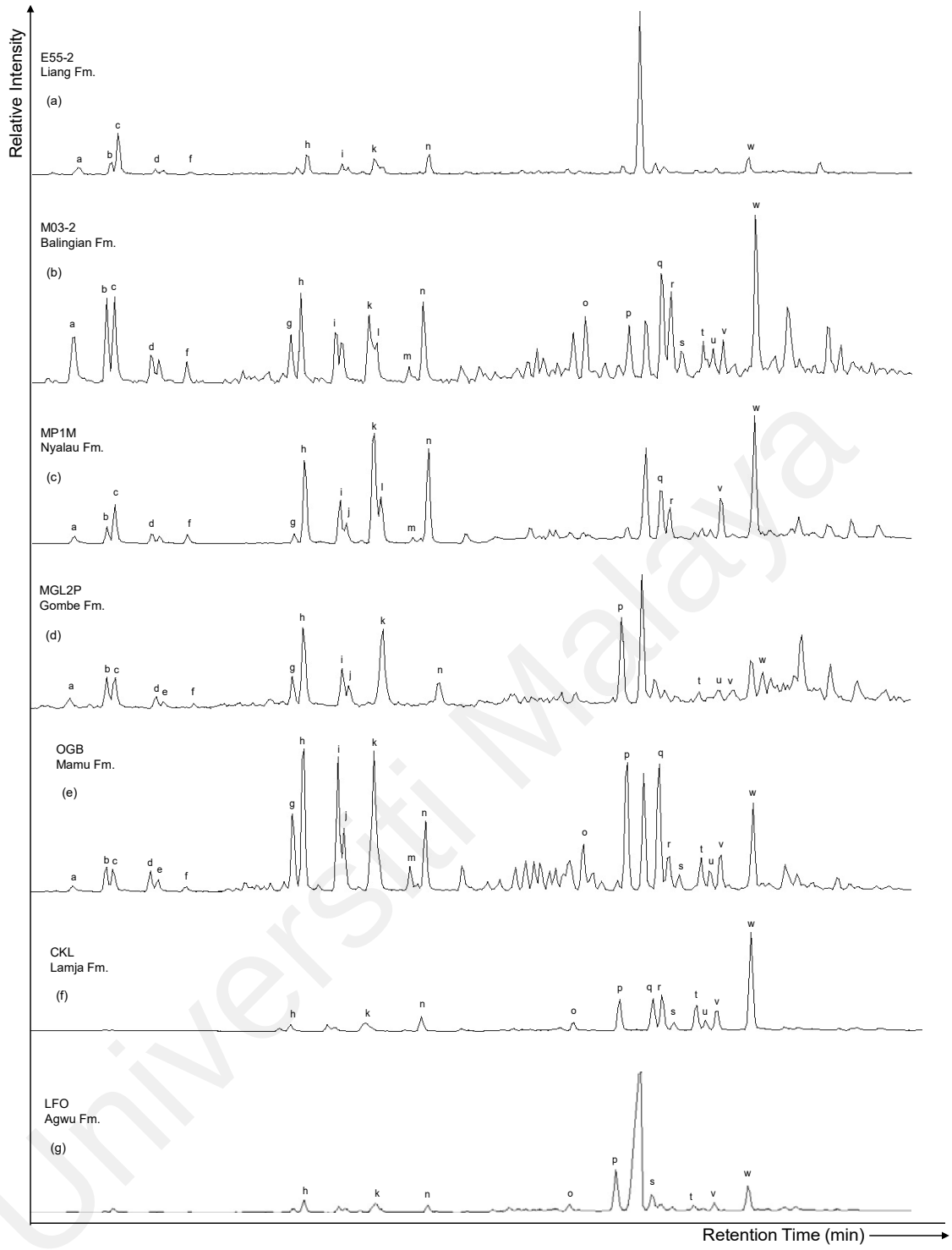

Figure 5.26: Partial *m/z* 156 + 170 + 184 mass chromatograms showing distribution of dimethylnaphthalene (DMN), trimethylnaphthalene (TMN) and tetramethylnaphthalene (TeMN) isomers in the aromatic fractions of the studied coals. Labelled compounds are listed in Table 5.23.

Table 5.25: Alkylated naphthalene-based parameters for the Sarawak Basin coals.

Sample	MNR	%R_c MNR	DNRx	DMR	DNR-1	TNR-1	TNR-2	%R_c TNR-2	TMR	TMNr	TeMNr	Log (1,2,5- / 1,3,6-TMN)
B01-1	0.81	0.96	0.29	4.54	2.14	0.60	0.65	0.79	4.48	0.19	-	0.65
B01-4	0.45	0.90	0.39	3.15	1.36	1.10	0.53	0.72	2.00	0.23	0.16	0.30
B01-5	0.80	0.96	0.40	3.57	2.31	0.93	0.39	0.64	4.15	-	-	0.62
B02-4	0.39	0.89	0.23	3.92	2.25	0.73	0.51	0.70	4.67	0.11	0.10	0.67
B03-2	0.64	0.93	1.33	8.50	14.86	0.57	0.63	0.78	6.75	0.11	0.31	0.83
B03-3	1.48	1.07	0.54	3.38	4.33	0.93	0.48	0.69	2.54	0.25	-	0.40
B03-6	0.56	0.91	0.38	13.77	1.54	0.89	0.77	0.86	2.87	0.19	-	0.46
E55-2	1.21	1.02	0.16	3.67	1.60	0.59	0.42	0.65	3.12	0.24	0.31	0.49
L04A-1	0.38	0.88	1.58	7.50	13.25	-	-	-	-	-	0.33	-
L04B-1	-	-	-	-	-	-	-	-	-	-	0.12	-
ML46A-6	0.86	0.97	0.22	10.40	5.50	0.41	0.39	0.63	5.83	0.19	-	0.77
ML46A-7	-	-	-	-	-	0.65	0.40	0.64	3.24	0.18	0.28	0.51
BG1	-	-	-	-	-		-	-	-		-	-
BG2	-	-	-	-	-	0.89	0.69	0.81	2.25	0.21	-	0.35
0464A	-	-	1.67	2.55	0.79	0.79	0.67	0.80	4.74	0.17	0.14	0.68
M03-2	1.43	1.06	0.54	1.29	1.93	0.80	0.63	0.78	2.04	0.37	0.23	0.31
MK1	1.61	1.09	-	-	-	-	-	-	-	-	0.39	-
MK2	2.66	1.27	1.32	-	-	-	-	-	-	-	-	-
MK3A	1.69	1.11	0.66	1.91	2.50	-	-	-	-	0.44	0.19	-
MK3B	1.52	1.08	0.69	1.59	2.17	0.66	1.59	1.36	0.95	0.60	0.13	-0.02

MN: Methylnaphthalene; DMN: Dimethylnaphthalene; TMN: Trimethylnaphthalene; TeMN: Tetramethylnaphthalene; MNR = 2-MN/1-MN; %R_c MNR = (0.17 x MNR + 0.82); DNR_x = (2,6-+2,7-DMN)/1,6-DMN; DMR = (1,5-+1,6-DMN)/(1,3-+1,7-DMN); DNR-1 = (2,6-+2,7-DMN)/1,5-DMN; TNR-1 = 2,3,6-TMN/(1,4,6-+1,3,5-DMN); TNR-2 = (1,3,7-+2,3,6-TMN)/(1,3,5-+1,3,6-+1,4,6-TMN); %R_c TNR-2 = 0.4 + (0.6 x TNR-2) ; TMR = 1,2,5-TMN/2,3,6-TMN; TMNr = 1,3,7-TMN/(1,3,7-1,2,5-TMN); TeMNr = 1,3,6,7-TeMN/(1,3,6,7-+1,2,5,6-TeMN).

Table 5.25, continued.

Sample	MNR	%R_c MNR	DNRx	DMR	DNR-1	TNR-1	TNR-2	%R_c TNR-2	TMR	TMNr	TeMNr	Log (1,2,5- / 1,3,6-TMN)
MP1L	-	-	0.33	2.48	1.71	1.00	0.39	0.63	2.57	0.10	0.08	0.41
MP1M	0.39	0.89	0.20	2.74	1.05	0.45	0.23	0.54	4.80	0.09	0.09	0.68
MP1U	1.79	1.12	0.15	3.10	0.54	0.75	0.33	0.60	4.07	0.11	0.18	0.61
MP2L	0.51	0.91	0.47	1.29	1.66	0.56	0.58	0.75	1.08	0.54	0.18	0.03
MP2U	1.36	1.05	0.67	2.70	-	0.61	0.44	0.66	3.09	0.19	0.24	0.49
MP3L	0.98	0.99	0.53	1.91	2.90	1.04	0.87	0.92	1.83	0.31	0.14	0.26
MP3M	0.86	0.97	0.14	-	2.79	1.13	0.50	0.70	6.22	-	0.12	0.79
MP3U	1.37	1.05	0.38	4.67	3.30	1.50	0.70	0.82	5.00	0.05	0.08	0.70
MP4L	0.95	0.98	0.69	4.36	4.00	0.60	0.47	0.68	4.71	0.15	0.21	0.67
MP4M	-	-	0.46	-	-	-	-	-	-	-	-	-
MP4U	-	-	0.41	3.88	1.83	0.38	0.18	0.51	-	-	0.18	0.71
MP5L	1.77	1.12	0.26	4.00	1.40	0.70	0.57	0.74	3.71	0.16	0.17	0.57
MP5M	1.05	1.00	0.32	6.16	3.09	0.95	0.70	0.82	2.80	0.15	0.26	0.45
MP5U	0.99	0.99	0.17	6.37	1.73	1.00	0.52	0.71	4.13	0.08	0.10	0.62
MP6L	7.32	2.06	0.15	7.63	1.70	-	-	-	-	-	-	-
MP6M	-	-	-	-	-	-	-	-	-	-	-	-
MP6U	0.64	0.93	0.39	3.61	2.75	2.00	0.73	0.84	2.50	0.07	0.08	0.40
MP7L	0.88	0.97	0.25	-	3.20	3.00	0.89	0.93	4.08	0.08	-	0.61
MP7M	-	-	0.15	8.54	3.68	-	-	-	-	-	-	-
MP7U	-	-	0.37	-	-	-	-	-	-	-	0.48	-

Table 5.26: Alkylated naphthalene-based parameters for the Benue Trough coals.

Sample	MNR	%R_c MNR	DNRx	DMR	DNR-1	TNR-1	TNR-2	%R_c TNR-2	TMR	TMNr	TeMNr	Log (1,2,5- / 1,3,6-TMN)
MGL3A	-	-	0.61	1.01	2.48	0.81	0.57	0.74	0.56	0.67	0.71	-0.25
MGL4A	-	-	1.10	2.39	-	1.11	0.61	0.76	0.82	0.49	0.50	-0.09
MGL1C	1.41	1.06	0.53	2.13	4.43	1.28	0.85	0.91	1.10	0.37	0.36	0.04
MGL2A	1.08	1.00	0.33	1.23	1.25	0.61	0.39	0.63	0.77	0.62	0.74	-0.12
MGL2B	2.00	1.16	0.35	1.28	1.28	1.00	0.55	0.73	0.67	0.52	0.70	-0.17
MGL2H	1.32	1.04	0.44	1.29	2.25	0.63	0.45	0.67	1.00	0.51	0.73	0.00
MGL2I	1.79	1.12	0.40	1.69	1.79	2.10	0.90	0.94	0.54	0.53	0.79	-0.27
MGL2O	0.98	0.99	0.38	1.38	2.00	1.42	0.76	0.86	0.73	0.48	0.70	-0.14
MGL2P	0.89	0.97	0.32	1.18	1.48	0.53	0.43	0.66	1.16	0.56	0.61	0.06
MGL2T	-	0.82	0.31	1.92	1.90	0.87	0.64	0.79	1.35	0.46	0.61	0.13
AFZ	1.55	1.08	0.67	1.44	2.29	-	-	-	-	-	0.20	-
ENG	0.73	0.94	0.37	2.21	2.40	0.86	0.78	0.87	1.66	0.33	0.35	0.22
IMG	0.72	0.94	0.54	1.10	1.47	0.90	0.69	0.81	3.21	0.16	0.24	0.51
OGB	-	-	0.25	1.40	0.46	-	-	-	-	-	0.61	-
OKB	-	-	0.20	2.91	0.84	1.04	0.87	0.92	2.50	0.22	-	0.40
WKP	0.99	0.99	0.67	1.12	1.68	0.50	0.44	0.67	2.83	0.20	0.16	0.45
CKL	1.23	1.03	0.42	1.05	0.95	0.61	0.51	0.71	3.65	0.16	0.24	0.56
LMZ1	1.15	1.02	0.61	1.00	2.00	0.98	0.77	0.86	1.26	0.37	-	0.10
LFO	1.15	1.02	0.20	3.07	1.60	0.71	0.44	0.66	1.59	0.35	0.59	0.20
SKJ	-	-	-	-	-		-	-	-	-	0.66	-

MN: Methylnaphthalene; DMN: Dimethylnaphthalene; TMN: Trimethylnaphthalene; TeMN: Tetramethylnaphthalene; MNR = 2-MN/1-MN; %R_c MNR = (0.17 x MNR + 0.82); DNR_x = (2,6-+2,7-DMN)/1,6-DMN; DMR = (1,5-+1,6-DMN)/(1,3-+1,7-DMN); DNR-1 = (2,6-+2,7-DMN)/1,5-DMN; TNR-1 = 2,3,6-TMN/(1,4,6-+1,3,5-DMN); TNR-2 = (1,3,7-+2,3,6-TMN)/(1,3,5-+1,3,6-+1,4,6-TMN); %R_c TNR-2 = 0.4 + (0.6 x TNR-2) ; TMR = 1,2,5-TMN/2,3,6-TMN; TMNr = 1,3,7-TMN/(1,3,7-1,2,5-TMN); TeMNr = 1,3,6,7-TeMN/(1,3,6,7-+1,2,5,6-TeMN).

5.11.3 Fluorene, Dibenzofuran, Dibenzothiophene, and Methyl Derivatives

Dibenzofuran (DBF), Dibenzothiophene (DBT), and Fluorene (F) are important aromatic compounds in source rocks and crude oils. The compounds are abundant in the studied coal samples and their distributions are shown in Figure 5.27.

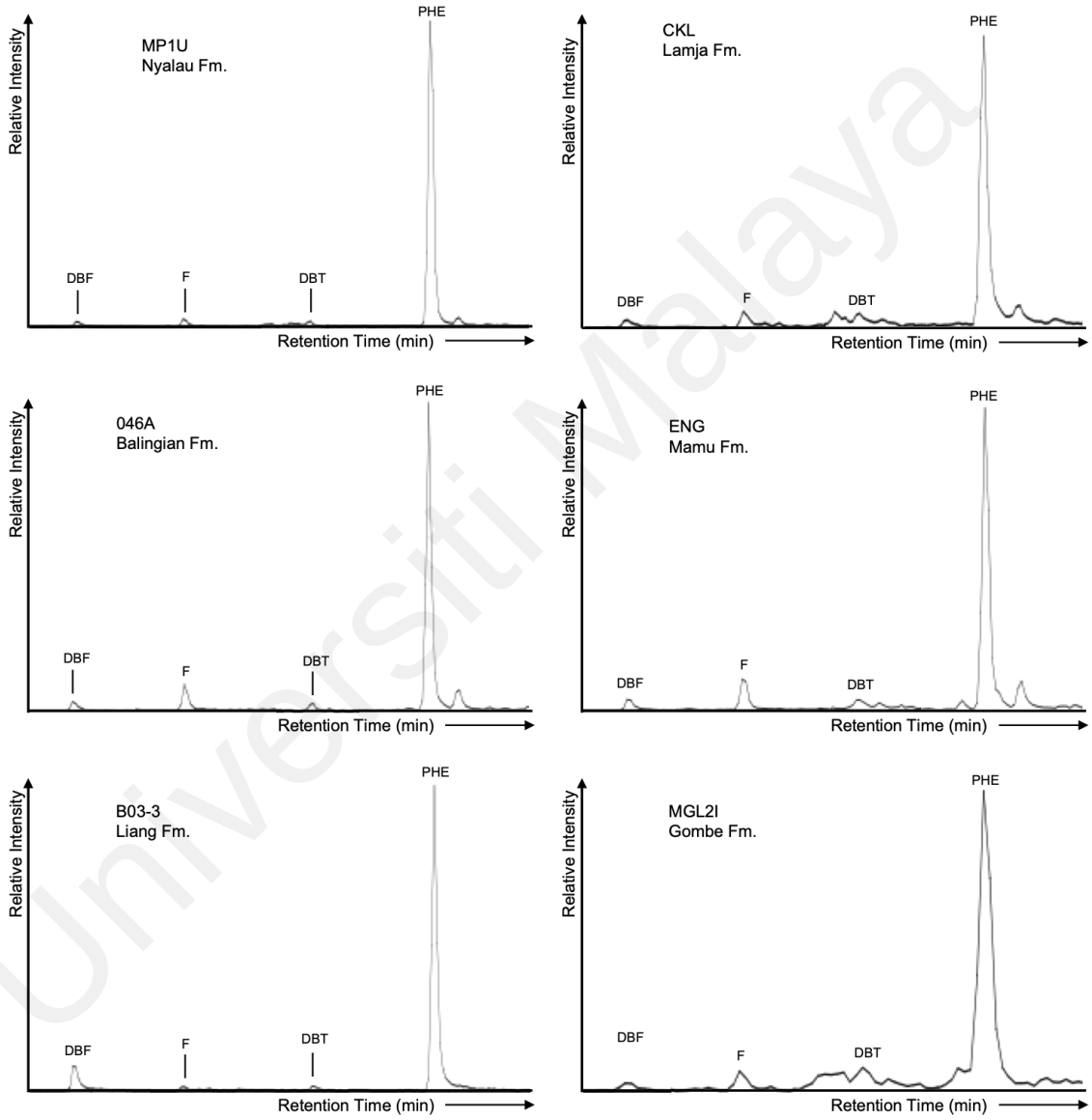

Figure 5.27: Summed partial chromatograms showing the distribution of aromatic compounds (*m/z* 166 + 168 + 178 + 184) in representative samples.
DBF: dibenzofuran; F: fluorene; DBT: dibenzothiophene; PHE: phenanthrene

In addition, their methylated derivatives, methyldibenzothiophenes (MDBT), methyldibenzofurans (MDBF) and methylfluorenes (MF), are present in the coal extracts (Figure 5.28).

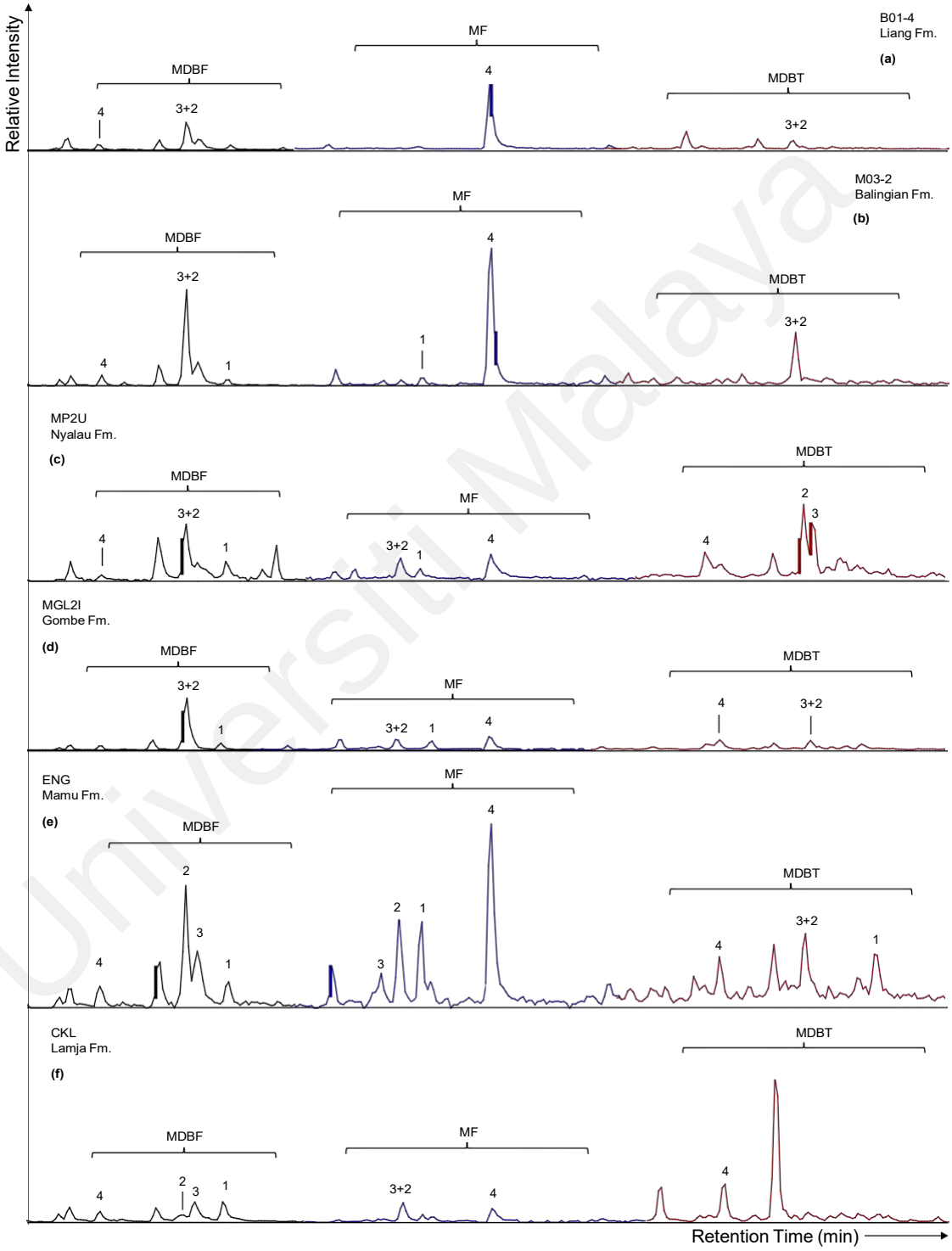

Figure 5.28: Summed partial chromatograms showing the distribution of aromatic compounds (*m/z* 182 + 180 + 198) in representative samples.

The distributions of these heterocyclic compounds have been employed as indicators of thermal maturity (Chakhmakhchev et al., 1997), source facies (Radke et al., 2000; Li et al., 2013; Asif & Wenger, 2019), lithologies and depositional environments (Pu et al., 1990; Hughes et al., 1995). For example, the relative abundances of DBT and MDBT have been established to predominate in marine sediments, whereas F and MF predominate in freshwater lacustrine source rocks. Furthermore, previous studies have shown that DBF and MDBF dominate terrigenous organic matter deposited in oxic environments due to the enrichment of O-species (Pu et al., 1990; Li et al., 2013; Asif & Wenger, 2019).

Compared with PHE, DBT abundances in the studied coals are considerably low with DBT/PHE ratios mostly < 1 (Table 5.27), which are typical of source rocks from non-marine environments (Hughes et al., 1995). Similarly, DBF/PHE ratios are all < 1, with average ratios of 0.11 and 0.09 for Sarawak Basin and Benue Trough samples, respectively. In addition, DBF/F ratios for the Sarawak Basin and Benue Trough samples range from 0.11 to 47.43 (avg. 4.99) and 0.20 to 3.64 (avg. 1.09), respectively. The lower DBF/F ratios for the Benue Trough coals imply a greater influence of the freshwater-lacustrine depositional environment. For the Sarawak Basin coals, the MDBF distribution of the Nyalau and Liang Formations are generally dominated by a high relative abundance of 3+2-MDBF with subordinate abundances of other MDBFs (Figure 5.28b). Similarly, the Balingian Formation coals are dominated by 2-MDBF but other MDBF are either absent or present in trace amounts. Although MDBTs are either absent or present in low abundance in the Liang Formation coals (Figure 5.28a), their distributions are mainly composed of 4-MDBT in the Balingian and Nyalau Formation coals (Figure 5.28c).

Table 5.27: Aromatic parameters based on relative abundance of methylated dibenzothiophene and dibenzofuran derivatives.

Sample	DBF/ PHE	DBF/ F	DBT/ PHE	DBT/ DBF	MDBF/ MP	MDBT/ MDBF	MDBF/ MF	MDR
B01-1	0.13	25.47	0.01	0.09	0.56	0.06	0.45	-
B01-4	0.09	1.97	0.03	0.25	0.01	0.32	0.84	-
B01-5	0.13	5.74	0.04	0.29	1.04	0.10	0.53	-
B02-4	0.05	0.56	0.05	0.87	0.18	0.34	1.02	-
B03-2	0.09	3.89	0.04	0.40	3.56	0.08	0.82	-
B03-3	0.11	4.62	0.06	0.52	0.02	0.10	0.68	-
B03-6	0.12	5.61	0.04	0.38	1.94	0.07	0.71	-
E55-2	0.18	8.44	0.04	0.23	0.45	0.12	0.88	2.39
L04A-1	0.10	4.47	0.06	0.65	1.96	0.05	0.63	-
L04B-1	0.02	0.90	0.06	2.43	1.17	0.13	0.49	-
ML46A-6	0.12	47.43	0.03	0.23	0.18	0.15	0.29	-
ML46A-7	0.03	0.41	0.03	1.16	0.01	1.04	0.80	1.51
BG1	-	-	-	-	-	-	-	-
BG2	0.13	0.42	0.09	1.66	0.18	0.30	4.79	-
0464A	0.04	0.46	0.05	1.18	0.25	0.89	0.58	-
M03-2	0.14	1.09	0.05	0.38	0.36	0.36	0.86	-
MK1	0.09	0.11	0.55	5.82	0.50	0.81	1.13	-
MK2	0.04	0.30	0.34	8.52	1.41	-	6.30	-
MK3A	0.18	1.57	0.36	2.03	0.52	0.46	1.14	0.63
MK3B	0.05	0.45	0.27	5.35	0.39	0.18	1.35	-
MP1L	0.54	6.74	0.10	0.36	0.50	0.72	2.34	1.04
MP1M	0.53	13.28	0.10	0.49	0.37	0.33	2.22	-
MP1U	0.03	0.90	0.04	5.49	0.24	0.06	0.74	-
MP2L	0.07	0.44	-	-	0.79	0.64	1.96	0.67
MP2U	0.04	1.46	-	-	0.46	0.66	1.76	0.77
MP3L	0.06	1.61	-	-	0.65	0.36	3.99	1.24
MP3M	0.14	5.44	-	-	1.72	0.13	4.88	1.17
MP3U	0.07	2.81	-	-	0.52	0.60	2.48	0.84
MP4L	0.01	0.65	-	-	0.34	1.46	0.82	0.33
MP4M	-	-	-	-	0.69	0.20	5.35	-
MP4U	0.02	0.93	-	-	0.58	0.62	1.19	2.66
MP5L	0.03	7.36	-	-	0.52	0.55	2.47	0.53
MP5M	0.02	-	-	-	0.41	0.31	2.42	1.37
MP5U	0.31	-	-	-	1.40	0.27	4.12	1.78
MP6L	0.07	1.31	-	-	1.44	0.59	-	-
MP6M	-	-	-	-	0.93	0.94	1.82	1.22
MP6U	0.12	2.95	-	-	0.59	0.54	3.12	0.79
MP7L	-	-	-	-	0.53	1.84	2.30	0.92
MP7M	-	-	-	-	0.47	0.70	5.54	0.80
MP7U	-	-	-	-	0.38	0.87	-	0.73

DBF: dibenzofuran; PHE: phenanthrene; F: fluorene; DBT: dibenzothiophene; MDBF: methyldibenzofurans; MP: methylphenanthrenes; MF: methylfluorenes; MDBT: methyldibenzothiophenes; MDR: methyldibenzothiophene ratio = 4-MDBT/1-MDBT.

Table 5.27 continued.

Sample	DBF/ PHE	DBF/ F	DBT/ PHE	DBT/ DBF	MDBF/ MP	MDBT/ MDBF	MDBF/ MF	MDR
MGL3A	0.05	0.83	0.05	0.95	0.09	0.48	0.96	0.71
MGL4A	0.04	0.52	0.05	1.32	0.40	0.25	1.98	0.96
MGL1C	0.11	1.50	-	-	1.34	0.10	2.40	-
MGL2A	0.03	2.05	0.05	2.04	0.15	0.49	1.37	-
MGL2B	-	0.20	0.05	9.68	0.08	0.29	1.36	0.14
MGL2H	0.16	2.78	0.14	0.92	0.86	0.22	2.20	0.06
MGL2I	0.04	0.70	0.16	4.01	0.30	0.17	1.52	-
MGL2O	0.16	1.33	0.17	1.05	0.74	0.09	2.07	-
MGL2P	0.11	3.64	-	-	1.61	-	1.90	-
MGL2T	0.02	0.37	-	-	0.44	0.23	1.85	0.40
AFZ	0.11	0.82	0.06	0.58	0.13	0.27	1.91	-
ENG	0.05	0.47	0.06	1.05	0.21	-	0.73	-
IMG	0.02	0.97	0.09	3.62	0.09	1.25	1.26	2.96
OGB	0.01	0.59	0.04	2.83	0.06	0.64	0.74	-
OKB	0.08	0.54	0.07	0.86	0.26	-	0.46	-
WKP	0.09	1.31	0.04	0.46	0.22	0.11	0.56	-
CKL	0.05	0.74	0.10	1.95	0.07	-	1.72	-
LMZ1	0.04	0.63	0.04	1.04	0.12	-	0.73	-
LFO	0.07	1.12	0.33	4.90	0.43	-	2.35	-
SKJ	0.04	0.77	0.04	0.99	1.21	-	3.16	-

The MF distributions of the studied humic coal are dominated by 4-MF. Other MF isomers are generally absent in the Liang and Balingian Formation coals but present in the Nyalau Formation coals. For the Benue Trough samples, the distribution of MDBF is dominated by 3+2-MDBF in the Mamu and Gombe Formation coals, while dominated by 3-MDBF and 1-MDBF in the Lamja Formation coals, and 1-MDBF in the Agwu Formation coals (Figure 5.28d-f). In addition, 4-MF and 1-MF are the most abundant isomers in the MF distribution. Aromatic parameters based on the abundances of F, DBF, DBT and their methyl derivatives are presented in Tables 5.27.

5.11.4 Polycyclic Aromatic Hydrocarbons

Alkylphenanthrenes and alkylnaphthalenes dominate the total ion chromatograms of the aromatic hydrocarbon fractions of the studied coals. Nevertheless, unsubstituted and substituted polycyclic aromatic hydrocarbons (PAHs) with 3-7 rings are also present in relatively lower abundances (Figure 5.29). Fluoranthene (Fl) and pyrene (Py) were observed in the *m/z* 202 mass chromatograms of the aromatic fractions of the coal extracts, and the abundances of fluoranthene mostly predominate that of pyrene in the analysed samples. Benzo[*a*]anthracene (BaA), chrysene (Ch), and triphenylene (Tph) were detected in the *m/z* 228 mass chromatograms. The co-eluting chrysene and triphenylene are present in all the samples while benzo[*a*]anthracene is present in most of the samples but particularly absent in the Nyalau Formation coals.

Additionally, benzo[*b,j,k*]fluoranthene (BFl), benzo[*e*]pyrene (BePy), benzo[*a*]pyrene (BaPy), and perylene (Per) were identified in the *m/z* 252 mass chromatograms of all Benue Trough and some Sarawak Basin coals. In contrast, perylene is markedly absent in the Lamja Formation coals, possibly due to the relative higher maturity of the samples as the abundance of perylene has been established to rapidly decrease at maturation levels higher than 0.6 %R_o (Marymowski et al, 2015). For the Sarawak Basin coals, benzo[*b,j,k*]fluoranthene, benzo[*e*]pyrene, and benzo[*a*]pyrene are mainly absent in the Nyalau and Balingian Formations while BaPy and perylene are mostly absent in the Liang Formation. Furthermore, ≥ 6-ring PAHs such as indeno[*1,2,3-cd*]pyrene (InPy), benzo[*ghi*]perylene (BgPer) and coronene (Cor) were also detected. These ≥ 6-ring PAHs, which are products of high-temperature events (Zakir Hossain et al., 2013; Zakrzewski et al., 2020), were observed in some Benue Trough coals but not in the Sarawak Basin coals (Figure 5.29).

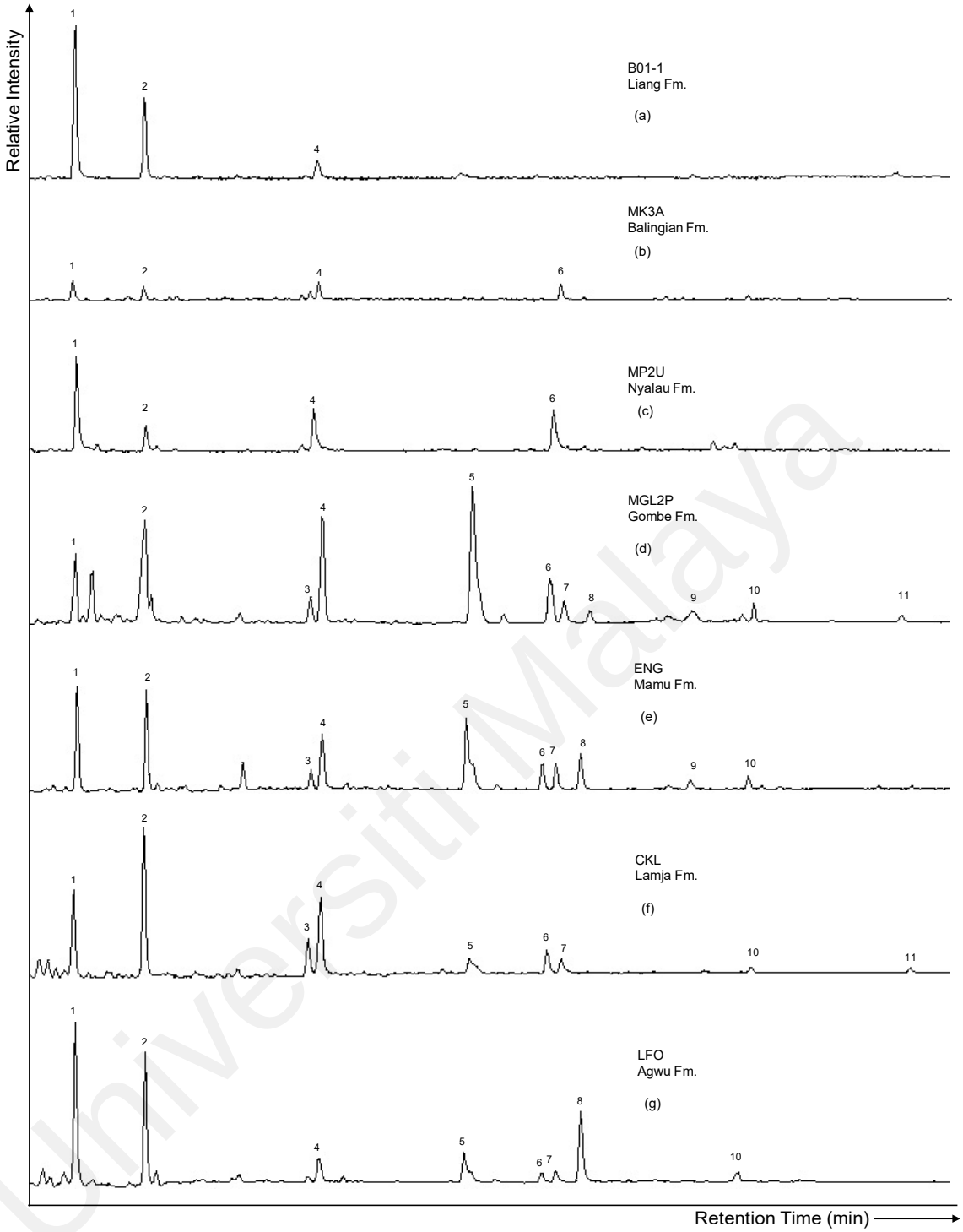

Figure 5.29: Summed partial chromatograms of the aromatic hydrocarbon fractions showing the distribution of combustion-derived polycyclic aromatic hydrocarbons (*m/z* 202 + 228 + 252 + 276 + 300) of representative samples. 1: fluoranthene; 2: pyrene; 3: benzo[*a*]anthracene; 4: chrysene + triphenylene; 5: benzo[*b*]fluoranthene + benzo[*k*]fluoranthene; 6: benzo[*e*]pyrene; 7: benzo[*a*]pyrene; 8: perylene; 9: indeno[1,2,3-cd]pyrene; 10: benzo[*ghi*]perylene; 11: Coronene

Generally, the abundances of PAHs are relatively higher in Benue Trough coals than in the Sarawak Basin coals. This finding suggests seasonal drier conditions suitable for thermal oxidation or relatively lower water table in the paleomires of the Benue Trough during the Late Cretaceous (Jiang et al., 1998; Zakir Hossain et al., 2013). Hence, the PAHs evaluated in this thesis were expressly utilized to distinguish between petrogenic and pyrogenic origin, and accordingly, to reconstruct environmental conditions. Source parameters based on the relative abundances of PAHs are tabulated in Tables 5.27 and 5.28.

5.11.5 Higher Plant-derived Aromatic Biomarkers

Aromatic biomarkers such as cadalene, retene, and 6-*iso*propyl-1-*iso*hexyl-2-methylnaphthalene (ip-iHMN) are important constituents of sedimentary rocks that originate from terrestrial plants due to their structural similarities to precursors (Ellis et al., 1996; Otto & Wilde, 2001; Otto et al. 2002a). Aromatic compounds considered for this research include sesquiterpenoids and diterpenoids. Conversely, aromatic triterpenoid biomarkers are not studied.

The aromatic distributions of the sesquiterpenoids and diterpenoids in the analysed coals are dominated by cadalene and retene, respectively (Figure 5.30). Retene was identified based on mass fragmentograms of *m/z* 219 and *m/z* 234 while cadalene was recognized by the intersecting mass fragmentograms of *m/z* 183 and *m/z* 198. Retene is generally regarded as a conifer vegetation biomarker as it is found primarily in gymnosperm species (Otto et al., 1997; Nakamura et al., 2010). In addition, conifer resin acids have been found to yield aromatics derivatives after undergoing oxidation and decarboxylation processes (Venkatesan et al., 1986). Whilst cadalene has been

found to be abundant in angiospermous vegetation (Widodo et al., 2009; Jiang & George, 2019), it is a generic and non-specific biomarker (van Aarssen et al., 2000; Romero-Sarmiento et al., 2011; Cesar & Grice, 2019) that originates from the degradation of cadinenes and cadinols in the resins of vascular plants during diagenesis (Hautevelle et al., 2006; Grice et al., 2015). Additionally, *ip*-iHMN is a marker of higher plant input in crude oils and sediments and according to Ellis et al. (1996), the compound is derived from the aromatization and rearrangement of terpenoids natural products. Additionally, its origin has also been attributed to non-vascular plants such as bryophytes which are less affected by climate (Cesar & Grice, 2019). The compound was detected in minor proportion in the *m/z* 197 of the aromatic fractions of some Benue Trough coal extracts but mostly absent in the Sarawak Basin coals. Other plant-derived aromatic hydrocarbons such as 1,2,3,4-tetrahydroretene, dehydroabietane, totarane and simonellite were either absent in the coal samples or detected in minor amounts.

The changes in abundances of the plant-derived aromatic biomarkers could be applied to track changes in paleoflora due to fluctuating paleoenvironmental conditions (van Aarssen et al., 2000; Haberer et al., 2006; Romero-Sarmiento et al., 2011; Hautevelle et al. 2006; Marynowski et al., 2013; Grice et al., 2015; Cesar & Grice, 2019; Jiang & George, 2019; Jiang et al. 2020). The plant-derived biomarker parameters for the studied coals are calculated and recorded in Tables 5.28 and 5.29.

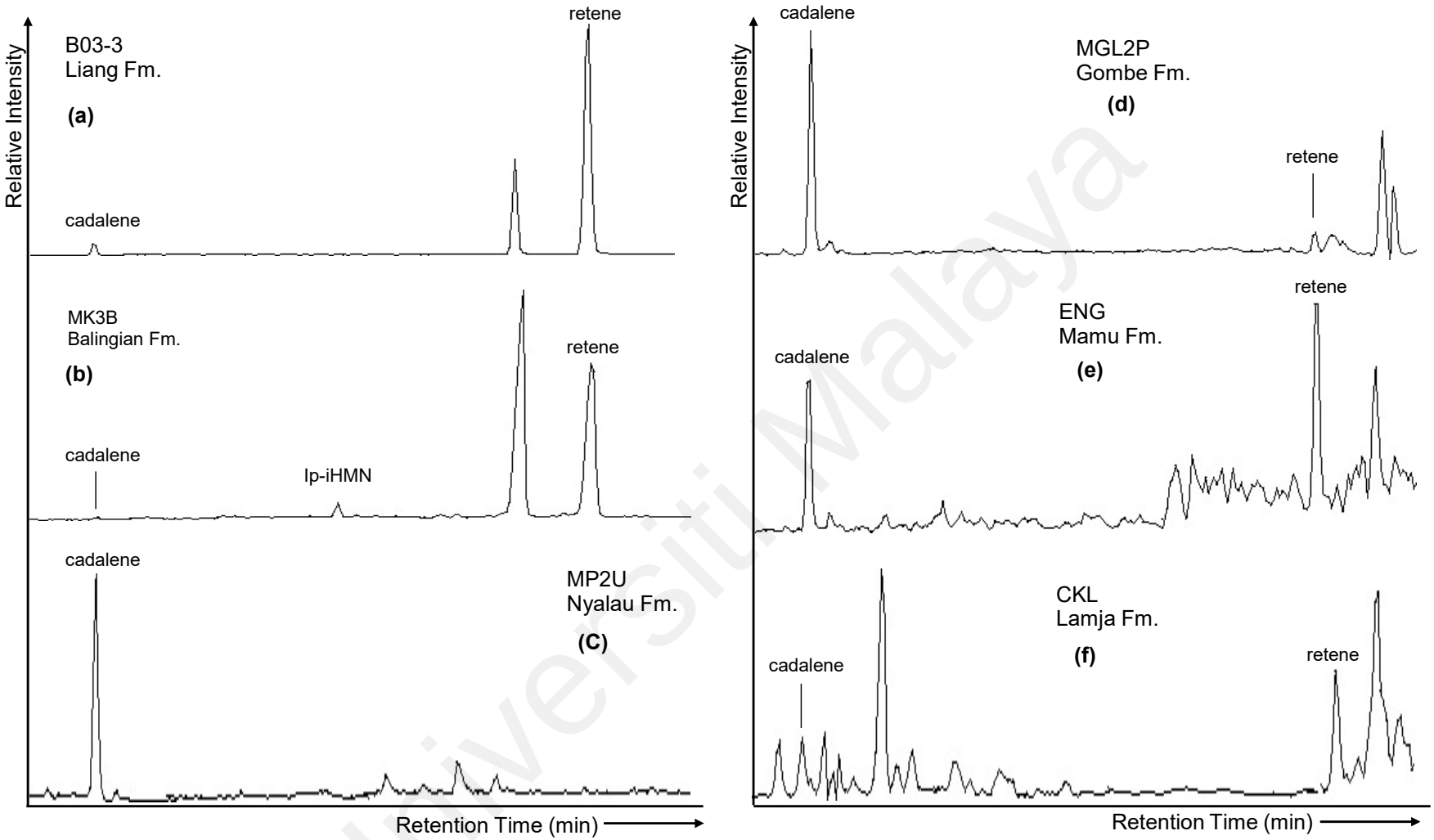

Figure 5.30: Summed partial chromatograms of the aromatic hydrocarbon fractions showing the distribution of plant-derived PAHs (*m/z* 183 + 197 + 219), of representative samples. ip-iHMN = 6-*iso*propyl-1-*iso*hexyl-2-methylnaphthalene.

Table 5.28: Partial land plant- and combustion-derived polycyclic aromatic hydrocarbon (PAH) ratios of the Sarawak Basin coals.

Sample	PHE/A	A/(A + PHE)	BaA/PHE	BaA/228	Fl/(Fl + Py)	Py/(Py + Per)	BFl/(BFl + BePy)
B01-1	-	-	-	-	0.67	-	-
B01-4	-	-	0.06	0.35	0.57	-	0.74
B01-5	252.4	0.00	0.04	0.19	0.69	-	0.75
B02-4	55.4	0.02	0.10	0.41	0.57	-	0.74
B03-2	-	-	0.05	0.22	0.71	-	0.71
B03-3	-	-	0.02	0.22	0.61	-	0.55
B03-6	-	-	-	-	0.77	-	0.73
E55-2	-	-	0.04	0.24	0.61	0.95	-
L04A-1	-	-	0.08	0.16	0.77	-	0.71
L04B-1	-	-	0.08	0.20	0.70	-	0.78
ML46A-6	-	-	0.01	0.17	0.62	-	-
ML46A-7	138.0	0.01	0.04	0.39	0.57	0.88	-
BG1	2.2	0.32	-	-	0.58	0.06	-
BG2	5.0	0.17	-	-	0.50	0.10	-
0464A	9.4	0.10	0.21	0.25	0.49	0.67	0.72
M03-2	11.0	0.08	0.21	0.26	0.59	0.54	0.73
MK1	6.2	0.14	0.12	0.21	0.62	0.01	-
MK2	12.1	0.08	-	-	0.57	0.18	-
MK3A	-	-	1.06	0.27	0.59	0.42	-
MK3B	-	-	0.67	0.25	0.46	-	-
MP1L	-	-	-	-	0.34	0.86	-
MP1M	-	-	-	-	0.20	0.92	-
MP1U	24.6	0.04	0.12	0.27	0.55	0.80	0.63
MP2L	8.4	0.11	-	-	0.92	0.27	-
MP2U	-	-	0.18	0.10	0.82	0.26	-
MP3L	-	-	0.09	0.12	0.70	0.28	-
MP3M	7.7	0.11	-	-	0.56	0.52	-
MP3U	-	-	-	-	0.60	0.27	-
MP4L	-	-	-	-	0.84	0.20	-
MP4M	-	-	-	-	0.74	0.22	-
MP4U	-	-	-	-	0.78	0.21	-
MP5L	-	-	0.01	0.06	0.83	0.56	-
MP5M	-	-	-	-	0.83	0.17	-
MP5U	-	-	-	-	0.60	0.34	-
MP6L	-	-	-	-	-	-	-
MP6M	-	-	-	-	-	-	-
MP6U	-	-	-	-	0.42	0.33	-
MP7L	-	-	-	-	0.81	0.16	-
MP7M	-	-	-	-	0.84	0.13	-
MP7U	-	-	-	-	0.69	0.38	-

A: anthracene; PHE: phenanthrene; BaA: benzo[*a*]anthracene; Ch: chrysene; Tph: triphenylene; Fl: fluoranthene; Py: pyrene; BbFl: benzo[*b*]fluoranthene; BePy: benzo[*e*]pyrene; BaPy: benzo[*a*]pyrene; Per: perylene; Ret: retene; Cad: cadalene; 228 = BaA + Ch + Tph; 252 = BFl + BePy + BaPy + Per; HPP: higher plant parameter = Ret/(Ret + Cad); HPI: higher plant input = (Ret + Cad + *ip*-iHMN)/1,3,6,7-tetramethylnaphthalene; mHPI: modified HPI = (Ret + Cad + *ip*-iHMN)/(Ret + Cad + *ip*-iHMN + 1,3,6,7-TeMN); PAHr = (PHE + Py + Fl)/(PHE + Py + Fl + Ret + Cad).

Table 5.28, continued.

Sample	BePy/ 1,3,6,7- TeMn	Cad/1,3,6,7 - TeMn	Ret/ Cad	HPP	HPI	mHPI	PAHr
B01-1	-	-	5.37	0.84	-	-	0.57
B01-4	1.14	20.43	-	-	20.43	0.95	0.83
B01-5	-	-	11.50	0.92	-	-	0.71
B02-4	4.61	8.96	-	-	8.96	0.90	0.97
B03-2	4.22	7.23	2.81	0.74	27.56	0.96	0.89
B03-3	-	-	25.98	0.96	-	-	0.19
B03-6	-	-	2.91	0.74	-	-	0.88
E55-2	1.01	102.91	0.22	0.18	125.88	0.99	0.35
L04A-1	6.10	5.42	1.90	0.65	15.69	0.94	0.91
L04B-1	7.54	5.57	4.64	0.82	31.41	0.97	0.91
ML46A-6	-	-	1.77	0.64	-	-	0.64
ML46A-7	-	19.56	-	-	19.56	0.95	0.63
BG1	-	-	3.88	0.80	-	-	0.03
BG2	-	-	20.66	0.95	-	-	0.06
0464A	5.68	1.52	22.26	0.96	35.38	0.97	0.86
M03-2	2.39	7.78	2.09	0.68	25.22	0.96	0.80
MK1	-	5.69	4.53	0.82	31.47	0.97	0.58
MK2	-	-	23.50	0.96	-	-	0.48
MK3A	-	6.55	31.24	0.97	211.16	1.00	0.12
MK3B	-	5.00	91.79	0.99	463.80	1.00	0.24
MP1L	-	9.82	-	-	9.82	0.91	0.54
MP1M	-	46.27	-	-	46.27	0.98	0.22
MP1U	0.54	38.04	5.66	0.85	253.50	1.00	0.11
MP2L	-	12.99	0.24	0.19	16.09	0.94	0.63
MP2U	-	12.88	-	-	12.88	0.93	0.68
MP3L	-	4.81	-	-	4.81	0.83	0.83
MP3M	-	39.64	-	-	39.64	0.98	0.37
MP3U	-	9.90	-	-	9.90	0.91	0.69
MP4L	-	12.05	-	-	12.05	0.92	0.63
MP4M	-	-	-	-	-	-	0.65
MP4U	-	33.34	-	-	33.34	0.97	0.56
MP5L	-	8.78	-	-	8.78	0.90	0.86
MP5M	-	4.37	-	-	4.37	0.81	0.87
MP5U	-	63.38	-	-	63.38	0.98	0.31
MP6L	-	-	-	-	-	-	0.66
MP6M	-	-	-	-	-	-	0.30
MP6U	-	29.76	-	-	29.76	0.97	0.26
MP7L	-	-	-	-	-	-	0.18
MP7M	-	-	0.17	0.14	-	-	0.32
MP7U	-	6.12	-	-	6.12	0.86	0.21

Table 5.29: Partial land plant- and combustion-derived polycyclic aromatic hydrocarbon (PAH) ratios of the Benue Trough coals.

Sample	PHE/ A	A/(A + PHE)	2-MP/ 2-MA	BaA/ PHE	BaA/ 228	Fl/(Fl + Py)	Py/(Py + Per)	Per/ 252	BePy/ (BePy + Per)	BaPy/(BePy + BaPy)	BePy/(BePy + BaPy)
MGL3A	17.8	0.05	11.5	0.22	0.45	0.84	0.94	0.06	0.71	0.43	0.57
MGL4A	11.0	0.08	6.3	0.29	0.36	0.60	0.90	0.06	0.71	0.38	0.62
MGL1C	13.8	0.07	3.8	0.21	0.10	0.43	0.24	0.20	0.50	0.36	0.64
MGL2A	34.2	0.03	12.0	0.89	0.34	0.86	0.74	0.05	0.77	0.38	0.62
MGL2B	117.6	0.01	-	1.00	0.43	0.85	0.85	0.05	0.74	0.41	0.59
MGL2H	27.2	0.04	4.7	0.34	0.11	0.61	0.40	0.35	0.23	0.52	0.48
MGL2I	32.5	0.03	10.3	1.09	0.17	0.72	0.90	0.05	0.79	0.31	0.69
MGL2O	28.8	0.03	5.0	0.89	0.13	0.70	0.70	0.09	0.68	0.35	0.65
MGL2P	14.3	0.07	3.0	1.92	0.13	0.76	0.17	0.10	0.66	0.25	0.75
MGL2T	-	-	-	0.80	0.18	0.67	0.29	0.39	0.23	0.41	0.59
AFZ	8.1	0.11	4.6	0.23	0.29	0.42	0.97	0.12	0.63	0.45	0.55
ENG	9.0	0.10	3.8	0.23	0.22	0.52	0.70	0.18	0.42	0.51	0.49
IMG	27.0	0.04	8.5	0.17	0.31	0.38	0.97	0.11	0.70	0.41	0.59
OGB	22.4	0.04	22.5	0.06	0.29	0.62	0.93	0.30	0.28	0.60	0.40
OKB	7.3	0.12	1.9	0.53	0.24	0.62	0.43	0.19	0.41	0.50	0.50
WKP	21.2	0.05	5.0	0.04	0.29	0.55	0.99	0.12	0.55	0.51	0.49
CKL	9.3	0.10	4.7	0.43	0.29	0.38	-	-	-	0.45	0.55
LMZ1	29.8	0.03	87.5	0.22	0.09	0.40	-	-	-	0.19	0.81
LFO	7.4	0.12	5.3	0.27	0.17	0.57	0.58	0.54	0.10	0.59	0.41
SKJ	5.7	0.15	3.2	0.12	0.30	0.63	0.78	0.32	0.24	0.53	0.47

A: anthracene; PHE: phenanthrene; MP: methylphenanthrene; MA: methylanthracene; BaA: benzo[*a*]anthracene; Ch: chrysene; Tph: triphenylene; Fl: fluoranthene; Py: pyrene; BbFl: benzo[*b*]fluoranthene; BkFl: benzo[*k*]fluoranthene; BePy: benzo[*e*]pyrene; BaPy: benzo[*a*]pyrene; Per: perylene; InPy:indeno[*1,2,3-cd*]pyrene; BgPer: benzo[*ghi*]pyrelene; Cor: coronene; Ret: retene; Cad: cadalene; 228 = BaA+Ch+Tph; 252 = BFl + BePy + BaPy + Per; HPP: higher plant parameter = Ret/(Ret + Cad); HPI: higher plant input = (Ret + Cad + *ip*-iHMN)/1,3,6,7-tetramethylnaphthalene; mHPI: modified higher plant input = (Ret + Cad + *ip*-iHMN)/(Ret + Cad + *ip*-iHMN + 1,3,6,7-tetramethylnaphthalene); PAHr = (PHE + Py + Fl)/(PHE + Py + Fl + Ret + Cad).

Table 5.29, continued.

Sample	BbFl/(BbFl + BePy)	InPy/(InPy + BgPer)	BgPer/ (BgPer + Per)	Cor/(Cor + BaPy)	BePy/1,3,6,7-TeMn	Cad/1,3,6,7-TeMn	Ret/ Cad	HPP	HPI	mHPI	PAHr
MGL3A	0.84	0.62	0.31	0.14	0.50	0.30	3.88	0.80	1.52	0.61	0.95
MGL4A	0.81	0.60	0.49	0.07	4.95	1.12	3.38	0.75	4.90	0.83	0.93
MGL1C	0.71	0.64	0.32	0.14	39.86	1.12	2.13	0.68	4.07	0.80	0.90
MGL2A	0.81	0.64	0.51	0.07	2.47	1.15	-	-	1.42	0.72	0.94
MGL2B	0.82	0.64	0.41	0.02	2.33	0.04	48.00	0.98	1.83	0.66	0.95
MGL2H	0.81	0.68	0.08	0.17	1.28	6.36	0.07	0.06	6.99	0.87	0.56
MGL2I	0.78	0.61	0.52	0.26	2.33	0.53	1.11	0.53	1.37	0.58	0.95
MGL2O	0.77	0.63	0.39	0.11	4.73	1.27	0.46	0.31	1.99	0.66	0.91
MGL2P	0.77	0.59	0.36	0.07	18.97	8.46	-	-	9.08	0.91	0.53
MGL2T	0.79	0.60	0.08	0.23	5.97	1.42	0.92	0.48	3.08	0.77	0.91
AFZ	0.70	-	0.33	-	0.38	14.91	0.05	0.05	15.62	0.94	0.54
ENG	0.81	0.47	0.27	-	9.40	4.12	1.85	0.65	11.75	0.91	0.88
IMG	0.61	0.15	0.61	-	0.84	3.77	0.24	0.19	4.79	0.82	0.85
OGB	0.77	0.32	0.27	-	0.10	5.10	0.04	0.04	5.31	0.84	0.74
OKB	0.80	0.50	0.25	-	41.21	11.11	1.22	0.55	24.62	-	0.89
WKP	0.81	0.44	0.37	-	0.27	12.54	0.08	0.07	13.53	0.92	0.84
CKL	0.56	0.20	-	0.23	0.62	0.19	1.93	0.66	0.68	0.36	0.94
LMZ1	0.57	0.30	-	0.24	24.80	1.35	2.65	0.73	6.02	-	0.98
LFO	0.83	0.66	0.04	-	0.16	38.33	0.00	0.00	38.42	-	0.11
SKJ	0.83	0.42	0.18	-	0.58	58.56	0.04	0.04	61.02	0.99	0.32

CHAPTER 6: DISCUSSIONS

6.1 Thermal Maturity

The thermal maturity of the studied samples was assessed using several maturity parameters. First, the generally low vitrinite reflectance values (< 0.5% *R*o) for most of the samples indicate that all the coals are immature for hydrocarbon generation (Table 5.1; Peters et al., 2005). Conversely, the Lamja Formation coals (CKL and LMZ1) from Benue Trough have relatively higher reflectance values (0.57-0.61% R_o) that indicate early thermal maturity. This low to early maturity interpretation is generally supported by the low T_{max} (<438 ℃) and production index (PI) (< 0.10) values of the coal samples (Tables 5.3-5.4; Peters & Cassa, 1994). The generally low thermal maturity nature of these coals is shown in the cross-plots of vitrinite reflectance against T_{max}, and PI against T_{max} in Figure 6.1. Although the Lamja Formation coals plot in the early mature zones, all other samples plot in the immature zones of the diagrams. Additionally, Figure 6.1 indicates that the Benue Trough coals have attained relatively higher thermal maturity levels than the Sarawak Basin coals.

Liquid petroleum generation from humic coals is described as a complex three-stage process that involves the onset of generation, kerogen/coal matrix saturation, and initial expulsion followed by efficient expulsion (Petersen, 2006). The oil generation stage is reportedly characterized by a sharp increase in the bitumen index (BI) while the initial oil expulsion stage is typified by a decrease in the quality index (QI). The BI, QI and T_{max} values for the analysed coal samples are plotted in Figure 6.2. The Sarawak Basin coals mostly plot away from the oil generation window, while the Benue Trough coals mostly plot near the window (Figure 6.2a). Nevertheless, both groups of coals mostly plot away from the oil expulsion window (Figure 6.2b), suggesting generally low thermal maturity for oil generation and expulsion. In contrast, some coals of the Lamja

and Mamu formations from the Benue Trough appear to have generated some oil and reached the third stage of initial oil expulsion (Figure 6.2).

The proportion of hydrocarbon fractions in extractable organic matter (EOM) is another indicator of thermal maturity (Peters et al., 2005). The coal extracts are dominated by polar compounds and the ratio of aliphatic to aromatic hydrocarbons in the extracts ranges from 0.20 to 2.00 (avg. 0.41) and 0.29 to 3.75 (avg. 0.68) for the Sarawak Basin and Benue Trough Coals, respectively, are mostly lower than ~ 1.5 found in early mature extracts (Killops & Killops, 2013). The proportion of aliphatic hydrocarbon fractions in the Sarawak Basin and Benue Trough coal extracts ranges, accordingly, from 1.9 to 21.0 (avg. 8.0%) and 6.2 to 41.7 (avg. 15.7%). The values are mostly lower than 25%; thus, consistent with samples with low thermal maturity (Miles, 1994; Figure 6.3a). In addition, the values show relatively higher thermal maturity for the Benue Trough coals. In addition, the CPI and OEP values of the studied coals are ≥ 1.0, indicating that the samples are mostly immature as CPI and OEP values tend towards unity as maturity increases and *n*-alkanes with no predominance are generated (Peters et al., 2005; Killops & Killops, 2013). The CPI and OEP values, however, indicate that the Benue Trough coals have higher maturity than the Sarawak Basin coals. In addition, the values also indicate that for the Sarawak Basin coals, the Nyalau Formation and Balingian Formation have slightly higher thermal maturity than the Liang Formation (Figure 6.3b).

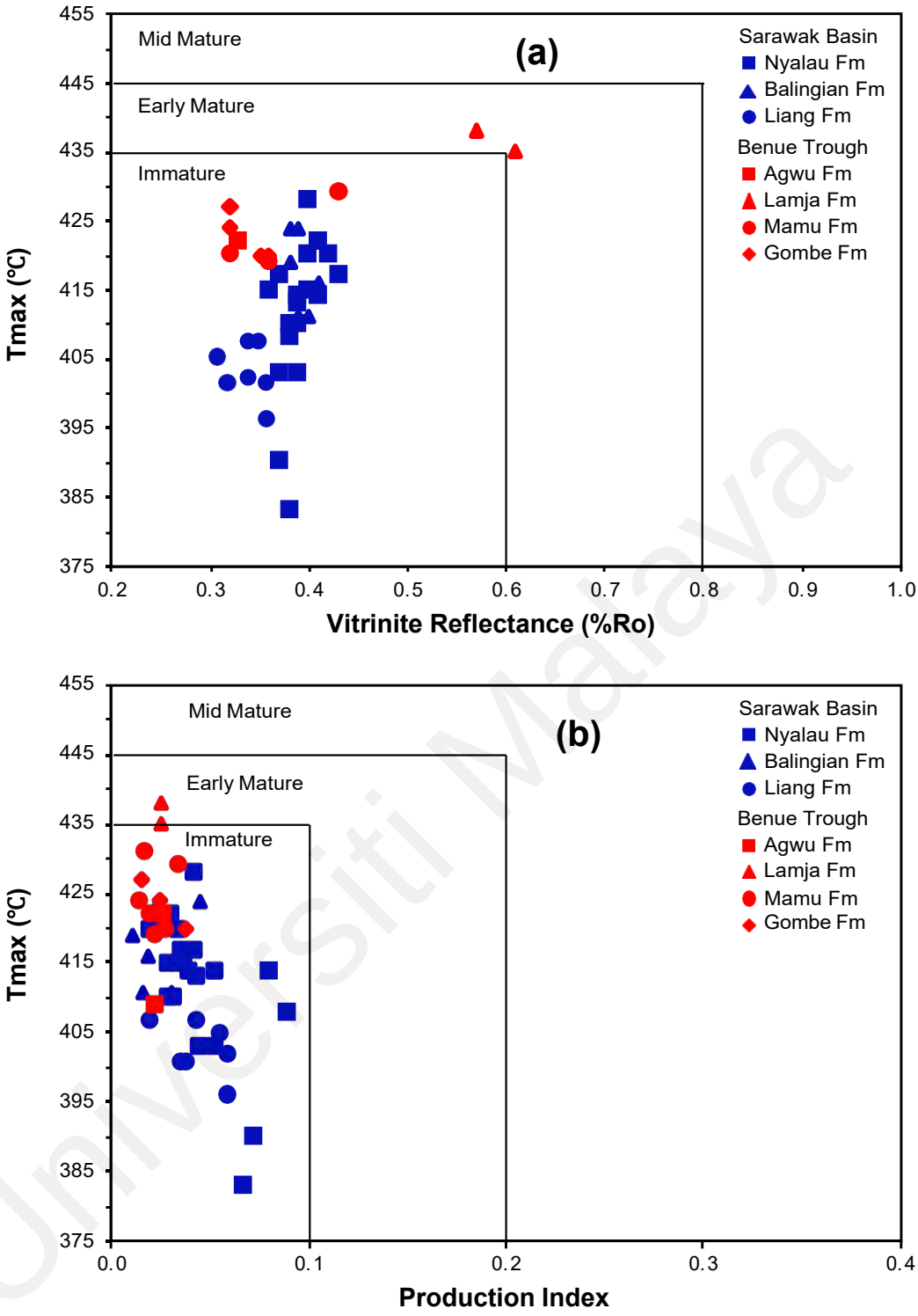

Figure 6.1: Maturity cross-plots of (a) – vitrinite reflectance vs. T_{max}, and (b) – production index vs. T_{max}.

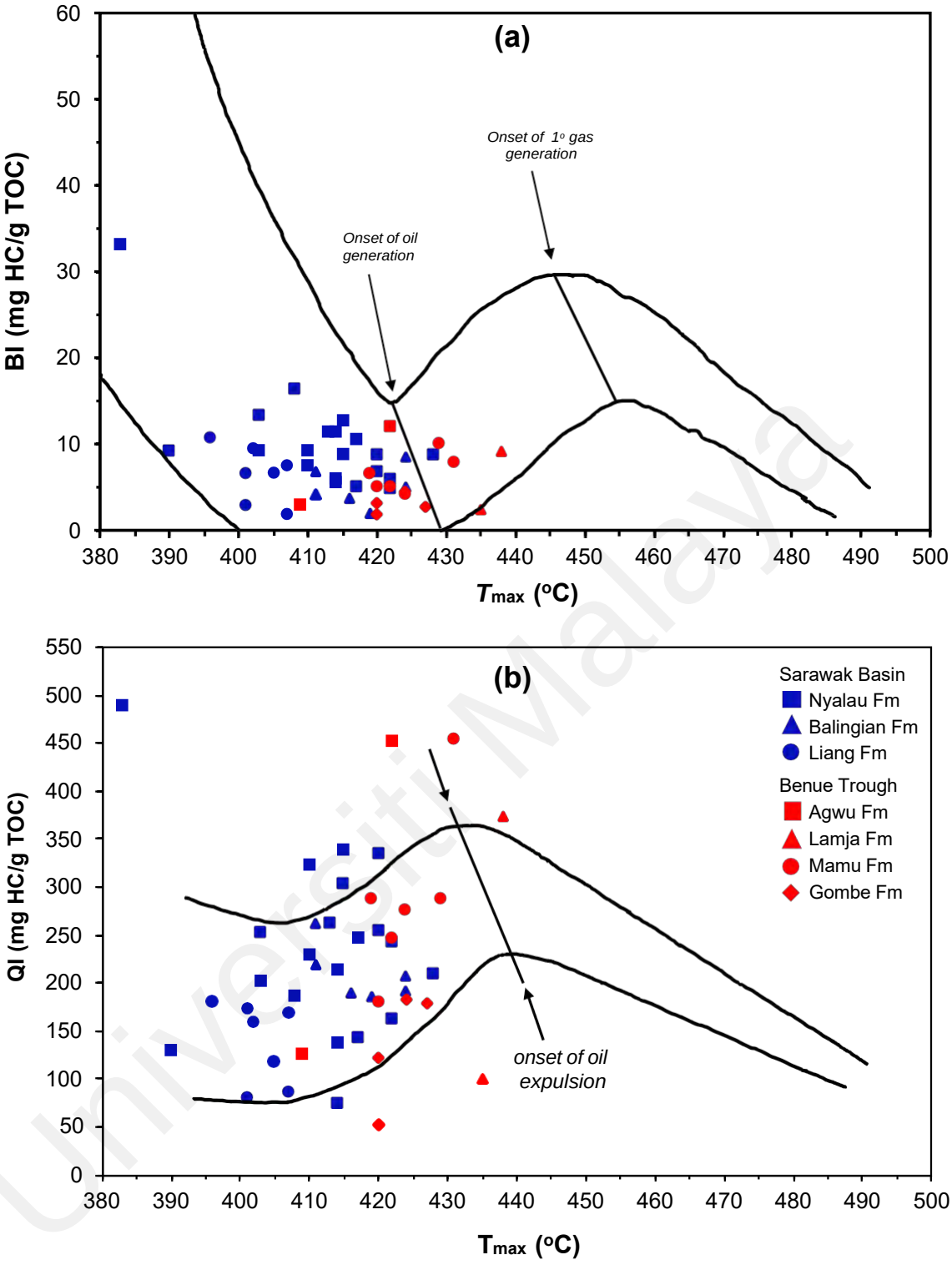

Figure 6.2: Plots of (a) – bitumen index (BI) vs. T_{max}, and (b) – quality index (QI) vs. T_{max}. Marked bands are oil generation and expulsion trends of New Zealand coals (after Sykes & Snowdon, 2002).

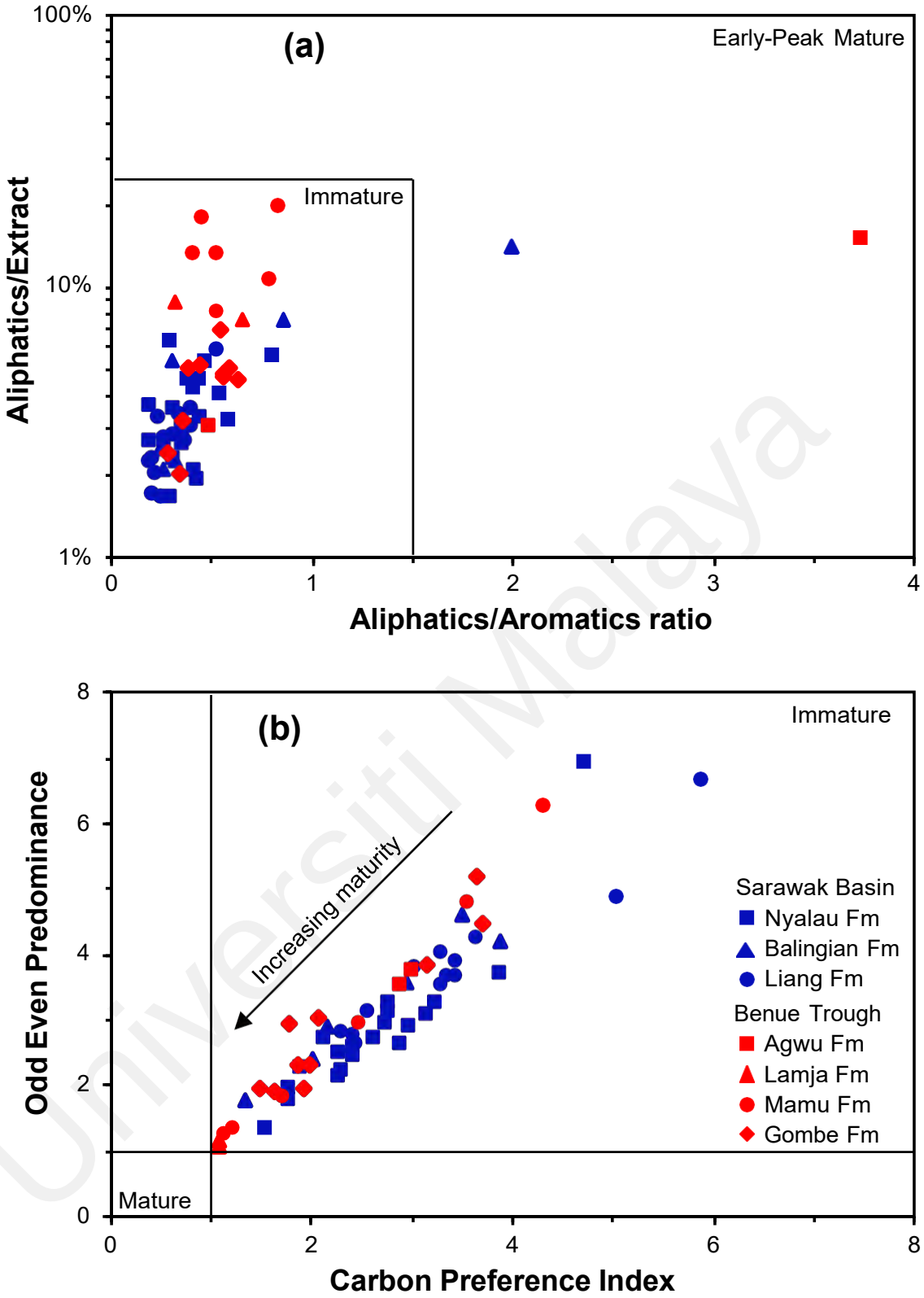

Figure 6.3: Cross-plots of (a) – Aliphatic/aromatic ratio vs. %aliphatics in extracts, and (b) – *n*-alkane proxies, showing thermal maturity of the coals.

Furthermore, the presence of hopenes and ββ-hopanes, high abundance of C_{31} αβ-homohopane (22R) and no clear presence of steranes in the coal samples (except the Lamja Formation) suggests low thermal maturity (Seifert & Moldowan, 1980; van Dongen et al., 2008). The C_{30} ββ/(ββ+βα+αβ) ratio applies over the early maturity to peak maturity range and the values decrease as maturity increases (Farrimond et al., 1998). Given the absence of C_{30} moretane in most of the samples, the ββ-hopane parameter was modified to C_{30} ββ/(ββ+αβ) (Sinninghe Damsté et l., 1995; van Dongen et al, 2008). According to Miles (1994), values > 0.4 indicates immaturity while values between 0.4 and 0.05 indicate early maturity. The C_{30} ββ/(ββ+αβ) hopane ratio ranges from 0.85 to 0.39 (avg. 0.72) and 0.81 to 0.22 (avg. 0.69) for the studied Malaysian and Nigerian samples, indicating low to early maturity (Table 5.17).

The C_{31} αβ-homohopane 22S/(22S+22R) parameter attains equilibrium values of 0.55-0.60 over the low to early maturity range (Farrimond et al., 1998; Peters et al., 2005). Values of the hopanoid parameter for the Sarawak Basin coals, which generally increase from Liang Formation (0.10 to 0.22) to Nyalau Formation (0.07 to 0.27) and Balingian Formation (0.19 to 0.29), are significantly lower than the equilibrium values and therefore, signifies low thermal maturity. For the studied Benue Trough coals, the C_{31} αβ-homohopane 22S/(22S+22R) ratios range from 0.17 to 0.60 with average values of 0.24, 0.36, 0.60, and 0.25 for the Gombe, Mamu, Lamja, and Agwu formations, respectively, signifying low to early thermal maturity levels. The parameter equilibrium values for the Lamja Formation corroborate the earlier interpretation of early thermal maturity. Although these findings are in agreement with earlier studies of the Gombe, Mamu, and Lamja Formation coals (Obaje et al., 2004b; Jauro et al., 2007; Akande et al., 2012; Ayinla et al., 2017a), the low thermal maturity of the investigated Agwu Formation contradicts earlier studies by Ehinola et al. (2002), Obaje et al. (2004b) and

Adedosu et al. (2012), which had concluded the coals are in the peak to late thermal maturity stage.

In addition, the presence of the less stable 8α(H)-epimers of drimane and homodrimane in the Sarawak Basin and Benue Trough coals suggest generally low thermal maturity as the 8α(H)-epimers are degraded before the onset of oil generation (Weston et al., 1989; Yan et al., 2019). Nevertheless, values of the drimane and homodrimane maturity parameters mostly indicate relatively higher thermal maturity for the Benue Trough coals (Figure 6.4).

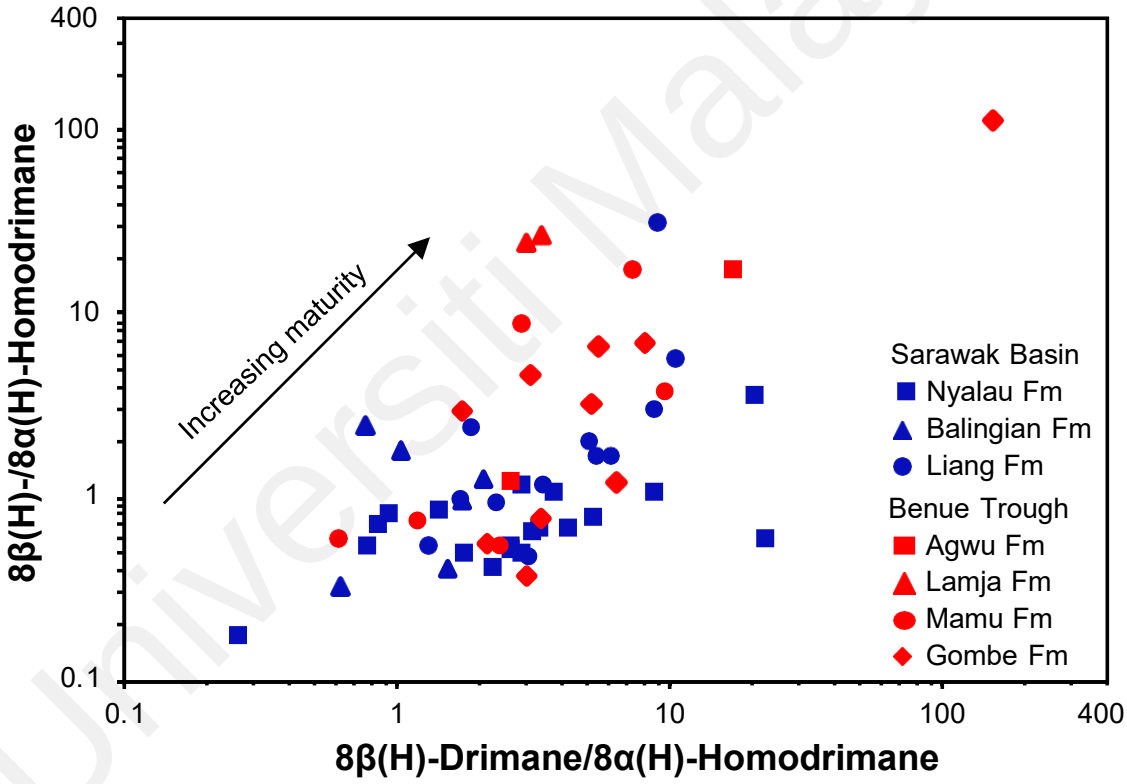

Figure 6.4: Cross-plot of drimane and homodrimane maturity parameters.

The variation in the distributions of methylated phenanthrenes and naphthalenes has been widely applied to evaluate the thermal maturity of sediments and oils (Radke & Welte, 1983; Radke et al., 1984; Radke et al. 1986; Alexander et al., 1985; Budzinski et al., 1995; van Aarssen et al., 1999). Aromatic maturity parameters are typically based

on the thermal stability of compounds as the more stable isomer increases with maturity while the less stable isomer decreases (Chakhmakhchev et al., 1997; van Aarssen et al., 1999). Maturity parameters calculated for the samples include methylphenanthrene ratio (MPR), methylphenanthrene indices (MPI-1 and MPI-2), methylphenanthrene distribution fraction (MPDF), dimethylphenanthrene ratio (DPR), methylnaphthalene ratio (MNR), dimethylnaphthalene ratios (DNR-1, and DNRx), trimethylnaphthalene ratios (TNR-2, and TMNr), tetramethylnaphthalene ratio (TeMNr), and methyldibenzothiophene ratio (MDR). These and other aromatic maturity-related parameters are presented in Tables 5.21-5.24.

The MPR, MPI-1 and MPI-2 ratios for the Sarawak Basin coals range from 0.01 to 1.43 (avg. 0.73), 0.01 to 1.51 (avg. 0.45), and 0.02 to 2.41 (avg. 0.66), respectively (Table 5.21). In contrast, MPR ratios for the Benue Trough coals are relatively higher, ranging from 0.41 to 1.53 (avg. 0.92) while MPI-1 and MPI-2 ratios are relatively lower, varying from 0.16 to 0.71 (avg. 0.35) and 0.20 to 0.85 (avg. 0.46), respectively (Table 5.22). According to Miles (1994), values (< 2.65) of MPR in the coals indicate low thermal maturity. Figure 6.5, a cross-plot of methylphenanthrene indices, shows that the Sarawak Basin coals have relatively lower thermal maturity than the Benue Trough coals. Calculated reflectance values from MPI-1 values range from 0.41 to 1.31 (avg. 0.67%) and 0.50 to 0.83 (avg. 0.61%) for the Sarawak Basin and Benue Trough coals, respectively. The calculated reflectance values are noticeably higher than the measured reflected values, especially for Nyalau Formation coals (Table 5. 21).

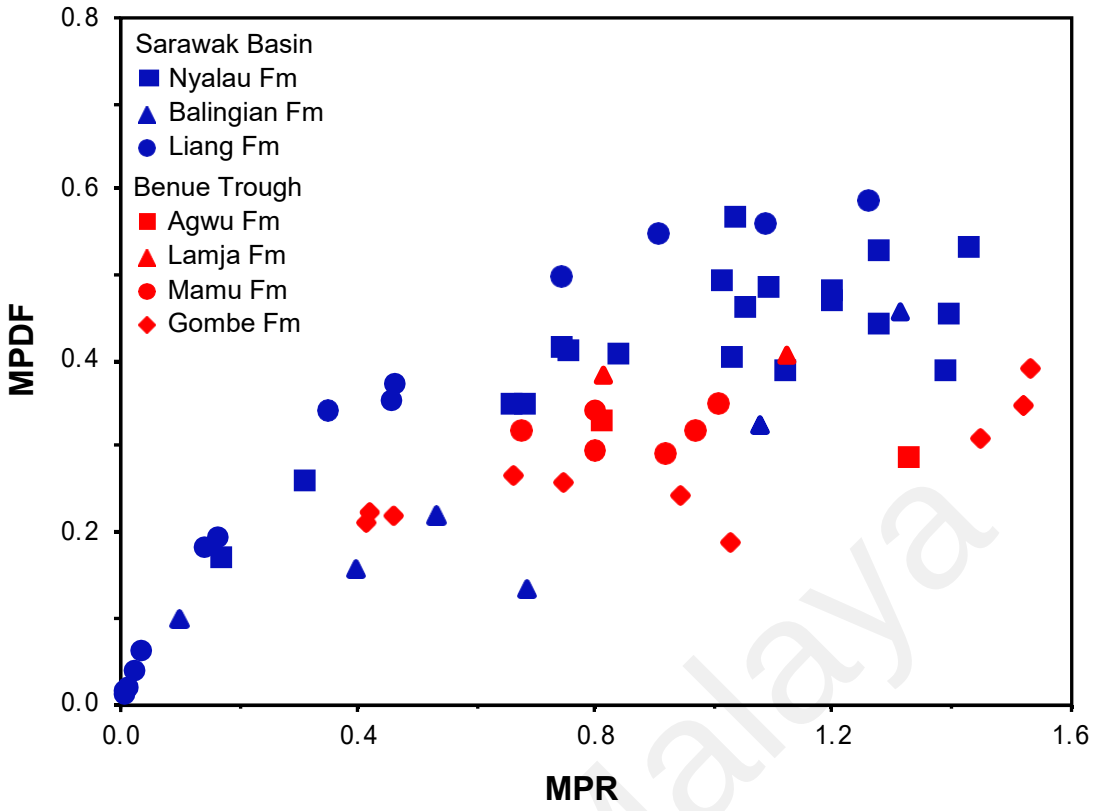

Figure 6.5: Cross-plot of methylphenanthrene ratio (MPR) vs. methylphenanthrene distribution fraction (MPDF), showing relative thermal maturity.

As shown in the merged 156 + 170 +184 mass chromatograms of alkylated naphthalene (Figure 5.23) of representative samples, the studied coals are dominated by 1,6-DMN, 1,3,6-TMN and 1,3,6,7-TeMN, which suggests relatively higher thermal maturity (van Aarssen et al., 1999). The MNR, DNRx, TNR-2, TMNr and TeMNr ranges from 0.38 to 7.32 (avg. 1.29), 0.14 to 1.67 (avg. 0.50), 0.18 to 1.59 (avg. 0.58), 0.05 to 0.60 (avg. 0.21) and 0.08 to 0.48 (0.20), respectively, for the Sarawak Basin coals (Table 5.24). The MNR, DNRx, TNR-2, TMNr and TeMNr parameters are relatively higher for the Benue Trough coals, varying from 0.72 to 2.00 (avg. 1.21), 0.20 to 1.10 (avg. 0.46), 0.39 to 0.90 (avg. 0.63), 0.16 to 0.67 (avg. 0.41), and 0.16 to 0.79 (avg. 0.53), respectively (Table 5.25; Figure 6.6a). Additionally, the cross-plots of DNR_x versus DNR-1 and TMNr versus TeMNr generally show relatively higher maturity levels for the Benue Trough coals (Figure 6.6). However, Figure 6.6b implies

the highest thermal maturity for the Gombe Formation coals (van Aarssen et al., 1999), which contradicts earlier interpretations of vitrinite reflectance, Rock-Eval and aliphatic biomarkers data.

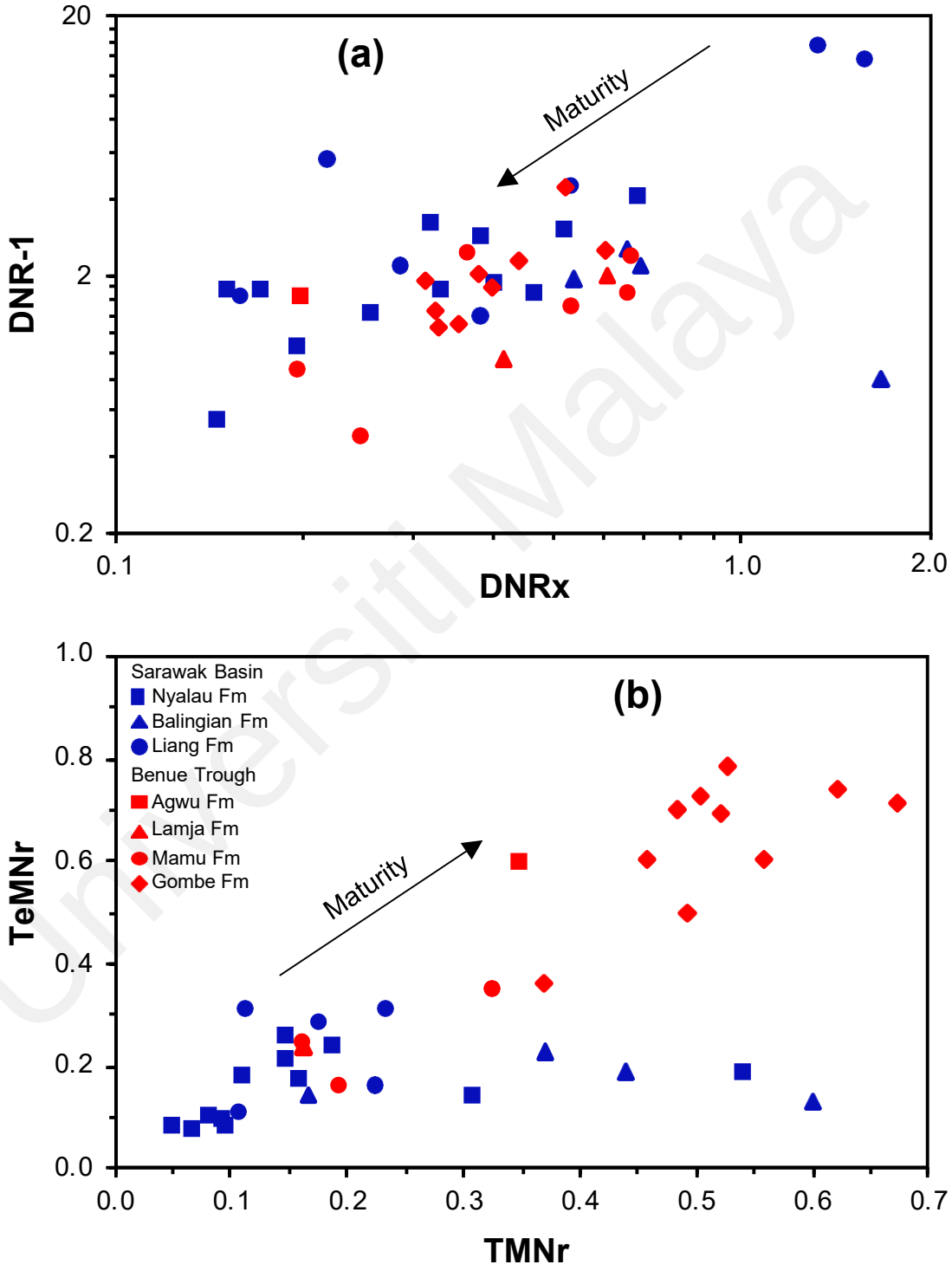

Figure 6.6: Cross-plots of (a) – dimethylnaphthalene ratios (DNR_x and DNR-1), and (b) – trimethylnaphthalene ratio (TMNr) vs. tetramethylnaphthalene ratio (TeMNr), showing relative thermal maturity of the coal samples.

Reflectance values from calibrated MNR and TNR-2 ratios range from 0.82 to 2.06 (avg. 1.02%) and 0.51 to 1.36 (avg. 0.75%) for the Sarawak Basin coals. Similarly, values of calculated reflectance from MNR and TNR-2 vary from 0.82 to 1.16 (avg. 1.01%) and 0.63 to 0.94 (avg. 0.78%). These calculated reflectance values indicate early to peak maturity for the studied Sarawak Basin and Benue Trough coals. Again, the calculated reflectance values are noticeably higher than the measured reflected values (Appendix F). The aromatic maturity parameters have greater applicability over a wider maturity range than aliphatic maturity parameters, while the methylated phenanthrene and naphthalene parameters infer anomalously higher maturity than measured vitrinite reflectance and aliphatic biomarker maturity parameters. Hence, these results signify their non-suitability for low-maturity type-III source rocks. This is mostly due to the higher influence of organic matter type on the abundance of aromatic compounds at lower maturity levels (Radke et al., 1986; Schou & Myhr, 1988; Strachan et al., 1988). In addition, a recent study by Li et al. (2022) attributed the unusual occurrence of the alkylnaphthalene isomers in some Australian sediments to microorganisms, considering 1,3,6-TMN, 1,3,6,7-TeMN and 1,2,3,6,7-PMN to be diagenetic products of drimane-type sesquiterpenes or hopanes from bacteria.

In summary, the studied Sarawak Basin and Benue Trough coals rank lignite to high volatile bituminous C, indicating generally low thermal maturity levels. However, the Lamja Formation coals of the Benue Trough have comparably higher maturity with average vitrinite reflectance and T_{max} values of 0.60% and 437 °C, respectively, which indicates an early level of thermal maturity.

6.2 Hydrocarbon Generation Potential

Bulk and organic geochemical data were applied to assess the hydrocarbon generation potential of the studied Sarawak Basin and Benue Trough coals. The TOC contents and *S*2 values for all coal samples are exceedingly greater than 4 wt. % and 20 mg HC/g rock, respectively (Tables 5.3-5.4), indicating excellent petroleum generation potential (Peters & Cassa, 1994). Similarly, the genetic potential (GP), which ranges from 40.2 to 277.9 (avg. 116.0 mg HC/g rock) and 33.4 to 337.4 (avg. 139.8 mg HC/g rock), respectively, for the Sarawak Basin and Benue Trough coals, indicate excellent hydrocarbon-generating potential (Peters & Cassa, 1994). The cross-plot of TOC versus *S*2, however, shows that some of the Benue Trough coals possess marginally better potential than the Sarawak Basin coals (Figure 6.7a). It also shows that for the Sarawak Basin coals, the potential generally increases from Liang Formation (avg. 68.0 mg HC/g rock) to Balingian Formation (avg. 103.3 mg HC/g rock), and Nyalau Formation (avg. 129.0 mg HC/g rock). In addition, the Gombe Formation (avg. 79.7 mg HC/g rock) have the lowest potential of the Benue Trough coals, with increasing potential from Lamja Formation (avg. 137.7 mg HC/g rock) to Mamu Formation (avg. 164.4 mg HC/g rock), and Agwu Formation (avg. 188.6 mg HC/g rock).

This interpretation is partly supported by high EOM yields ranging from 21596 to 224779 ppm and 13296 to 125596 ppm, with average values of 63532 ppm and 37352 ppm for the Malaysian and Nigerian coals, respectively. The EOM yields for the Malaysian coals are generally higher for the Nyalau Formation (avg. 89073 ppm) and relatively lower in Liang (avg. 37794) and Balingian (avg. 38450 ppm) Formations. For the Benue Trough coals, EOM yields are highest in the Agwu Formation (avg. 93359) and lowest in the Gombe Formation (avg. 24685 ppm) while Lamja (avg. 40412 ppm) and Mamu (avg. 38774 ppm) Formations show intermediate EOM yields. Similarly, the

concentration of hydrocarbons in the investigated Sarawak Basin and Benue Trough coals are high, varying from 2763 to 58922 (avg. 8167 ppm) and 1794 to 23650 (avg. 6786 ppm), respectively. Immature source rocks with extract yield and hydrocarbon concentration greater than 4000 ppm and 2400 ppm, respectively, are deemed to possess excellent generation potential (Peter & Cassa, 1994). The cross-plot of EOM yield and hydrocarbon concentration in Figure 6.7b indicates that Gombe Formation coals from Benue Trough possess the least generation potential of the studied coals while the Nyalau Formation coals from Sarawak Basin generally have the highest potential for hydrocarbon generation.

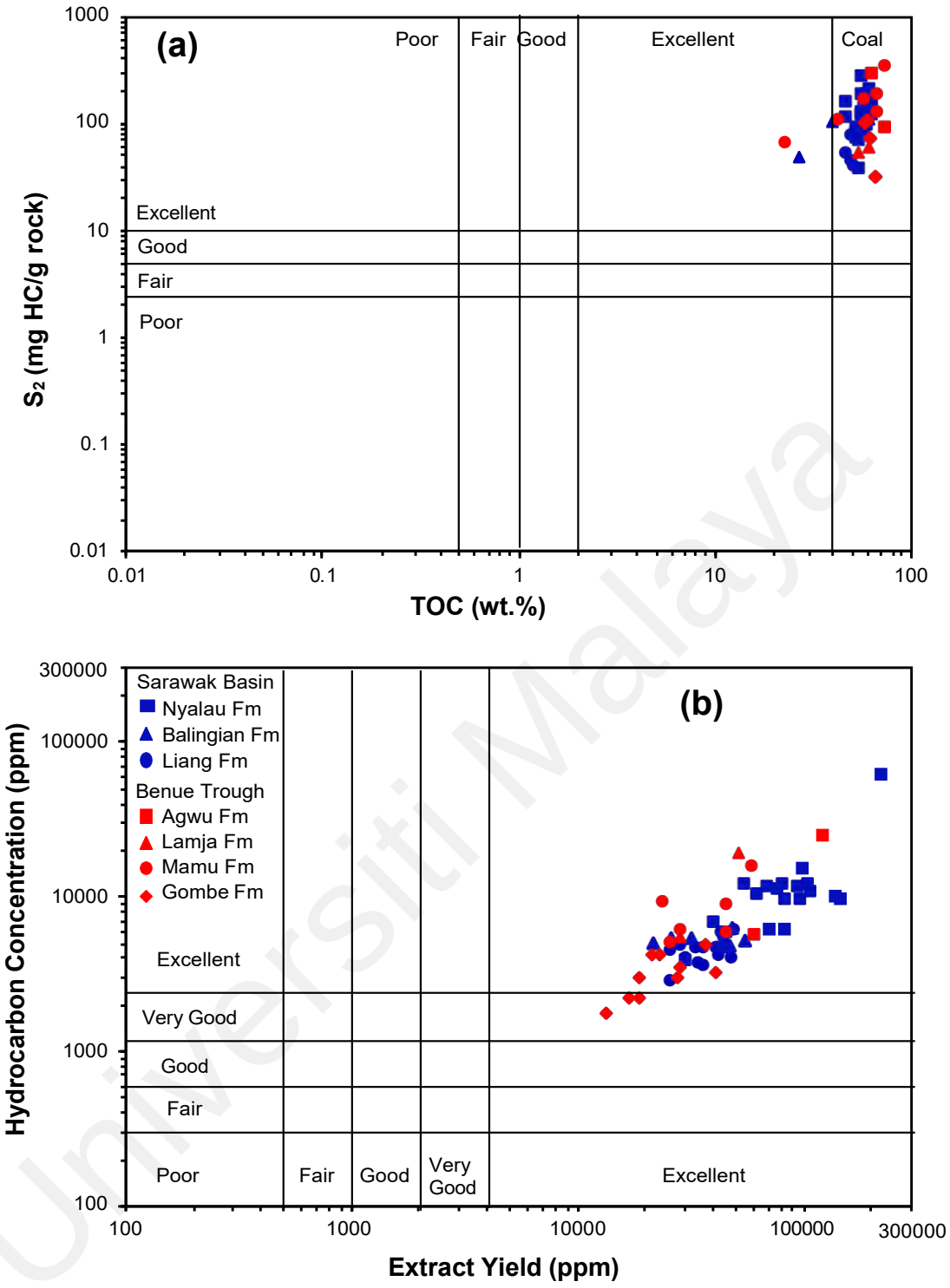

Figure 6.7: Cross-plots of (a) – total organic carbon (TOC) vs. Rock-Eval *S2* (after Dembicki, 2009), and (b) – extract yield vs. hydrocarbon concentration (after Peter & Cassa, 1994), showing the hydrocarbon generation potential of the studied coals.

Furthermore, the studied coals fall mostly within the gas and gas/oil source zones of the TOC vs. HI diagram (Figure 6.8), indicating the potential for gas to mixed oil and gas generation. Nevertheless, the higher HI values of the Mamu and Nyalau Formation coals suggest the capacity for oil generation. This interpretation is corroborated by a petrographic study by Abdullah (1997) which found that the Nyalau Formation coals contain a considerable amount of liptinitic maceral, suberinite, that may contribute to oil generation (Hunt 1991; Fleet & Scott, 1994). In contrast, the Gombe Formation coals which possess the least hydrocarbon-generating potential of the investigated coals contain a considerable amount of liptinitic macerals (Ayinla et al., 2017b), suggesting that the amount of liptinitic content in the Benue Trough coals is no control on its oil-generating capacity.

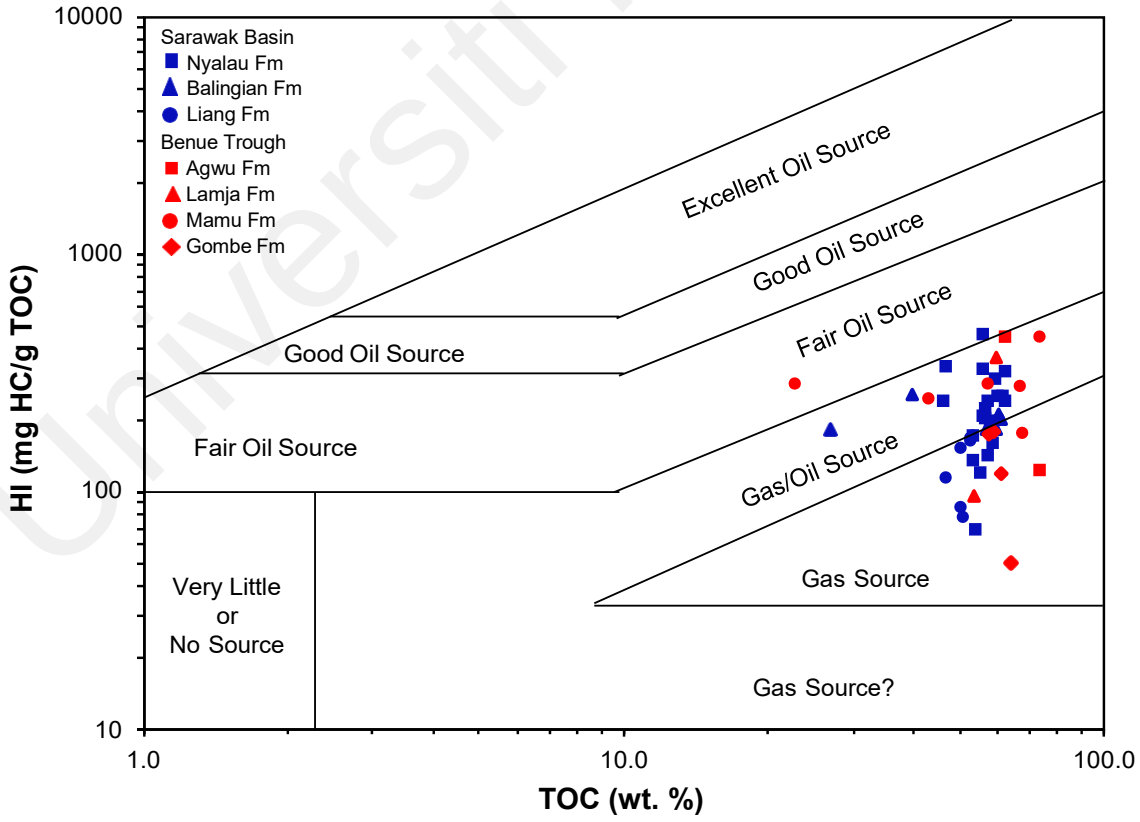

Figure 6.8: Cross-plot of total organic carbon (TOC) vs. hydrogen index (HI), indicating the oil-generating capacity of the studied coals.

Based on a study of Late Cretaceous-Cenozoic coals from New Zealand, Sykes & Snowdon (2002) established that the *S*2 values of coals increase as maturity increases towards the expulsion thresholds due to the reorganisation of the coal structure *via* reincorporation of the H-rich volatile components. Hence, the authors concluded that early mature samples are more appropriate to assess the potential of coaly source rocks as HI values of immature samples underestimate the oil generation potential. Consequently, Sykes & Snowdon (2002) postulated that effective HI (HI') values, which are translated from measured HI values at the onset of oil expulsion, are a better indicator of petroleum potential. The maturation pathway diagram based on the HI and T_{max} values of New Zealand coals by Sykes & Snowdon (2002) was employed to determine the effective HI values of the analysed coals (Figure 6.9). Estimated effective HI values range from 209 to 523 (avg. 302 mg HC/g TOC) and 151 to 453 (avg. 297 mg HC/g TOC) for the Sarawak Basin and Benue Trough coals, respectively (Tables 5.3-5.4). The effective HI values are slightly higher than HI values for all samples (except AFZ). The TOC versus HI diagram in Figure 6.8 was redrawn with effective values (Figure 6.10). The coals now plot mainly in the mixed oil and gas zone while some samples plot in the fair oil zone, suggesting a greater capacity for liquid hydrocarbon generation (Peters & Cassa, 1994).

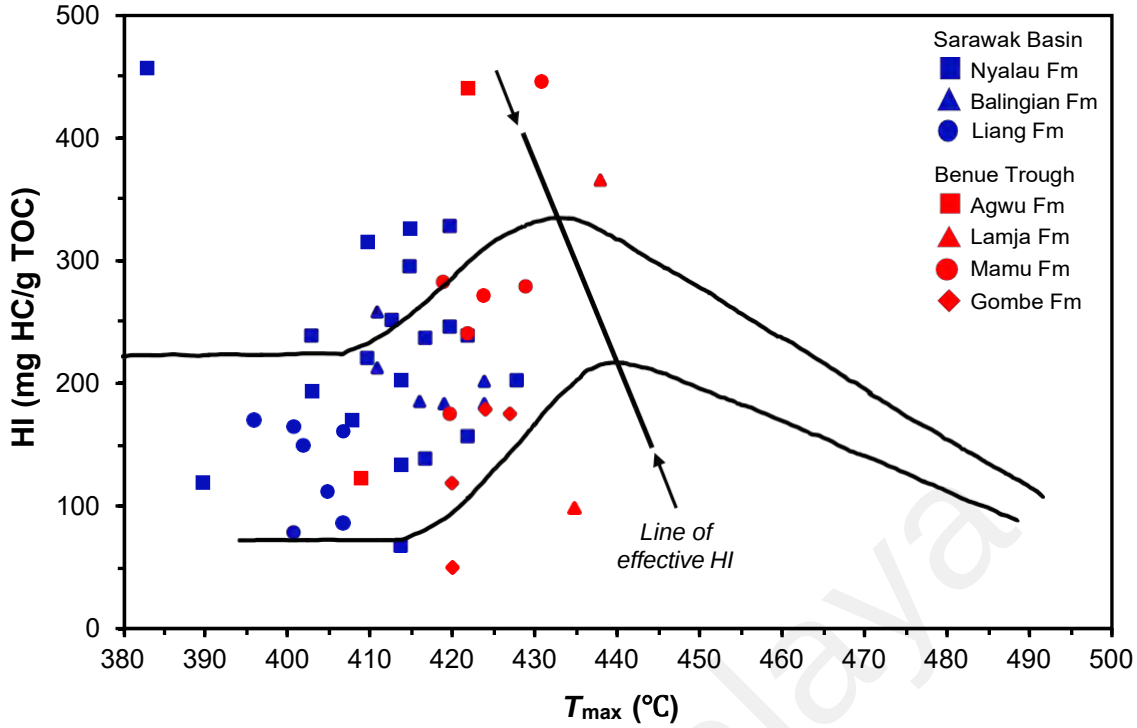

Figure 6.9: Cross-plot of hydrogen index (HI) against T_{max}. Marked band is the maturation pathway of New Zealand coals (after Sykes & Snowdon, 2002).

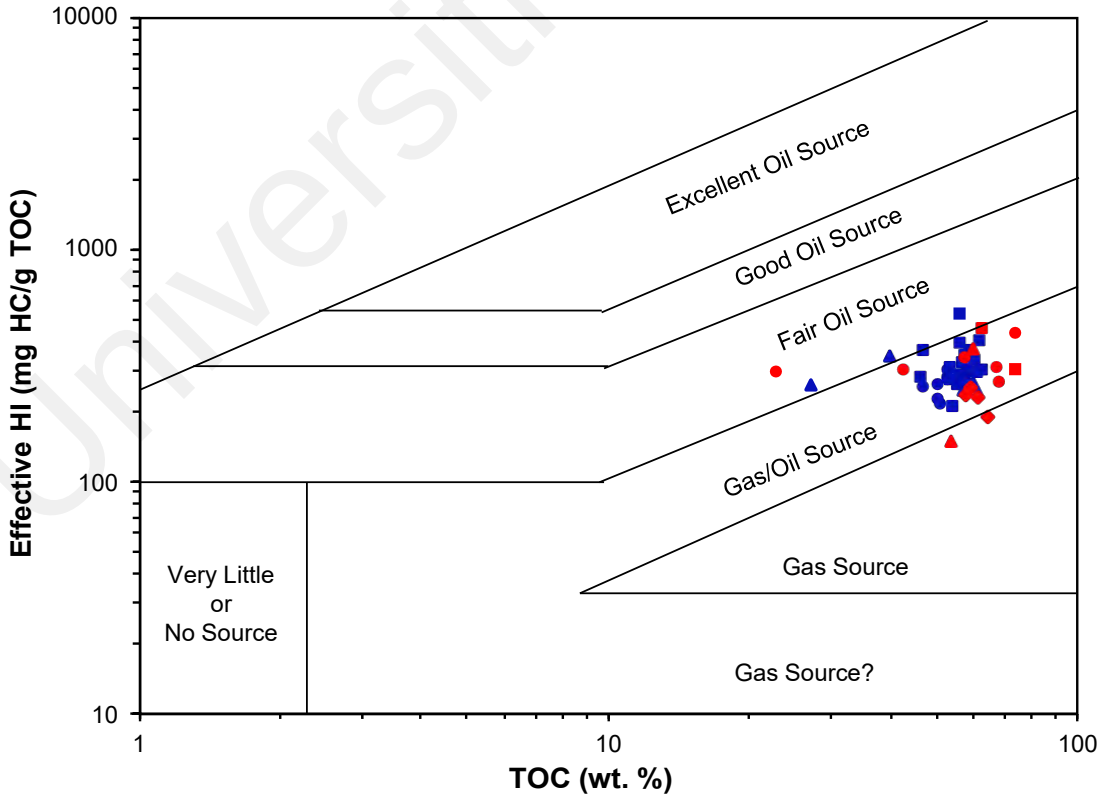

Figure 6.10: Plot of total organic carbon (TOC) vs. effective hydrogen index (HI).

Previous studies have shown that the oil-generating potential of coals depends on the length and type of aliphatic chains in its structure (Ganz & Kalkreuth, 1987; Ganz & Kalkreuth, 1991; Mastalerz et al., 2013; Petersen, 2005). Hence, FTIR spectra-based parameters have been used to evaluate the hydrocarbon-generating potential of the Sarawak coals (Wang et al., 2013; Misra et al., 2018; Biswas et al., 2020). First, calculated A_F values for all the studied coals (except MP1L and MGL2I) are > 0.4, which indicates generally good hydrocarbon-generating potential (Patricia et al., 2020). In addition, according to Petersen (2005), the relative intensity of CH_2 peak at 2850 cm^{-1} indicates the proportion of aliphatic structure in the coal structure and thus the oil-generating potential. The intensity at 2850 cm^{-1} is highest in the Nyalau Formation coals and lowest in the Liang Formation coals, which suggests the highest and lowest oil-generating potential for the Nyalau and Liang Formation coals, respectively (Figure 5.5). Similarly, the intensity of the CH_3 peak at 2955 cm^{-1}, which is indicative of the gas-generating potential, is highest for the Nyalau Formation coals and lowest for the Balingian coals.

The above interpretation is supported by the I_{HG} values which range from 26 to 280 mg HC/gTOC and generally increase from Gombe (avg. 54 mg HC/gTOC) to Liang (avg. 70 mg HC/gTOC) to Balingian (avg. 111 mg HC/gTOC) to Nyalau (avg. 125 mg HC/gTOC), Lamja (avg. 132 mg HC/gTOC), to Agwu (avg. 160 mg HC/gTOC) and Mamu Formation (avg. 160 mg HC/gTOC; Table 5.5). In support, the cross-plots of Rock-Eval's GP versus A_F in Figure 6.11a shows that the coals plot mostly in the gas to gas/oil zones, signifying the potential for gas to mixed oil and gas generation. In addition, Figure 6.11b shows that the Nyalau, Mamu and Agwu Formation coals possess relatively higher oil-generating potential.

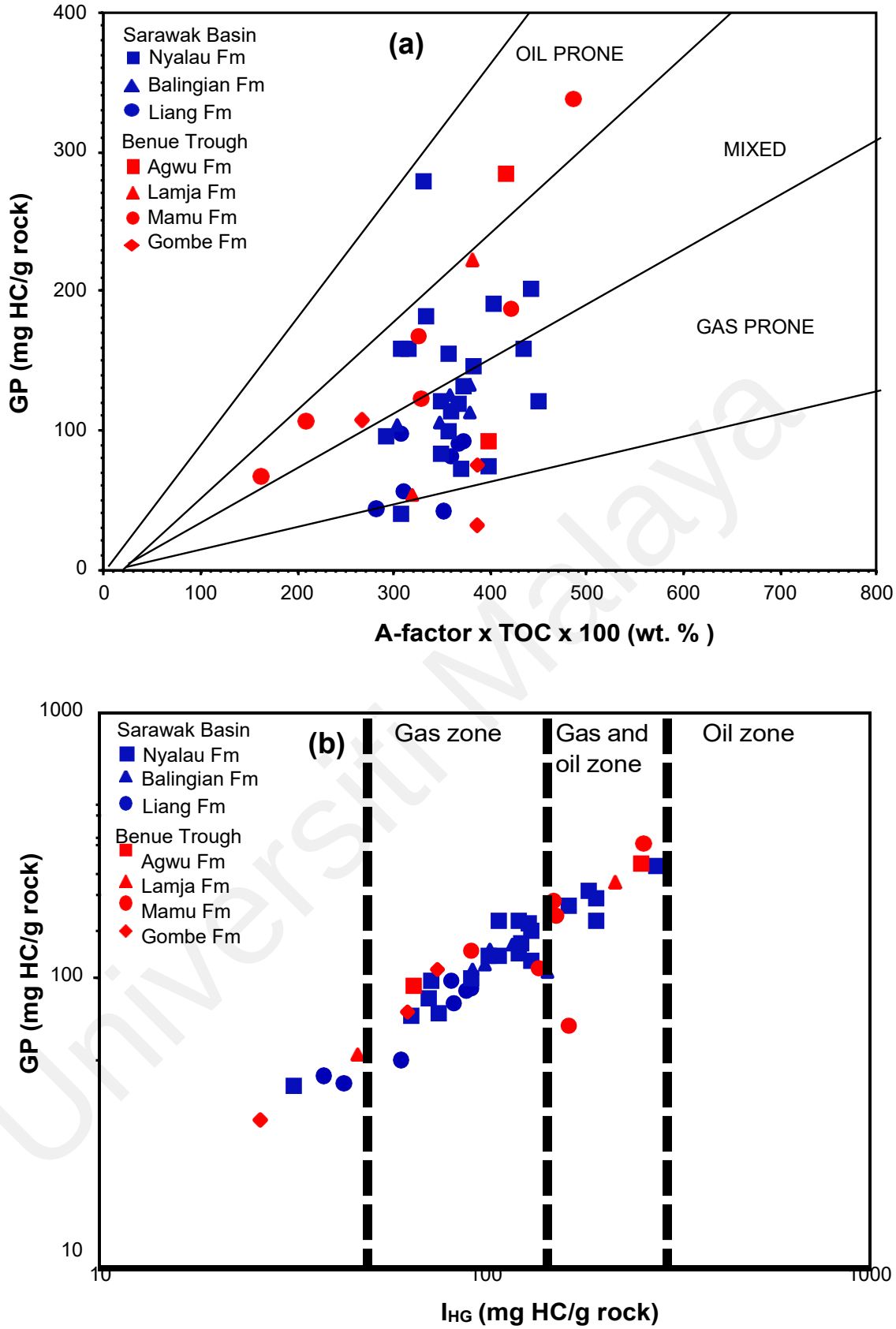

Figure 6.11: The correlation plots of genetic potential (GP) vs. (a) – *A*-factor (after Ganz & Kalkreuth, 1991), and (b) index for hydrocarbon generation (I_{HG}; after Misra et al., 2018), showing the oil-gas generative character.

Overall, Rock-Eval and FT-IR parameters, and the amount of extractable organic matter for the studied Sarawak Basin and Benue Trough coals indicate that the coals possess excellent potential to generate gas and mixed oil and gas.

6.3 Kerogen Type and Origin of Organic Matter

Source rocks often contain two or more kerogen types and thus, Rock-Eval pyrolysis data alone is not sufficient to accurately assess kerogen type (Dembicki, 2009). In this study, Rock-Eval, PyGC, FTIR, biomarker and atomic data were combined to determine the type and origin of organic matter in the Sarawak Basin and Benue Trough kerogens.

Based on a modified Van Krevelen diagram of HI versus OI (Figure 6.12a), the coal samples are dominated by type-III kerogen. Two trends of relatively lower and higher OI values were however observed in the modified Van Krevelen diagram. The Liang and Nyalau formations form a trend of samples with relatively higher OI values, while the Balingian Formation and Benue Trough coals plot along the low OI trend. The observed trends are possibly due to the varying OM source inputs. The interpretation of dominant type-III kerogen is supported by the *S*2 versus TOC diagram showing that the studied coals plot mainly in the type-III kerogen zone (Figure 6.12b). The relatively higher *S*2 and HI values of some Nyalau, Agwu and Mamu Formation coals possibly imply a mixed type III-II kerogen source. This observation is supported by the T_{max} versus HI diagram (Figure 6.13) which shows a mixed type III-II kerogen source for some of the studied coals. Additionally, the correlation diagram of FTIR spectra parameters, A_F and C_F, suggests the presence of some type II kerogen (Ganz & Kalkreuth, 1987; Figure 6.14). Hence, whilst dominated by type-III kerogen, the studied coals are a mixture, in varying proportions, of type III and type II kerogens.

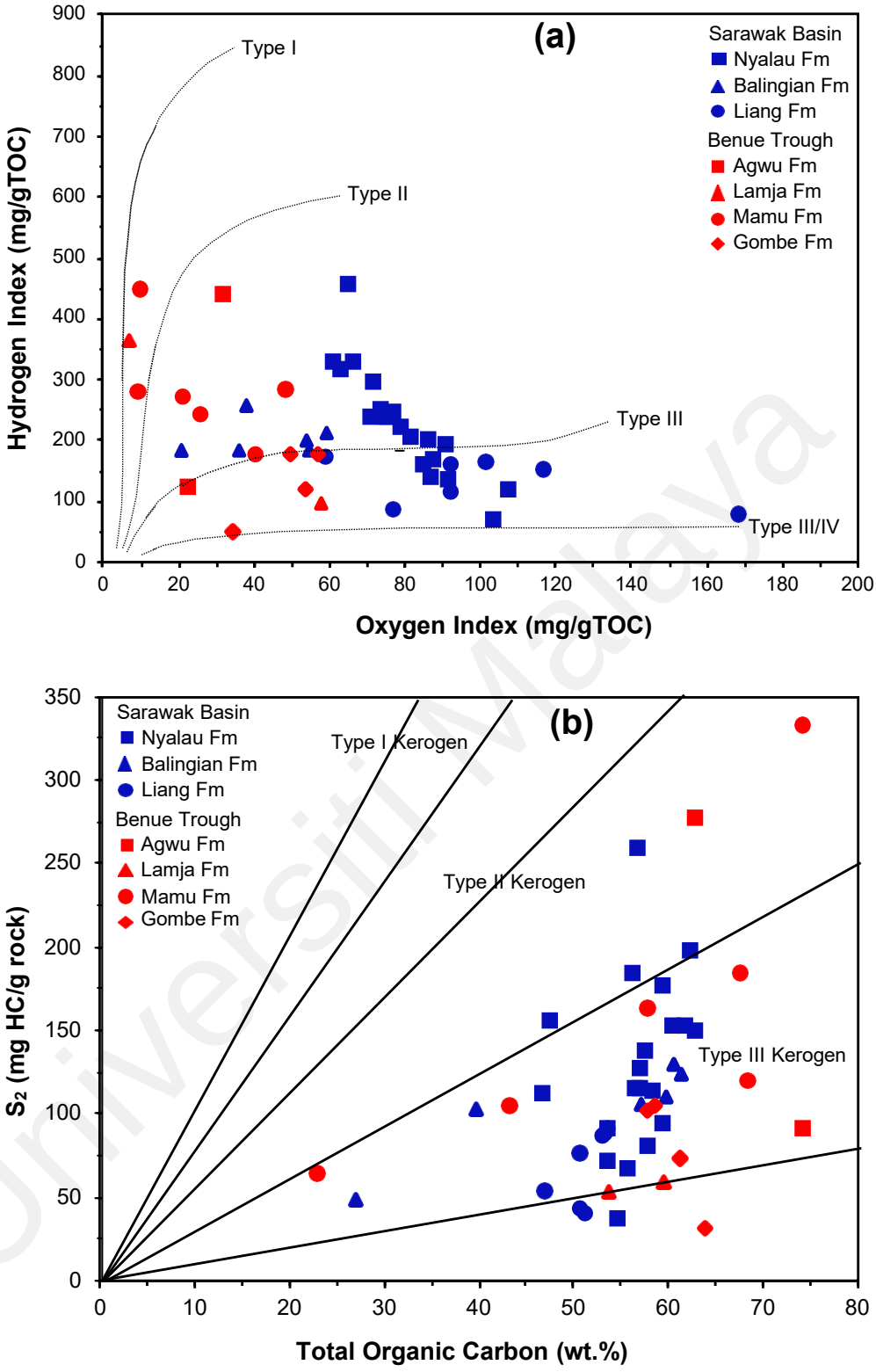

Figure 6.12: (a) – pseudo-Van-Krevelen diagram of Oxygen Index vs. Hydrogen Index (after Peters, 1986), and (b) – cross-plot of total organic carbon vs. *S2* (after Langford & Blanc-Valleron, 1990), showing kerogen type.

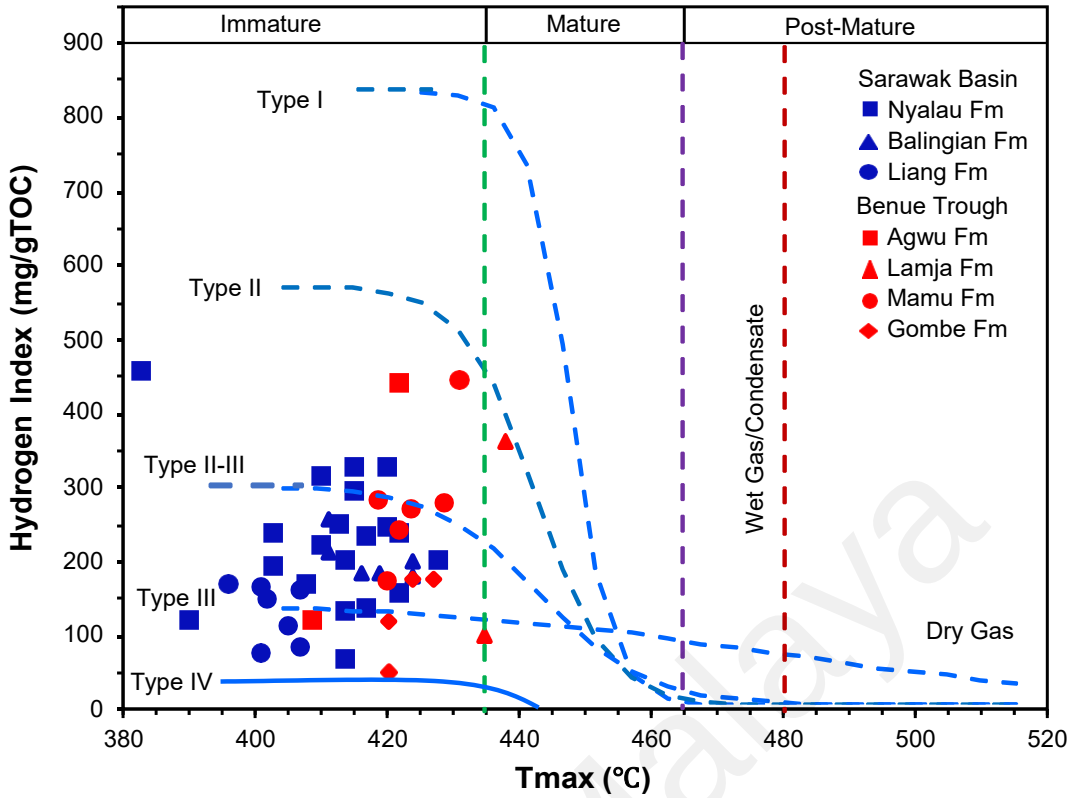

Figure 6.13: Diagram of T_{max} vs. Hydrogen Index showing kerogen type and thermal maturity.

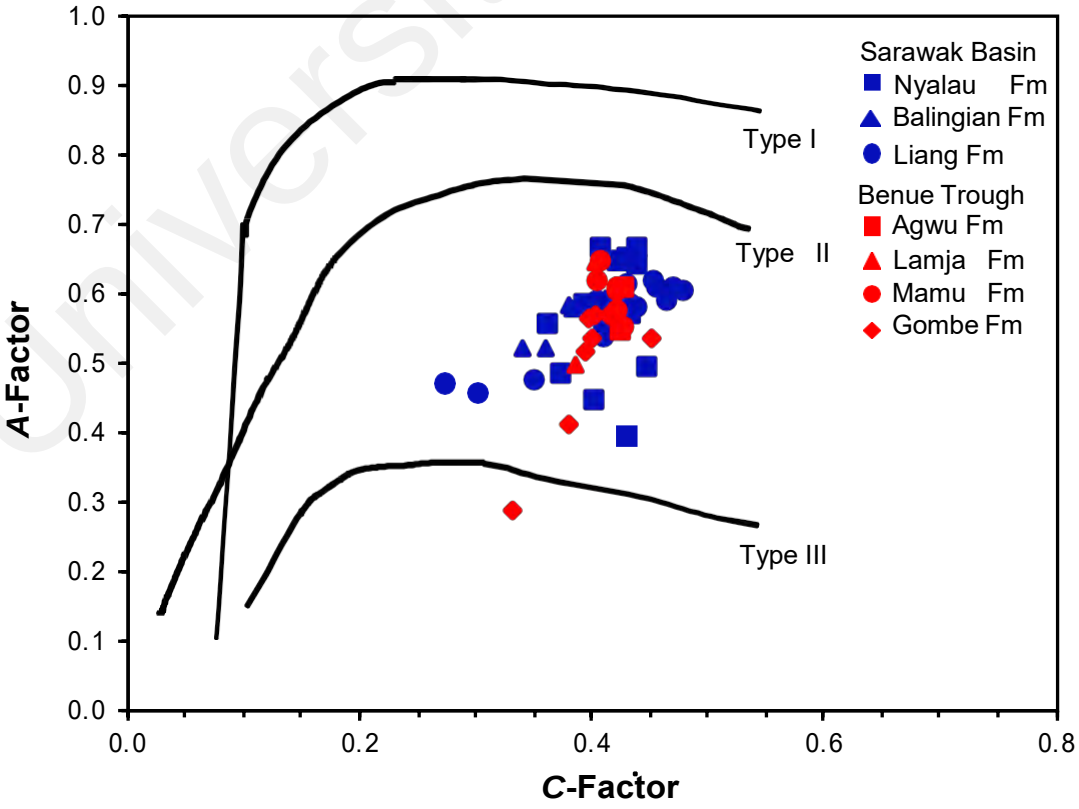

Figure 6.14: Correlation diagram of *A*-Factor and *C*-Factor showing kerogen type (after Ganz & Kalkreuth, 1987).

Furthermore, the Py-GC results provide additional and more accurate information on kerogen type when supplemented with Rock-Eval data. According to Dembicki (2009), the pyrograms of typical type-I and type-III kerogens are characterised by abundant peaks in the > C_{15} and < C_{10}, respectively, while the pyrolysate gas chromatograms of type-II kerogens are dominated by naphthalenic compounds and large unresolved complex mixtures (UCM) in the > C_{15} zone. The pyrograms of the Sarawak Basin coals largely show dominating peaks in the < C_{10} zone, typical of type-III kerogens. However, the pyrograms, particularly those of Balingian and Nyalau Formation coals, also show abundant peaks in the > C_{15} zone, which is indicative of the presence of type-II kerogen (Figures 5.12b-c). This interpretation supports the earlier Rock-Eval data interpretation of the presence of type-II kerogen. Although the higher HI values of Nyalau Formation (avg. 226 mg HC/g TOC) relative to the Balingian Formation (avg. 204 mg HC/g TOC) coals suggest a higher contribution of type-II kerogen (Figure 6.12a), the relatively higher proportion of peaks in the > C_{15} zone of the Balingian Formation pyrograms indicates a higher proportion of type-II kerogen (Figures 5.12b). Similarly, the pyrolysate gas chromatograms of the Benue Trough coals generally show dominating peaks in the < C_{10} zone and subordinate peaks in the > C_{15} zone, which is characteristic of predominant type-III kerogen mixed with varying proportions of type II kerogen. The Lamja Formation coals, however, contain relatively lower abundances of < C_{10} hydrocarbons and elevated proportions of C_{10} to C_{15} hydrocarbons (Figure 5.12h). This observation is indicative of the relatively higher contribution of Type-II kerogen to the Lamja Formation kerogens.

Additionally, the kerogen types in the analysed coals can be determined based on the abundances of *n*-alkane/alkene doublets and aromatic compounds in the whole-rock pyrograms (Larter & Douglas, 1980; Larter, 1984). For example, the Type Index is defined as the abundance of m(+p)-xylene relative to *n*-1-octene (xy/C_8) and according

to Larter & Douglas (1980), xy/C_8 values < 0.4, between 0.4 and 1.3 and > 1.3 are characteristic of type I, type II and type-III kerogens, respectively. Calculated values of the Type Index are > 0.4, varying from 0.6 to 2.9 (avg. 1.7) and 0.6 to 3.0 (avg. 1.2) for the Sarawak Basin and Benue Trough coals, respectively. The values imply a mixture of type II and type III kerogens in the coals. However, the relatively lower values for the Benue Trough coals suggest a higher proportion of type-II kerogen in the samples.

The C_8/xy ratio is reportedly a proxy for estimating the relative abundance of aliphatic to aromatic hydrocarbons. The calculated C_8/xy ratios range correspondingly from 0.34 to 1.58 (avg. 0.66) and 0.33 to 1.81 (avg. 1.02) for the Sarawak Basin and Benue Trough coals (Table 5.12). The generally lower C_8/xy values for the Sarawak coals indicate a higher abundance of aromatic hydrocarbons and input of humic materials that is typical of type-III kerogen (Farhaduzzaman et al., 2012; Adegoke et al., 2015). In agreement with earlier findings, the generally higher C_8/xy values for the Benue Trough coals indicate a higher abundance of aliphatic hydrocarbons which could be related to higher input of type-II kerogen (Dembicki et al., 2009). Larter (1984) proposed the ternary diagram of the relative abundances of *n*-1-octene, m(+p)-xylene and phenol to distinguish kerogen types. Whilst some coals plot near the type-II zone, the analysed coals mostly plot in the type-III zone of the diagram (Figure 6.15), indicating the predominant proportion of type-III kerogen in the coals.

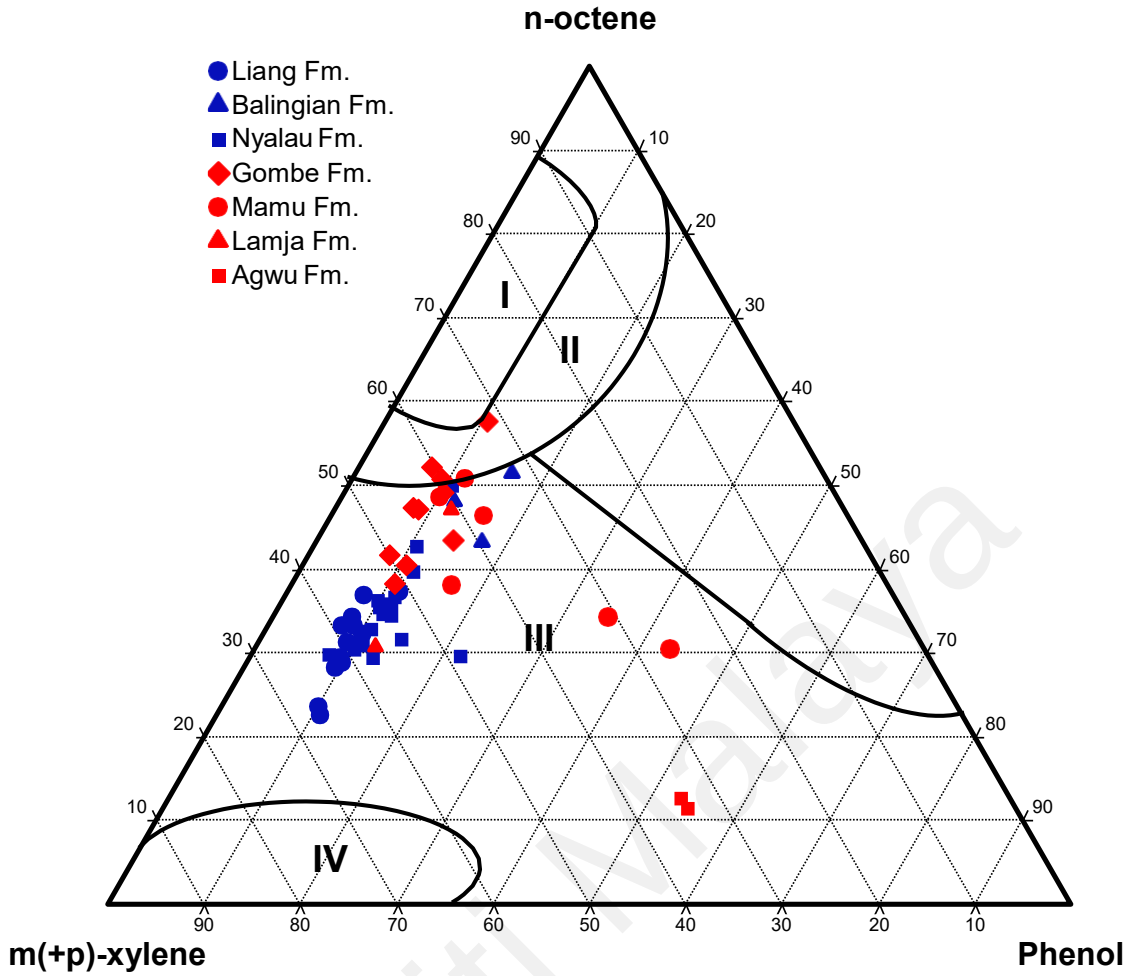

Figure 6.15: Ternary diagram of the relative abundances of *n*-1-octene, m(+p)-xylene and phenol, showing kerogen classification (after Larter, 1984).

The distribution of *n*-alkanes could be a useful indicator of organic matter input. High amounts of low MW (< C_{21}) *n*-alkanes are indicative of lacustrine OM input while high amounts of medium MW (C_{21} – C_{25}) and high MW (> C_{27}) *n*-alkanes signify aquatic macrophytes and terrestrial vascular plant inputs, respectively (Cranwell et al., 1987; Peters et al., 2005; Zheng et al., 2007). The ternary diagram of the relative proportions of the lower, medium, and higher MW *n*-alkanes is shown in Figure 5.16. The studied coals are dominated by higher MW homologues with mean proportions of 67.0% and 54.8%, respectively, in the Sarawak Basin and Benue Trough coals. The predominant abundance of long-chain *n*-alkanes suggests that the humic coals are sourced from highly aliphatic, resistant biopolymers associated with cuticular materials

of higher land plants (Collinson et al., 1994; Curry et al., 1994). Although the abundances of the medium MW *n*-alkanes are generally similar for both groups of coals, the proportions of lower MW *n*-alkanes are higher in the Benue Trough (avg. 17.3%) than in the Sarawak Basin (avg. 8.9%) coals. The Balingian Formation (avg. 21.3%) coals contain a relatively higher proportion of lower MW *n*-alkanes when compared with coals of Liang (avg. 7.3%) and Nyalau (avg. 6.3%) formations. In addition, lower MW *n*-alkanes are abundant in the Benue Trough coals with the average proportion generally increasing from Mamu (avg. 13.2%) to Agwu (avg. 17.2%), Gombe (avg. 19.1.3%) and Lamja (avg. 21.3%) formations. These findings are suggestive of the elevated contribution of marine algal organic matter to the Balingian Formation and Benue Trough coals.

Aquatic algae have been found to show a characteristic *n*-C_{17} signature (Bourbonniere & Meyers, 1996). Hence, $C_{27}/(C_{17} + C_{27})$ and C_{31}/C_{17} *n*-alkane ratios are veritable proxies for estimating the relative contribution of terrigenous and aquatic organic matter. Higher ratios of both proxies signify a higher contribution of terrigenous organic matter. Measured $C_{27}/(C_{17} + C_{27})$ ratios are relatively higher in the Sarawak Basin coals, varying from 0.71 to 0.99 (avg. 0.91), than in the Benue Trough coals with lower ratios that vary from 0.70 to 0.95 (avg. 0.86). Similarly, ratios of *n*-C_{31}/*n*-C_{17} are higher in the Malaysian coal extracts, varying from 1.84 to 50.50 (avg. 22.25) while ratios for Nigerian coals vary between 1.86 and 16.57 (avg. 5.46). The cross-plot of $C_{27}/(C_{17} + C_{27})$ and C_{31}/C_{17} *n*-alkane ratios shows a generally higher terrigenous OM input in the Sarawak Basin coals (Figure 6.16). However, the Balingian Formation coals plot lower along with the Benue Trough coals, indicating the coals contain a relatively lower proportion of terrigenous OM.

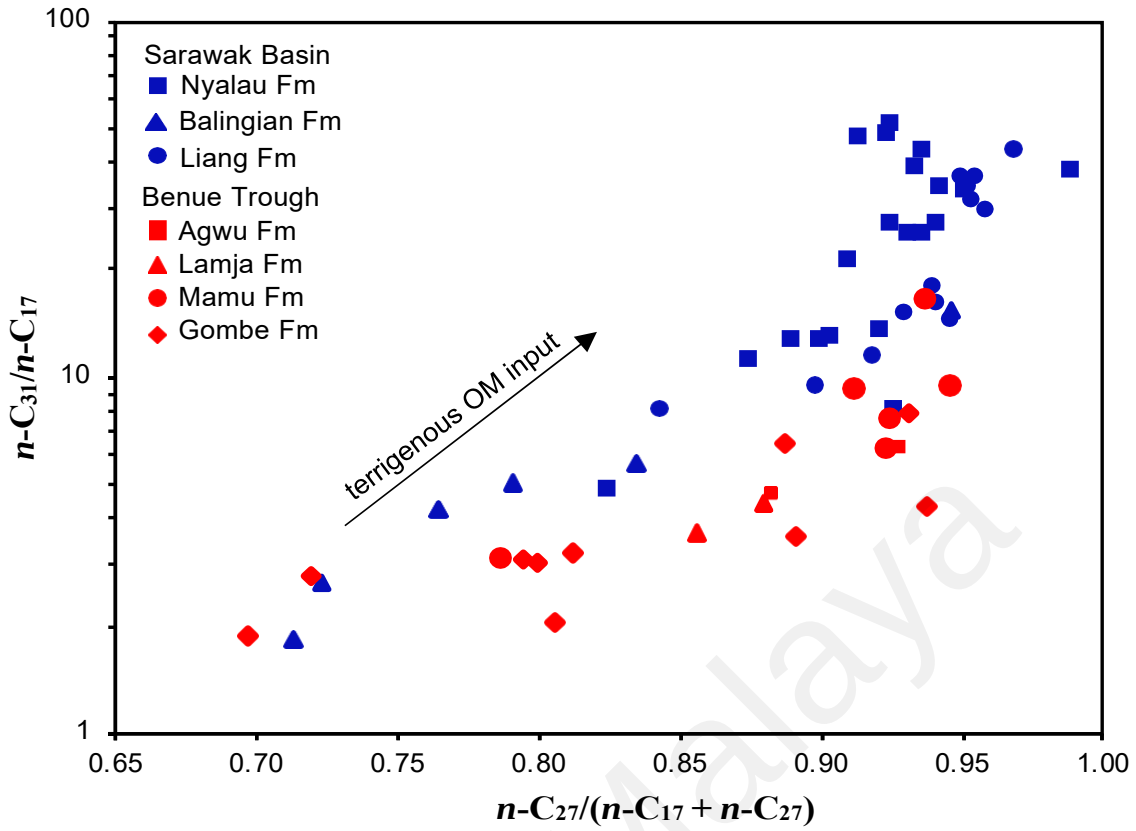

Figure 6.16: Cross-plot of *n*-C_{27}/(*n*-C_{17} + *n*-C_{27}) vs. *n*-C_{31}/*n*-C_{17} showing organic matter source input.

The TAR values, which are a measure of the relative contribution of terrigenous and aquatic organic matter (Bourbonniere & Meyers, 1996), are higher for the Sarawak Basin coals (3.0-32.4) than the Benue Trough coals (2.2-20.9). Similarly, values of the wax index (WI) are higher for the Sarawak Basin coals (2.4-24.8) than the Benue Trough coals (2.5-12.5). The studied coals all have TAR and WI values > 1, which signifies the predominant contribution of terrestrial organic matter (Bourbonniere & Meyers, 1996). Nevertheless, the cross-plot of WI versus TAR in Figure 6.17, indicates a relatively higher proportion of terrestrial organic matter in the Sarawak Basin coals. Furthermore, some of the Balingian Formation and Benue Trough coals have TAR values < 4, which again implies that the coals contain a considerable proportion of marine algal organic matter. The ratios of isoprenoids over *n*-alkanes are commonly employed to infer the type of organic matter (Shanmugam, 1985). Pr/*n*-C_{17} and Ph/*n*-C_{18}

ratios for the coal samples are generally > 1 and < 1, respectively. The cross-plot of Ph/*n*-C_{18} versus Pr/*n*-C_{17} is displayed in Figure 6.18. Even though two Liang Formation coals plot in the mixed type II-III to marine algal Type II kerogen zones, the studied coals mostly plot in type-III kerogen zone, corroborating the predominant terrestrial organic matter origin.

The distributions of alkylated phenanthrenes and naphthalenes have been widely employed as indicators of OM origin. Elevated abundances of 9-MP, 2,10-DMP, 3,9-DMP and 3,10-DMP have been observed in sediments of marine origin while high amounts of 1-MP and 1,7-DMP (pimanthrene) are found in sediments with higher plant origin (Budzinski et al., 1995). The cross-plot of Log (1-MP/9-MP) and Log (1,7-DMP/1,3+2,10+3,9+3,10-DMP) in Figure 6.19a delineates the organic matter source inputs. The Liang and Nyalau Formation coals plot mainly in the top right quadrant, signifying a predominant input of 1-MP and 1,7-DMP that is typical of terrestrial organic matter input. However, the Balingian Formation and Benue Trough coals plot in the bottom zone, signifying high input of 9-MP that is characteristic of considerable marine algal OM input (Budzinski et al. 1995). Similarly, the relative abundance of 1,2,5-TMN and 1,3,6-TMN is reported to reflect source effects in immature to low-maturity terrestrial sediments (Strachan et al., 1988; van Aarssen et al., 1999). Hence, log (1-MP/9-MP) is plotted against (1,2,5-TMN/1,3,6-TMN) in Figure 6.19b. The Benue Trough coals plot mainly in the bottom left quadrant due to the relatively higher abundances of 9-MP and 1,3,6-TMN, which is characteristic of a substantial contribution of marine organic matter. Conversely, the Sarawak Basin coals plot mostly in the top right, indicating high input of 1-MP and 1,2,5-TMN that is characteristics of high terrigenous input and low thermal maturity, respectively (Budzinski et al., 1995; van Aarssen et al., 1999).

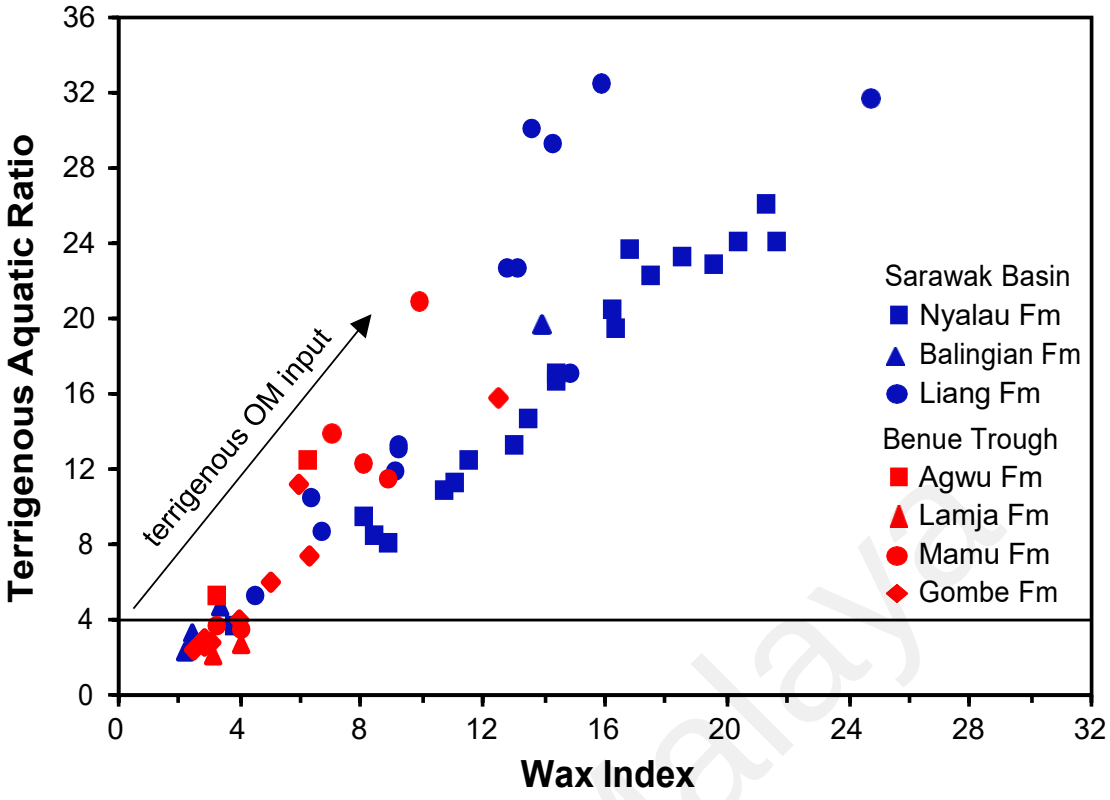

Figure 6.17: Cross-plot of wax index (WI) vs. terrigenous aquatic ratio (TAR) for the studied coals.

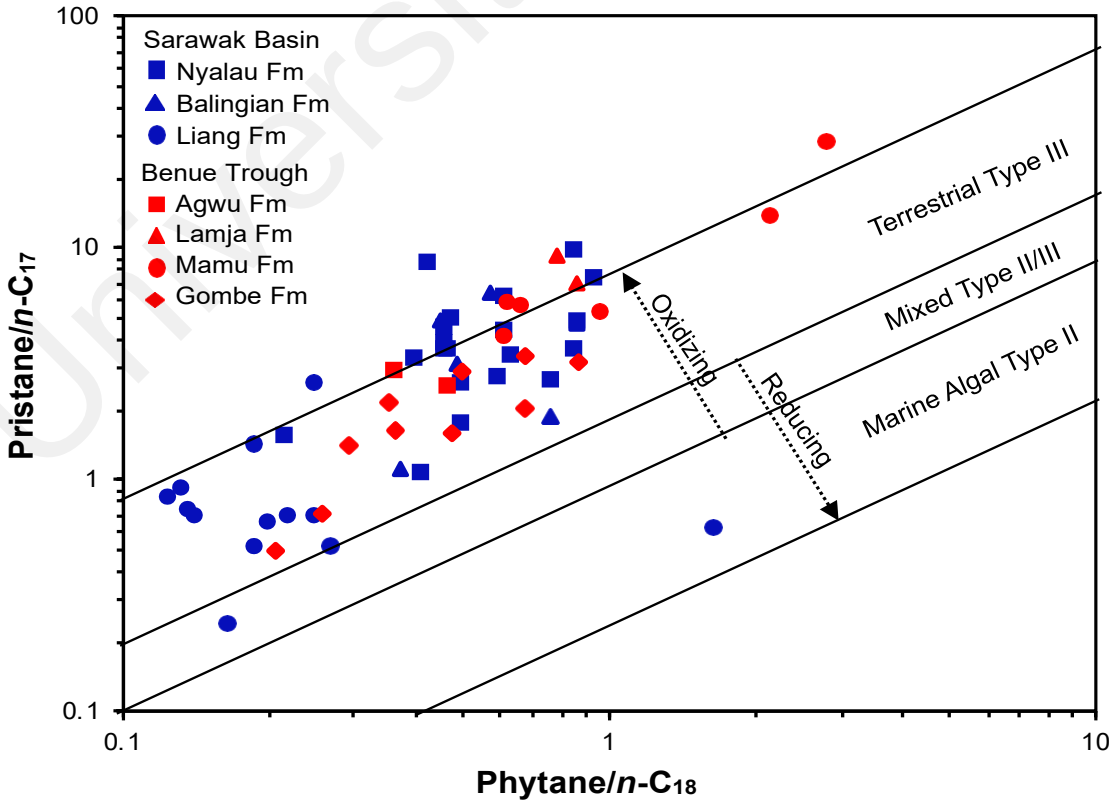

Figure 6.18: Diagram of phytane/*n*-C_{18} vs. pristane/*n*-C_{17} showing organic matter type for the Sarawak Basin and Benue trough coals (after Peters et al., 1999).

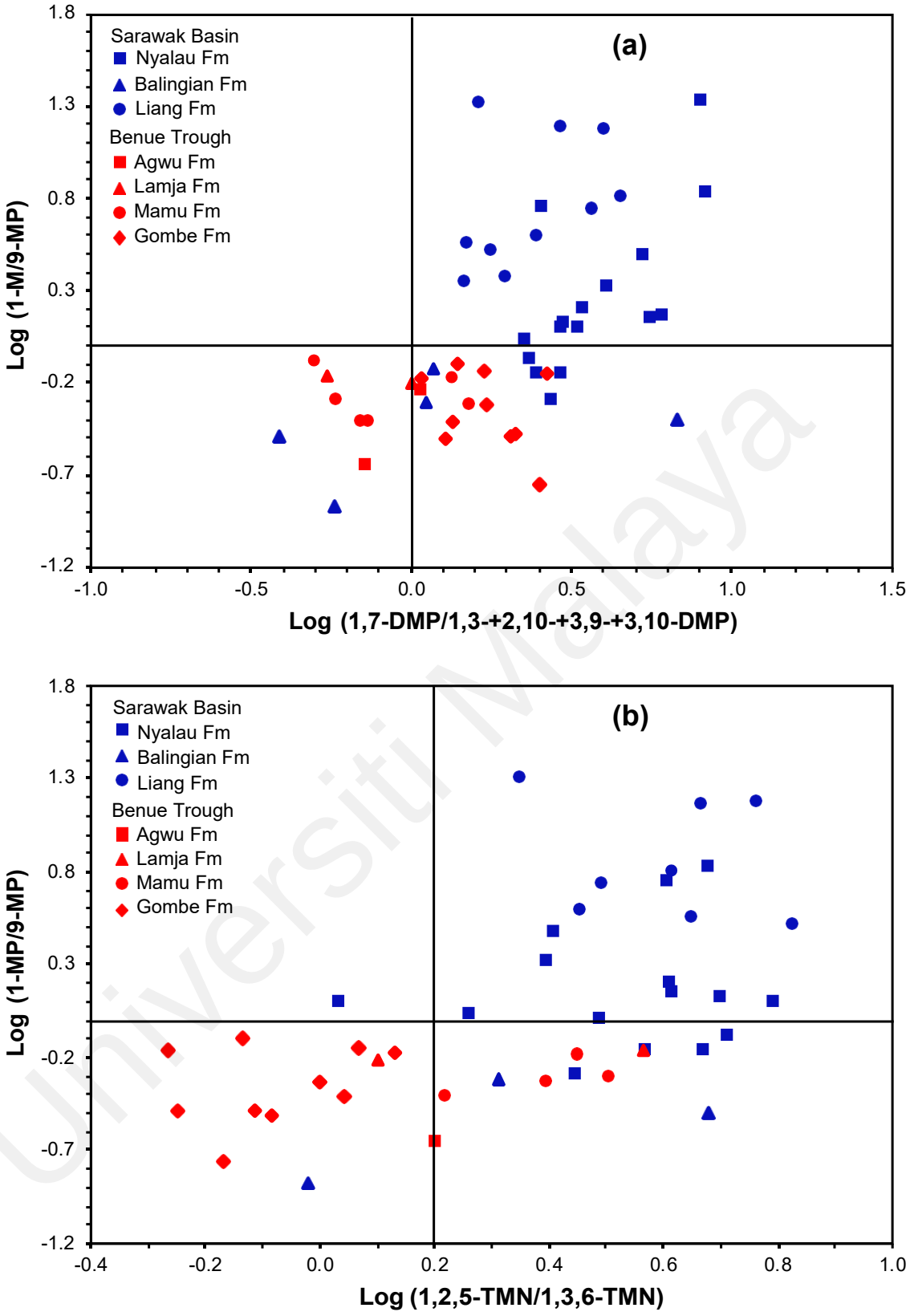

Figure 6.19: Cross-plots of (a) – Log (1,7-DMP/1,3+2,10+3,9+3,10-DMP) vs Log (1-MP/9-MP), and (b) – Log (1,2,5-TMN/1,3,6-TMN) vs Log (1-MP/9-MP) for the studied coals.

Asahina & Suzuki (2018) proposed ratios of alkylated naphthalenes as potential indicators of organic matter input and concluded that dimethylnaphthalene (DMR) and trimethylnaphthalene ratio (TMR) values greater than 1.0 and 0.8, respectively, in oils and condensates indicate terrestrial organic matter origin. Calculated DMR values for the studied Sarawak Basin coals are > 1, ranging from 1.3 to 13.8 (avg. 4.6), while the TMR values are > 0.8, varying from 1.0 to 6.8 (avg. 3.6). Similarly, DMR values for the Benue Trough coals are ≥ 1.0, ranging from 1.0 to 3.1 (avg. 1.6). However, some samples show TMR values < 0.8, ranging from 0.5 to 3.6 (avg. 1.5). The cross-plot of TMR and DMR illustrates the relatively higher contribution of terrigenous organic matter in the Sarawak Basin coals (Figure 6.20). In addition, it shows that the Benue Trough coals, particularly the Gombe Formation coals, are sourced mainly from terrestrial OM but with a considerable contribution of marine algal OM.

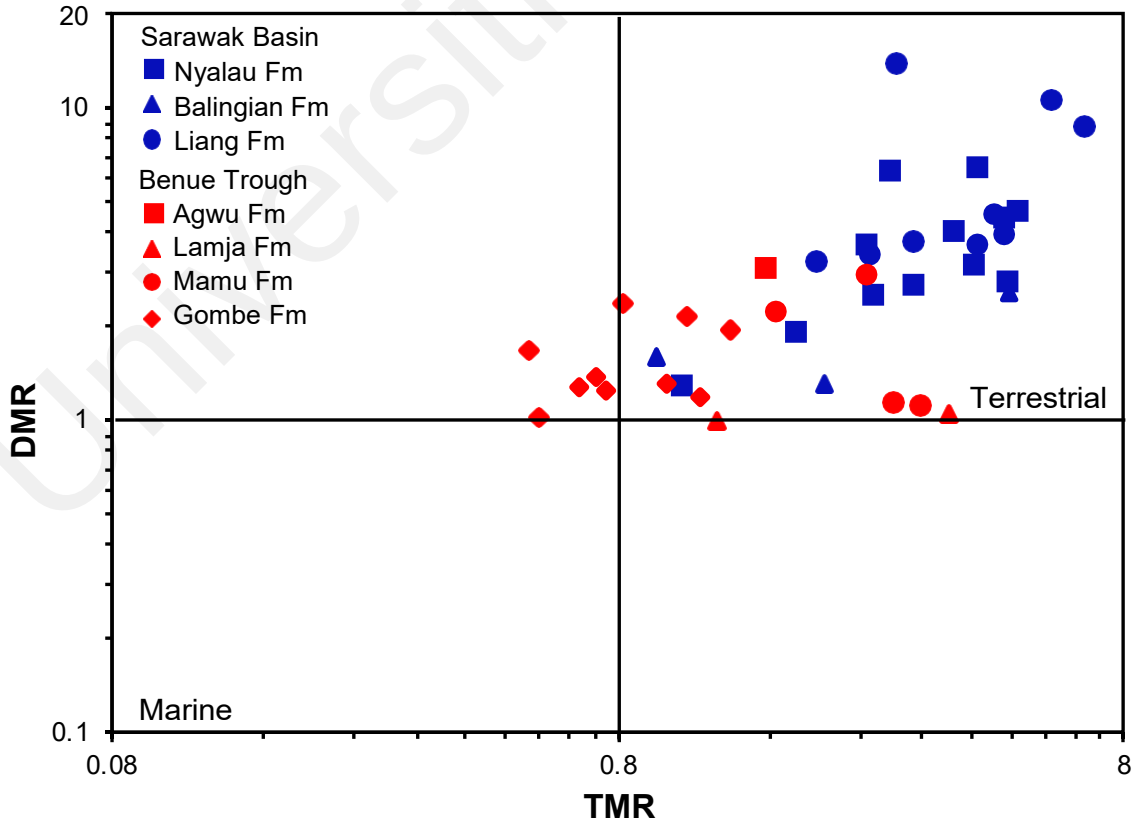

Figure 6.20: Plot of trimethylnaphthalene ratio (TMR) vs. dimethylnaphthalene (DMR), showing organic matter source input (after Asahina & Suzuki, 2018).

Dibenzofuran (DBF) and its methylated derivatives could also be useful indicators of organic matter source input as their concentration are higher in terrestrial-sourced OM than in marine-derived OM (Radke et al., 2000; Asif & Wegner, 2019). Baydjanova & George (2019) proposed the cross-plot of MDBF/MP versus DBF/P to differentiate organic matter source and lithology. The DBF/P ratios are relatively higher for the Sarawak Basin coals (0.01-0.54) than the Benue Trough coals (0.01-0.16). Similarly, MDBF/MP ratios for the Sarawak Basin coals (0.01-3.56) are generally higher when compared with the Benue Trough coals (0.06-1.61). The studied coals mostly plot near the terrestrial organic matter axis of the Baydjanova & George (2019) diagram (Figure 6.22). However, some Liang Formation coals from Sarawak Basin plot near the marine axis, which corroborates the earlier Ph/*n*-C_{18} versus Pr/*n*-C_{17} diagram interpretation of some marine algal OM input (Figure 6.18). Regardless, this interpretation is contradicted by the high TAR, WI, DMR, TMR values and abundance of 1-MP in the Liang Formation coals, which all signify the predominant contribution of terrigenous organic matter.

The atomic carbon to nitrogen (C/N) ratio is an excellent proxy for organic matter source input. Due to the absence of cellulose in algae, its C/N ratios typically range from 4-10 while vascular plants with high cellulose content have C/N ratios > 20 (Meyers, 1994; Meyers 1997). The C/N ratios for all the studied coals are > 20, with mean values of 42.1 and 42.4 in the Sarawak Basin and Benue trough coals, respectively (Table 5.11). The high C/N ratios indicate the predominant contribution of vascular plants to organic matter. This interpretation is supported by cadalene to m(+p)-xylene (cad/xy) ratios which vary from 0.03 to 0.35 and 0.04 to 0.24 (Table 5.12). These ratios imply a predominant input of higher land plants to peat formation and thus kerogen formation (Solli et al., 1984; Adegoke et al., 2015).

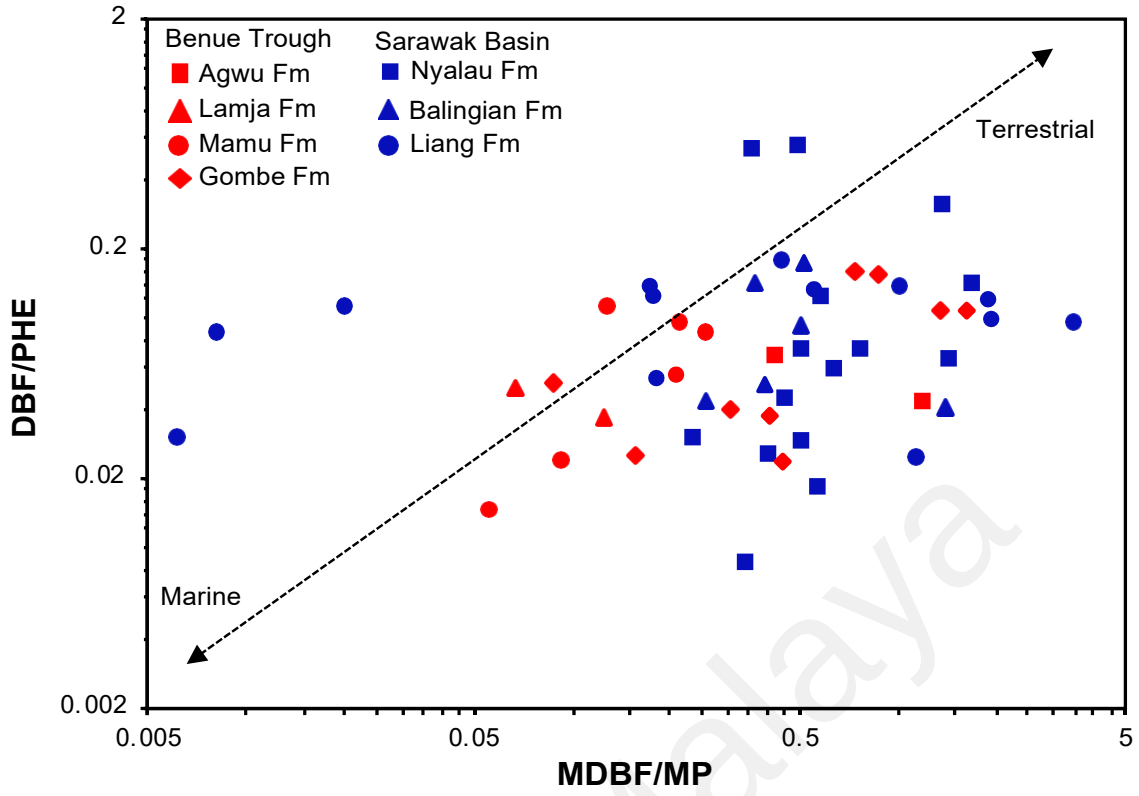

Figure 6.21: Cross-plot of methyldibenzofurans/methylphenanthrenes (MDBF/MP) vs. dibenzofuran/phenanthrene (DBF/PHE) (after Baydjanova & George, 2019).

In summary, the investigated Sarawak Basin and Benue Trough coals are dominated by type-III kerogen with varying proportions of type-II kerogen. The coals are derived mainly from terrigenous organic matter but with varying inputs of marine algal organic matter. Nevertheless, the contribution of marine OM is relatively higher in the Benue Trough coals and the Balingian Formation coals of the Sarawak Basin.

6.4 Provenance of Source Areas

The abundances of trace elements have been widely employed to determine the provenance of clastic sediments and the composition of their source areas (McLennan et al., 1993; Hayashi et al., 1997; Dai et al., 2012; Vosoughi Moradi et al., 2016; Tao et

al., 2017; Krzeszowska et al., 2019; Han et al., 2020). Although the abundances of elements in sediments may not reflect abundance in parent igneous source rocks, the abundances of immobile elements such as Al, Nb, Ti, Hf, Zr, Sn, Th, and REY are relatively unchanged during transportation, reworking, deposition, and diagenesis due to their low solubility (Kiipli et al., 2017). Hence, the elemental composition of coals is a potential information resource on the provenance of their inorganic constituents (Li et al. 2019; Lv et al., 2019; Liu et al., 2021).

The Al_2O_3/TiO_2 ratio is a widely utilized proxy for inferring the source area composition of sedimentary rocks. According to Hayashi et al. (1997), sedimentary rocks derived from mafic, intermediate, and felsic igneous rocks have Al_2O_3/TiO_2 ratios ranging from 3 to 8, 8 to 21, and 21 to 70, respectively. The Al_2O_3/TiO_2 ratios are comparably higher for the Sarawak Basin coals, ranging from 3.3 to 43.6 with an average of 22.3, while the ratios for the Benue Trough coals range from 1.7 to 21.8 with an average of 10.5. These ratios suggest that the parent rocks of the Sarawak Basin and Benue Trough coals were mostly derived from intermediate to felsic igneous rocks, and mafic igneous rocks, respectively (Figure 6.22a). Furthermore, the relative abundance of TiO_2 and Zr has been employed to evaluate provenance. TiO_2/Zr ratios > 200 signify mafic igneous rocks, while ratios < 55 indicate felsic rocks (Hayashi et al., 1997). TiO_2/Zr ratios for the studied Sarawak Basin coals range from 55.6 to 2000.0 (avg. 1264.0) and are suggestive of a dominantly mafic rock source composition. Similarly, TiO_2/Zr ratios for the investigated Benue Trough coals vary widely between 88.3 and 2750.0 (avg. 664..6), which are suggestive of the predominant abundance of intermediate to mafic rocks in the Benue Trough areas (Figure 6.22b).

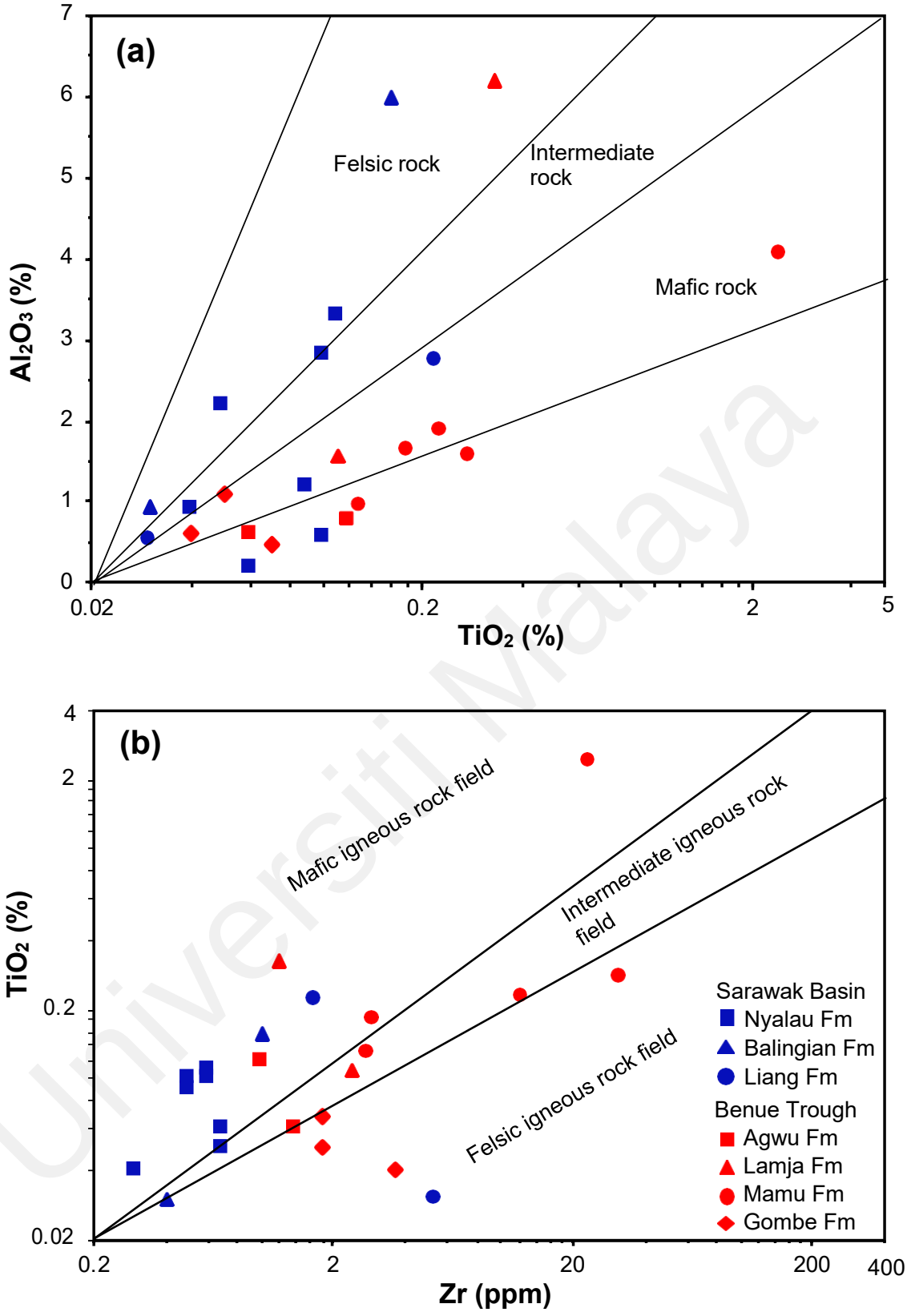

Figure 6.22: Source composition discrimination plots of (a) – TiO_2 vs. Al_2O_3, and (b) – Zr vs. TiO_2 (after Hayashi et al., 1997).

Elemental ratios based on the relative abundances of heavier and lighter elements or incompatible and compatible elements are also used to determine source composition (McLennan et al., 1993; Roy & Roser, 2013). For instance, high (> 1.0) and low (< 0.6) Th/Sc ratios imply felsic and mafic igneous rock source composition, respectively (McLennan et al., 1993). Th/Sc ratios range from 0.21 to 1.50 (avg. 0.63) and 0.41 to 2.57 (avg. 1.31) for the Sarawak Basina and Benue Trough coals, respectively. The cross plot of Th and Sc in Figure 6.23a suggests the dominance of mafic to intermediate rocks in the Sarawak areas, and mostly intermediate to felsic igneous rocks in the Benue Trough areas (Krzeszowska, 2019; Han et al., 2020).

In addition, the La/Th ratios of the studied coals show various values, ranging from 0.71 to 51.75 (avg. 8.70) for the Sarawak Basin, and 0.73 to 7.38 (avg. 2.18) for Benue Trough (Figure 6.23b). The ratios for most of the Benue Trough samples are lower than the La/Th ratio of the upper continental crust (2.8), suggesting a felsic to an intermediate source (Taylor & McLennan, 1985). In contrast, the Sarawak Basin coals show a wide range across the Formations. The La/Th ratios of the Nyalau Formation are < 2.8, which could indicate a felsic to an intermediate source. The Liang and Balingian Formations show very high (> 10) ratios that imply an intermediate to mafic igneous rock source (Taylor & McLennan, 1985). Furthermore, the bivariate plot of Zr/Sc and Th/Sc ratios indicates the lack of sediment sorting and recycling in the source areas of the studied samples (McLennan et al., 1993; Figure 6.24).

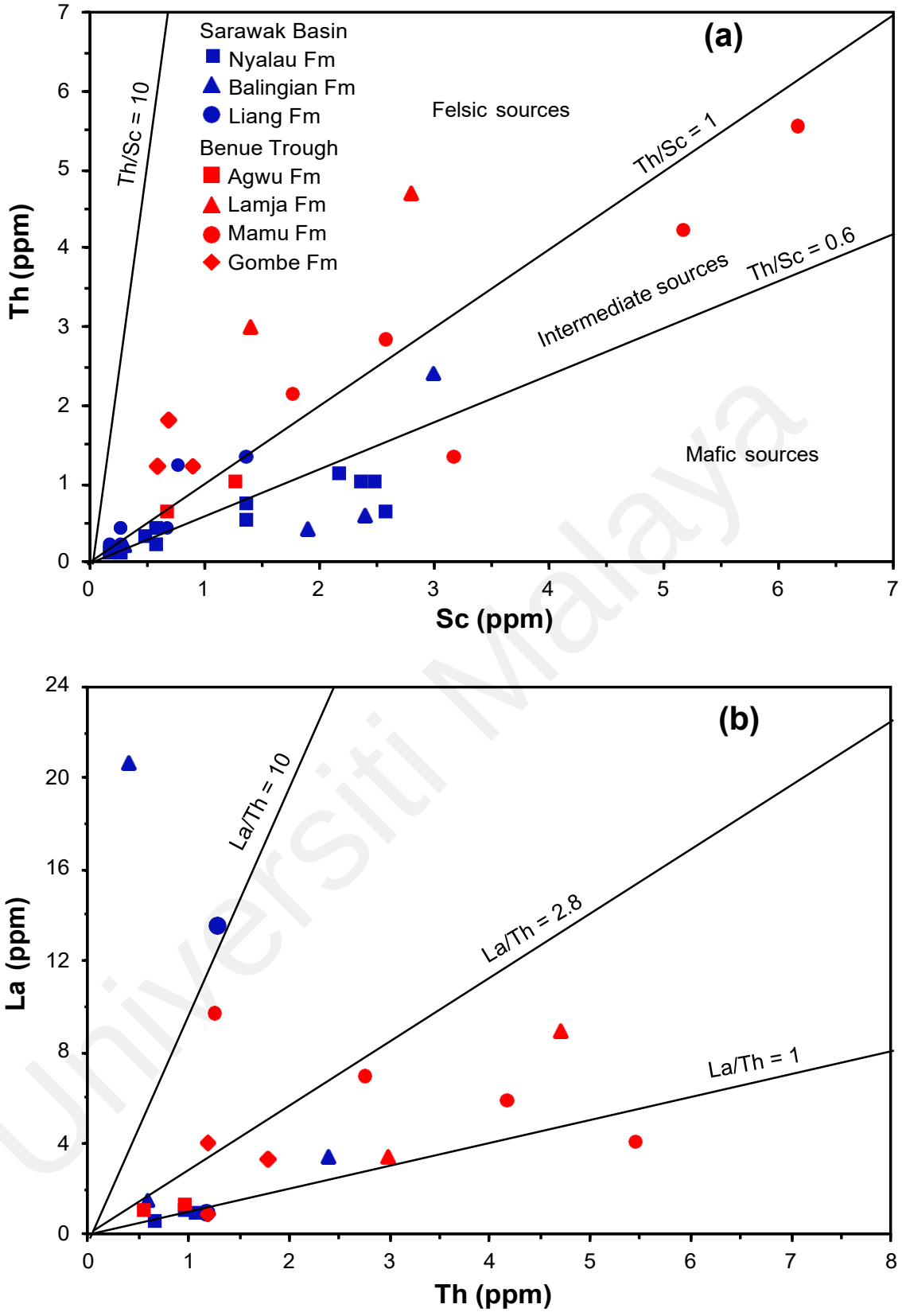

Figure 6.23: Binary plots of (a) – Sc vs. Th, and (b) – La vs. Th (after Taylor & McLennan, 1985).

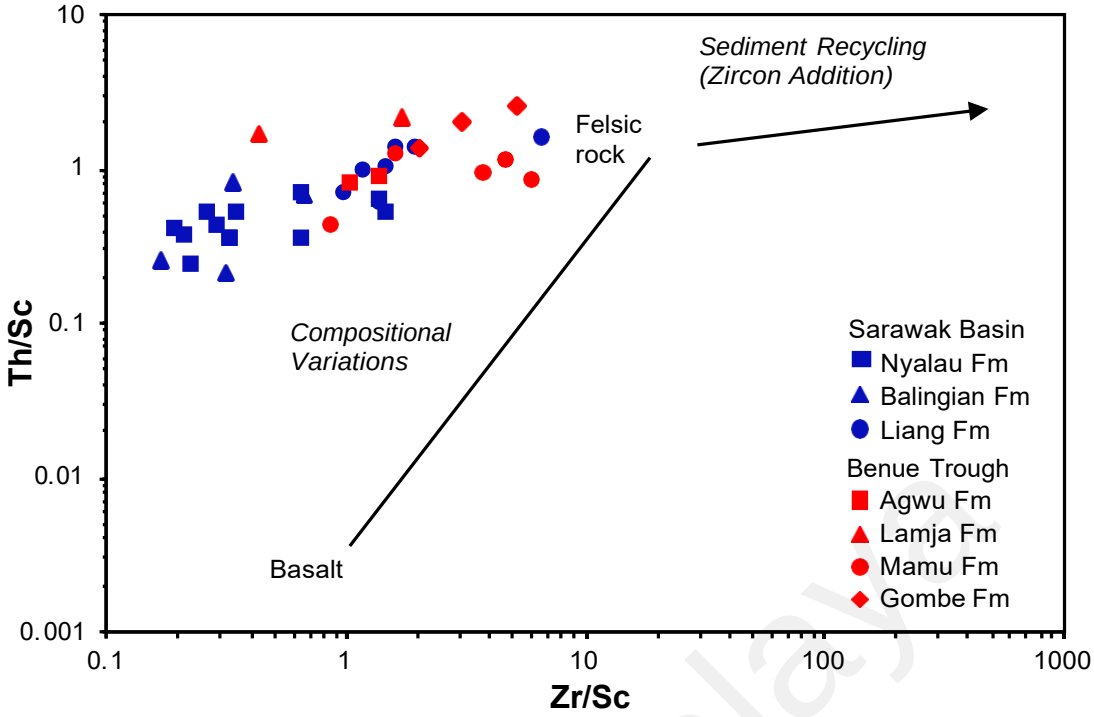

Figure 6.24: Source-composition discrimination plot of Zr/Sc vs. Th/Sc (after McLennan et al., 1993).

The relative abundance of high field strength trace elements (HFSTE; e.g., Th, La, Y, Zr and Hf) to transition trace elements (TTE; e.g., Cr, Co, and Sc) has been shown to provide information on the composition of sedimentary rocks (Edegbai et al, 2019b). According to Cullers (2000), relatively higher and lower Th/Co, Th/Cr, Th/Sc, and La/Sc ratios are indicative of felsic and mafic parent rocks, respectively. The calculated ratios for the analysed samples are presented in Table 5.10. Th/Co ratios of the Sarawak Basin (avg. 0.36) coals are mostly lower than those of the Benue Trough coals (avg. 0.66). Similarly, Th/Cr and Th/Sc ratios are lower in the Sarawak Basin (avg. 0.13 and 1.02) samples than in the Benue Trough samples (avg. 0.30 and 1.31). However, La/Sc ratios are in general higher for the Malaysian coals (avg. 3.10) than the Nigerian coals (avg. 2.56). In summary, the relatively lower HFSTE/TTE ratios of the Sarawak Basin coals generally support the interpretation of mafic igneous parent rocks while higher ratios indicate intermediate to felsic igneous parent rocks in the Benue Trough coals (Figures 6.25).

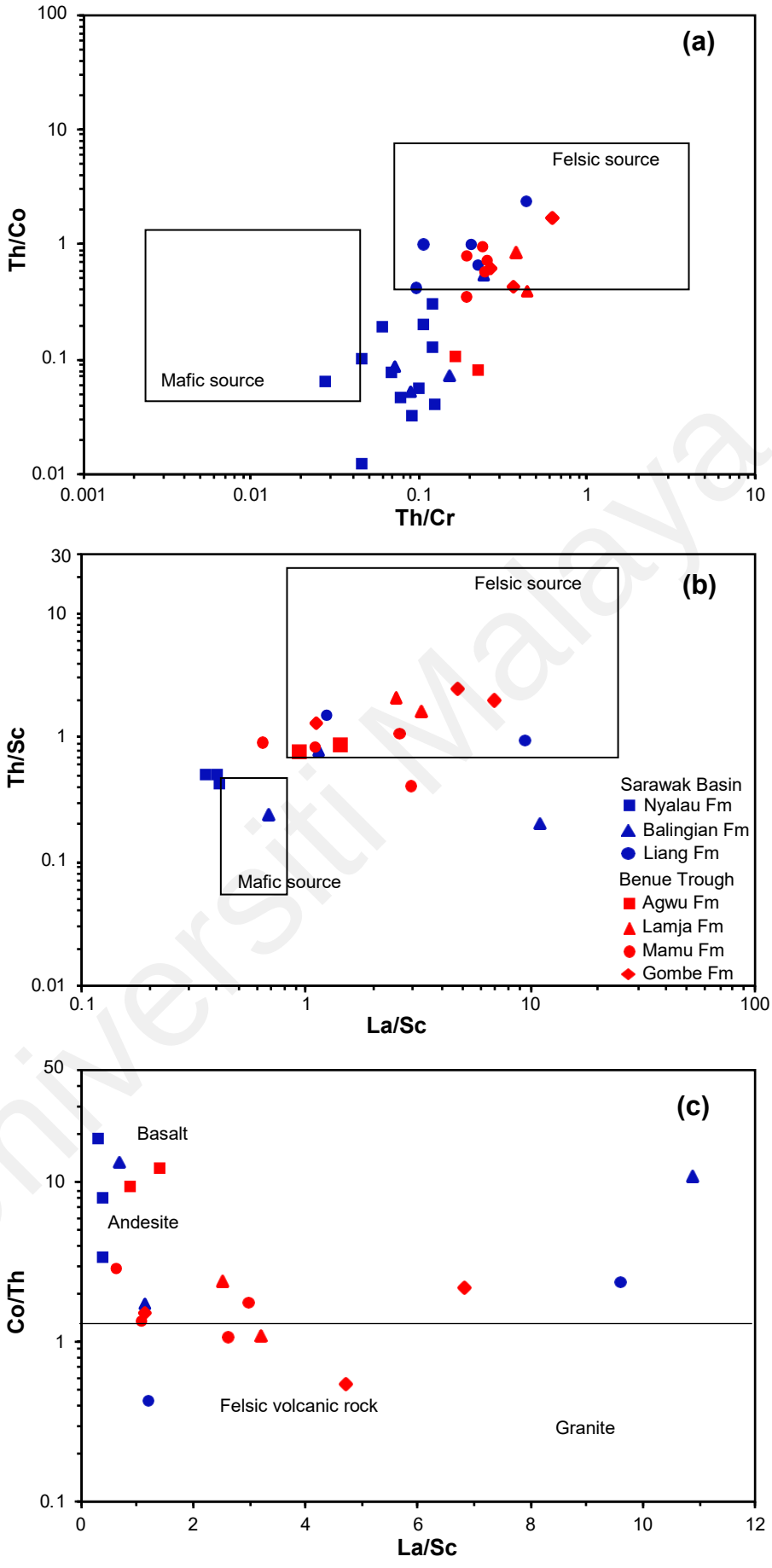

Figure 6.25: Bivariate plots of (a) – Th/Cr vs. Th/Co (after Cullers, 2000), (b) – La/Sc vs. Th/Sc, and (c) – La/Sc vs. Co/Th (after Wronkiewicz & Condie, 1987).

The abundance of trace elements in coals is often primarily determined by the nature of the sediment-source region (Dai et al., 2012). Overall, the various elemental parameters employed in this research generally indicate the abundance of felsic to intermediate rocks in the Benue Trough source area and mixed but dominantly mafic rocks in the Sarawak Basin source area.

6.5 Paleovegetation and Paleoclimate

The abundance of plant-derived biomarkers in sediments is mainly dependent on the original biological source input; therefore it is greatly influenced by prevailing climatic conditions during and after deposition (Jiang et al., 1998; van Aarssen et al., 2000; Hautevelle et al., 2006; Diefendorf & Freimuth, 2017). Peat-forming plants, generally, grow in warm and humid climates, while arid climates are unfavourable for their growth (Ortiz et al., 2013). In addition, other factors such as seasonality, proximity to the coast and soil conditions also influence vegetation type. Hence, plant macrofossils are veritable proxies to reconstruct paleovegetation and consequently, paleoclimate. A summary of biomarker proxies for the reconstruction of past vegetation, environment and climate is provided by Naafs et al. (2019).

6.5.1 Bulk Isotopes

The carbon isotopic composition of plants is widely used to differentiate between C_3 and C_4 land plants (Meyers, 1994; Meyers, 1997; Bi et al., 2005; Diefendorf & Freimuth, 2017). C_4 plants are isotopically heavier than C_3 plants with mean $\delta^{13}C$ mean bulk values of -13‰ and -25‰, respectively (Stein, 1991). The bulk $\delta^{13}C$ values (-

29.4‰ to -24.2‰) for the studied coals signify a C_3 vegetation origin (Figure 6.26). Furthermore, stable carbon signatures are a proven indicator of plant groups (i.e. angiosperms and gymnosperms). Plant wax derived from angiosperms are isotopically lighter than those sourced from gymnosperm vegetation (Diefendorf et al., 2011) and in coals, $\delta^{13}C$ values are strongly correlated with the proportion of plant groups (Lücke et al., 1999; Widodo et al., 2009; Radhwani et al., 2018). According to Lücke et al. (1999), mean $\delta^{13}C$ values for fossil wood fragments from angiosperms (-26.0‰) and gymnosperms (-23.3‰) in the Garzweiler seam, Lower Rhine Embayment, Germany indicate a 2.8‰ isotopic offset between angiosperms and gymnosperms. The angiosperms-dominated Miocene Embalut lignite and sub-bituminous samples from Kutai Basin, Indonesia show $\delta^{13}C$ values between -28.0‰ and -27.0‰ (Widodo et al., 2009) while the gymnosperm-dominated Miocene lignite deposits from Zillingdorf deposit, Austria show $\delta^{13}C$ values between -27.2‰ and -24.6‰ (Bechtel et al., 2007).

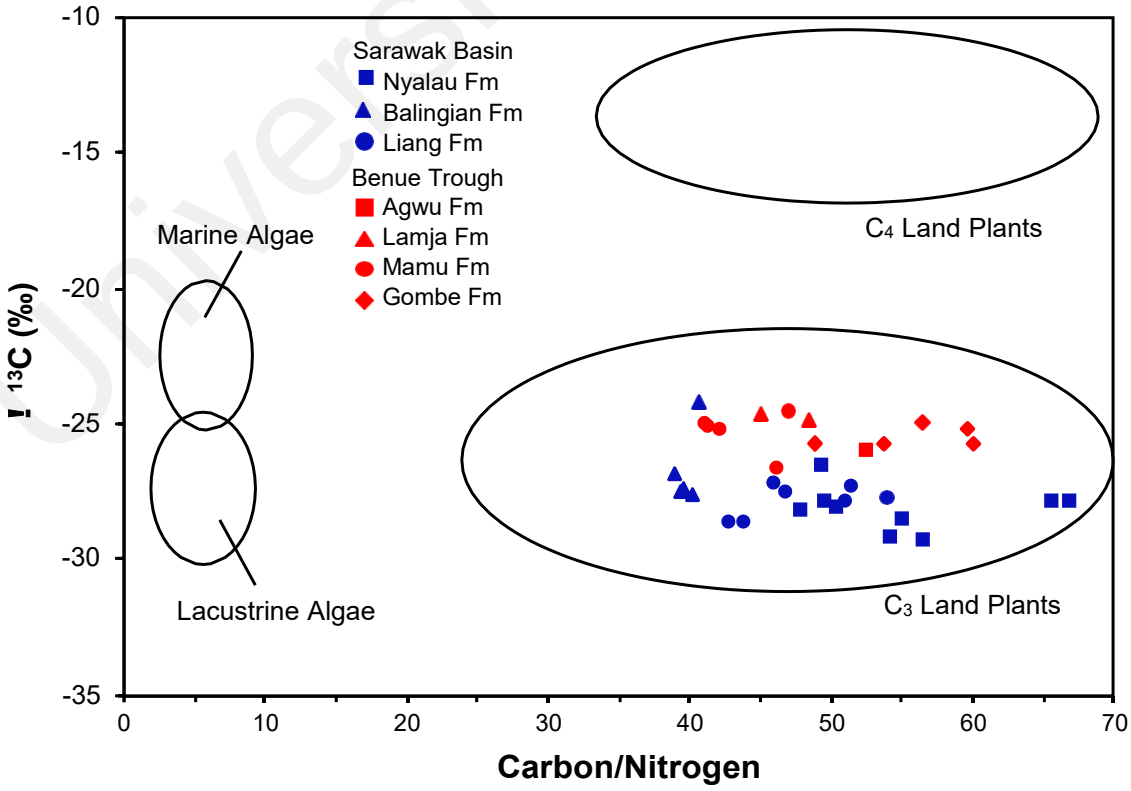

Figure 6.26: Source input diagram of atomic ratio vs. bulk carbon isotopic value (after Meyers, 1994).

The $\delta^{13}C$ values for the Tertiary coals from Sarawak Basin, Malaysia vary between -29.4‰ and -24.2‰ with a mean of -27.8‰. $\delta^{13}C$ values for the Tertiary coals are lower than -26.5‰ except in one sample (MK2) with an anomalous value of -24.2‰ (Table 5.11). In contrast, $\delta^{13}C$ values for the Late Cretaceous coals from Benue Trough, Nigeria fluctuate between -26.8‰ and -24.7‰ with a mean of -25.4‰. The Sarawak Basin coals are generally isotopically lighter than coals from the Benue Trough with a mean isotopic offset of 2.4‰. The studied coals from both basins are mostly of similar lignite to sub-bituminous rank, the varying carbon isotopic composition cannot be explained by thermal maturity. Additionally, the coals are of different ages and from different localities; therefore, the varying isotopic composition can be adduced to varying climatic and environmental conditions, and their influence on plant physiology (Bechtel et al., 2008). These details all imply that the peat-forming vegetation of the Sarawak Basin and Benue Trough areas is considered to be generally dominated by angiosperm and gymnosperm taxa, respectively. This is also supported by the reported $\delta^{13}C$ values of recent higher plants (Smith & Epstein, 1971). Gymnosperm plants such as Araucariaceae (-25.9‰), Ginkgoaceae (-25.6‰), and Taxodiaceae (-25.4‰) show relatively higher values.

This interpretation is supported by the predominant presence of diterpenoids in the Benue Trough coals and their low abundance to near absence in the Sarawak Basin coals (Figure 5.19). The distribution of diterpenoids in coals implies a dominant angiosperm and conifer contribution to the paleovegetation of the Sarawak Basin and Benue Trough, respectively. Furthermore, this interpretation is corroborated by the positive relationships between $\delta^{13}C$ values and angiosperm-gymnosperm parameters for the studied coals (Figure 6.27). The AGI ($R^2 = 0.576$) and di-/tri-terpenoid ($R^2 = 0.620$) proxies are moderately and positively correlated with $\delta^{13}C$ while the al-AGI' parameter is strongly and positively correlated ($R^2 = 0.720$).

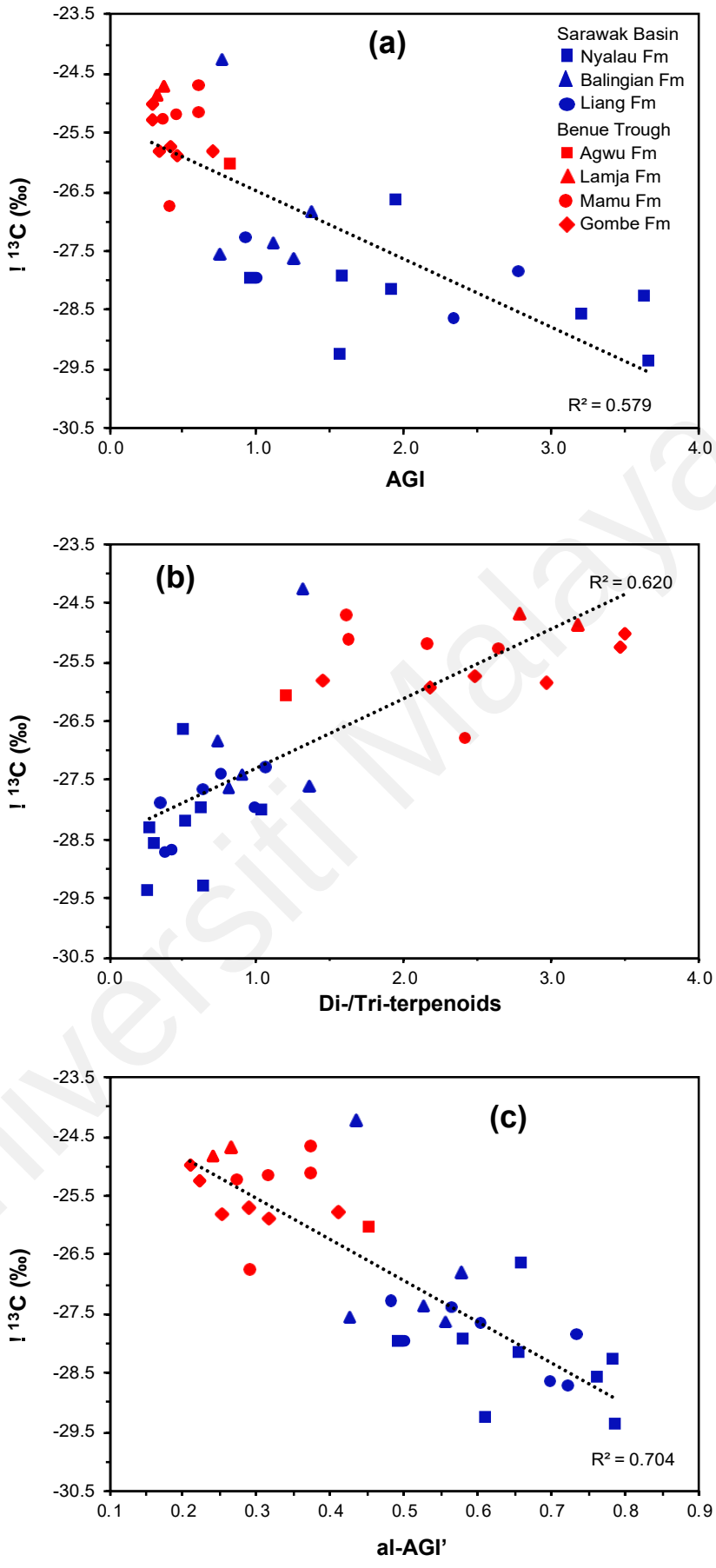

Figure 6.27: Plots showing the relationship between bulk carbon isotopic ratios ($\delta^{13}C$) and (a) – angiosperm/gymnosperm index (AGI), (b) – di-/tri-terpenoid ratios, and (c) – aliphatic angiosperm/gymnosperm index (al-AGI').

Similarly, the stable hydrogen isotopic composition of plants and sediments has been employed as a proxy for reconstructing paleoflora and past environmental conditions such as precipitation, temperature and humidity (Dawson et al., 2004; Schimmelmann et al., 2004; Bi et al., 2005; Hou et al., 2007; Duan & Xu, 2012; Duan et al., 2014). For instance, terrestrial plants have been shown to produce *n*-alkanes that are isotopically heavier than aquatic plants whilst woody plants are isotopically heavier than herbaceous plants mainly due to the different source water δD values (Sachse et al., 2006; Duan & Xu, 2012). Additionally, sediments from low-latitude locations and under humid climates are relatively enriched in deuterium than sediments deposited under glacial conditions in high-latitude areas (Dawson et al., 2004). The δD values of meteoric water reportedly have also been shown to depend on temperature, length of moisture transport and amount of moisture. However, the amount of moisture is the most important control on δD values in tropical latitudes (Randlett et al., 2017). Furthermore, δD values have been shown to mainly reflect continental rainfall fluctuations and, relatively negative δD values reportedly indicate wetter conditions (Schefuß et al. 2005; Sachse et al., 2012).

Paleogeographical and paleoclimatic reconstruction studies have established that both the Benue Trough and Sarawak Basin were located within the tropical region and under humid climate during the Late Cretaceous and Cenozoic, respectively (Hay & Floegel, 2012; Friederich et al., 2016). In addition, the studied coals are dominated by C_3 land plants; hence, the observed varying hydrogen isotopic composition can be attributed to past hydrological conditions. The δD values of the coals are generally higher for the Benue Trough samples (-117‰ to -66.4‰) than for the Sarawak Basin samples (-173.5‰ to -91‰), which imply relatively wetter conditions during the accumulation of the Sarawak peats in the Miocene and Pliocene. However, some of the Sarawak Basin coals, particularly the Liang Formation samples, have δD values

comparable to those from Benue trough coals, which are suggestive of frequent dry episodes in the Pliocene (Figure 6.28).

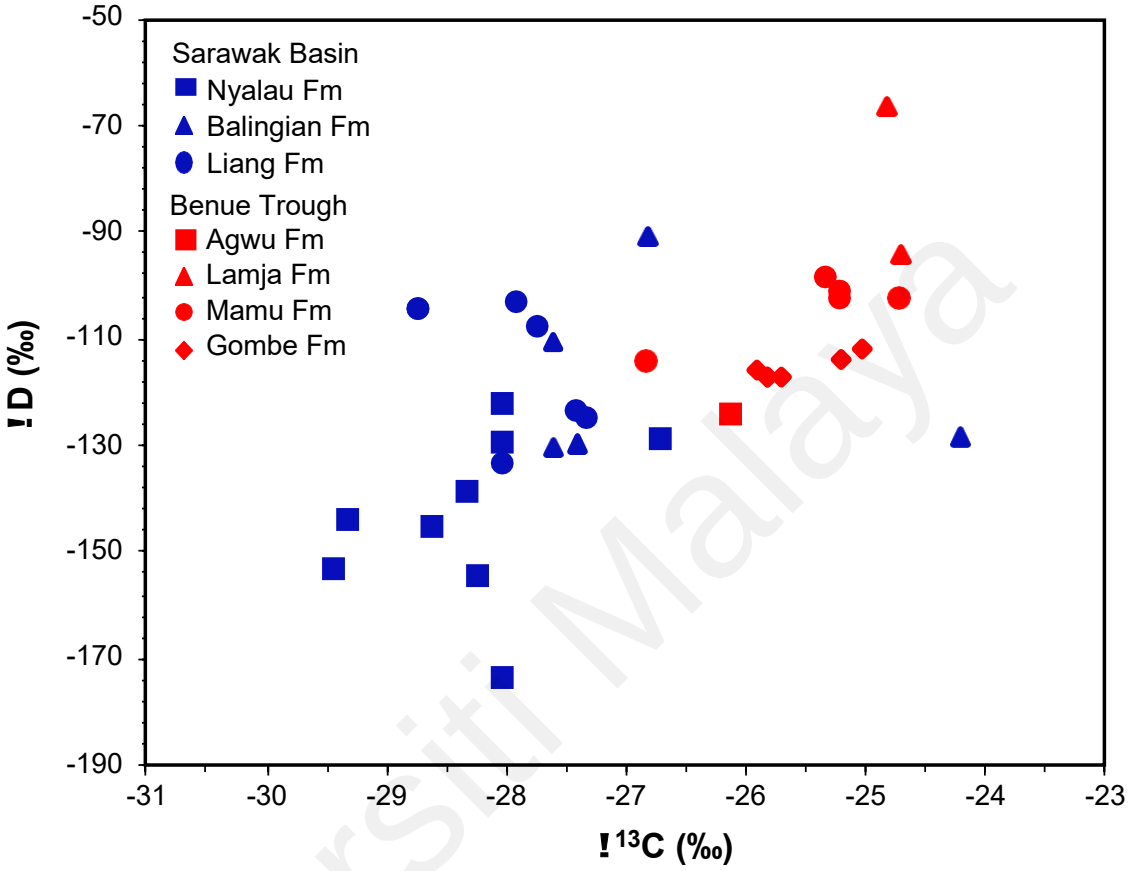

Figure 6.28: Bulk carbon and hydrogen isotopic ratios of the studied coals.

Additionally, bulk δD values varied widely within the Sarawak Basin as coals of the Early Miocene Balingian (avg. -117.9‰) and Nyalau (avg. -143.4‰) formations show generally distinct values. This is possibly due to the different distances of the coal seams from the ocean as the Merit-Pila coalfield is further inland (Figure 3.1). According to Dawson et al. (2004), meteoric water becomes increasingly depleted in deuterium with increasing distance from the ocean due to the 'raining out' of heavier isotopes.

6.5.2 *n*-Alkanes

Leaf waxes from *Sphagnum* mosses and terrestrial higher plants are correspondingly dominated by medium MW (C_{23} and C_{25}) and high MW (> C_{27}) *n*-alkanes (Baas et al., 2000; Ficken et al., 2000; Nott et al., 2000; Bush & McInerney, 2013). In addition, *Sphagnum* mosses and terrestrial higher plants prevail under wetter and drier bog conditions, respectively. Hence, given the abundance of *n*-alkanes and rapidity of GC-MS analysis, various studies have applied *n*-alkane proxies such as P_{wax}, P_{aq}, and average chain length (ACL) to reconstruct past hydrology and accordingly, the vegetation and climate of peatlands (Nichols et al., 2006; Zheng et al., 2007; Bingham et al., 2010; Andersson et al., 2011). The use of these proxies is based on the established control of hydrology on peatland vegetation and peat decomposition rates (McCabe, 1987; Moore, 1987; Diessel, 1992).

The distribution of high MW *n*-alkanes is also an indicator of the diagenetic process and paleoenvironment conditions. Maximum abundances of *n*-C_{27}, *n*-C_{29}, and *n*-C_{31} are reportedly suggestive of predominant contributions of deciduous trees, conifers, and grasses, respectively. Hence, the relative abundances of *n*-C_{27}, *n*-C_{29}, and *n*-C_{31} relative to their summed abundances are often used to distinguish the type and changes in land plant inputs (Schwark et al., 2002; Ortiz et al., 2013). The ternary plot of the relative abundances of C_{27}, C_{29}, and C_{31} *n*-alkanes is shown in Figure 6.29. The Sarawak Basin and Benue Trough samples mostly show maximum abundances at *n*-C_{31} and *n*-C_{29}, which are respectively indicative of predominant contributions of herbaceous and coniferous vegetation to peat formation (Ortiz et al., 2013).

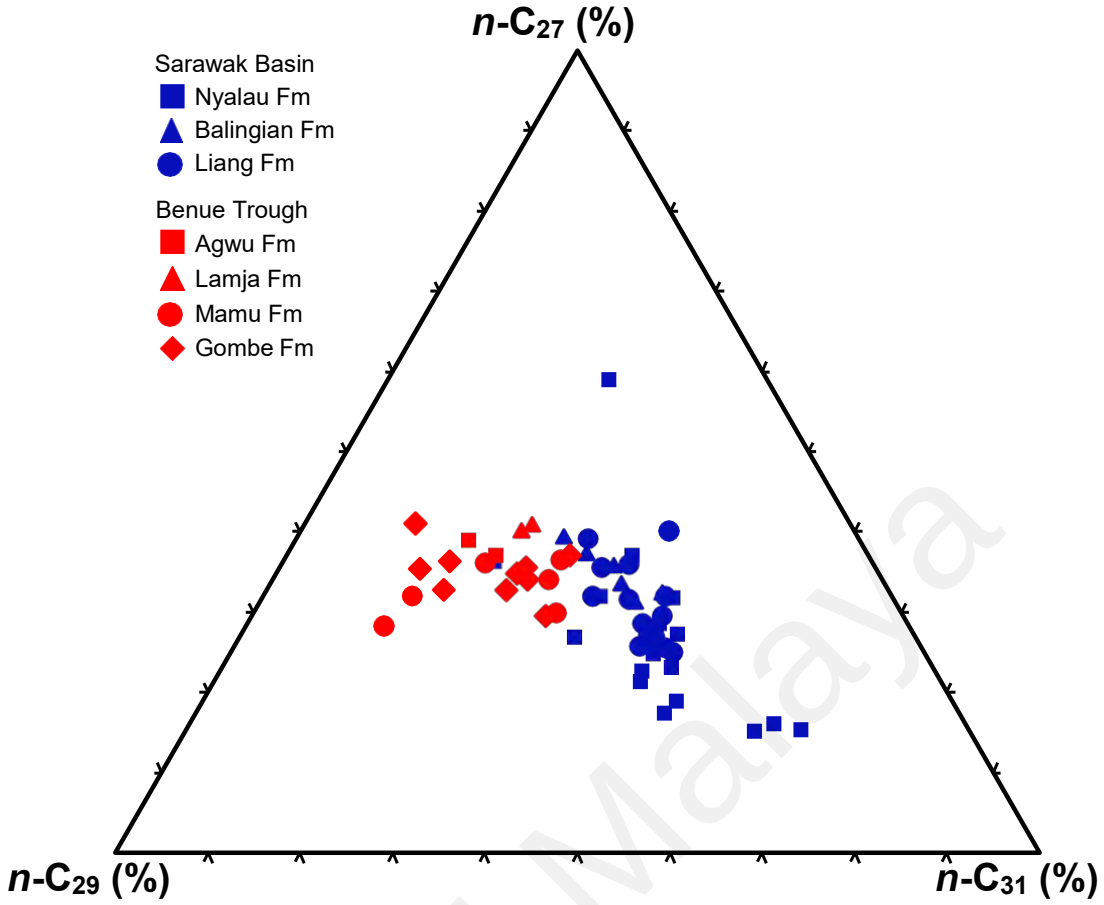

Figure 6.29: Ternary diagram of relative abundances of *n*-C_{27}, *n*-C_{29}, and *n*-C_{31} alkanes in the coals.

The *n*-C_{27}/*n*-C_{31} ratio is also widely used to estimate the contribution of woody versus herbaceous inputs to paleovegetation (Schwark et al., 2002; López-Días et al., 2013). The *n*-C_{27}/*n*-C_{31} ratios indicate a much higher proportion of woody vegetation in the Benue Trough (0.91-3.42) than in the Sarawak Basin (0.23-2.47). Similarly, the (C_{27} + C_{29})/(C_{23} + C_{25} + C_{27} + C_{29} + C_{31} + C_{33}) *n*-alkane ratio was developed by Hanisch et al. (2003) to measure the contribution of deciduous trees to paleovegetation. The *n*-alkane ratios of the studied Sarawak Basins coals (0.22-0.57) are lower than in the Benue Trough (0.41-0.75). These values indicate a higher abundance of deciduous trees and conifers in the Benue Trough areas, which is consistent with a cool and humid climate in the Late Cretaceous (Schwark et al., 2002; Jiang et al., 2020).

The ACL measures the average length of high MW *n*-alkanes (Poynter & Eglinton, 1990). Previous studies have established that plants produce higher MW *n*-alkanes in warmer climates, and that non-woody plants produce leaf wax with longer ACL values than woody plants (Rommerskirchen et al., 2006). However, a few studies have noted that ACL is more influenced by precipitation than temperature or vegetation type (Schefuß et al., 2003; Sachse et al., 2006). ACL values > 27 are reportedly indicative of emergent macrophytes and terrestrial plants input (Duan & Xu, 2012; Diefendorf & Freimuth, 2017) and values generally increase under warmer and drier conditions (Andersson et al., 2011; Silva et al., 2012; Bush & McInerney, 2015). Given these conflicting results, Hoffmann et al. (2013) recommend obtaining information on past vegetation structures before employing ACL as a proxy for paleoclimatic conditions.

ACL values for the Sarawak Basin and Benue Trough coals vary from 28.3 to 30.0 (avg. 29.3) and 28.4 to 29.1 (avg. 28.8), respectively. The higher ACL values for the Malaysian samples suggest peat accumulation under relatively warmer climatic conditions. For all the studied coals, the ACL parameter shows a strong, positive correlation with $\%C_{31}$ ($r = 0.953$) but a strong, negative correlation with $\%C_{27}$ ($r = -0.865$) and a moderate, negative correlation with $\%C_{29}$ ($r = -0.575$). The strong correlations with the $\%C_{27}$ and $\%C_{29}$ parameters, which are proxies for woody and herbaceous vegetation, therefore validate the established influence of vegetation type on ACL values (Table 6.1). Furthermore, the δD values of leaf waxes reportedly generally decrease with increasing ACL values (Duan & Xu, 2012; Duan et al. 2014). The moderate, negative correlation ($r = -0.519$) between ACL and δD values of the studied coals supports this finding (Figure 6.30).

Table 6.1: Pearson's correlation coefficients of *n*-alkane and isotopic parameters for the studied coals.

Variable	TOC	HI	$\delta^{13}C$	δD	C/N	CPI	TAR	ACL	P_{aq}	P_{wax}	$\%C_{27}$	$\%C_{29}$	$\%C_{31}$	$C_{23}/(C_{27}+C_{31})$	C_{23}/C_{29}
TOC	1.000														
HI	-0.038	1.000													
$\delta^{13}C$	0.012	0.662	1.000												
δD	-0.374	0.617	0.566	1.000											
C/N	0.148	-0.419	-0.195	-0.465	1.000										
CPI	-0.114	-0.528	-0.192	-0.06	0.053	1.000									
TAR	-0.152	-0.706	-0.469	-0.136	0.209	0.762	1.000								
ACL	0.248	-0.615	-0.544	-0.519	0.365	0.297	0.466	1.000							
P_{aq}	-0.222	0.519	0.221	0.195	-0.101	-0.733	-0.617	-0.584	1.000						
P_{wax}	0.182	-0.514	-0.203	-0.167	0.066	0.761	0.613	0.503	-0.99	1.000					
$\%C_{27}$	-0.350	0.479	0.284	0.396	-0.372	-0.355	-0.428	-0.865	0.739	-0.647	1.000				
$\%C_{29}$	0.084	0.429	0.595	0.422	-0.146	-0.006	-0.205	-0.575	-0.056	0.068	0.093	1.000			
$\%C_{31}$	0.160	-0.616	-0.612	-0.554	0.336	0.222	0.413	0.953	-0.413	0.347	-0.682	-0.792	1.000		
$C_{23}/(C_{27}+C_{31})$	-0.026	0.637	0.387	0.369	-0.18	-0.777	-0.663	-0.44	0.823	-0.857	0.478	0.101	-0.368	1.000	
C_{23}/C_{29}	-0.165	0.420	0.087	0.147	-0.181	-0.684	-0.488	-0.361	0.874	-0.877	0.619	-0.294	-0.164	0.825	1.000

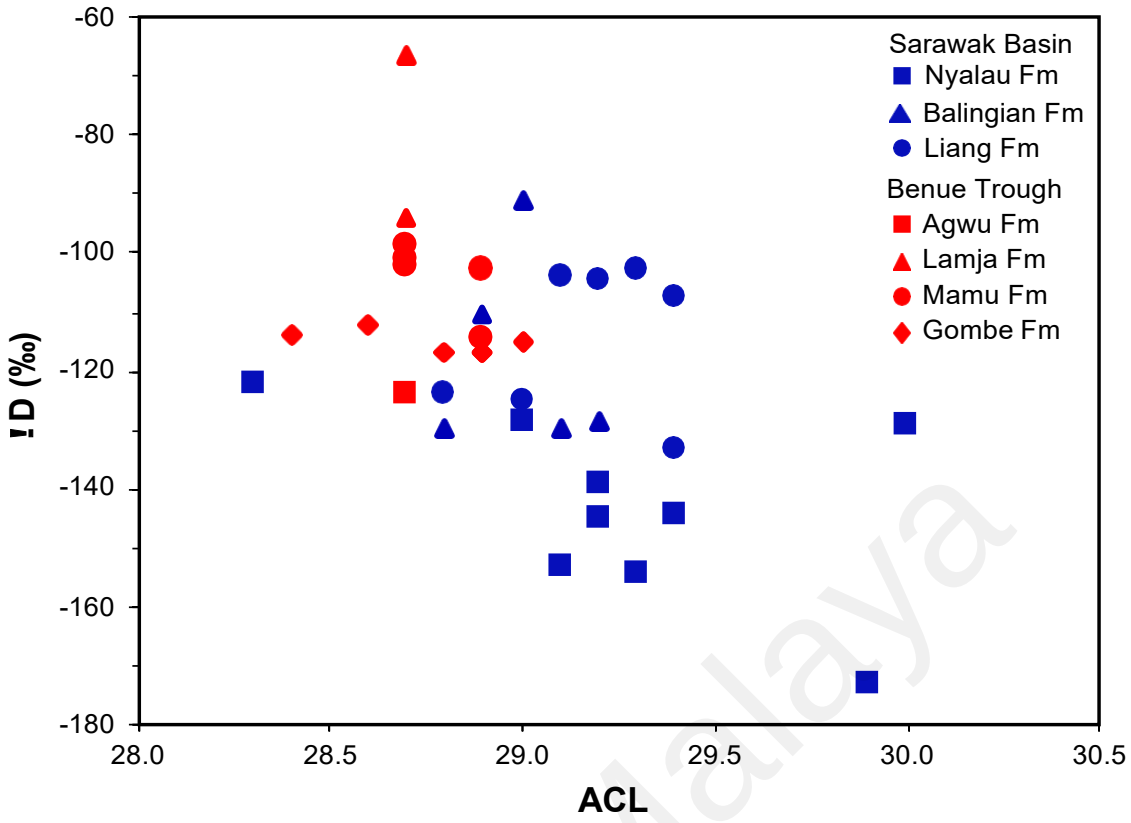

Figure 6.30: Cross-plot of *n*-alkane average chain length (ACL) and hydrogen isotopic ratios of the studied coals.

The P_{aq} parameter was proposed by Ficken et al. (2000) to measure the abundance of non-emergent aquatic plants relative to emergent aquatic and terrestrial plants. Values < 0.1 and > 0.4 characterise the predominant abundance of terrestrial plants and non-emergent aquatic plants, respectively, while values between 0.1 and 0.4 signify mixed input of terrestrial plants and aquatic macrophytes. The P_{aq} values for the Sarawak Basin and Benue Trough coals vary over the 0.12-0.69 (avg. 0.28) and 0.12-0.56 (avg. 0.33) range, respectively. The values generally indicate a mixed input of terrestrial plants and aquatic macrophytes for the studied coals. Furthermore, Zheng et al. (2007) introduced the P_{wax} parameter to determine the relative proportion of waxy hydrocarbons derived from emergent aquatic and terrestrial plants. The calculated P_{wax} values, which are similar for Sarawak Basin (0.52-0.91) and Benue Trough (0.56-0.91) coals, are mostly > 0.7 with mean values of 0.79 and 0.75, respectively (Figure 6.31).

These values indicate the predominant input of terrestrial plants under relatively lower water levels (Zheng et al., 2007).

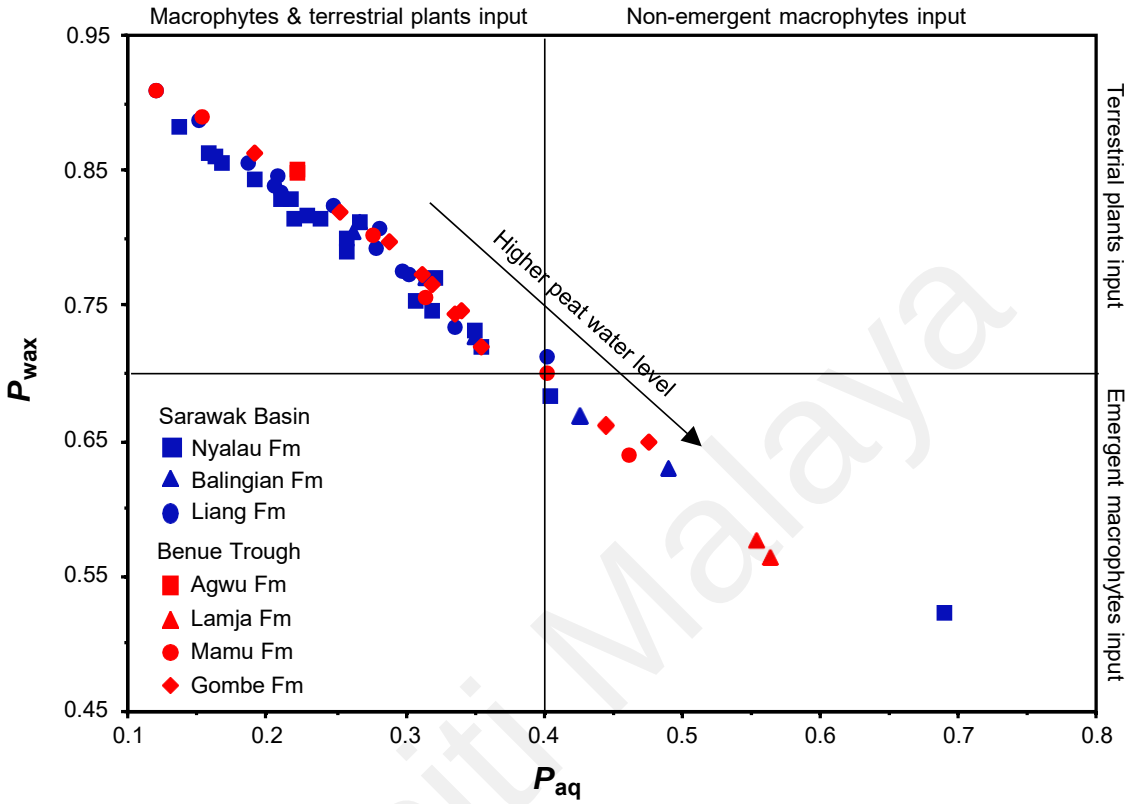

Figure 6.31: Cross-plot of *n*-alkane proxies P_{aq} and P_{wax}, showing paleovegetation.

The *n*-C_{23}/*n*-C_{29} and *n*-C_{23}/*n*-C_{31} ratios measure the relative contribution of *Sphagnum* and vascular plants to peat formation (Nichols et al., 2006). Except for a few samples, values of the *n*-C_{23}/*n*-C_{29} ratio are < 1, with similar average values of 0.34 and 0.35 for the Sarawak Basin and Benue Trough coals, respectively (Tables 5.15-5.16). Similarly, values of the *n*-C_{23}/*n*-C_{31} ratio are mostly < 1, with average values of 0.24 and 0.55 for the Malaysian and Nigerian coals, respectively. Values of both ratios suggest a relatively higher contribution of *Sphagnum* to the Benue Trough paleo-peats, which signifies higher water table levels and thus, relatively wetter mire conditions possibly due to rising sea levels. However, *n*-C_{23} can supposedly be derived from both

aquatic macrophytes and terrestrial plants (Sachse et al., 2006). Hence, the *n*-C_{23}/*n*-C_{29} ratio can be misleading when *Betula* and *Sphagnum fuscum* are abundant in the paleopeat (Andersson et al., 2011). Consequently, Andersson et al. (2011) proposed the $C_{23}/(C_{27} + C_{31})$ *n*-alkane parameter to improve interpretations of the *n*-C_{23}/*n*-C_{29} proxy by more accurately reconstructing past water table levels in peat deposits. According to He et al. (2019), *n*-C_{23}/(*n*-C_{27} + *n*-C_{31}) ratios > 0.2 are indicative of a significant contribution of *Sphagnum* in wetter habitats. The $C_{23}/(C_{27} + C_{31})$ *n*-alkane ratios for the Sarawak Basin and Benue Trough coals vary correspondingly from 0.05 to 0.39 (avg. 0.13) and 0.09 to0.59 (avg. 0.22). In general, the higher average ratio for the Benue Trough coals corroborates the interpretation of the higher contribution of *Sphagnum* to paleovegetation and higher water levels in the Benue Trough paleopeats (Figure 6.32).

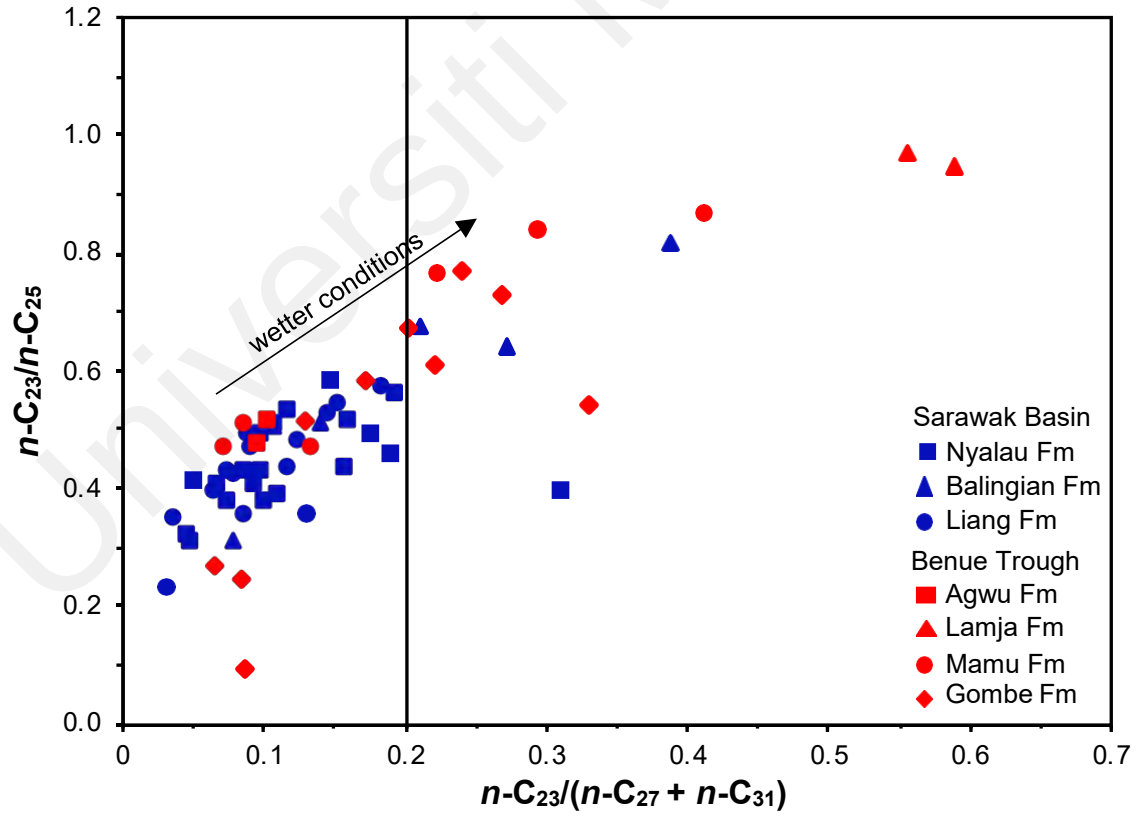

Figure 6.32: Cross-plot of *n*-alkane paleohydrology proxies.

The *n*-C_{23}/*n*-C_{25} ratio is another paleohydrological proxy that was proposed by Bingham et al. (2010). This parameter measures the relative abundance of *Sphagnum* species derived from wetter and drier microhabitats in ombrotrophic peat bogs. The workers concluded that higher ratios indicate higher input of C_{23}-dominated *Sphagnum* species in wetter conditions. *n*-C_{23}/*n*-C_{25} ratios for all the studied coals are less than 1.0, thus indicating predominant input of C_{25}-dominated species under drier peatland conditions. However, the ratios are relatively higher for the Benue Trough coals (0.09-0.97) than the Sarawak Basin coals (0.23-0.82). The cross plot of $C_{23}/(C_{27} + C_{31})$ and C_{23}/C_{25} *n*-alkane ratios generally indicates relatively wetter conditions in the Benue Trough peatlands during the Late Cretaceous (Figure 6.32).

Overall, *n*-C_{23}/*n*-C_{31}, *n*-C_{23}/(*n*-C_{27} + *n*-C_{31}), *n*-C_{27}/*n*-C_{31}, and P_{aq} ratios of the investigated Sarawak Basin coals are generally highest for the Balingian Formation, and lowest for the Liang Formation. These ratios suggest relatively lower and higher water levels for paleopeats of the Liang and Balingian Formations, respectively. In addition, the widely varying ratios observed for Nyalau Formation imply intermittent low-high water table levels during the accumulation of the Merit-Pila paleopeat. When compared with Sarawak Basin, the *n*-alkane proxies mostly signify relatively higher water levels in the Benue Trough paleopeats. However, the lower ratios for the Agwu and Gombe Formations indicate relatively lower water table levels.

6.5.3 Land Plants-derived Biomarkers

Aromatic hydrocarbon parameters such as plant fingerprint (PF), higher plant parameter (HPP), higher plant input (HPI) and the modified higher plant input (mHPI) have been employed to evaluate the contribution of land-derived higher plants (van

Aarssen et al., 2000; Cesar & Grice, 2019; Zakrzewski et al., 2020), using the relative distribution of retene, cadalene, *ip*-iHMN and 1,3,6,7-TeMN (Tables 5.27-5.28). Retene, cadalene and *ip*-iHMN are higher plant biomarkers, while 1,3,6,7-TeMN is mostly derived from microbial action and is abundant in both marine and terrestrial sediments (Jiang et al., 1998; van Aarssen et al., 1999). Hence, the abundances of retene and cadalene relative to that of 1,3,6,7-TeMN are indicators of land-plant input. Retene/1,3,6,7-TeMN and cadalene/1,3,6,7-TeMN ratios for the analysed samples are relatively higher for the Sarawak Basin coals, indicating a greater contribution of organic matter from terrigenous land plants (Figure 6.33).

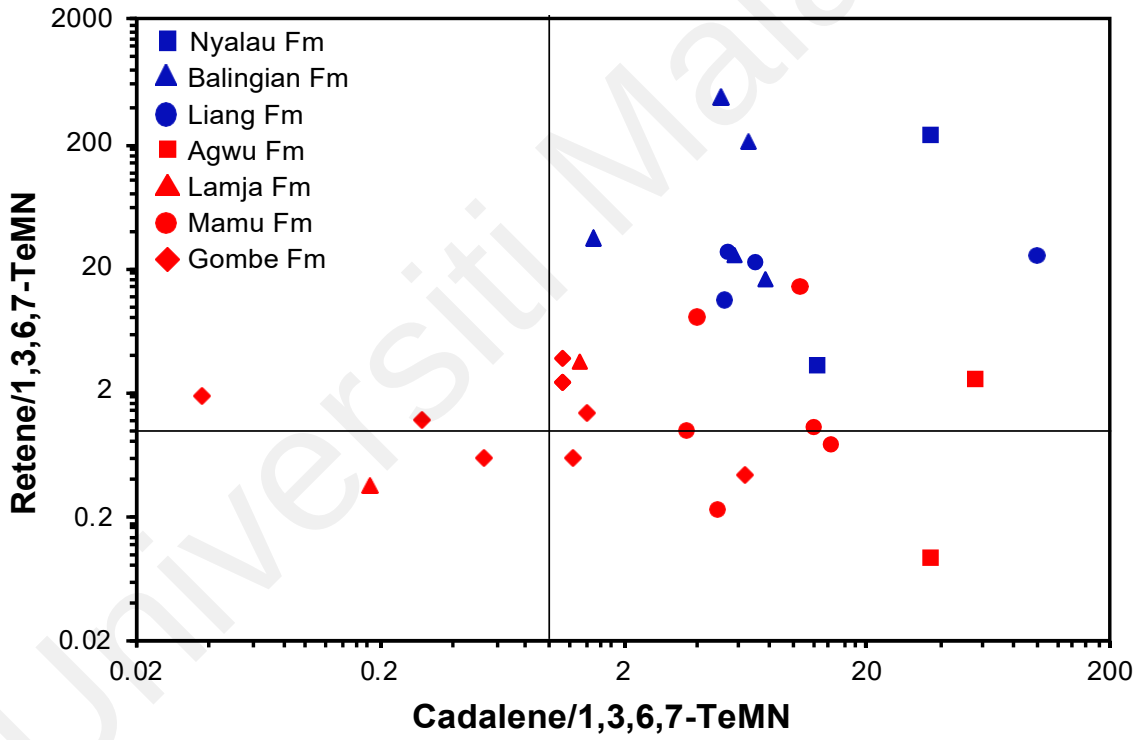

Figure 6.33: Cross-plot of cadalene/1,3,6,7-TeMN vs. retene/1,3,6,7-TeMN ratios for the analysed coals.

The HPI is applied to evaluate the contribution of land plants to organic matter. The index is calculated from the formula (retene + cadalene + *ip*-iHMN)/1,3,6,7-TeMN. HPI values of all samples are > 1, except in sample CKL, varying significantly from 4.4 to 463.8 (avg. 58.0) and 0.7 to 61.0 (avg. 10.9) for the Sarawak Basin and Benue Trough

coals, respectively. The generally high HPI values indicate the predominant input of land plants to organic matter. However, the relatively lower HPI values for the Lamja (avg. 3.6) and Gombe (avg. 3.6) Formation coals imply a significant contribution of marine algae to organic matter. Additionally, the relatively higher HPI values for the Sarawak Basin coals corroborate earlier interpretations of the greater contribution of terrigenous organic matter. Furthermore, the modified HPI (mHPI) proposed by Zakrzewski et al. (2020) and which is calculated from (retene + cadalene + *ip*-iHMN)/(retene + cadalene + *ip*-iHMN + 1,3,6,7-TeMN) ranges from 0.81 to 1.00 (avg. 0.94) and 0.40 to 0.98 (avg. 0.79) for the Sarawak Basin and Benue Trough, respectively. The mHPI values are indicative of the dominant proportion of higher plant-derived terrigenous organic matter. Also, the relatively higher mHPI values for the Sarawak Basin coals again corroborate the finding of greater contribution of land plants to organic matter.

Previous studies have found that higher plants that adapt to humid and arid climates are accordingly the main sources of retene and cadalene (Hautevelle et al., 2006; Grice et al., 2015; Cesar & Grice, 2019; Xu et al. 2019). Additionally, Hautevelle et al. (2006) established that the retene/cadalene ratio is unaffected by depositional and diagenetic conditions but by climatic conditions. Hence, the retene/cadalene ratios for the Sarawak Basin and Benue Trough coals range widely from 0.2 to 91.8 (avg. 13.2) and 0.0 to 48.0 (avg. 3.8), respectively, supporting the interpretation of relatively drier conditions in the Benue Trough during the Late Cretaceous. Furthermore, the mostly low retene/cadalene ratios for the Campanian-Maastrichtian Mamu Formation and Maastrichtian Gombe Formation coals imply an increasingly relatively drier and cooler climate. This interpretation is further corroborated by studies that have reported a global cooler climate in the Maastrichtian (Linnert et al., 2014; Jiang & George, 2018; Jiang & George, 2019).

The HPP is expressed as retene/(retene + cadalene) and is often used to estimate the proportion of conifer relative to vascular plants (van Aarssen et al., 2000). However, recent studies have highlighted two limitations of the HPP. First, the abundance of retene has often been associated with gymnosperm contribution to paleoflora; however, Grice et al. (2007) found no strong correlation between gymnosperm pollen and the relative abundance of retene. Second, variations in the HPP have been associated with global sea level fluctuations or aridity (van Aarssen et al., 2000). Nevertheless, a recent study by Cesar & Grice (2019) determined that the HPP cannot be applied to ascertain global climate effects. The HPP ranges between 0.14 and 0.99 and 0.00 to 0.98 for the Sarawak Basin and Benue Trough coals, respectively. For the Late Cretaceous Benue Trough, the HPP decreases from Coniacian-Santonian to Campanian and then increases in the Maastrichtian, showing a similar trend to the published global sea level curve. Global climate studies on the Late Cretaceous established the warmest conditions in the Cenomanian-Turonian after which declining atmospheric pCO_2 levels resulted in sea level fall and major climate cooling from the Late Turonian to Maastrichtian (Ladant et al., 2020; Linnert et al., 2018). However, the earliest Campanian was warm but the climate further cooled by ca. 7 °C over the Campanian-Maastrichtian period (Linnert et al., 2014; DeConto et al., 1999). This Maastrichtian cooling event was characterised by high detrital influx, higher $\delta^{13}C$ values, high but reducing $\delta^{18}O$ values, and low Sr/Ca ratios (Stüben et al., 2003). For the Tertiary Sarawak Basin, the HPP generally decreases from the Miocene to the Pliocene, thus implying increasingly drier conditions (Cesar & Grice, 2019).

Similarly, the PF compares the relative abundances of retene, cadalene and *ip*-iHMN. The Benue Trough coals are generally characterised by high abundances of retene (0-99%) and cadalene (2-100%) while *ip*-iHMN is observed only in low abundance (0-20%). Coal samples of the Coniacian-Santonian Lamja Formation show a predominant

abundance of retene (avg. 56%) with a subordinate abundance of cadalene (avg. 25%) and *ip*-iHMN (avg. 19%) while the Campanian-Maastrichtian Mamu Formation samples are dominated by cadalene (avg. 74%) and retene (avg. 26%). The Maastrichtian Gombe Formation show similar abundances of retene (avg. 43%) and cadalene (avg. 49%). In the Cenozoic Sarawak Basin, cadalene predominated in the earliest Miocene as retene was mostly absent in the Nyalau Formation coals. This was perhaps due to the warm and moderately dry climate that prevailed from the Late Oligocene to the earliest Miocene (Jablonski, 2005). The Early Miocene Balingian Formation coals are, however, dominated by retene (avg. 89%) with a subordinate contribution of cadalene (avg. 10%), which coincides with the reported return of humid climate around 20 Ma (Morley, 1998; Morley, 2012). The Upper Pliocene Liang Formation coals are typified by a mostly dominant abundance of retene (avg. 59%) with a significant contribution of cadalene (avg. 41%) and the complete absence of *ip*-iHMN. This finding is supportive of the earlier interpretation of seasonal dry conditions in the Sarawak Basin during the Late Pliocene.

6.5.4 Combustion-derived Biomarkers

Combustion-derived polycyclic aromatic hydrocarbons (PAHs) are unsubstituted hydrocarbons with 3 or more rings produced by forest and peat fires that result in the incomplete burning of biomass (Jiang et al., 1998). The abundance of combustion-derived PAHs is therefore dependent on the frequency and extent of fire events, which in turn depends on climatic conditions as fire incidents occur mostly during dry periods. Volcanic activity and igneous intrusion have also been reported to produce PAHs *via* the recombination at lower temperatures of the small molecular fragments produced at abnormal heating rates (Romero-Sarmiento et al., 2011). PAHs are also often produced

via catagenetic modification (Zakir Hossain et al., 2013). However, while the thermal alteration of sediments during burial produces alkyl-substituted compounds, rapid heating due to fire or hydrothermal events accelerates the aromatization process, yielding unsubstituted PAHs.

According to H. Huang et al. (2015), the presence of combustion-derived PAHs in sediments indicates past high-temperature events and the consequent reworking of organic matter. Hence, the presence of PAHs with 5-7 rings in some of the Benue Trough coals suggests the occurrence of past fire events (Jiang et al., 1998; Zakir Hossain et al., 2013; H. Huang et al., 2015; Xu et al., 2019; Zakrzewski et al., 2020). However, Xu et al. (2019) investigated the lacustrine sediments from Bohai Bay Basin, China and concluded that the observed PAHs were diagenetically derived from algal OM origin. Furthermore, benzo[*e*]pyrene can also originate from algal and plankton sources, and perylene may be diagenetically derived by wood-degrading fungi (Grice et al., 2007; Marynowski et al., 2013; Zakrzewski et al., 2020). Nevertheless, the significant amount of inertinite maceral in the Benue Trough coals, particularly the Gombe Formation samples (Jimoh & Ojo, 2016; Ayinla et al., 2017b; Akinyemi et al., 2020; Akinyemi et al., 2022), provides evidence in support of fire events (Scott & Glasspool, 2007; Romero-Sarmiento et al., 2011) and frequent dry periods during peat accumulation.

The relative distributions of ≥ 3-ring unsubstituted PAHs in the studied coals are shown in Figure 5.26. The PAHs detected in the studied coals include phenanthrene (PHE), anthracene (A), fluorene (F), fluoranthene (Fl), pyrene (Py), benzo[*a*]anthracene (BaA), chrysene (Ch), triphenylene (TPh), benzo[*b*]fluoranthene (BbFl), benzo[*k*]fluoranthene (BkFl), benzo[*e*]pyrene (BePy), benzo[*a*]pyrene (BaPy), perylene (Per), indeno[*1,2,3-cd*]pyrene (InPy), benzo[*ghi*]perylene (BgPer) and coronene (Cor).

The PAHs are present in significant amounts in the Benue Trough samples but mostly absent or present in low amounts in the Sarawak Basin samples. The abundance of combustion-derived PAHs relative to land plants-derived aromatic biomarkers (PAHr) is expressed by the formula (phenanthrene + pyrene + fluoranthene)/(phenanthrene + pyrene + fluoranthene + cadalene + retene). The PAHr values of the studied Sarawak Basin and Benue Trough coals range broadly from 0.03 to 0.97 (avg. 0.54) and 0.11 to 0.98 (avg. 0.78), respectively. First, these values support the finding of greater amounts of combustion-derived PAHs in the Benue Trough. Within the Sarawak Basin, PAHr values are generally highest for the Pliocene Liang Formation (avg. 0.61) with relatively lower, similar values for the Miocene Nyalau (avg. 0.49) and Balingian (avg. 0.51) Formations (Table 5.27). Average PAHr values for the Late Cretaceous Benue Trough coals are highest for the Lamja Formation (0.98) and lowest for the Agwu Formation (0.22) while Gombe (0.85) and Mamu (0.79) Formations show intermediate values (Table 5.28).

Based on the difference in relative thermodynamic stability, various ratios of PAHs have been proposed to distinguish between diagenetic/catagenic/petrogenic and combustion/pyrogenic origins of PAHs in sedimentary rocks and oils (Yunker et al., 2002; H. Huang et al., 2015; Xu et al., 2019; Zakrzewski et al., 2020). The relative abundance of anthracene to phenanthrene is a widely applied parameter to distinguish the sources of PAHs. Phenanthrene predominates in all the studied samples; however, anthracene, a linearly fused 3-ring aromatic compound, was mostly absent in the Sarawak Basin coals and present in the Benue Trough coals. High abundances of anthracene with A/(A+PHE) ratios > 0.10 reportedly signify high-temperature events (H. Huang et al., 2015). The measured A/(A+PHE) ratios in the Benue Trough coals vary from 0.01 to 0.15. Average A/(A+PHE) ratios indicate petrogenic origins for the Lamja (0.07), Mamu (0.08) and Gombe (0.04) Formations, and pyrogenic origin for the

Agwu Formation (0.13). The ratio of methylphenanthrenes to phenanthrene (MP/P) is another often utilized parameter. MP/P ratios < 1.0 and > 2.0 correspondingly signify pyrogenic and petrogenic origins (Yunker et al., 2002; Xu et al., 2019). The calculated MP/P ratios vary broadly from 0.2 to 44.0 (avg. 5.5) and 0.5 to 5.2 (avg. 2.3) for the Sarawak Basin and Benue Trough coals, respectively. These ratios imply a mixed origin of pyrogenic and petrogenic sources for the PAHs in both groups of coals. However, the relatively lower ratios for the Benue Trough samples imply that more of the PAHs are derived from pyrogenic sources, thus suggesting drier paleoclimatic conditions.

The relative abundances of 4-ring PAHs are important combustion markers (Xu et al., 2019). Pyrene and fluoranthene are identified in the *m/z* 202 mass chromatograms of most of the investigated samples. Also, the abundance of fluoranthene mostly predominates that of pyrene, except in a few samples where pyrene predominates. Fl/(Fl+Py) ratios < 0.4 and > 0.5 indicate petrogenic-related and pyrogenic-related sources, respectively (Yunker et al., 2002). The Fl/(Fl+Py) ratio for the Sarawak Basin and Benue Trough coals ranges accordingly from 0.20 to 0.92 (avg. 0.64) and 0.38 to 0.86 (avg. 0.61). The ratios are mostly > 0.5, signifying a pyrogenic or combustion origin. Additionally, 4-ring PAHs, benzo[a]anthracene, chrysene and triphenylene, are detected in the *m/z* 228 mass chromatograms of the aromatic fractions. Chrysene and triphenylene coelutes, and are observed in all studied samples, while benzo[a]anthracene is present in a relatively low amount in the Sarawak Basin coals. The summed abundances of chrysene and triphenylene prevail over that of benzo[a]anthracene in all samples. Yunker et al. (2002) concluded that BaA/(BaA+Ch+TPh) ratios < 0.20 and > 0.35 implies petrogenic and pyrogenic origins, respectively. BaA/(BaA+Ch+TPh) ratios are similar for the Sarawak Basin and Benue Trough, varying respectively from 0.06 to 0.41 (avg. 0.23) and 0.09 to 0.45 (avg. 0.24).

The cross-plots of Fl/(Fl+Py) against MP/P and BaA/(BaA+Ch+TPh) ratios in Figure 6.34 indicate petrogenic to mixed sources for the PAHs.

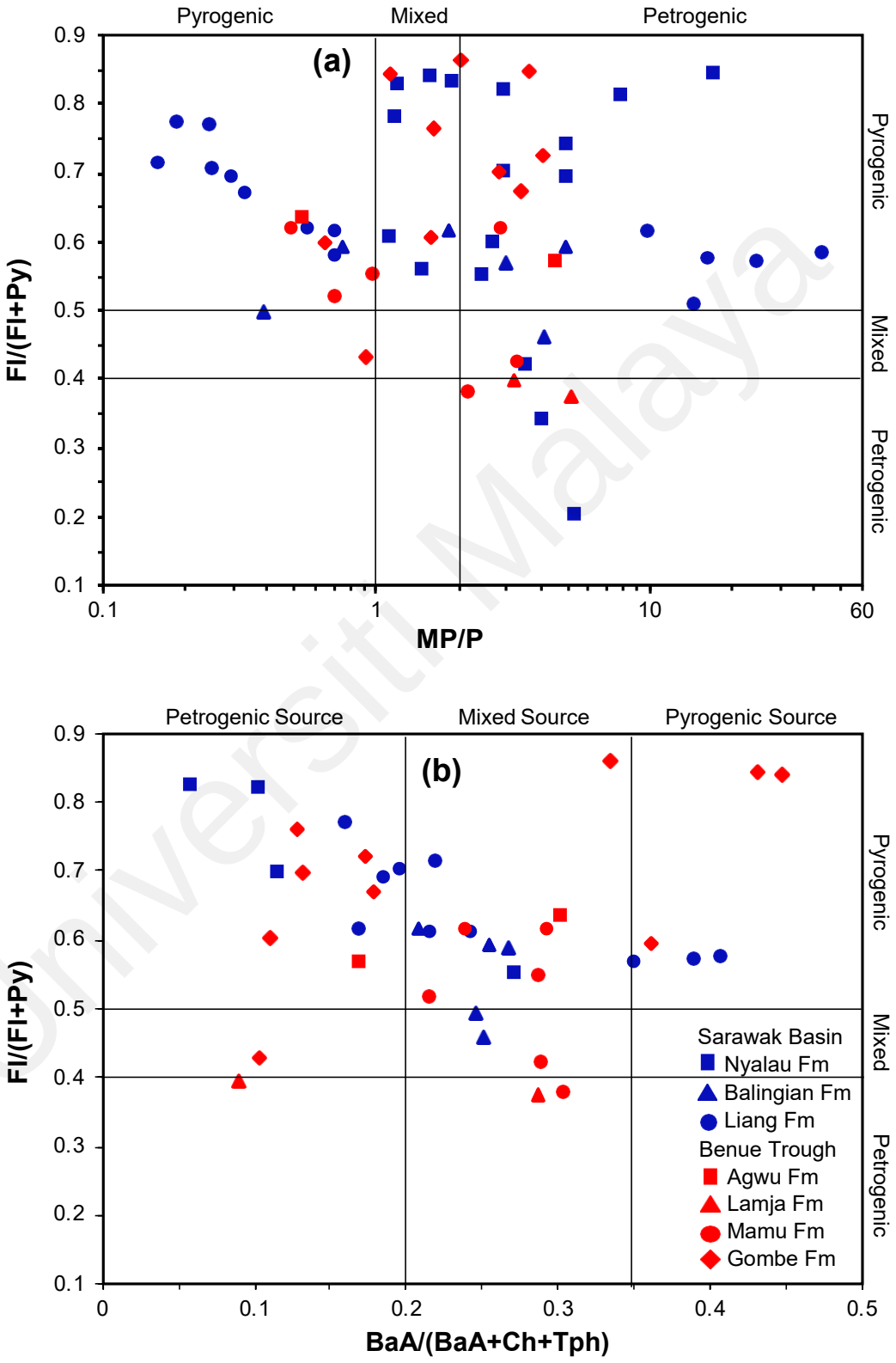

Figure 6.34: Cross-plots of MP/P versus Fl/(Fl+Py) – (a) and BaA/(BaA+Ch+Tph) versus Fl/(Fl+Py) – (b). Abbreviations are defined in Table 5.27.

The *m/z* 252 mass chromatograms show the distribution of 5-ring PAHs such as benzopyrenes, benzofluoranthenes and perylene (Figure 5.26). Whereas pyrogenic-derived PAHs can be altered by the subsequent alkylation process during catagenesis, benzopyrenes and benzofluoranthenes have been found to be less susceptible to such alteration (Jiang et al., 1998). Hence, the relative abundance of summed benzofluoranthenes over benzo[e]pyrene is an effective indicator of the origin of PAHs. The (BFl)/(BFl+BePy) values range from 0.55 to 0.78 (avg. 0.71) and 0.56 to 0.84 (avg. 0.76) for the Sarawak Basin and Benue Trough coals, respectively. According to Xu et al. (2019), values > 0.7 imply a pyrogenic or combustion origin. Hence, the calculated (BFl)/(BFl+BePy) ratios suggest a predominant combustion source. Furthermore, 6-ring PAHs such as indeno[1,2,3-cd]pyrene, benzo[ghi]perylene and coronene were observed in the *m/z* 276 and *m/z* 300 mass chromatograms of some analysed Benue Trough samples. InPy/(InPy+BgPer) ratios < 0.2 and > 0.5 indicate petrogenic and pyrogenic origins, respectively (Yunker et al., 2015). The calculated values for the Nigerian coals range from 0.15 to 0.68 with average ratios of 0.54, 0.62, 0.38, and 0.25 for the Agwu, Gombe, Mamu and Lamja formations, respectively. The coals plot mostly in the mixed to pyrogenic source zones of the cross-plot of (BFl)/(BFl+BePy) and InPy/(InPy+BgPer), indicating a mixed to pyrogenic/combustion origin (Figure 6.35a). However, the relatively lower ratios of the Lamja Formation coals imply a petrogenic source for the PAHs, and thus relatively wetter conditions during the Coniacian-Santonian.

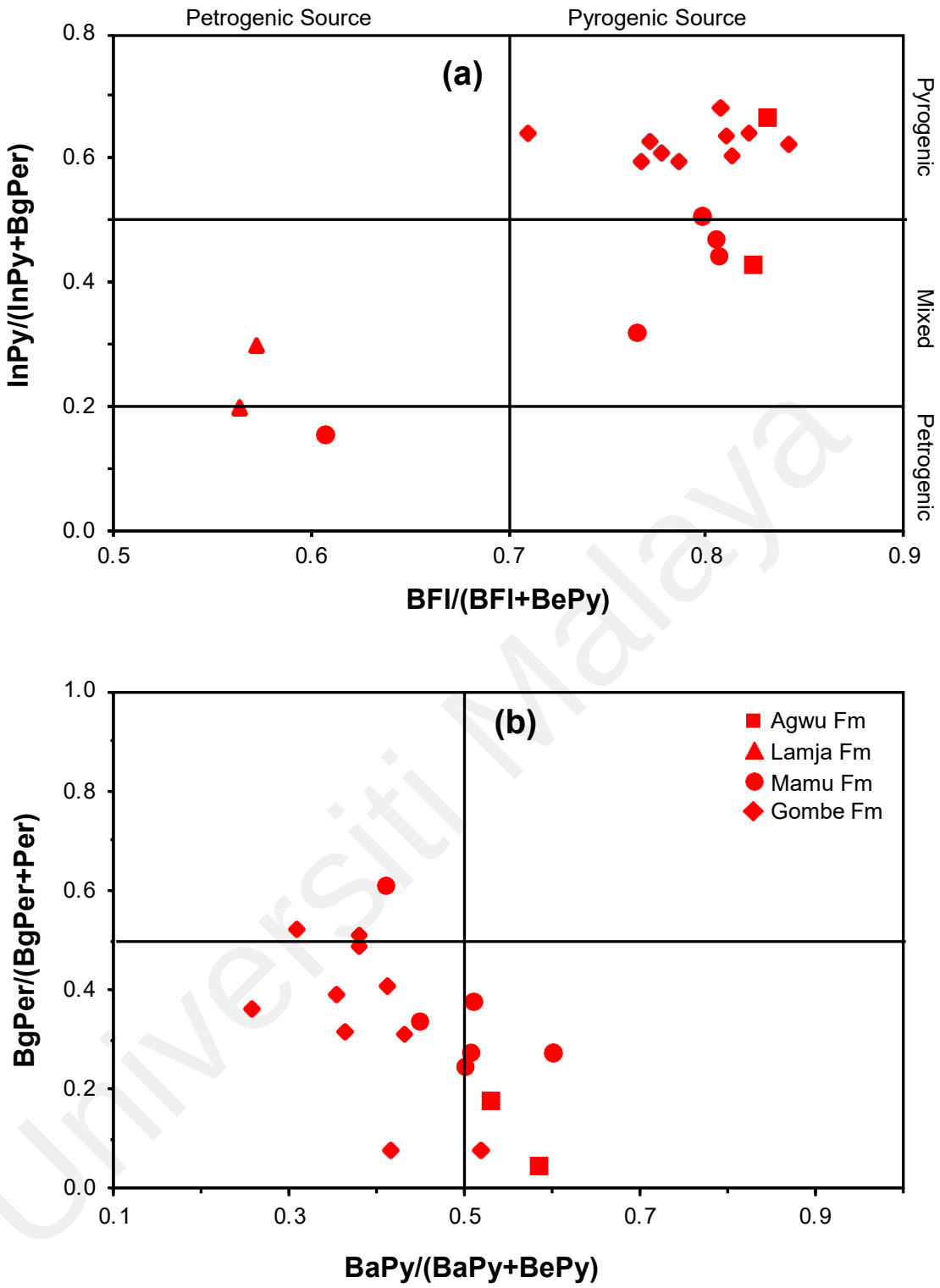

Figure 6.35: Cross-plots of (a) – (BFl)/(BFl+BePy) vs. InPy/(InPy+BgPer) ratios, and (b) – BaPy/(BaPy+BePy) vs. BgPer/(BgPer+Per) ratios, for the Benue Trough coals. Abbreviations are defined in Table 5.27.

Following work by Marynowski et al. (2015) on the thermal degradation of perylene and benzo[ghi]perylene, Zakrzewski et al. (2020) proposed the BgPer/(BgPer+Per) ratio to estimate the proportion of burnt and unburnt terrigenous OM in immature to low thermal maturity sediments. High values (> 0.5) of the ratio signify a higher proportion of charred OM and thus, pyrolytically sourced PAHs from high-temperature wildfires. The BgPer/(BgPer+Per) ratios for the Benue Trough coals range from 0.04 to 0.61 (avg. 0.32), suggesting a greater proportion of unburnt OM possibly due to either moderately intense and/or shorter-duration wildfires. In addition, Zakrzewski et al. (2020) posited that BaPy/(BaPy+BePy) values > 0.5 signify a high influence of paleofire events on deposited organic matter. The BaPy/(BaPy+BePy) values of the analysed Benue Trough coals vary from 0.19 to 0.60 with average ratios of 0.56, 0.38, 0.50 and 0.32 for the Agwu, Gombe, Mamu and Lamja Formations, respectively. The BgPer/(BgPer+Per) and BaPy/(BaPy+BePy) ratios are, together, suggestive of limited to moderate influence of high-temperature paleo-wildfires or fire events in the Benue Trough during the Late Cretaceous (Figure 6.35b).

These findings are all corroborated by the absence, or presence in relatively low abundance, of coronene in the Gombe Formation coals. The Cor/(Cor+BaPy) ratios of the studied Benue trough coals range between 0.02 and 0.26 (avg. 0.14). In contrast, Middle Jurassic sediments from the Polish Basin investigated by Zakrzewski et al. (2020) show higher values (0.12-0.67). The cross-plot of the Cor/(Cor+BaPy) ratio and total inertinite content for the Nigerian coals and Polish sediments suggests a correlation between both parameters as samples with high Cor/(Cor+BaPy) ratios generally contain a high amount of inertinite macerals (Figure 6.36).

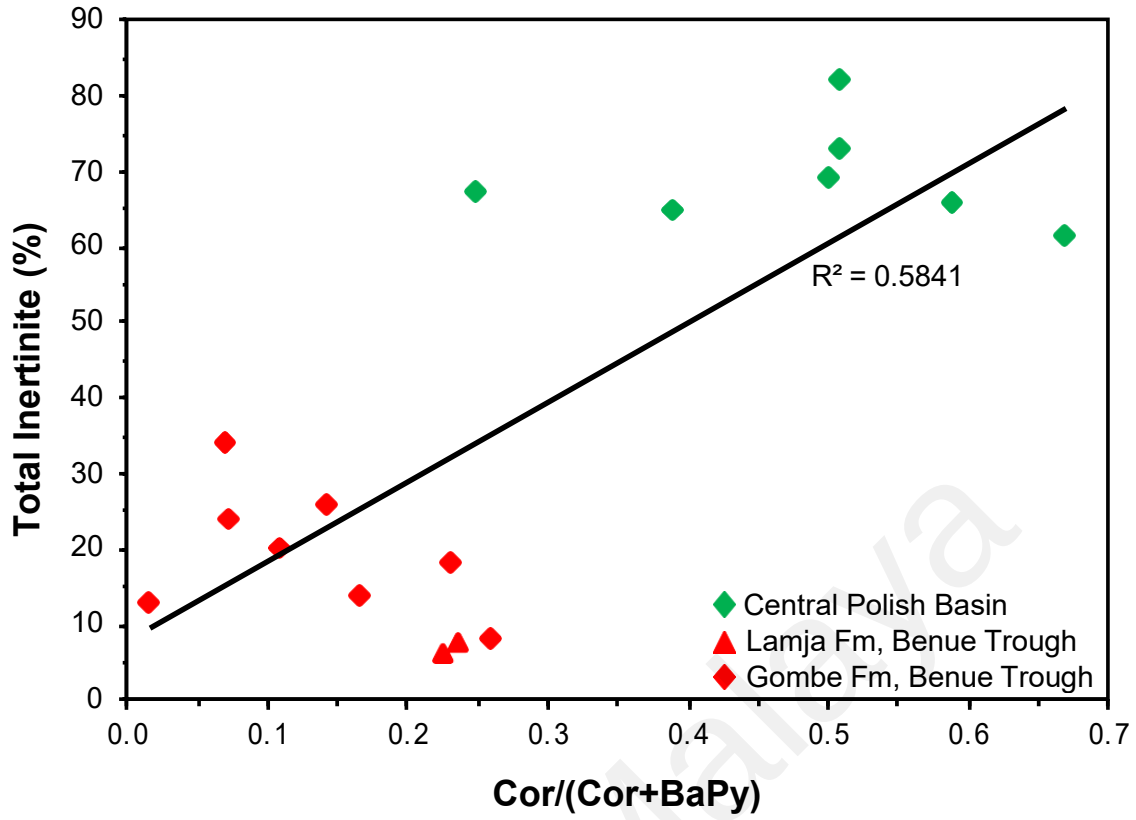

Figure 6.36: Correlation diagram of Cor/(Cor + BaPy) and total inertinite content for the studied Benue Trough coals and Polish Basin sediments reported by Zakrzewski et al. (2020). Cor = coronene; BaPy = benzo[*a*]pyrene.

6.5.5 Elemental Composition

The abundance of elements in coals provides important information on paleoenvironmental conditions and several studies have documented the effect of paleoclimate on the elemental composition of coals (Bai et al., 2015; Li et al., 2019; Lv et al., 2019; Liu et al., 2021; Zhou et al., 2021; Akinyemi et al., 2022). Elements such as Fe, Mn, Co and Ni are often enriched under humid climatic conditions, while Ca, Mg and Sr are often enriched under arid conditions (Cao et al., 2012). Hence, bimetal ratios such as Sr/Cu, Rb/Sr and Ga/Rb are employed as paleoclimate proxies (Cao et al., 2012; Vosoughi Moradi et al., 2016; Krzeszowska, 2019).

The low Rb/Sr ratios (<1) for all the coals generally indicate warmer climatic conditions (Vosoughi Moradi et al., 2016; Krzeszowska, 2019). Furthermore, the relative abundance of strontium over copper has been used to determine climatic conditions. Sr/Cu ratios between 1.5 and 5.0 reportedly indicate a humid climate while ratios > 5.0 indicate an arid climate (Sarki Yandoka et al., 2015a; Han et al., 2020). The Sr/Cu ratio for Sarawak Basin coals varies widely between 1.1 and 108.1, mostly increasing from Nyalau Formation (avg. 9.8) and Balingian Formation (avg. 10.8) to Liang Formation (avg. 52.8). The Sr/Cu ratios are suggestive of relatively drier climatic conditions for the Liang Formation coals and fluctuating wet and dry conditions during accumulation of the Nyalau and Balingian Formation paleopeats. Similarly, Sr/Cu ratios for the Benue Trough coals vary widely between 0.2 and 132.9, with correspondingly average values of 1.1, 3.1, 7.9 and 54.6 for the Mamu, Agwu, Lamja and Gombe Formations. These values suggest mostly wetter conditions in the Late Cretaceous until drier conditions developed in the Maastrichtian during the accumulation of the Gombe Formation paleopeats.

The Sr/Ba ratio is another widely utilized bimetal proxy for paleoclimate, and ratios < 1 and > 1 generally imply humid and arid climatic conditions, respectively (Dai et al., 2020). Calculated Sr/Ba ratios range from 0.07 to 13.78 (avg. 1.57) and 0.16 to 8.40 (avg. 1.09) for the analysed Sarawak Basin and Benue Trough coals, respectively (Table 5.10). For the Sarawak Basin coals, ratios for the Miocene Balingian (avg. 0.54) and Nyalau (avg. 0.15) Formations are < 1 but > 1 for the Pliocene Liang Formation (avg. 4.58). In contrast, Sr/Ba ratios for the Benue Trough coals are < 1 except in two samples (MGL3A and LMZ1). The cross-plot of Sr/Ba and Sr/Cu ratios in Figure 6.37a shows that the Malaysian Balingian and Nyalau Formation coals were deposited under wetter conditions of a warm and humid climate in the Early Miocene while the Liang Formation coals accumulated under relatively drier conditions in Late Pliocene.

In addition, Figure 6.37a shows that the Nigerian coals accumulated under humid climatic conditions during the Late Cretaceous. However, high Sr/Cu ratios suggest frequent drier periods during the accumulation of the Lamja and Gombe Formation peats in the Turonian-Coniacian and Maastrichtian, respectively. Furthermore, the C-value, defined as [Fe + Mn + Cr + Ni + V + Co]/[Ca + Mg + Sr + Ba + K + Na], is an effective proxy of paleoclimate in mudstones and its values reduce with increasing aridity (Cao et al., 2012). Ratios of the C-value parameter < 0.2 and > 0.8 corresponds, respectively, to arid and humid climate (Cao et al., 2012). The C-value ratios are > 0.2 in all the studied Sarawak Basin and Benue Trough coals, ranging from 0.24 to 6.94 (avg. 1.93) and 0.26 to 28.27 (avg. 6.14), signifying accumulation under humid climatic conditions (Figure 6.37b).

In a study of coals and shales from Huangxian Basin, China, Lv et al. (2019) established that SiO_2/Al_2O_3 ratios are indicative of redox and climatic conditions during deposition. According to Lv et al. (2019), SiO_2/Al_2O_3 ratios increase with decreasing humidity. The SiO_2/Al_2O_3 ratios are mostly relatively higher for Benue Trough coals, varying broadly from 1.32 to 9.36 with an average of 3.42, which indicate relatively drier climatic conditions. Similarly, the ratios vary broadly from 0.18 to 7.30 with an average of 2.09 for the Sarawak Basin coals. Comparing the SiO_2/Al_2O_3 ratios of the Sarawak samples generally shows the highest ratios for the Pliocene Liang Formation (avg. 2.84) and the lowest ratios for the Miocene Balingian Formation (avg. 1.18). These ratios corroborate the interpretation of less humid and more humid paleoclimate during peat accumulation in the Pliocene and Miocene, respectively. Additionally, consistent with previous interpretations, the Nyalau Formation coals show varying SiO_2/Al_2O_3 ratios (avg. 1.96) that are suggestive of fluctuating wetter-drier conditions.

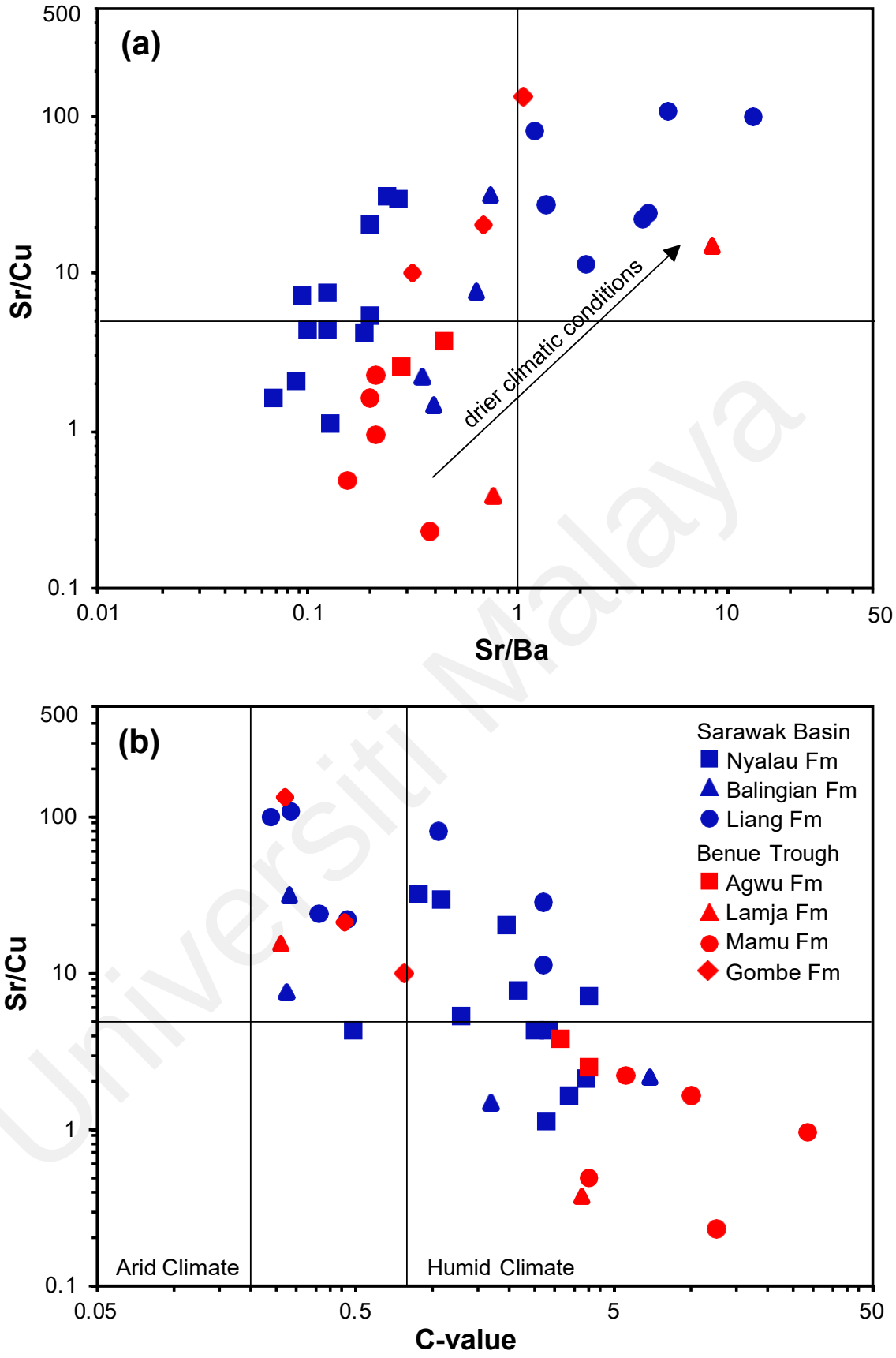

Figure 6.37: Cross-plots of (a) – strontium/barium (Sr/Ba) ratio vs. strontium/copper (Sr/Cu) ratio, and (b) – C-value vs. Sr/Cu ratio, showing paleoclimatic conditions.

The interpretations of considerably drier conditions during the accumulation of the Liang Formation peats in the Late Pliocene, and a warm, tropical wet-dry climate when peats of the Balingian and Nyalau formations accumulated in the Late Oligocene to Early Miocene are corroborated by published paleovegetation (Morley 1998; Barry et al., 2002; Widodo et al., 2009) and paleoclimate (Zachos et al., 2001; Jablonski, 2005; Morley, 2012; Holbourn et al., 2014; Friederich et al., 2016) studies. According to Morley (1998, 2012), plant dispersal in the SE Asia region has been mainly controlled by climate since the Eocene and the climate in the Late Oligocene to the earliest Miocene was warm and considerably drier. However, moist climate and tropical rain forests became widespread in the Early Miocene (~ 20 Ma) until the Middle Miocene (~ 15 Ma) when warming peaked. This was followed by a period of gradual cooling, increased aridity, the recession of rain forests and, the expansion of grasslands from the Middle Miocene to the Early Pliocene (Barry et al., 2002; Chamberlain et al., 2014). In contrast, the Early Pliocene was marked by a subtle warming trend that ended in the Late Pliocene (~ 3.2 Ma) when glaciation resumed with pronounced seasonal climates in the Late Pliocene and Quaternary (Morley, 1998; Zachos et al., 2001; Jablonski, 2005).

The wide variation in values of *n*-alkane proxies (n-C_{23}/n-C_{29}, ACL, P_{wax}, *P*aq) for the Nyalau Formation and, to a lesser degree in the Balingian Formation coals suggests fluctuating peat hydrological conditions (Zheng et al., 2007). This further suggests that the Nyalau Formation coals at Merit-Pila coalfield were deposited under the tropical wet-dry seasonal climate that prevailed in the Late Oligocene and earliest Miocene and are probably stratigraphically older than the Balingian Formation coals which accumulated under the relatively stable humid conditions of the Early to Middle Miocene, possibly between 20 and 15 Ma (Morley, 1998; Jablonski, 2005; Morley, 2012). Palynological and sedimentological investigation of the Balingian Formation by

Murtaza et al. (2018) showed the occurrence of *Florscheutzia trilobata* and *Florscheutzia levipoli*, and based on this finding, the authors assigned an Early to Middle Miocene age. In addition, Hennig-Breitfeld et al. (2019) ascribed Oligocene to Early Miocene, and uppermost Early to Middle Miocene ages to the Nyalau and Balingian Formations, respectively. Hence, the geochemical interpretations of this research support the conclusions by Murtaza et al. (2018) and Hennig-Breitfeld et al. (2019) of the latest Oligocene to Early age for the Nyalau Formation, and Early to Middle Miocene age for the Balingian Formation (Figure 6.38).

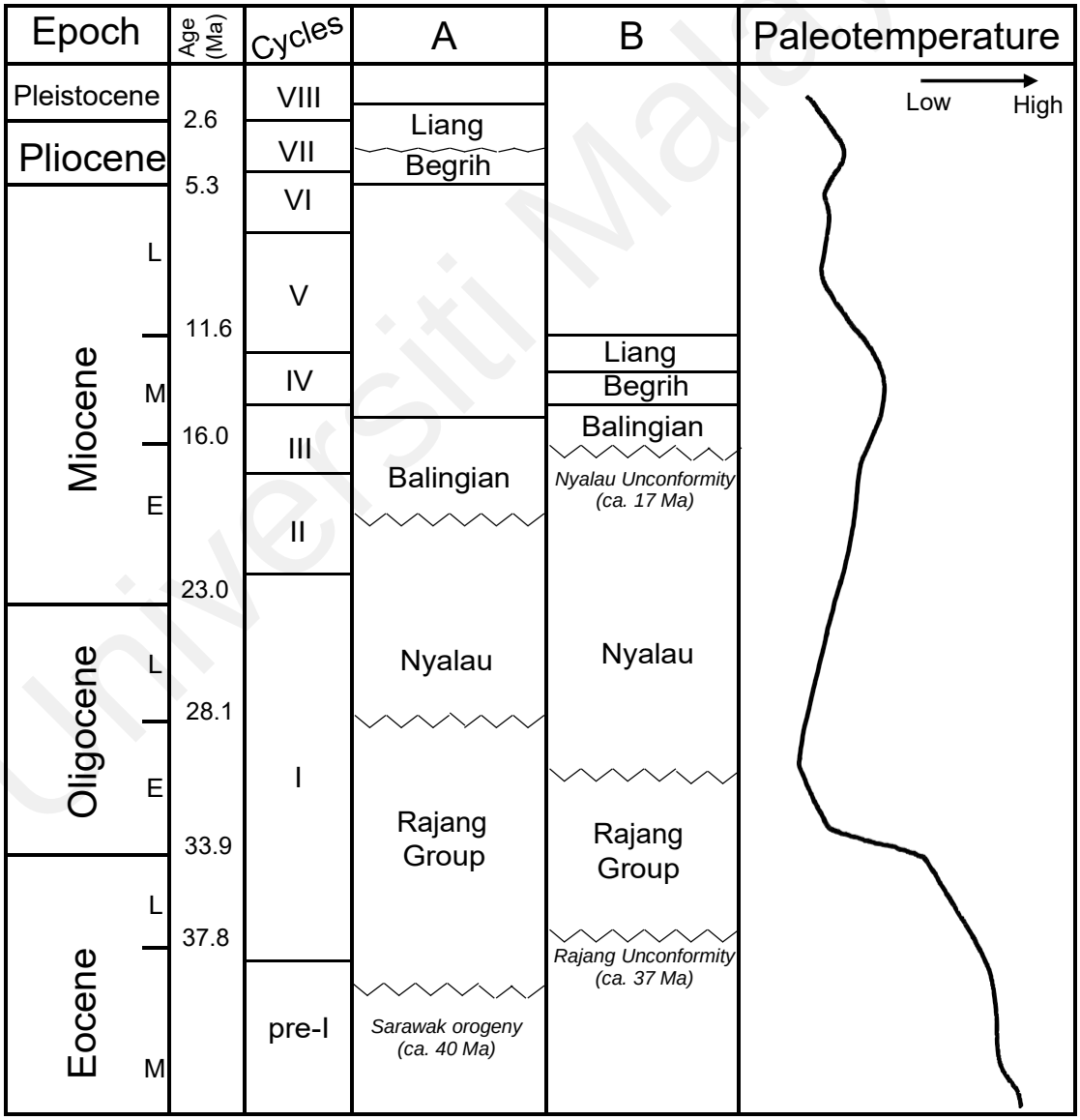

Figure 6.38: Simplified stratigraphic framework of Mukah-Balingian and Merit-Pila coalfields (after A: Hageman, 1987; Madon, 1999b; Mukah et al., 2014; Murtaza et al., 2018; this research, and B: Hennig-Breitfeld et al., 2019)

Although most studies have ascribed a Late Pliocene to Pleistocene age to the Liang Formation (Wolfenden, 1960; Hutchison, 2005), the revised stratigraphy proposed by Hennig-Breitfeld et al. (2019) suggests a latest Middle Miocene age. Interpretations of *n*-alkane proxies, bimetal ratios and δD values indicate relatively warmer and drier conditions during the accumulation of the Liang Formation paleopeats. This interpretation is further corroborated by preliminary results of the oxygen isotopic ($\delta^{18}O$) analysis of the studied coals which show a 2‰ decline in $\delta^{18}O$ values from the Balingian Formation to the Liang Formation that signifies relatively warmer climatic conditions (Zachos et al., 2001). However, the Middle Miocene is generally characterised by cooler climatic conditions after warming peak at ~ 15 Ma (Holbourn et al., 2014). A global climate study by Zachos et al. (2001) established that $\delta^{18}O$ values increased after Middle Miocene Climate Optimum (MMCO) until the Early Pliocene when $\delta^{18}O$ values declined due to warming between 6 Ma and 3.2 Ma. Warming events are often accompanied by sea level rise and decreasing surface productivity that are accordingly reflected by higher Sr/Ca and lower $\delta^{13}C$ values (Stüben et al., 2003). Average $\delta^{13}C$ values of the Sarawak Basin coals are lower for the Liang Formation (-28.0‰) than the Balingian Formation (-26.7‰), while average Sr/Ca ratios are higher for Liang Formation (0.029) than the Balingian Formation (0.016), validating the finding of relatively warmer depositional conditions for the Liang Formation. Although the geochemical evidence presented in this thesis does not conclusively support a Late Pliocene age for the Liang Formation, elemental and isotope data however contradict the latest Middle Miocene age recently assigned by Hennig-Breitfeld et al. (2019).

Nevertheless, the palynological study by Sia et al. (2019) concluded that the Liang Formation coals were dominated by palynomorphs, and characterized by a strong diversity of species, which according to the authors suggests wet climatic conditions. Furthermore, a review of the climate in the Cenozoic by Morley (2012) concluded that

the Borneo Island areas have, without interruption, experienced ever-wet climates since the Late Miocene. These petrography and palynology interpretations of ever-wet conditions in the Late Pliocene contradict this research's biomarker and elemental data interpretation of relatively drier conditions. This is possibly due to the highly seasonal climate in the Late Pliocene which limited peat fires and ensured minimal diversity of species (Jablonski, 2005).

6.6 Paleodepositional Conditions

6.6.1 Paleoenvironments

Previous studies have shown that variations in the relative abundances of aromatic compounds such as phenanthrene (PHE), naphthalene (Np), dibenzofuran (DBF), fluorene (F), and dibenzothiophene (DBT) are effective markers of facies and depositional environments (Pu et al., 1990; Hughes et al., 1995; Radke et al., 2000; Li et al., 2013; Asif & Wenger, 2019). In general, the relative abundances of PHE, F and DBF are higher in source rocks from freshwater sedimentary environments than in those from marine environments whilst the abundances of DBT and Np are relatively higher in source rocks from marine environments.

The analysed Sarawak Basin and Benue Trough coals are dominated by PHE with subordinate abundances of DBF and DBT (Figure 6.39a), generally signifying non-marine depositional environments (Pu et al., 1990); however, the elevated abundance of DBT observed in a few samples is suggestive of marine influence (Radke et al., 2000). Although the dominance of MPs over MDBFs and MDBTs is less pronounced (Figure 6.39b), the moderately high abundance of MDBFs supports the interpretation of a non-marine depositional environment (Radke et al., 2000).

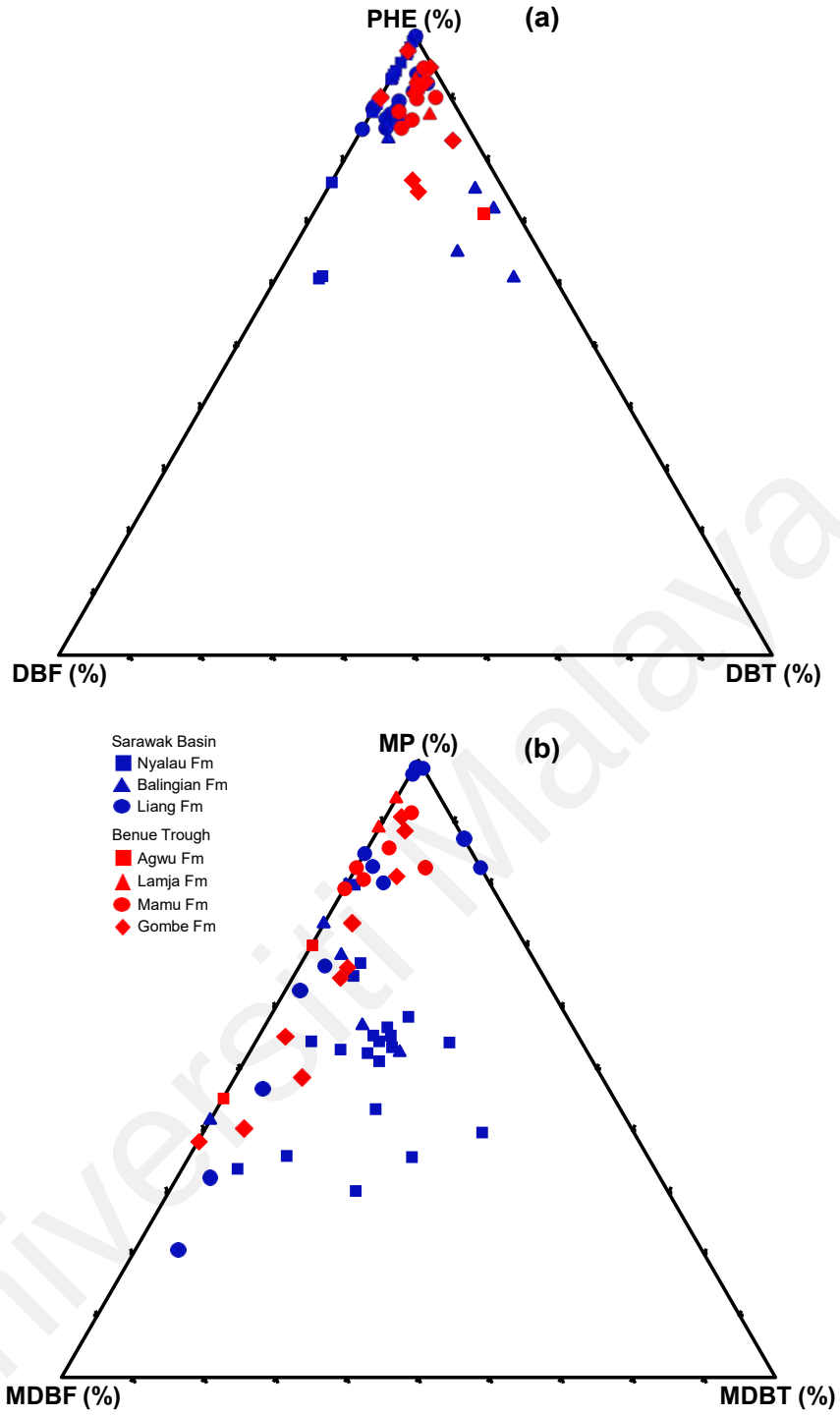

Figure 6.39: Ternary diagrams showing relative abundances of (a) – phenanthrene (PHE), dibenzofuran (DBF), and dibenzothiophene (DBT), and (b) – methylphenanthrenes (MP), methyldibenzofurans (MDBF) and methyldibenzothiophenes (MDBT) in the studied coals.

Furthermore, Asif & Wegner (2019) utilized the ternary diagram of the relative abundances of F, DBF and DBT to differentiate source facies. The authors reported that freshwater lacustrine-, coaly-, and marine carbonate-sourced oils have the highest

abundances of F, DBF and DBT, respectively. The relative abundance of F, DBF and DBT in the Sarawak Basin coals vary broadly from 0.0 to 100.0%, 0.0 to 100.0, and 0.0 to 66.6%, respectively, while varying accordingly from 13.1 to 73.0%, 6.4 to 78.5%, and 0.0 to 72.1% in the Benue Trough coals. The ternary plot of %F, %DBF and %DBT mostly shows similar average abundances of F (34.2%), DBF (30.7%) and DBT (35.1%) in the Benue Trough samples that is typical of freshwater to brackish-water lacustrine environment (Figure 6.40a). In contrast, the Sarawak Basin samples are characterised by predominant abundances of DBF (avg. 46.3%) and F (avg. 38.9%) which indicates terrestrial organic matter deposited in freshwater- to lacustrine-mire environment (Pu et al., 1990; Radke et al., 2000; Li et al., 2013; Asif & Wenger, 2019). Additionally, the higher variance in the abundances of the heterocyclic compounds in the Sarawak Basin coals is indicative of fluctuating depositional conditions during peat accumulation in the Tertiary. For example, the Nyalau and Balingian Formation coals are dominated by DBF (avg. 50.1%) and DBT (avg. 44.1), which suggests peat accumulation occurred under relatively oxidizing and less-oxidizing conditions of a deltaic environment (Pu et al., 1990).

The methylated homologue distributions of the heterocyclic compounds are slightly comparable for both groups of coals (Figure 6.40b). The Sarawak Basin coals are dominated by MF (avg. 35.9%) and MDBF (avg. 45.7%), with a subordinate abundance of MDBT (avg. 18.4%). Similarly, MF (avg. 38.1%) and MDBF (avg. 51.9%) predominate in the Benue Trough coals with a low abundance of MDBT (avg. 10.0%). However, MDBF/MF ratios range from 0.29 to 6.30 and 0.46 to 3.16 for the Sarawak Basin and Benue Trough coals, respectively. Within the Sarawak Basin, MDBF/MF ratios are highest for the Nyalau Formation (avg. 2.75) and lowest for the Liang Formation (avg. 1.00). The wider range of MDBF/MF ratios for the Sarawak Basin coals supports the finding of varying depositional sub-environments as higher

MDBF/MF ratios imply peat mire paleoenvironment for Nyalau Formation, while lower ratios suggest freshwater lacustrine paleoenvironment for the Liang Formation (Li et al., 2013; Asif & Wegner, 2019).

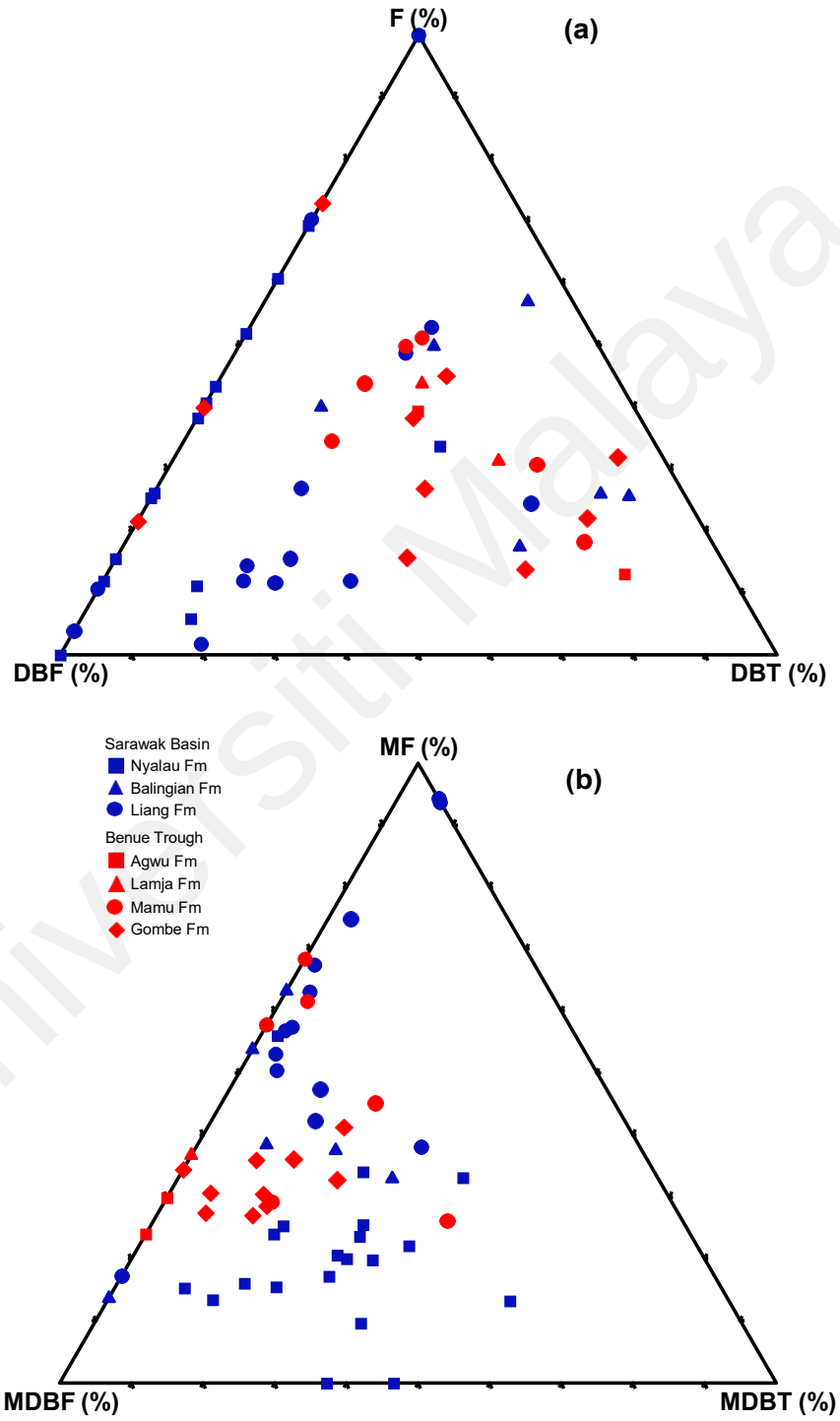

Figure 6.40: Ternary plots of the relative proportions of (a) – fluorene (F), dibenzofuran (DBF), and dibenzothiophene (DBT) and (b) – methylfluorenes (MF), methyldibenzofurans (MDBF), and methyldibenzothiophenes (MDBT) in the studied Sarawak Basin and Benue Trough coals.

Hughes et al. (1995) utilized the cross-plot of dibenzothiophene/phenanthrene (DBT/PHE) and pristane/phytane (Pr/Ph) ratios to differentiate five distinct environments and lithologies. DBT/PHE and Pr/Ph ratios for the studied coals are plotted in Figure 6.41a. The Sarawak Basin coals plot across zones C, D and E, corresponding to lacustrine (sulfate-poor), marine and lacustrine, and fluvio-deltaic depositional environments, respectively. However, the Benue Trough coals mostly plot in the boundary between zones D and E, which indicates marine/lacustrine to fluvial-deltaic depositional environments. Again, the Sarawak Basin coals show broad ranges of DBT/PHE and Pr/Ph ratios that indicate differing sub-depositional environments. Whereas the Liang Formation plots across zones C, D and E, the Balingian Formation plot in zones D and E, and the Nyalau Formation mostly within zone E of the Hughes et al. (1995) diagram (Figure 6.41a).

Due to the dominant abundance of PHE over DBT in terrestrial sedimentary environments (Figure 5.24), Radke et al. (2000) modified the Hughes et al. (1995) diagram to differentiate high-rank coals and mature mudstones by plotting Pr/Ph ratios against MDBT/MDBF ratios. Similarly, the studied coals plot in the zones C, D and E of the modified diagram (Figure 6.41b), thus corroborating the interpretation of peat accumulation in a lacustrine swamp to fluvial/deltaic depositional environments.

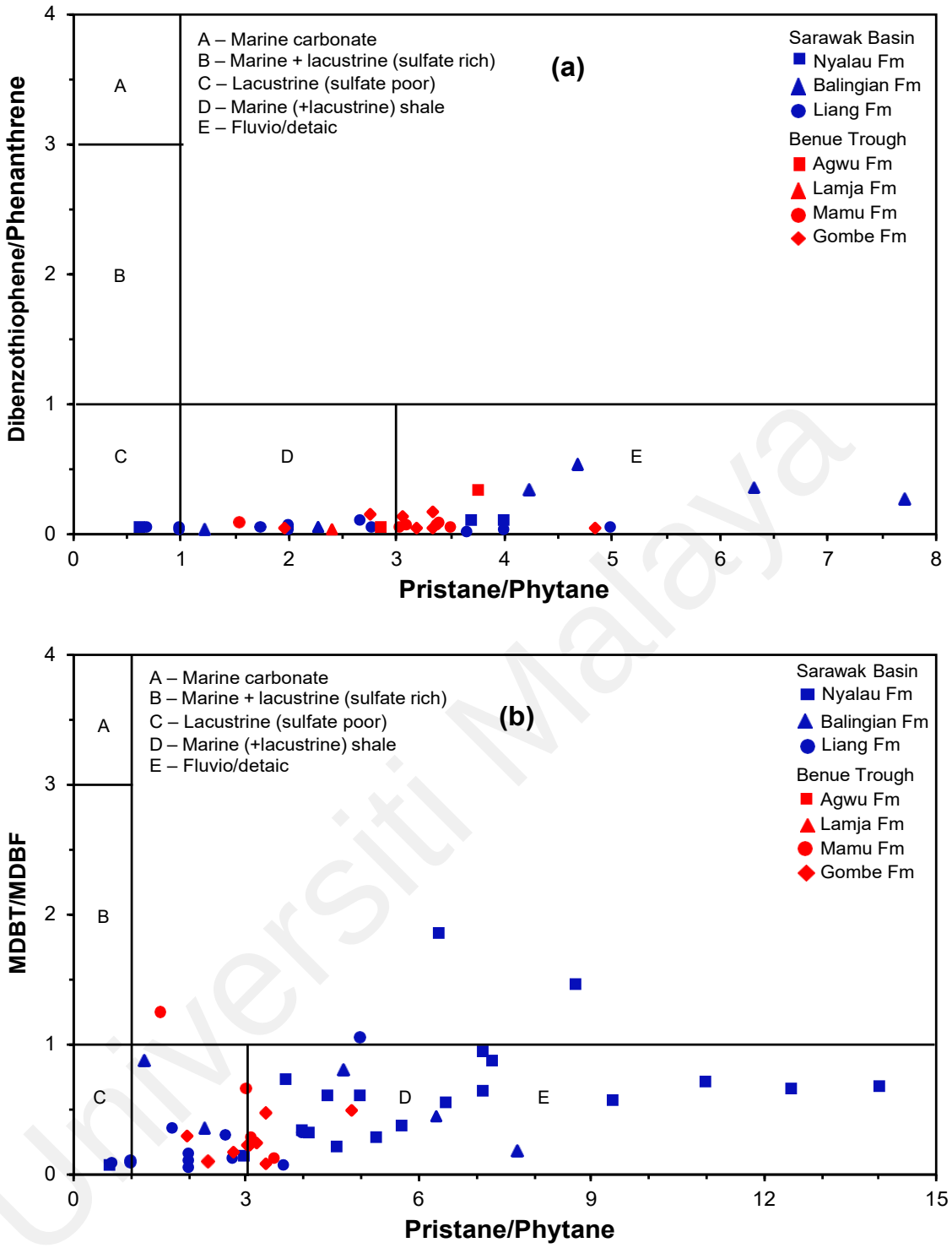

Figure 6.41: Cross-plots of pristane/phytane ratios vs. (a) – dibenzothiophene/phenanthrene ratios (after Hughes et al., 1995) and (b) – methyldibenzothiophenes/methyldibenzofurans (MDBT/MDBF) ratios (after Radke et al., 2000), indicating depositional environment of the studied coals.

6.6.2 Paleoredox Conditions

The pristane-to-phytane (Pr/Ph) ratio is an important indicator of paleoredox condition (Didyk et al., 1978). Pr/Ph values < 0.8 indicate saline to hypersaline conditions, while values > 3 suggest terrigenous organic matter deposited under oxic conditions (Peters et al., 2005). The Pr/Ph ratios for the studied Sarawak Basin and Benue Trough range from 0.6 to 14.0 (avg. 4.8) and 1.5 to 4.8 (avg. 3.0), respectively (Tables 5.15-5.16). The ratios are mostly indicative of terrestrial organic matter deposited under fully oxidizing conditions. The Pr/Ph ratios for the Liang Formation are > 1 (except in samples B03-6 and BG1) with an average of 2.3, which indicate deposition under suboxic to dysoxic paleoenvironmental conditions. Coals of the Balingian and Nyalau formations have Pr/Ph ratios > 3 (except in M03-2, 046A and MP1U) with respective average values of 4.4 and 6.5 that signify oxic conditions.

The abundances of trace elements and bimetal proxies such as V/Cr, V/Ni and Ni/Co have been widely used to infer paleoredox conditions (Jones and Manning, 1994; Algeo & Maynard, 2004; Tribovillard et al., 2006; Kombrink et al., 2008; Bennet & Canfield, 2020). For instance, the concentrations of Mo, U and V have been found to increase under reducing conditions (Rimmer, 2004; Tribovillard et al., 2006), while V and Ni are more abundant in minerotrophic than ombrotrophic peats (Shotyk, 1988). However, a recent study by Algeo & Liu (2020) re-examined the thresholds for bimetal proxies established by Jones & Manning (1994). The authors noted that the universal adoption of proxy thresholds established for sediments of specific formations and ages is problematic, and concluded that thresholds must be applied cautiously. Although these paleoredox proxy thresholds may not be suitable for determining the specific redox conditions in coal depositional environments, the parameters are nonetheless useful for a comparative evaluation of the degree of varying redox conditions.

The low concentrations of Mo (< 1 ppm), U (< 0.2 ppm), V (< 20 ppm), and Ni (< 20 ppm) in the studied coals indicate oxic to suboxic depositional conditions (Tribovillard et al., 2006; Galarraga et al., 2008). However, the relatively higher Zn, U, and V abundances in some of the studied coals suggest intermittent relatively less oxidizing conditions (Algeo & Maynard, 2004; Kombrink et al., 2008). Furthermore, according to Jones & Manning (1994), Ni/Co and V/Cr ratios < 5 and < 2, respectively, indicate oxic conditions, while ratios > 5 and > 2 imply reducing conditions. V/Cr ratios vary from 0.36 to 2.03 (avg. 1.06) and 068 to 1.96 (avg. 1.30), respectively, for the Malaysian and Nigerian coals. The Ni/Co ratios for the studied coals (except MP6M) are < 5.0, with an average ratio of 1.71 and 1.90 for the Sarawak Basin and Benue Trough samples, respectively. Hence, the V/Cr and Ni/Co ratios for the studied coals generally indicate oxic depositional conditions (Figure 6.42).

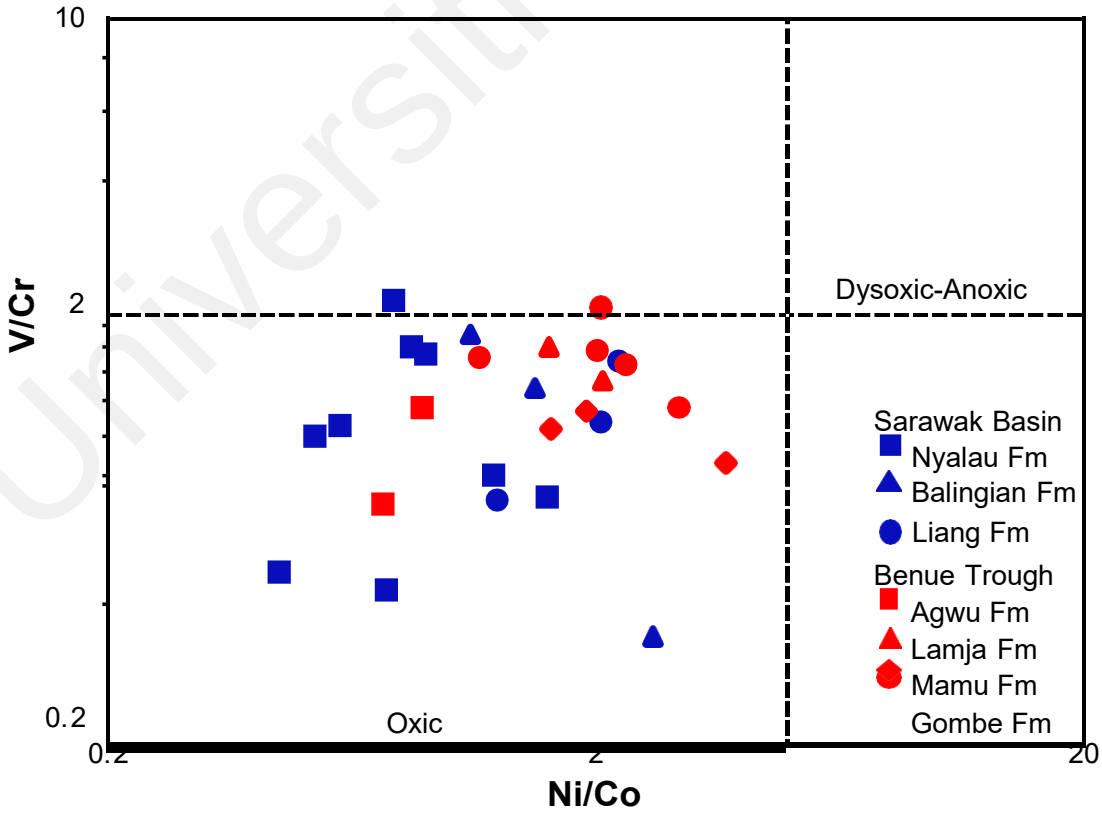

Figure 6.42: Cross-plot of nickel/cobalt (Ni/Co) and vanadium/chromium (V/Cr) ratios, showing paleoredox condition.

The Fe/Al ratio is another indicator of paleoredox condition as Fe enrichment is favoured by reducing conditions (Tribovillard et al., 2006; Algeo & Liu, 2020). Fe/Al ratios for the Sarawak Basin and Benue Trough coals vary widely from 0.14 to 28.00 and 1.47 to 15.21, respectively. Within the Sarawak Basin, Fe/Al ratio generally increases from Balingian (avg. 4.7) to Nyalau (avg. 5.2) and Liang (avg. 13.4) formations. For the Benue Trough coals, Fe/Al ratios are generally lower for Lamja (avg. 2.10) and Gombe (avg. 3.48) Formations and higher for Mamu (avg. 7.54) and Agwu (avg. 9.58) Formations. These ratios suggest that the Liang, Agwu, and Mamu Formation coals accumulated under relatively less oxidizing conditions (Tribovillard et al., 2006).

6.6.3 Paleosalinity and Marine Influence

The Sr/Ba ratio could also be a useful indicator of freshwater and seawater influence in depositional environments, and ratios > 1 and < 1 are indicative of marine-influenced and freshwater-influenced environments, respectively (Gayer et al., 1999; Dai et al., 2020). For the Sarawak Basin coals, the Sr/Ba ratios are > 1 in the Liang Formation (1.4-13.8) and < 1 for the Balingian Formation (0.4-0.7) and Nyalau Formation (0.1-0.3), suggesting some marine-influence in the Liang Formation coals. Sr/Ba ratios for the Benue Trough coals are mostly < 1, except in two Gombe and Lamja Formation samples (MGL3A and LMZ1), indicating a mostly freshwater-influenced depositional environment. Furthermore, the total abundance of B is an effective indicator of paleosalinity (Diessel, 1992; Dai et al., 2020). According to Goodarzi & Swaine (1994), boron concentrations in coals < 50 ppm and > 110 ppm, respectively, indicate freshwater and brackish water influence, while concentrations between 50 and 110 ppm indicate mildly brackish water influence. Boron concentration in the studied Sarawak

Basin and Benue Trough coals, which ranges from 24 to 248 ppm and 22 to 72 ppm, respectively, are suggestive of some degree of brackish water influence.

For the Sarawak Basin coals, B concentration in the Nyalau Formation is generally below the detection limit of 20 ppm, with only one sample (MP1M) recording an abundance of 24 ppm. However, B concentration ranges from 47 to 248 (avg. 119 ppm) and 53 to 91 (avg. 68 ppm), respectively, for the Liang and Balingian Formations. Hence, the low (< 50 ppm) concentration of boron in the Nyalau Formation coal is indicative of low salinity typical of a freshwater depositional environment, while higher concentrations (> 50 ppm) in the Liang Formation and Balingian Formation coals infer brackish-water influenced depositional environments (Goodarzi & Swaine, 1994). Within the Benue Trough, B concentration is below the detection limit in the investigated Lamja Formation coals but its concentration generally increases from Gombe Formation (22-31 ppm) to Agwu Formation (33-72 ppm) and Mamu Formation (34-71 ppm) coals. The measured B concentrations in the Benue Trough coals are indicative of freshwater-influenced environments for the Lamja and Gombe Formations, and brackish-water-influenced environments for the Agwu and Mamu Formations. The cross-plot of B concentration and Sr/Ba ratio in Figure 6.43 shows that the studied coals mostly accumulated in freshwater-influenced depositional environments. However, the high B concentration and Sr/Ba ratios of the Liang Formation coals suggest a mild but increasingly brackish-water-influenced environment.

The elevated abundance of U and low Th/U ratios in coals have also been linked to sea-water influence (Gayer et al., 1999). U concentrations in the studied are considerably lower in the Sarawak Basin coals (0.1-0.2 ppm) than in the Benue Trough coals (0.1-5.6 ppm). Similarly, Th concentrations are relatively lower for the Sarawak coals (0.1-2.4 ppm) and higher for the Benue Trough samples (0.6-5.5 ppm) and

accordingly, Th/U ratios range from 6.0 to 12.0 (avg. 8.3) and 0.2 to 18.0 for (avg. 7.3). Therefore, the low (< 0.1 ppm) U concentration and high (> 4.8) Th/U ratios for the Sarawak coals suggests little or no marine influence on the coals (Gayer et al., 1999; Kombrink et al., 2008). Conversely, the relatively higher U concentrations and lower Th/U ratios in some Benue Trough samples, particularly the Mamu Formation coals with an average Th/U ratio of 3.5, suggest some marine influence on the coals (Table 5.10; Gayer et al., 1999).

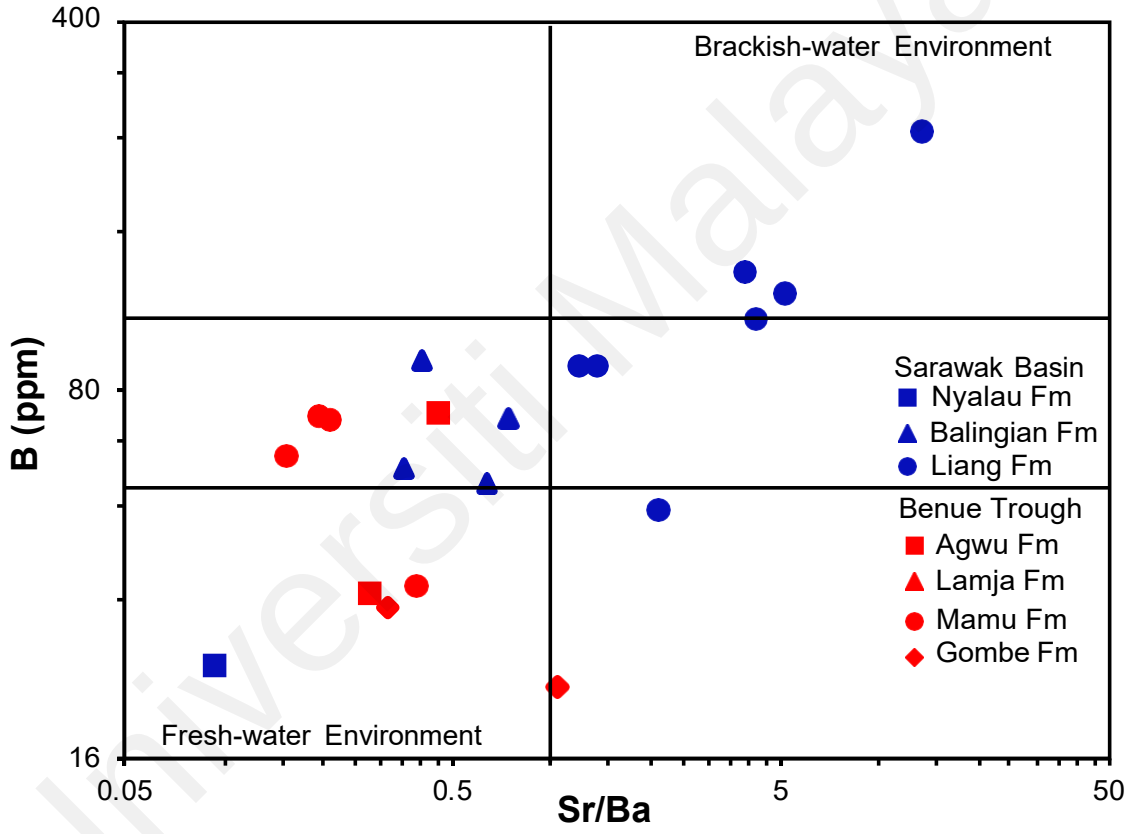

Figure 6.43: Plot of strontium/barium (Sr/Ba) ratio vs. boron concentration in the studied coals.

The generally low sulfur and uranium abundances and high Th/U ratios for the Liang Formation coals suggest no marine influence, while high B concentration and Sr/Ba ratios signify brackish-water marine influence on the coals (Figure 6.44). These contradictory interpretations highlight the drawbacks of the use of elemental paleosalinity proxies, which are summarized by Dai et al. (2020).

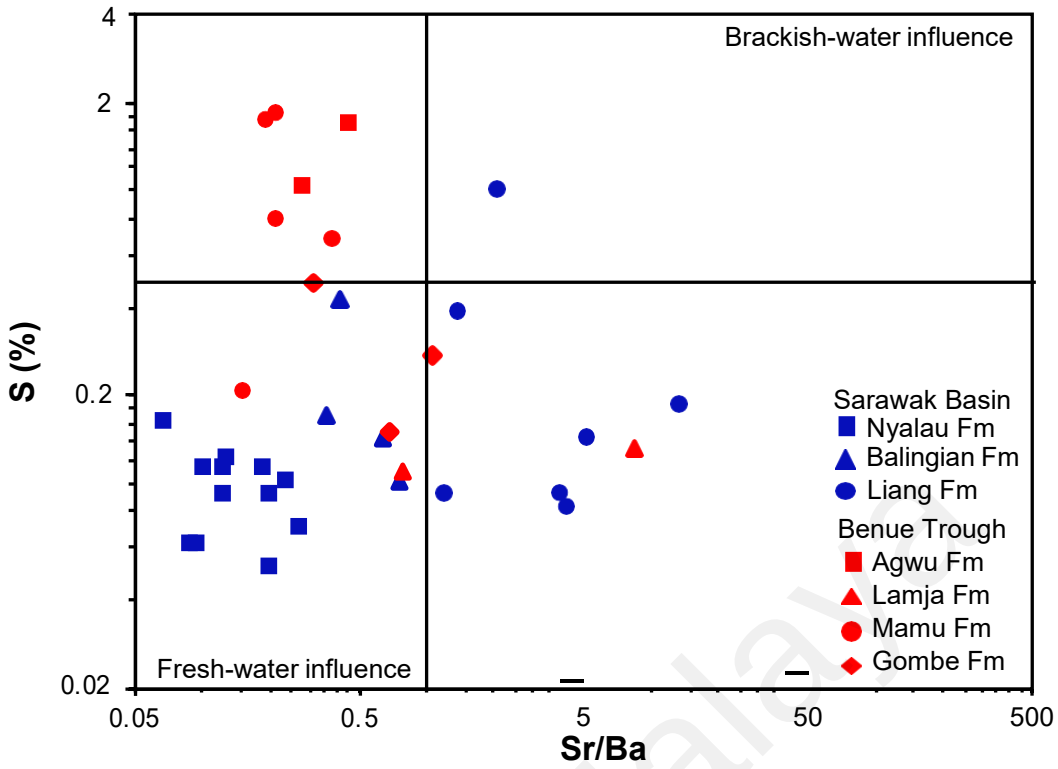

Figure 6.44: Plots of Sr/Ba ratio vs. sulfur content in the studied coals.

High B concentrations with no syngenetic marine influence have been reported for some New Zealand coals. Moore et al. (2005) attributed the high B concentration (up to 7000 ppm) in the Waikato region coals to a hydrothermal source. Similarly, Gürdal & Bozcu (2011) reported high S_T content (up to 12.2 wt.%) in some Miocene Çan Basin coals from Çanakkale, Turkey. The authors concluded that organic sulfur is the dominant sulfur form in the coals and therefore attributed the high S_T content to regional volcanic activity. Hence, S_T content in coals is no indicator of the type/time of marine influence. The average boron concentration (1838 ppm) for the New Zealand coals investigated by Moore et al. (2005) is two orders of magnitude higher than the global average value (52 ppm) reported by Ketris & Yudovich (2009). In contrast, B concentrations (< 248 ppm) in the studied Liang Formation coals are significantly lower and can thus be plausibly explained by post-burial marine influence. This hypothesis is corroborated by the reported presence of cleat-filling epigenetic pyrite in the Liang

Formation coals (Sia & Abdullah, 2012), which are incorporated after compaction/partial consolidation (Widodo et al., 2010).

Sulfur abundance in coal depends primarily on the degree of seawater influence during peat accumulation and diagenesis. Hence, S_T content is a widely applied proxy for marine influence on coal seams (Casagrande, 1987; Chou, 2012; Dai et al., 2020), and according to Sykes et al. (2014), S_T content > 0.5 wt.% indicates some degree of seawater influence. The authors regarded S_T contents between 0.5 and 1.5 wt.%, and > 1.5 wt.% as respectively indicating slight and strong marine influence (Sykes et al., 2014). S_T contents are generally < 0.5 wt.% for the coal formations in the Sarawak Basin, thus indicating freshwater conditions with slight or no marine influence. Conversely, average S_T contents are generally > 0.5 wt.% for the Benue Trough coals, with average values of 2.08, 0.59 and 1.73 wt.% for the studied Agwu, Lamja and Mamu Formation coals, respectively. However, the S_T content is marginally lower in the Gombe Formation coals, averaging 0.48 wt.%. Hence, the S_T content generally indicates a slight to strong brackish-water influence on the Benue Trough coal seams. Furthermore, the S_T contents also indicate that sulfur incorporation in the Sarawak Basin seams was primarily through an assimilatory reduction process by plant precursors while incorporation in the Benue Trough peats was through parent plant material and sulfate-rich seawater during accumulation and diagenesis (Lowe & Bustin, 1985; Casagrande, 1987; Haszeldine, 1989; Chou, 2012).

In addition, the Fe content of coals has been closely related to the abundance of pyritic sulfur (Kombrink et al., 2008; Spears & Tewalt, 2009; Widodo et al., 2010). The correlation coefficient (r = -0.40) between Fe and S content of the studied Sarawak Basin coals is negative and weak (Figure 5.45a). In contrast, the correlation coefficient (0.70) for the Benue Trough coals is positive and moderate (Figure 5.45b). Furthermore,

strong and positive relationships (0.86 and 0.92) were reported by Widodo et al. (2010) for the Indonesian coals from Sebulu and Central Busang mines, and by Spears & Tewalt (2009) for the marine-influenced British Parkgate coals from Yorkshire-Nottinghamshire coalfield. Hence, the weak, negative correlation between Fe and S corroborates the near absence of pyritic sulfur and the finding of little or no seawater influence in Sarawak Basin coals while the moderate, positive correlation supports the finding of brackish-water influence in the Benue Trough coals.

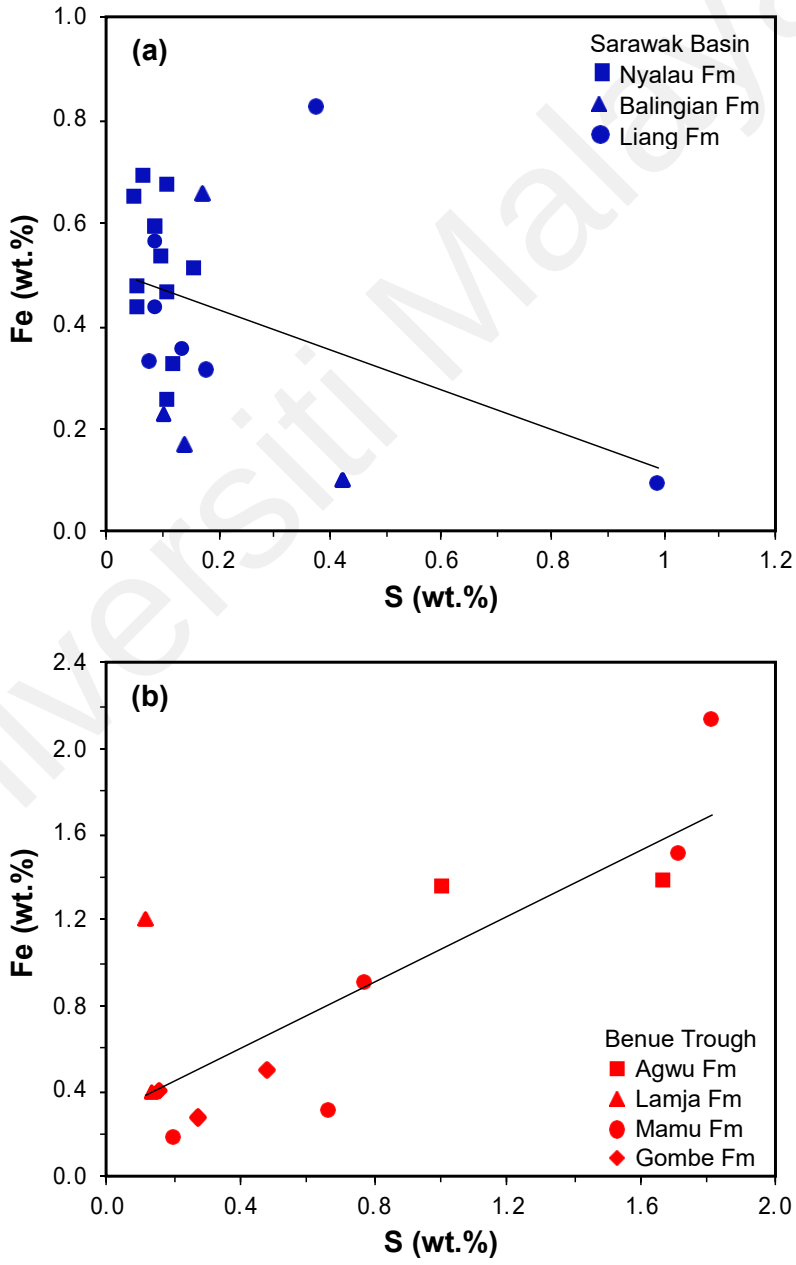

Figure 6.45: Correlation plot of elemental sulfur (S) and iron (Fe) in the studied Sarawak Basin and Benue Trough coals.

The availability of Fe has also been shown to be an important control on S geochemistry in mires (Dellwig et al., 2001; Marshall et al., 2015; Uguna et al., 2017). In a study of the Holocene coastal peats in Germany, Dellwig et al. (2001) concluded that pyrite formation is enhanced by the combination of sulfate-rich groundwater and Fe-rich mire waters. Furthermore, Marshall et al. (2015) established that the supply of sulfate-rich groundwater must be greater than Fe-rich mire waters to create a system that is Fe-deficient and thus with excess sulfur. Given that the atomic Fe/S ratio for pyrite (FeS_2) is 0.87, all available sulfur in peats with Fe/S ratios > 0.87 are presumably sequestered as pyrite and the excess Fe precipitated as Fe-carbonates (Marshall et al., 2015). However, with additional supplies of sulfate-rich groundwater, the Fe/S ratio becomes < 0.87, which creates excess sulfur that ultimately forms organosulfur compounds (Sinninghe Damste & De Leeuw, 1990; Marshall et al., 2015).

Calculated Fe/S ratios are relatively higher for the Sarawak Basin coals, ranging from 0.09 to 13.00 (avg. 4.52), and lower for the Benue Trough coals with values varying from 0.45 to 11.00 (avg. 2.13). Within the Sarawak Basin, Fe/S ratios are generally highest in the Nyalau Formation coals (avg. 6.22) and lowest in the Balingian Formation coals (avg. 1.91). These ratios suggest the absence of excess S required to form organosulfur compounds in the paleopeats. This is corroborated by the low DBT/PHE ratios of both groups of coals (Table 5.26). In addition, the Fe/S ratios suggest a relatively higher supply of sulfate-rich sea water into the Benue Trough mires, which corroborates the finding of higher marine influence in the seams. The higher average abundance of Fe in the Benue Trough (0.88 wt.%) relative to the Sarawak Basin (0.44 wt.%) coals also suggests peat accumulation under more minerotrophic conditions in the Benue Trough areas as Fe is more abundant in fen plants than in bog plants (Shotyk, 1988).

The ash content of coals has been found to correlate strongly and positively with mineral and S_T contents (Widodo et al., 2010). Ombrotrophic peats are often typified by low S_T and mineral contents, while rheotrophic peats are subjected to regular flooding and thus characterized by high ash content (Anderson 1964; Dehmer, 1993). Hence, the generally low S_T (avg. 0.29 wt.%) and low to moderately high ash (avg. 9.5 wt.%) contents of the Sarawak Basin coals indicate the presence of ombrotrophic and rheotrophic peat deposits, and their proportion connotes the evolutionary development of its paleopeats. In contrast, the considerably higher S_T (avg. 1.02 wt.%) and ash (avg. 16.3%) contents of the Benue Trough coals are indicative of peat accumulation under varying but prevailing rheotrophic conditions.

Within the Sarawak Basin, the varying ash content suggests different peat types. Lower ash contents in the basal layers of the Nyalau Formation suggest that peat accumulation in the Merit-Pila coalfield possibly originated under ombrotrophic mire settings but morphed into rheotrophic mire settings with the observed higher ash contents in samples of the upper coal zone. These fluctuations from ombrogenous to rheotrophic mire settings, possibly due to base level fluctuations, were established by Morley (2013) from the Southeast Asian peat mires. Similarly, the Balingian Formation coals are characterised by varying ash content (avg. 16.6 wt.%) which also suggests the presence of multiple mire facies. This finding is corroborated by Zainal Abidin et al. (2022), which found that due to rising water table levels during accumulation, peat accumulated originally in ombrotrophic mires but ultimately in rheotrophic mires. In contrast, the Liang Formation coals generally contain low ash (avg. 7.3 wt.%) and S_T (avg. 0.40 wt.%) contents, typical of ombrogenous peats (Anderson, 1964; Moore, 1987; Dehmer, 1993). This interpretation is corroborated by the observed absence of non-coal epiclastic partings in the seams (Sia & Abdullah, 2012).

6.6.4 Acidity of Paleomire

The S_T content of coals has been associated with the pH conditions of peat-forming mires (Casagrande, 1987; Bechtel et al., 2003). In addition, the acidity of peatlands is negatively correlated with the abundance of pyritic sulfur (Diessel, 1992). Therefore the generally low sulfur content in the studied Sarawak Basin coals signifies mostly low pH conditions during peat formation. The inundation of mostly freshwater severely limited the availability of sulfate-reducing bacteria, which ultimately created an oxidizing and acidic environment (Casagrande, 1987). In contrast, the higher S_T content of the Benue Trough coals indicates flooding by oxygenated and slightly less acidic or nearly neutral waters, which resulted in slight pyritic sulfur enrichment in the paleopeats (Esterle & Fern, 1994).

Hopanoids are important pentacyclic triterpenoids and their distribution could be useful for estimating depositional conditions. The presence of C_{31} αβ-22R-homohopane in immature peats has been observed to be strongly dependent on pH (Dehmer, 1995; Bechtel et al., 2003). Inglis et al. (2018) established a significant, positive correlation between the C_{31} ββ/(αβ + ββ) ratio and pH, and established that αβ-hopanes are products of the acid-catalyzed oxidation and subsequent decarboxylation reactions of bacteriohopanetetrol. Values of the C_{31} ββ/(αβ + ββ) ratio for the low-rank Sarawak Basin and Benue Trough coals show considerable variation from 0.10 to 0.42 and 0.11 to 0.34, respectively. The corresponding calibrated pH values vary from 3.7 to 5.3 and 3.7 to 4.9 and (Table 5.17), signifying a slightly acidic depositional environment for the studied coals. Within the Sarawak Basin, the average calibrated pH value for the Liang Formation (4.2), Balingian Formation (4.6), and Nyalau Formation (4.5) signify relatively less acidic conditions in the Mukah paleopeats.

6.7 Controlling Influences on Hydrocarbon Generation

A significant number of oil-prone coal-bearing sequences are found in Australasia and Southeast Asia (Isaksen et al., 1998). According to Macgregor (1994), these coal-bearing sequences can be classified into two broad paleoclimatic and paleobotanical associations: Tertiary tropical coals and Late Jurassic-Eocene coals. The first group is dominated by coal-bearing basins in Southeast Asia countries which were presumably supported by the tropical ever-wet climate in the Tertiary (Macgregor, 1994; Thompson et al., 1994). A recent regional study by Friederich et al. (2016) concluded that the combination of factors such as humid paleoclimate, depositional settings suitable for peat accumulation, and tectonics settings suitable for the development of extensive basins resulted in the formation of the extensive Cenozoic coal deposits in Indonesia. Plant growth and biomass production are markedly aided by warm and humid climates. In contrast, humification generally proceeds faster under cooler climates and in low-nutrient, highly acidic environments with less fluctuating hydrologic conditions (McCabe, 1987; Moore, 1987; Dehmer, 1993). Additionally, Moore & Shearer (2003) investigated four New Zealand peat mires and found no direct relationship between depositional environment, tectonic setting, climatic condition, and peat types. Furthermore, the oil-generating capacity of New Zealand humic coals depends primarily on the volume and type of mire petrofacies (Sykes et al., 2014;). Petrofacies are mainly classified based on the association of plant tissues and matrix types, and rheotrophic, planar mire facies have been shown to possess higher oil-generating potential than ombrotrophic, raised mire facies (Sykes,1994; Sykes et al., 2014).

In summary, studies have established that humification and the liquid hydrocarbon generation capacity of coals are dependent on factors such as stratigraphic age, paleobotany, paleoclimate, and depositional conditions (Collinson et al., 1994; Isaksen

et al, 1998; Wilkins & George, 2002; Petersen & Nytoft, 2006). Since both the Cenozoic Sarawak Basin and Upper Cretaceous Benue Trough coals are sourced mainly from terrigenous organic matter and of similar thermal maturity, the coals vary in age, and are derived from different paleoflora, and deposited under varying environmental conditions. Hence, a comparative analysis of their geochemical data should provide insight into the controlling influence(s) on the distribution of hydrocarbons in humic coals. These potential controlling factors were appraised by undertaking multivariate data analysis of relevant geochemical proxies. For each probable controlling factor, two runs of principal component analysis (PCA) were carried out. The first run compared the geochemical proxies, identifying correlations among the proxies while the second run compared proxies of hydrocarbon-generating potential and probable controlling factors, which include thermal maturity, source input, flora, hydrological, climatic and environmental conditions.

PCA result of 15 selected hydrocarbon-generating potential parameters shows that 100% of the total variance was accounted for by the two rotating components (RCs). Component 1 comprises of Rock-Eval and solvent extraction parameters of hydrocarbon potential. However, TOC and FTIR parameters such as chain length (CL_1 and CL_2), A-factor (A_F), and aliphaticity index (I_{AL}) show weak correlations with other generation potential parameters and thus are loaded on component 2 (Figure 6.46). Hence, 10 parameters, *S*2, GP, HI, BI HI_{max}, QI, A_F, I_{HG}, extract yield, and hydrocarbon concentration was preferred for correlation analyses with proxies of the identified probable controlling factors.

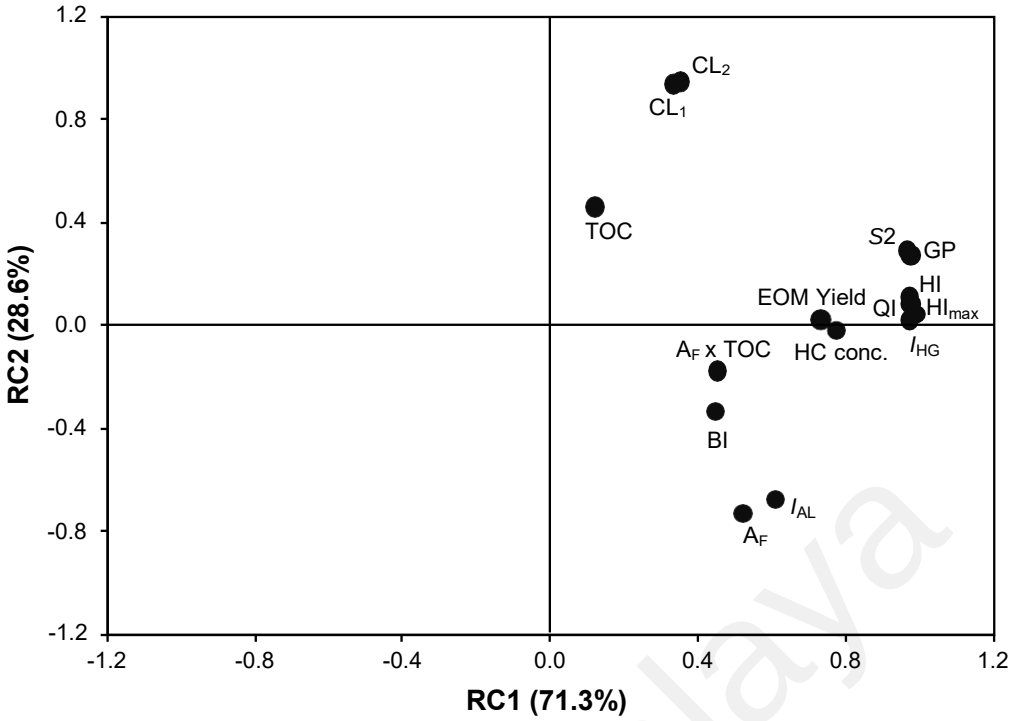

Figure 6.46: Rotated loadings of hydrocarbon potential parameters.

6.7.1 Thermal Maturity

The studied coals are mostly immature. Nonetheless, the Lamja Formation coals from the Benue Trough are in the early maturity stage. Hence, the effect of thermal maturity on the hydrocarbon-generating potential of the coals is evaluated. First, PCA results of the maturity parameters show that molecular parameters are weakly associated with measured vitrinite reflectance (Figure 6.47a).

Additionally, the result of the PCA analysis of thermal maturity and hydrocarbon potential parameters shows that thermal maturity is not a control on the petroleum potential of the studied coals (Figure 6.47b). The two principal components account for 100.0% of the total variance of the data distribution. The thermal maturity parameters are strongly loaded on RC2 while the petroleum potential parameters are positively and strongly loaded on RC1, therefore showing no correlation between thermal maturity and petroleum potential.

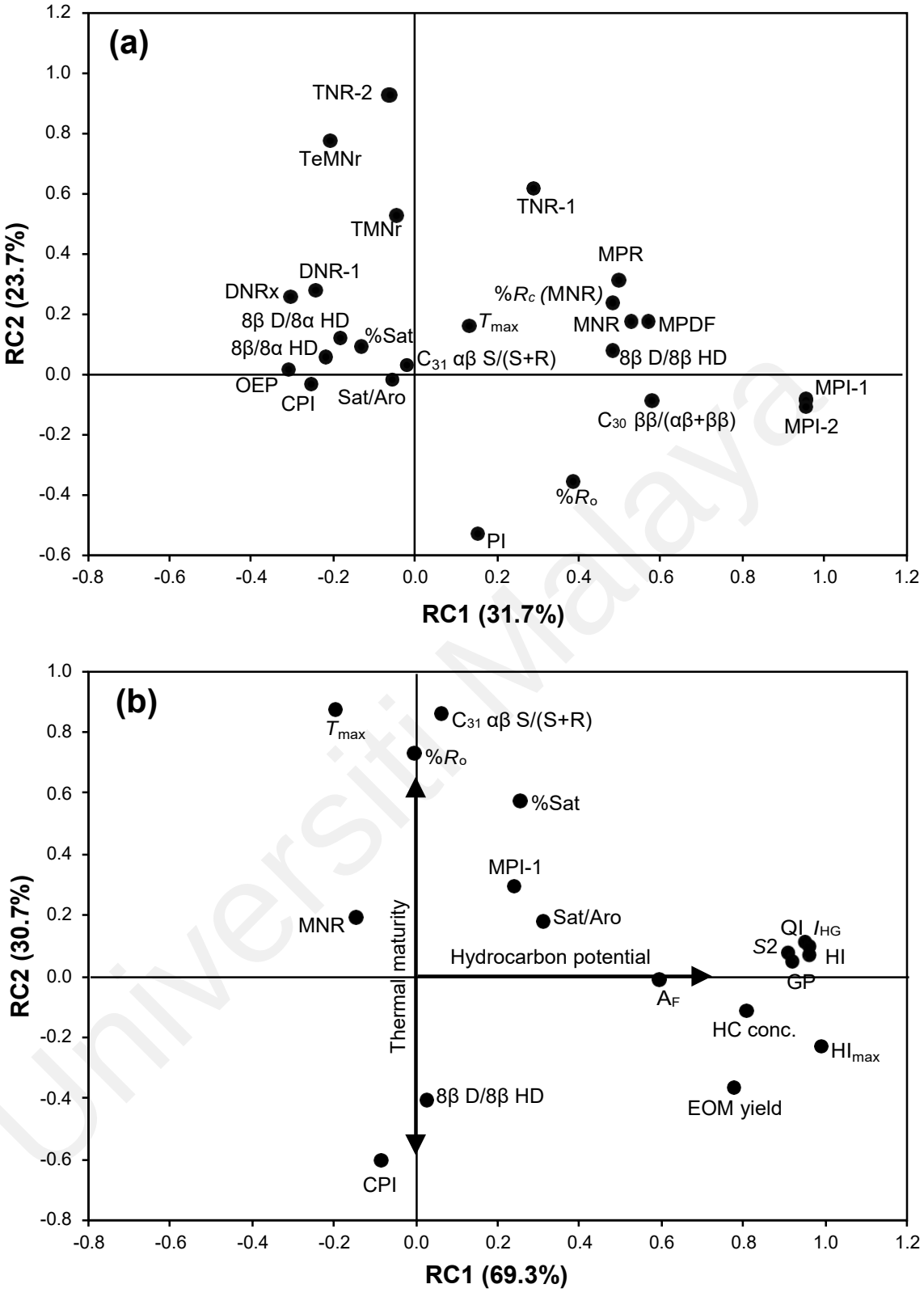

Figure 6.47: Rotated loadings of (a) – maturity parameters, and (b) – maturity and petroleum potential parameters for the studied coals.

6.7.2 Organic Matter Input

Organic matter of marine and terrigenous origin are generally regarded as oil-prone and gas-prone, respectively. Hence, the proportion of marine algal and terrigenous organic matter in kerogens is related to its hydrogen richness. The result of the principal component analysis of organic matter source parameters is shown in Figure 6.48a, with the first two components accounting for 71.6% of the total variance. Clusters 3 and 4 consist of parameters with the highest loadings on RC1 while clusters 1 and 2 are composed of parameters with the highest loadings on RC2. Py-GC source input parameters such as the Type Index and %*n*-1-octene are correlated with both RC1 and RC2, which suggests they are effective indicators of source inputs.

Furthermore, principal component analysis of the petroleum-potential and source input parameters was also carried out. The result indicates that the first two components account for 75.9% of the total variance, with the variance relatively higher for RC1 (41.7%) than RC2 (33.9%). The source input and petroleum potential parameters are mostly loaded on RC2 and RC1, respectively, which indicates little correlation (Figure 6.48b). However, source parameters such as C_F, cadalene/xylene ratio and the Type Index are positively loaded on RC1, suggesting some correlation.

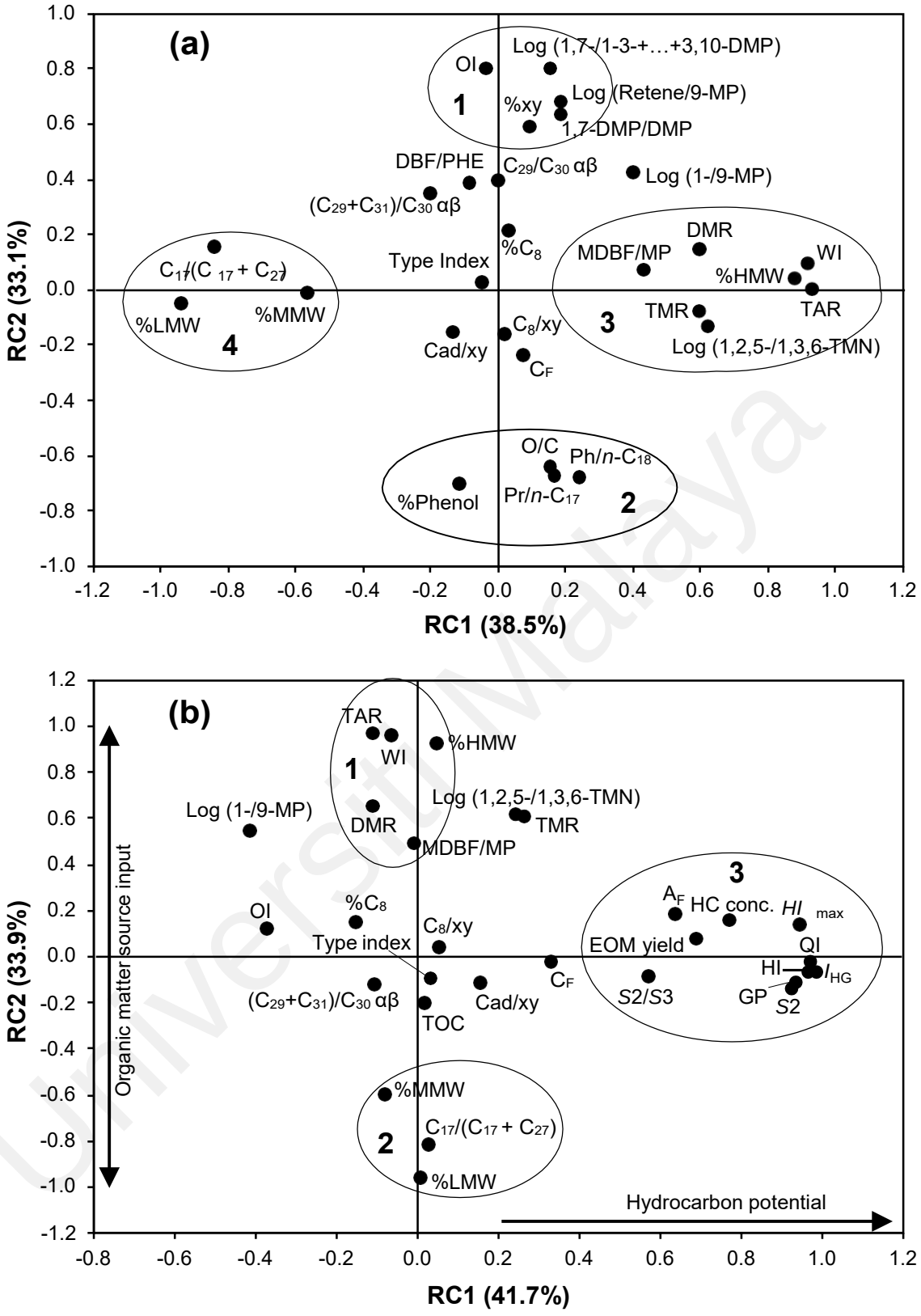

Figure 6.48: Rotated loadings of (a) – source input parameters, and (b) – source input and petroleum potential parameters for, the studied coals.

6.7.3 Paleoflora

The concentration of long-chain *n*-alkanes is generally lower in sediments derived from gymnosperms than from angiosperms (Diefendorf et al., 2011, Diefendorf et al., 2015; Lane, 2017). Hence, flora type has been identified as a possible control on the petroleum potential of coals.

The PCA result of the paleoflora proxies indicates that the proxies are mostly loaded on RC1 (Figure 6.49a). In contrast, HPP, %retene, %cadalene and retene/cadalene ratio are loaded on RC2, showing little or no correlation with paleoflora parameters loaded on RC1. This finding agrees with the conclusion by Grice et al. (2007) of no strong correlation between gymnosperm pollen and the relative abundance of retene. Consequently, the retene and cadalene parameters were excluded from the second principal component analysis of paleoflora and petroleum potential parameters (Figure 6.49b). The plotted rotated components account for 100.0% of the variance with similar variation for the RCs (RC1, 50.6%; RC2, 49.4%).

As shown on the loadings cross-plot in Figure 6.49b, paleoflora proxies (clusters 2 and 3) load strongly on RC1 while the petroleum potential parameters (cluster 1) load positively and strongly on RC2. Hence the loadings plot indicates no correlation between paleoflora and petroleum potential, thus rejecting hypothesis two (H_2).

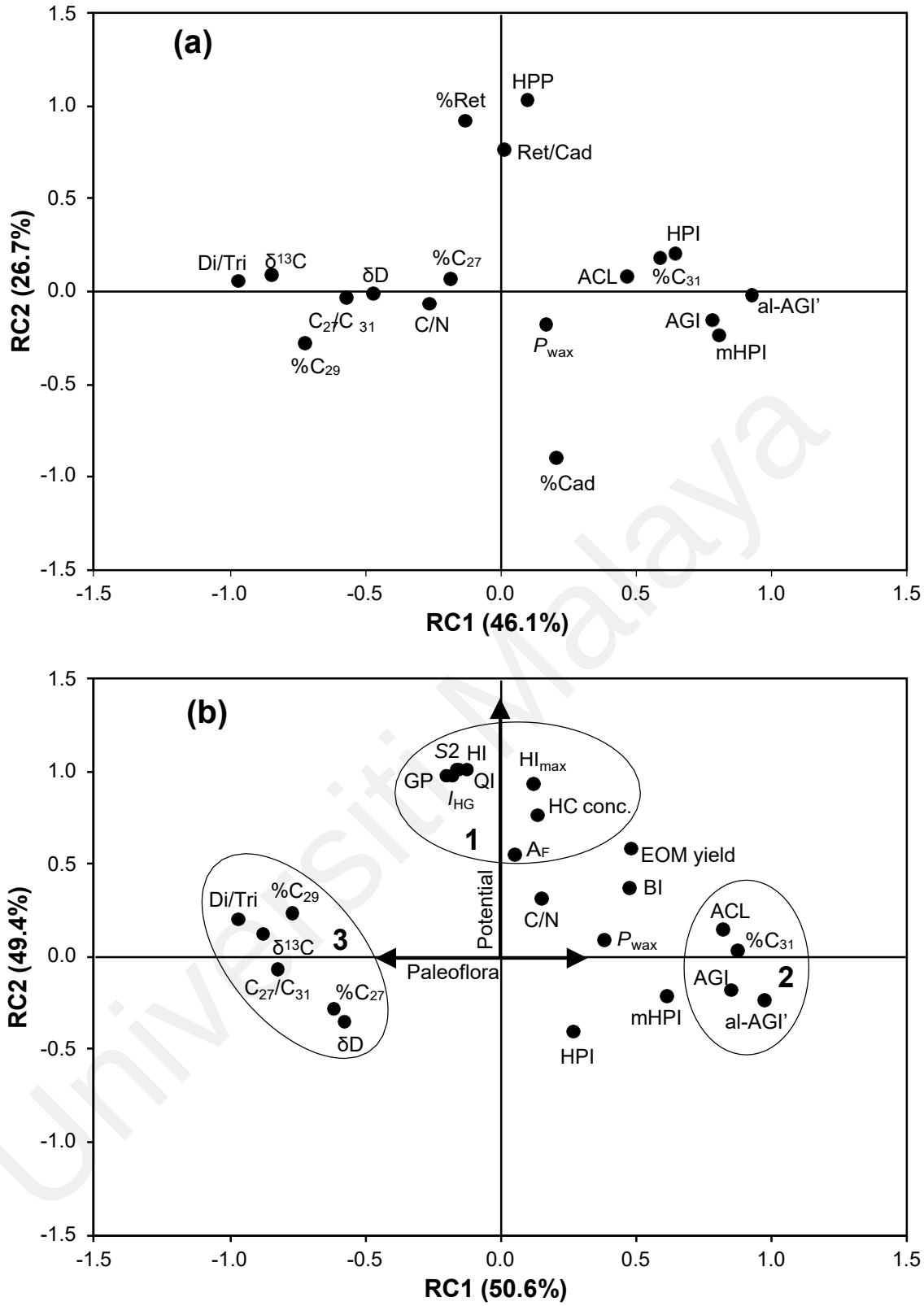

Figure 6.49: Rotated loadings of (a) – paleoflora proxies, and (b) – paleoflora and petroleum potential parameters, for the studied coals.

6.7.4 Paleohydrology and Paleoclimate

As discussed in Section 6.7 above, hydrological and climatic conditions are possible controls on the oil-generating potential of humic coals. PCA result indicates that paleohydrology and paleoclimate proxies are mostly positively loaded on RC1 and RC2, respectively, which both account for 74.7% of the total variation around the RCs (Figure 6.50a). Additionally, elemental paleoclimate ratios Sr/Cu and Sr/Ba are clustered with HPP and %retene and HPP, suggesting that the abundance of retene is more suitable as paleoclimate and not as paleoflora proxy (Hautevelle et al., 2006).

Rotated loadings of the paleohydrology, paleoclimate and petroleum potential parameters indicate three clusters (Figure 6.50b). Two clusters (1 and 3) of paleohydrology and paleoclimate proxies are mostly loaded on the RC2 while one cluster (2) of petroleum potential indicators is loaded positively on RC1 (Figure 6.50b). The plotted rotated components account for 77.5% of the total variation around the RCs. The paleohydrology cluster 1 shows no correlation with the petroleum potential cluster 2. However, paleoclimate cluster 3 is centred around the origin, which is indicative of weak correlations with both RC1 and RC2. This result is therefore suggestive of minor climatic control on the petroleum potential of the studied coals. Furthermore, the result fails to reject hypothesis three (H_3).

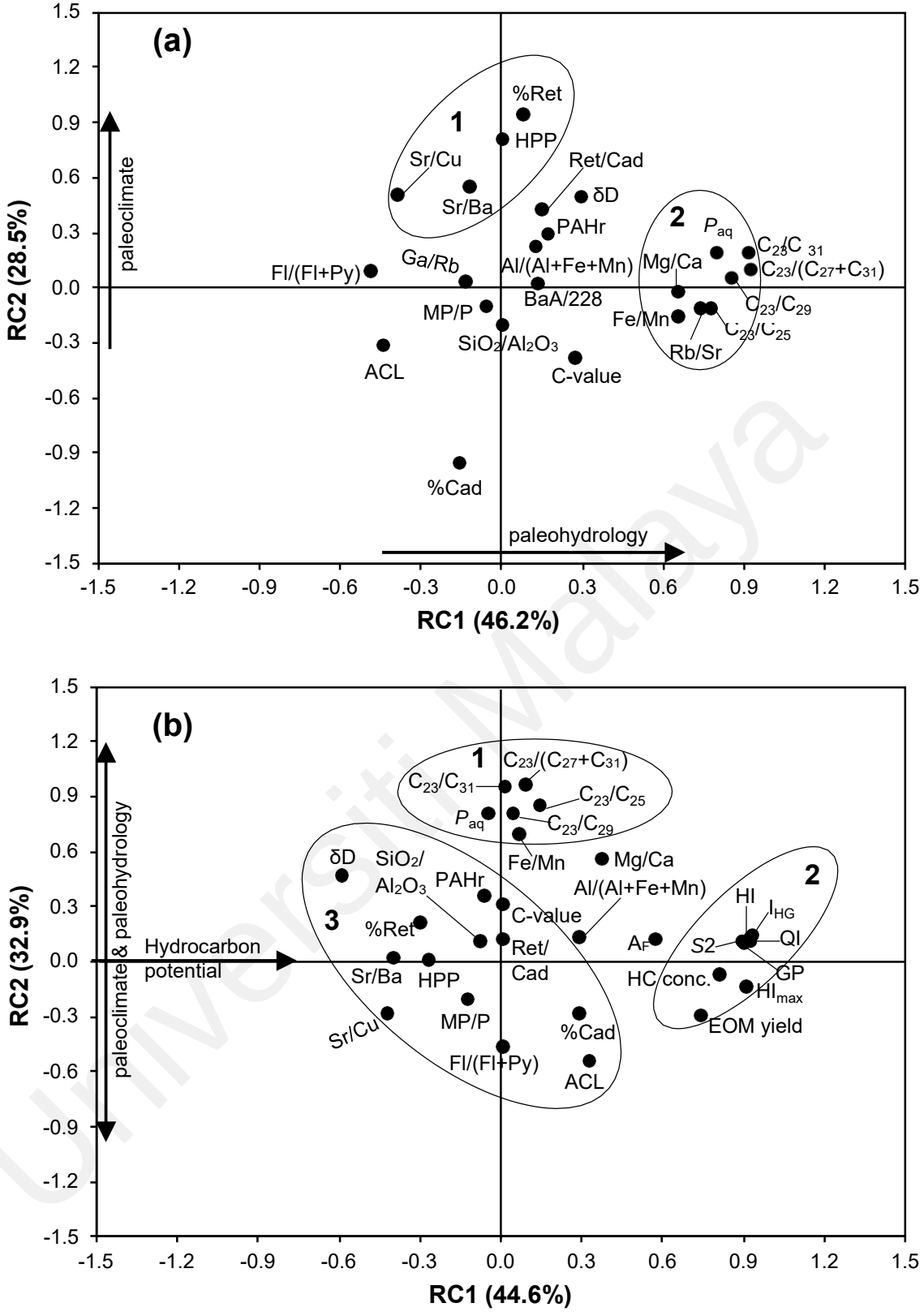

Figure 6.50: Rotated loadings of (a) – paleohydrology and paleoclimate proxies, and (b) – paleohydrology, paleoclimate and petroleum potential parameters, for the studied coals.

6.7.5 Paleodepositional conditions

Paleodepositional conditions such as marine influence and redox setting have been established to influence the petroleum-generating capacity of humic coals (Flores & Sykes, 1996; Sykes et al., 2014). PCA result of the paleodepositional environment proxies indicates that the first two RCs account for 71.9% of the total variance (Figure 6.51a). Proxies of seawater influence such as S_T, %DBT, and TOC/S are highly loaded on RC1 while redox proxies such as V/Cr and V/Ni are loaded on RC2, thus implying no association. However, another redox proxy, Ni/Co loads slightly away from the origins of RC1 and RC2, and plots in cluster 1 with other proxies such as Pr/Ph, Fe/S and pH (Figure 6.51a). This result implies that Ni/Co is a more effective bimetal redox indicator than V/Cr and V/Ni for peat depositional environments.

PCA study of 29 selected parameters of depositional environment and petroleum potential showed that 80.6% of the total variance is accounted for by the first two RCs (RC1, 48.8%; RC2, 31.3%). Additionally, four clusters were identified on the loadings plot of RC1 and RC2 (Figure 6.51b). Cluster 1 includes parameters mostly affected by sea-water influence while cluster 2 consists of petroleum potential indicators. Clusters 1 and 2 are positively and highly loaded on RC2 and RC1, respectively, thus signifying that marine influence has little or no influence on the petroleum potential of the studied humic coals. Clusters 3 and 4 consist mostly of redox and lithology/environment proxies and are loaded positively on RC1 and negatively on RC2 (Figure 6.51b). The result shows that petroleum potential is slightly influenced by redox conditions and depositional lithology/environments.

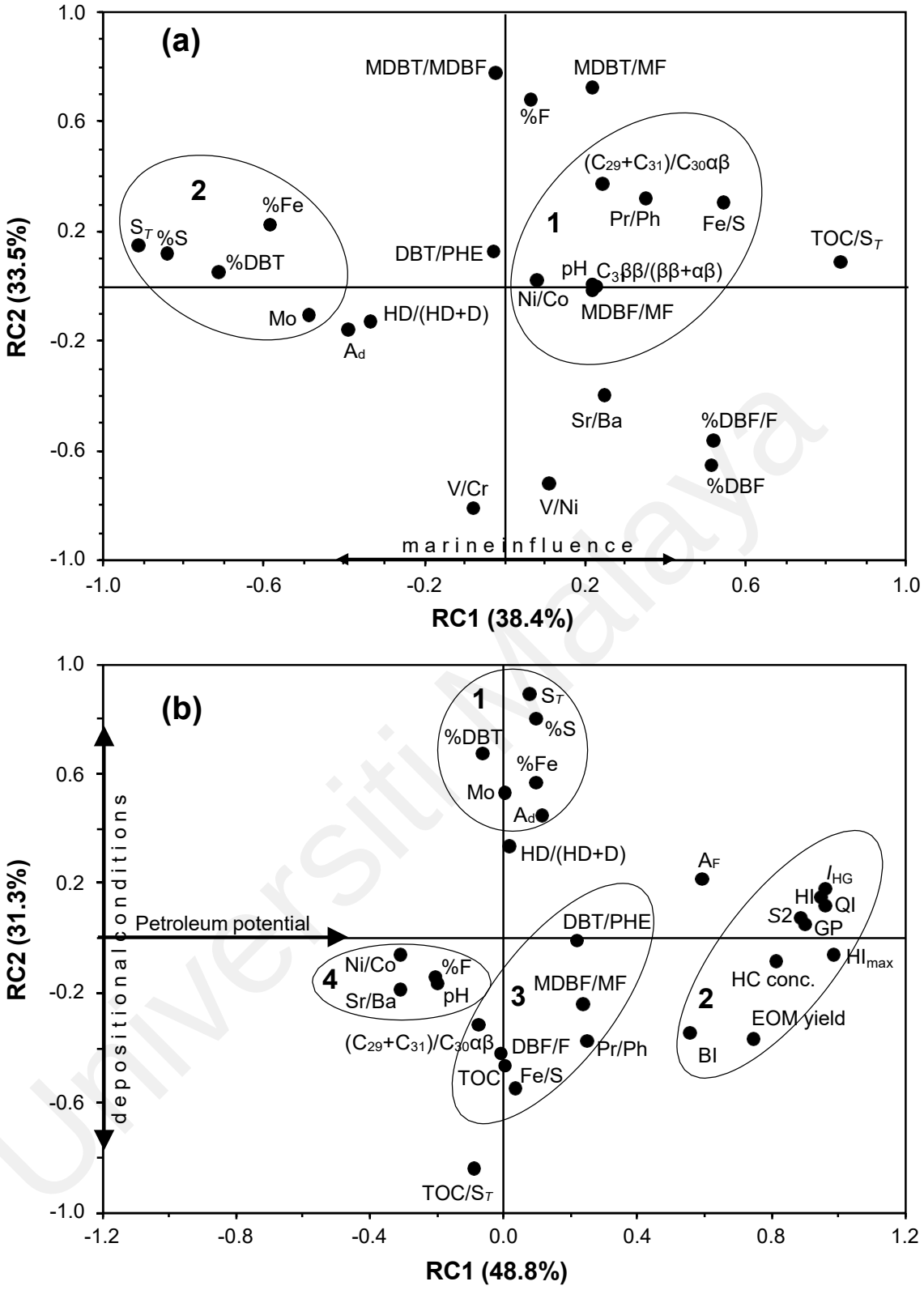

Figure 6.51: Rotated loadings of (a) – proxies for paleodepositional conditions, and (b) – paleodepositional conditions and petroleum potential parameters, for the studied coals.

Overall, the PCA result of 35 selected geochemical parameters indicates that 67.9% of the total variance in the dataset is accounted for by RC1 and RC2 (Figure 6.52; Appendix G). The loadings plot of RC1 and RC2 shows that the petroleum potential of the coals is not influenced by paleoflora, marine incursions, and hydrological conditions of the paleopeats. However, both climatic conditions and depositional sub-environments appear to slightly affect the petroleum potential of the investigated humic coals from Sarawak Basin and Benue Trough.

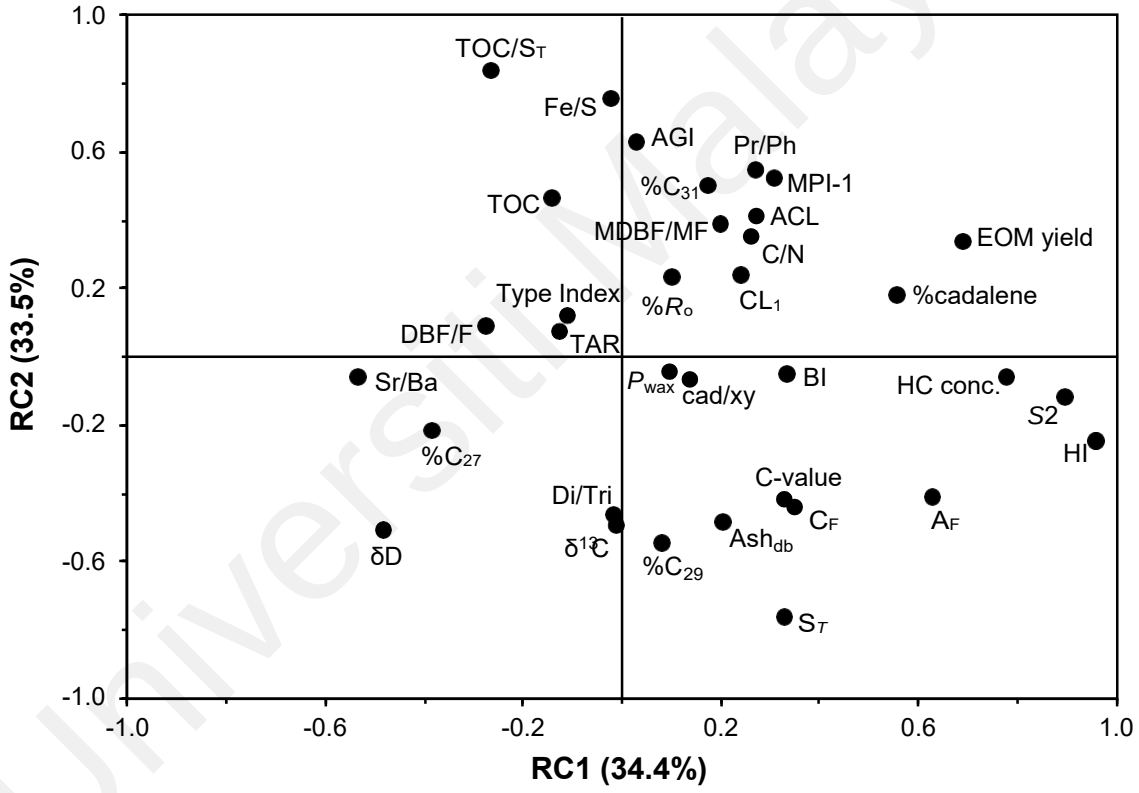

Figure 6.52: Rotated loadings of selected geochemical parameters of the studied coals.

CHAPTER SEVEN: CONCLUSION

7.1 Conclusion

Tertiary Sarawak Basin and Upper Cretaceous Benue Trough coals were analysed using organic geochemical techniques to determine their thermal maturity, petroleum generation potential, organic matter input, kerogen type and paleodepositional conditions. In addition, the paleovegetation and paleoclimate of the study areas were appraised. Furthermore, the distributions of hydrocarbons and non-hydrocarbon compounds in the Sarawak Basin and Benue Trough coals were compared and using statistical analytical tools, the geochemical controls on the distribution of hydrocarbons were determined. The summary of findings is presented in Table 7.1.

The studied Sarawak Basin and Benue Trough coals are mostly thermally immature and ranked as lignite to high volatile bituminous-C. This finding is supported by %Ro values < 0.61%, low T_{max} values < 438 °C, production index < 0.10, strong odd-even predominance, the abundance of hopenes and ββ hopanes, and low aliphatic/aromatic hydrocarbon ratios. Thermal maturity for the Sarawak Basin coals generally increases from Liang Formation to Balingian and Nyalau Formations. For the Benue Trough coals, it increases from Gombe and Agwu Formations to Mamu Formation and Lamja formations. The Lamja Formation coals show relatively higher maturity and are considered at the top of the petroleum generation window. Nonetheless, the Lamja Formation coals are thermally immature for significant hydrocarbon generation and expulsion.

High TOC (> 20 wt. %), genetic potential (> 30 mg HC/g rock), *A*-factor (> 0.4), extract yield (> 10000 ppm) and hydrocarbon concentration (> 1750 ppm) for all the analysed coals indicated excellent potential for petroleum generation. However, the

relatively lower HI values (< 300 mg HC/g TOC) for most of the coals suggest the capacity for gas and mixed condensate oil and gas generation.

Based on interpretations from Rock-Eval, Py-GC, FTIR, elemental and biomarker data, the studied coals are dominated by type-III kerogen but mixed with varying proportions of type II kerogen. Lower values of the Type Index parameter and higher *n*-1-octene/m(+p)-xylene ratios indicate the relatively higher contribution of type II kerogen in the Benue Trough coals. Furthermore, *n*-alkane and aromatic biomarker source proxies for all the coal samples signify the predominant contribution of terrigenous organic matter. However, higher TAR, WI, $C_{27}/(C_{17} + C_{27})$ and C_{31}/C_{17} ratios indicate relatively a higher proportion of terrigenous organic matter in the Sarawak Basin coals. This finding was corroborated by the higher abundance of aromatic compounds such as 1-MP and 1,7-DMP in the Sarawak Basin coals. Additionally, higher DBF/PHE, TMR and DMR values for Sarawak Basin coals, particularly the Liang and Nyalau Formations, evidently indicate greater input of terrigenous organic matter.

Results of the elemental analysis of the coals show that when compared with the published global average abundances, the Sarawak Basin and Benue Trough coals are mostly depleted in major oxides and trace elements, which reflects low input of detrital materials during mire development. Nevertheless, the average concentrations of the major oxides and trace elements are relatively higher in the Benue Trough coals than in the Sarawak Basin coals. Furthermore, provenance proxies based on the ratios of major oxides and trace elements generally indicate the abundance of felsic to intermediate rocks in the Benue Trough source area and mixed but dominantly mafic rocks in the Sarawak Basin source area.

Table 7.1: Summary of findings.

Basin/ Formation	Sarawak Basin			Benue Trough			
	Liang	**Balingian**	**Nyalau**	**Gombe**	**Mamu**	**Lamja**	**Agwu**
Epoch/Age	Late Pliocene	Early Miocene	Oligocene-Early Miocene	Late Cretaceous	Late Cretaceous	Late Cretaceous	Late Cretaceous
Coal rank	Lignite	Lignite to Sub-bituminous B	Lignite to Sub-bituminous B	Lignite	Sub-bituminous C, B	Bituminous C	Lignite to Sub-bituminous C
Thermal maturity	Immature	Immature	Immature	Immature	Immature	Early mature	Immature
Generation capacity	Excellent	Excellent	Excellent	Very good to excellent	Excellent	Excellent	Excellent
Petroleum potential	Gas	Gas to mixed oil and gas	Gas to mixed oil and gas	Gas	Gas to mixed oil and gas	Gas	Gas
Kerogen type	Predominantly Type III	Predominantly Type III with considerable Type II	Predominantly Type III	Predominantly Type III with considerable Type II and Type IV	Predominantly Type III	Predominantly Type III with considerable Type II	Predominantly Type III
Paleovegetation	Angiosperms	Angiosperms	Angiosperms	Gymnosperms	Gymnosperms	Gymnosperms	Gymnosperms
Paleomire setting	Dominantly ombrotrophic	ombrotrophic and rheotrophic	ombrotrophic and rheotrophic	Dominantly rheotrophic	Dominantly rheotrophic	Dominantly rheotrophic	Dominantly rheotrophic
Paleoclimate	Warm, Humid, strongly seasonal	Warm, Humid	Warm, Humid with wet-dry conditions	Cooler, Humid with drier conditions	Cooler, Humid	Warm, Humid	Warm, Humid
Paleoredox	Suboxic to dysoxic	Dysoxic to oxic	Oxic	Dysoxic to oxic	Dysoxic to oxic	Dysoxic to oxic	Dysoxic to oxic
Marine influence	Slight	None	None	Slight	Strong	Slight	Strong
Paleoenvironment	Lower delta plain	Lower delta plain	Upper delta plain	Lower delta plain	Lower delta plain	Lower delta plain	Lower delta plain

Stable bulk carbon isotopic ratios and the distribution of aliphatic and aromatic terpenoid biomarkers in the coals both indicate that paleovegetation of the Benue Trough was dominated by gymnosperm taxa while angiosperm taxa predominated in the Sarawak Basin. Additionally, the distribution of combustion-derived polycyclic aromatic hydrocarbons (PAHs) signifies a mixed to dominant origin of pyrogenic sources. However, the predominant input of terrigenous organic matter, a higher proportion of unburnt organic matter and low abundances of 6- and 7-ring PAHs such as benzo*[ghi]*perylene and coronene in the Benue Trough coals all suggest the occurrence of low-temperature wildfires and thus, prevailing humid paleoclimate with frequent drying episodes. In contrast, the absence of ≥ 6-ring PAHs in the Sarawak Basin coals signifies a mostly humid climate. However, *n*-Alkane and elemental paleoclimate proxies indicate that the Nyalau and Balingian Formation coals were deposited under humid and warm paleoclimate with wet-dry conditions in the Early Miocene while the Liang Formation coals were deposited under humid but strongly seasonal paleoclimate in the Late Pliocene.

The relative abundances of heterocyclic aromatic hydrocarbon imply freshwater to brackish-water lacustrine environment for the Benue Trough coals and freshwater- to lacustrine-swamp environment for the Sarawak Basin coals. Additionally, calculated DBT/PHE and Pr/Ph ratios for the Sarawak Basin and Benue Trough generally indicate deposition under oxic and sub-oxic conditions of a deltaic system, respectively. Sulfur content and bimetal ratios indicate slight to strong marine influence on the Benue Trough coal seams, and little or no marine influence on the Sarawak Basin coals. Within the Sarawak Basin, the Nyalau Formation coals were deposited in a freshwater environment with no marine influence while the Liang and Balingian Formation coals were deposited in fresh-water to mildly brackish-water swamp environment.

Principal component analysis result of over 100 geochemical proxies of thermal maturity, organic matter source input, paleoflora, paleoclimate and paleoredox indicates that the petroleum potential of the coals is not influenced by thermal maturity, source input, marine incursions, peat hydrology and paleoflora. Conversely, the fluctuating paleoclimatic conditions and distinct sub-environments appear to be the controlling influence on the oil generation capacity of the coals.

7.2 Limitations and Future Work

This research work employed various geochemical analytical techniques to resolve the research questions posed in Section 1.2. Nevertheless, the work was limited in a few ways. First, the relatively smaller sample size of the Benue Trough coals makes the interpretations quite tentative. Second, the work focused comprehensively on the geochemistry approach, excluding palynology and petrography.

Hence, for future work, facies association studies to identify the different facies and petrographic studies on thin sections and polished blocks to observe the shape of the minerals are suggested. The combination of this new information will provide valuable insights into the time of mineral formation and thus depositional environments. Additionally, pollen taxa of the coals will improve discussions on paleovegetation and thus paleoclimate. Bulk oxygen isotopic ratio, and carbon and hydrogen isotope ratios of *n*-alkanes will also improve discussions on paleoclimate while compositional kinetics study on the coals will provide supporting information on the mechanism and timing of hydrocarbon generation and expulsion.

REFERENCES

Abdullah, W. H. (1997). Common liptinitic constituents of Tertiary coals from the Bintulu and Merit-Pila coalfield, Sarawak and their relation to oil generation from coal. *Geol. Soc. Malaysia Bulletin*, *41*, 85–94.

Abdullah, W. H. (2001). A petrographic comparison of oil-generating coals from the tropics and non oil-generating coals from the arctic. In *Geological Society of Malaysia Annual Geological Conference* (pp. 33–38). Pangkor Island.

Abdullah, W. H. (2002). Organic petrological characteristics of limnic and paralic coals of Sarawak. In *Geological Society of Malaysia Annual Geological Conference* (pp. 65–70). Kota Bharu.

Abdullah, W. H. (2003). Coaly source rocks of NW Borneo: role of suberinite and bituminite in oil generation and expulsion. *Geol. Soc. Malaysia Bulletin*, *47*, 153–163.

Abubakar, M. B., Dike, E. F. C., Obaje, N. G., Wehner, H., & Jauro, A. (2008). Petroleum prospectivity of Cretaceous formations in the Gongola Basin, Upper Benue Trough, Nigeria: an organic geochemical perspective on a migrated oil controversy. *Journal of Petroleum Geology*, *31*(4), 387–407.

Adedosu, T. A., Alao, S. A., Ajayi, T. R., & Akinlua, A. (2020). Petroleum potential of Gombe Formation, Kolmani River-1 Well Gongola Basin, NE Nigeria. *Journal of Chemical Society of Nigeria*, *45*(5), 1–13.

Adedosu, Taofik A., Sonibare, O. O., Tuo, J., & Ekundayo, O. (2012). Biomarkers, carbon isotopic composition and source rock potentials of Awgu coals, middle Benue trough, Nigeria. *Journal of African Earth Sciences*, *66–67*, 13–21.

Adegoke, A. K., Abdullah, W. H., Hakimi, M. H., Sarki Yandoka, B. M., Mustapha, K. A., & Aturamu, A. O. (2014). Trace elements geochemistry of kerogen in Upper Cretaceous sediments, Chad (Bornu) Basin, northeastern Nigeria: Origin and paleo-redox conditions. *Journal of African Earth Sciences*, *100*, 675–683.

Adegoke, A. K., Abdullah, W. H., Yandoka, B. M. S., & Abubakar, M. B. (2015). Kerogen characterisation and petroleum potential of the late cretaceous sediments, chad (Bornu) basin, northeastern Nigeria. *Bulletin of the Geological Society of Malaysia*, *61*, 29–42.

Ahmed, M., Volk, H., George, S. C., Faiz, M., & Stalker, L. (2009). Generation and expulsion of oils from Permian coals of the Sydney Basin, Australia. *Organic Geochemistry*, *40*(7), 810–831.

Akande, S. O., Egenhoff, S. O., Obaje, N. G., Ojo, O. J., Adekeye, O. A., & Erdtmann, B. D. (2012). Hydrocarbon potential of Cretaceous sediments in the Lower and Middle Benue Trough, Nigeria: Insights from new source rock facies evaluation. *Journal of African Earth Sciences*, *64*, 34–47.

Akande, S. O., Lewan, M. D., Egenhoff, S., Adekeye, O., Ojo, O. J., & Peterhansel, A. (2015). Source rock potential of lignite and interbedded coaly shale of the Ogwashi-Asaba Formation, Anambra basin as determined by sequential hydrous pyrolysis. *International Journal of Coal Geology*, *150–151*, 224–237.

Akinyemi, S. A., Adebayo, O. F., Nyakuma, B. B., Adegoke, A. K., Aturamu, O. A., OlaOlorun, O. A., … Jauro, A. (2020). Petrology, physicochemical and thermal analyses of selected cretaceous coals from the Benue Trough Basin in Nigeria. *International Journal of Coal Science and Technology*, *7*(1), 26–42.

Akinyemi, Segun A., Adebayo, O. F., Madukwe, H. Y., Kayode, A. T., Aturamu, A. O., OlaOlorun, O. A., … Hower, J. C. (2022). Elemental geochemistry and organic facies of selected cretaceous coals from the Benue Trough basin in Nigeria: Implication for paleodepositional environments. *Marine and Petroleum Geology*, *137*, 105490.

Akinyemi, Segun A., Nyakuma, B. B., Adebayo, O. F., Kayode, A. T., Jauro, A., OlaOlorun, O. A., … Hower, J. C. (2021). Geochemistry, mineralogy and thermal analyses of Cretaceous coals from the Benue Trough basin Nigeria: Reconnaissance assessments. *Journal of African Earth Sciences*, *178*, 104167.

Alexander, G., Hazai, I., Grimalt, J., & Albaigés, J. (1987). Occurrence and transformation of phyllocladanes in brown coals from Nograd Basin, Hungary. *Geochimica et Cosmochimica Acta*, *51*(8), 2065–2073.

Alexander, R., Kagi, R. I., Rowland, S. J., Sheppard, P. N., & Chirila, T. V. (1985). The effects of thermal maturity on distributions of dimethylnaphthalenes and trimethylnaphthalenes in some Ancient sediments and petroleums. *Geochimica et Cosmochimica Acta*, *49*(2), 385–395.

Alexander, R., Kagi, R., & Noble, R. (1983). Identification of the bicyclic sesquiterpenes drimane and eudesmane in petroleum. *Journal of the Chemical Society, Chemical Communications*, (5), 226–228.

Algeo, T. J., & Liu, J. (2020). A re-assessment of elemental proxies for paleoredox analysis. *Chemical Geology*, *540*, 119549.

Algeo, T. J., & Maynard, J. B. (2004). Trace-element behavior and redox facies in core shales of Upper Pennsylvanian Kansas-type cyclothems. *Chemical Geology*, *206*(3–4), 289–318.

Ameh, E. G. (2019). Geochemistry and multivariate statistical evaluation of major oxides, trace and rare earth elements in coal occurrences and deposits around Kogi east, Northern Anambra Basin, Nigeria. *International Journal of Coal Science and Technology*, *6*(2), 260–273.

Amir Hassan, M. H., Johnson, H. D., Allison, P. A., & Abdullah, W. H. (2013). Sedimentology and stratigraphic development of the upper Nyalau Formation (Early Miocene), Sarawak, Malaysia: A mixed wave- and tide-influenced coastal system. *Journal of Asian Earth Sciences*, *76*, 301–311.

Amir Hassan, M. H., Johnson, H. D., Allison, P. A., & Abdullah, W. H. (2017). Sedimentology and stratigraphic architecture of a Miocene retrogradational, tide-dominated delta system: Balingian Province, offshore Sarawak, Malaysia. *Geological Society, London, Special Publications*, *444*(1), 215–250.

Anderson, J. A. R. (1964). Peat swamps of Sarawak and Brunei. *Journal of Tropical Geography*, *18*, 7–16.

Andersson, R. A., Kuhry, P., Meyers, P., Zebühr, Y., Crill, P., & Mörth, M. (2011). Impacts of paleohydrological changes on n-alkane biomarker compositions of a Holocene peat sequence in the eastern European Russian Arctic. *Organic Geochemistry*, *42*(9), 1065–1075.

Asahina, K., & Suzuki, N. (2018). Methylated naphthalenes as indicators for evaluating the source and source rock lithology of degraded oils. *Organic Geochemistry*, *124*, 46–62.

Asif, M., & Wenger, L. M. (2019). Heterocyclic aromatic hydrocarbon distributions in petroleum: A source facies assessment tool. *Organic Geochemistry*, *137*, 103896.

Awang Jamil, A. S., Anwar, M. L., & Seah, E. P. K. (1991). Geochemistry of selected crude oils from Sabah and Sarawak. *Bulletin of the Geological Society of Malaysia*, *28*, 123–149.

Ayinla, H. A., Abdullah, W. H., Makeen, Y. M., Abubakar, M. B., Jauro, A., Sarki Yandoka, B. M., … Zainal Abidin, N. S. (2017a). Source rock characteristics, depositional setting and hydrocarbon generation potential of Cretaceous coals and organic rich mudstones from Gombe Formation, Gongola Sub-basin, Northern Benue Trough, NE Nigeria. *International Journal of Coal Geology*, *173*, 212–226.

Ayinla, H. A., Abdullah, W. H., Makeen, Y. M., Abubakar, M. B., Jauro, A., Sarki Yandoka, B. M., & Zainal Abidin, N. S. (2017b). Petrographic and geochemical characterization of the Upper Cretaceous coal and mudstones of Gombe Formation, Gongola sub-basin, northern Benue trough Nigeria: Implication for organic matter preservation, paleodepositional environment and tectonic settings. *International Journal of Coal Geology*, *180*, 67–82.

Baas, M., Pancost, R., Van Geel, B., & Sinninghe Damsté, J. S. (2000). A comparative study of lipids in Sphagnum species. *Organic Geochemistry*, *31*(6), 535–541.

Bai, Y., Liu, Z., Sun, P., Liu, R., Hu, X., Zhao, H., & Xu, Y. (2015). Rare earth and major element geochemistry of Eocene fine-grained sediments in oil shale- and coal-bearing layers of the Meihe Basin, Northeast China. *Journal of Asian Earth Sciences*, *97*(PA), 89–101.

Barry, J. C., Morgan, M. E., Flynn, L. J., Pilbeam, D., Behrensmeyer, A. K., Raza, S. M., … Kelley, J. (2002). Faunal and environmental change in the late Miocene Siwaliks of northern Pakistan. *Paleobiology*, *28*(sp3), 1–71.

Bastow, T. P., Singh, R. K., van Aarssen, B. G. K., Alexander, R., & Kagi, R. I. (2001). 2-Methylretene in sedimentary material: A new higher plant biomarker. *Organic Geochemistry*, *32*(10), 1211–1217.

Baydjanova, S., & George, S. C. (2019). Depositional environment, organic matter sources, and variable 17α(H)-diahopane distribution in Early Permian samples, southern Sydney Basin, Australia. *Organic Geochemistry*, *131*, 60–75.

Bechtel, A., Gruber, W., Sachsenhofer, R. F., Gratzer, R., Lücke, A., & Püttmann, W. (2003). Depositional environment of the Late Miocene Hausruck lignite (Alpine Foreland Basin): Insights from petrography, organic geochemistry, and stable carbon isotopes. *International Journal of Coal Geology*, *53*(3), 153–180.

Bechtel, A., Gruber, W., Sachsenhofer, R. F., Gratzer, R., & Püttmann, W. (2001). Organic geochemical and stable carbon isotopic investigation of coals formed in low-lying and raised mires within the Eastern Alps (Austria). *Organic Geochemistry*, *32*(11), 1289–1310.

Bechtel, A., Reischenbacher, D., Sachsenhofer, R. F., Gratzer, R., & Lücke, A. (2007). Paleogeography and paleoecology of the upper Miocene Zillingdorf lignite deposit (Austria). *International Journal of Coal Geology*, *69*(3), 119–143.

Bechtel, Achim, Gratzer, R., Sachsenhofer, R. F., Gusterhuber, J., Lücke, A., & Püttmann, W. (2008). Biomarker and carbon isotope variation in coal and fossil wood of Central Europe through the Cenozoic. *Palaeogeography, Palaeoclimatology, Palaeoecology*, *262*(3–4), 166–175.

Behar, F., Beaumont, V., & De B. Penteado, H. L. (2001). Rock-Eval 6 Technology: Performances and Developments. *Oil & Gas Science and Technology*, *56*(2), 111–134.

Benkhelil, J. (1989). The origin and evolution of the Cretaceous Benue Trough (Nigeria). *Journal of African Earth Sciences*, *8*(2–4), 251–282.

Bennett, W. W., & Canfield, D. E. (2020). Redox-sensitive trace metals as paleoredox proxies: A review and analysis of data from modern sediments. *Earth-Science Reviews*, *204*, 103175.

Bi, X., Sheng, G., Liu, X., Li, C., & Fu, J. (2005). Molecular and carbon and hydrogen isotopic composition of n-alkanes in plant leaf waxes. *Organic Geochemistry*, *36*(10), 1405–1417.

Bingham, E. M., McClymont, E. L., Väliranta, M., Mauquoy, D., Roberts, Z., Chambers, F. M., … Evershed, R. P. (2010). Conservative composition of n-alkane biomarkers in Sphagnum species: Implications for palaeoclimate reconstruction in ombrotrophic peat bogs. *Organic Geochemistry*, *41*(2), 214–220.

Biswas, S., Varma, A. K., Kumar, M., Mani, D., Saxena, V. K., & Mishra, V. (2020). Influence of geochemical, organo-petrographical and palynofacies assemblages on hydrocarbon generation: A study from upper Oligocene coal and shale of the Makum Coal Basin, Assam, India. *Marine and Petroleum Geology*, *114,* 104206.

Boreham, C. J., Blevin, J. E., Radlinski, A. P., & Trigg, K. R. (2003). Coal as a source of oil and gas: a case study from the Bass Basin, Australia. *APPEA Journal*, *43*(1), 117–148.

Bourbonniere, R. A., & Meyers, P. A. (1996). Sedimentary geolipid records of historical changes in the watersheds and productivities of Lakes Ontario and Erie. *Limnology and Oceanography*, *41*(2), 352–359.

Bray, E. E., & Evans, E. D. (1961). Distribution of n-paraffins as a clue to recognition of source beds. *Geochimica et Cosmochimica Acta*, *22*(1), 2–15.

Breitfeld, H. T., Hennig-Breitfeld, J., BouDagher-Fadel, M. K., Hall, R., & Galin, T. (2020). Oligocene-Miocene drainage evolution of NW Borneo: Stratigraphy, sedimentology and provenance of Tatau-Nyalau province sediments. *Journal of Asian Earth Sciences*, *195*, 104331.

Budzinski, H., Garrigues, P., Connan, J., Devillers, J., Domine, D., Radke, M., & Oudins, J. L. (1995). Alkylated phenanthrene distributions as maturity and origin indicators in crude oils and rock extracts. *Geochimica et Cosmochimica Acta*, *59*(10), 2043–2056.

Bush, R. T., & McInerney, F. A. (2013). Leaf wax n-alkane distributions in and across modern plants: Implications for paleoecology and chemotaxonomy. *Geochimica et Cosmochimica Acta*, *117*, 161–179.

Bush, R. T., & McInerney, F. A. (2015). Influence of temperature and C4 abundance on n-alkane chain length distributions across the central USA. *Organic Geochemistry*, *79*, 65–73.

Cameron, C. C., Esterle, J. S., & Palmer, C. A. (1989). The geology, botany and chemistry of selected peat-forming environments from temperate and tropical latitudes. *International Journal of Coal Geology*, *12*(1–4), 105–156.

Cao, J., Wu, M., Chen, Y., Hu, K., Bian, L., Wang, L., & Zhang, Y. (2012). Trace and rare earth element geochemistry of Jurassic mudstones in the northern Qaidam Basin, northwest China. *Chemie Der Erde*, *72*(3), 245–252.

Carvajal-Ortiz, H., & Gentzis, T. (2015). Critical considerations when assessing hydrocarbon plays using Rock-Eval pyrolysis and organic petrology data: Data quality revisited. *International Journal of Coal Geology*, *152*, 113–122.

Casagrande, D. J. (1987). Sulfur in peat and coal. *Geological Society Special Publication*, *32*, 87–105.

Cesar, J., & Grice, K. (2019). Molecular fingerprint from plant biomarkers in Triassic-Jurassic petroleum source rocks from the Dampier sub-Basin, Northwest Shelf of Australia. *Marine and Petroleum Geology*, *110*, 189–197.

Chakhmakhchev, A., Suzuki, M., & Takayama, K. (1997). Distribution of alkylated dibenzothiophenes in petroleum as a tool for maturity assessments. *Organic Geochemistry*, *26*(7–8), 483–489.

Chakhmakhchev, A., & Suzuki, N. (1995). Aromatic sulfur compounds as maturity indicators for petroleums from the Buzuluk depression, Russia. *Organic Geochemistry*, *23*(7), 617–625.

Challinor, J. M. (2001). Review: The development and applications of thermally assisted hydrolysis and methylation reactions. *Journal of Analytical and Applied Pyrolysis*, *61*(1–2), 3–34.

Chamberlain, C. P., Winnick, M. J., Mix, H. T., Chamberlain, S. D., & Maher, K. (2014). The impact of neogene grassland expansion and aridification on the isotopic composition of continental precipitation. *Global Biogeochemical Cycles*, *28*(9), 992–1004.

Chattopadhyay, A., & Dutta, S. (2014). Higher plant biomarker signatures of Early Eocene sediments of North Eastern India. *Marine and Petroleum Geology*, *57*, 51–67.

Chen, S. P. (1986). Coal potential and exploration in Sarawak. *Geol. Soc. Malaysia Bulletin*, *20*, 649–665.

Chen, S. P. (1993). Coal as an energy resource in Malaysia. *Geol. Soc. Malaysia Bulletin*, *33*, 399–410.

Chou, C. L. (2012). Sulfur in coals: A review of geochemistry and origins. *International Journal of Coal Geology*, *100*, 1–13.

Clayton, J. L., Rice, D. D., & Michael, G. E. (1991). Oil-generating coals of the San Juan Basin, New Mexico and Colorado, U.S.A. *Organic Geochemistry*, *17*(6), 735–742.

Collinson, M. E., Van Bergen, P. F., Scott, A. C., & De Leeuw, J. W. (1994). The oil-generating potential of plants from coal and coal-bearing strata through time: a review with new evidence from Carboniferous plants. *Geological Society, London, Special Publications*, *77*(1), 31–70.

Courel, L. (1989). Organics versus clastics: conditions necessary for peat (coal) development. *International Journal of Coal Geology*, *12*(1–4), 193–207.

Cranwell, P. A., Eglinton, G., & Robinson, N. (1987). Lipids of aquatic organisms as potential contributors to lacustrine sediments-II. *Organic Geochemistry*, *11*(6), 513–527.

Curry, D. J., Emmett, J. K., & Hunt, J. W. (1994). Geochemistry of aliphatic-rich coals in the Cooper Basin, Australia and Taranaki Basin, New Zealand: implications for the occurrence of potentially oil-generative coals. *Geological Society, London, Special Publications*, *77*(1), 149–181.

Dai, S., Bechtel, A., Eble, C. F., Flores, R. M., French, D., Graham, I. T., … O'Keefe, J. M. K. (2020). Recognition of peat depositional environments in coal: A review. *International Journal of Coal Geology*, *219*, 103383.

Dai, S., Ren, D., Chou, C. L., Finkelman, R. B., Seredin, V. V., & Zhou, Y. (2012). Geochemistry of trace elements in Chinese coals: A review of abundances, genetic types, impacts on human health, and industrial utilization. *International Journal of Coal Geology*, *94*, 3–21.

Dai, S., Ren, D., Tang, Y., Shao, L., & Li, S. (2002). Distribution, isotopic variation and origin of sulfur in coals in the Wuda coalfield, Inner Mongolia, China. *International Journal of Coal Geology*, *51*(4), 237–250.

Dawson, D., Grice, K., Wang, S. X., Alexander, R., & Radke, J. (2004). Stable hydrogen isotopic composition of hydrocarbons in torbanites (Late Carboniferous to Late Permian) deposited under various climatic conditions. *Organic Geochemistry*, *35*(2), 189–197.

de Silva, S. (1986). Stratigraphy of the South Mukah - Balingian region, Sarawak. *Warta Geologi, Geological Society of Malaysia Newsletter*, *12*(5), 215–220.

DeConto, R. M., Hay, W. W., Thompson, S. L., & Bergengren, J. (1999). Late Cretaceous climate and vegetation interactions: Cold continental interior paradox. *Special Paper of the Geological Society of America*, *332*, 391–406.

Dehmer, J. (1993). Petrology and organic geochemistry of peat samples from a raised bog in Kalimantan (Borneo). *Organic Geochemistry*, *20*(3), 349–362.

Dehmer, J. (1995). Petrological and organic geochemical investigation of recent peats with known environments of deposition. *International Journal of Coal Geology*, *28*(2–4), 111–138.

Dellwig, O., Watermann, F., Brumsack, H. J., Gerdes, G., & Krumbein, W. E. (2001). Sulfur and iron geochemistry of Holocene coastal peats (NW Germany): A tool for palaeoenvironmental reconstruction. *Palaeogeography, Palaeoclimatology, Palaeoecology*, *167*(3–4), 359–379.

Dembicki, H. (2009). Three common source rock evaluation errors made by geologists during prospect or play appraisals. *AAPG Bulletin*, *93*(3), 341–356.

Didyk, B. M., Simoneit, B. R. T., Brassell, S. C., & Eglinton, G. (1978). Organic geochemical indicators of palaeoenvironmental conditions of sedimentation. *Nature*, *272*(5650), 216–222.

Diefendorf, A. F., Freeman, K. H., Wing, S. L., & Graham, H. V. (2011). Production of n-alkyl lipids in living plants and implications for the geologic past. *Geochimica et Cosmochimica Acta*, *75*(23), 7472–7485.

Diefendorf, A. F., & Freimuth, E. J. (2017). Extracting the most from terrestrial plant-derived n-alkyl lipids and their carbon isotopes from the sedimentary record: A review. *Organic Geochemistry*, *103*, 1–21.

Diefendorf, A. F., Leslie, A. B., & Wing, S. L. (2015). Leaf wax composition and carbon isotopes vary among major conifer groups. *Geochimica et Cosmochimica Acta*, *170*, 145–156.

Diessel, C. F. K. (1992). *Coal-Bearing Depositional Systems*. *Coal-Bearing Depositional Systems* (1st ed.). Springer-Verlag.

Donahue, C. J., & Rais, E. A. (2009). Proximate analysis of coal. *Journal of Chemical Education*, *86*(2), 222–224.

Du Bois, E. P. (1985). Review of principal hydrocarbon-bearing basins around the South China Sea. *Bulletin of the Geological Society of Malaysia*, *18*, 167–209.

Duan, Y., & He, J. (2011). Distribution and isotopic composition of n-alkanes from grass, reed and tree leaves along a latitudinal gradient in China. *Geochemical Journal*, *45*(3), 199–207.

Duan, Y., Wu, Y., Cao, X., Zhao, Y., & Ma, L. (2014). Hydrogen isotope ratios of individual n-alkanes in plants from Gannan Gahai Lake (China) and surrounding area. *Organic Geochemistry*, *77*, 96–105.

Duan, Y., & Xu, L. (2012). Distributions of n-alkanes and their hydrogen isotopic composition in plants from Lake Qinghai (China) and the surrounding area. *Applied Geochemistry*, *27*(3), 806–814.

Durand, B., & Paratte, M. (1983). Oil potential of coals: a geochemical approach. *Geological Society, London, Special Publications*, *12*(1), 255–265.

Edegbai, A. J., Schwark, L., & Oboh-Ikuenobe, F. E. (2019a). A review of the latest Cenomanian to Maastrichtian geological evolution of Nigeria and its stratigraphic and paleogeographic implications. *Journal of African Earth Sciences*, *150*, 823–837.

Edegbai, A. J., Schwark, L., & Oboh-Ikuenobe, F. E. (2019b). Campano-Maastrichtian paleoenvironment, paleotectonics and sediment provenance of western Anambra Basin, Nigeria: Multi-proxy evidences from the Mamu Formation. *Journal of African Earth Sciences*, *156*, 203–239.

Ehinola, O. A., Ekweozor, C. M., Oros, D. R., & Simoneit, B. R. T. (2002). Geology, geochemistry and biomarker evaluation of Lafia-Obi coal, Benue Trough, Nigeria. *Fuel*, *81*(2), 219–233.

Ellis, L., Singh, R. K., Alexander, R., & Kagi, R. I. (1996). Formation of isohexyl alkylaromatic hydrocarbons from aromatization-rearrangement of terpenoids in the sedimentary environment: A new class of biomarker. *Geochimica et Cosmochimica Acta*, *60*(23), 4747–4763.

Escobar, M., Márquez, G., Suárez-Ruiz, I., Juliao, T. M., Carruyo, G., & Martínez, M. (2016). Source-rock potential of the lowest coal seams of the Marcelina Formation at the Paso Diablo mine in the Venezuelan Guasare Basin: Evidence for the correlation of Amana oils with these Paleocene coals. *International Journal of Coal Geology*, *163*, 149–165.

Esterle, J. S., & Ferm, J. C. (1994). Spatial variability in modern tropical peat deposits from Sarawak, Malaysia and Sumatra, Indonesia: analogues for coal. *International Journal of Coal Geology*, *26*(1–2), 1–41.

Farhaduzzaman, M., Abdullah, W. H., & Islam, M. A. (2012). Depositional environment and hydrocarbon source potential of the Permian Gondwana coals from the Barapukuria Basin, Northwest Bangladesh. *International Journal of Coal Geology*, *90–91*, 162–179.

Farrimond, P., Taylor, A., & TelnÆs, N. (1998). Biomarker maturity parameters: the role of generation and thermal degradation. *Organic Geochemistry*, *29*(5), 1181–1197.

Fatoye, F. B., & Gideon, Y. B. (2013). Appraisal of the Economic Geology of Nigerian Coal Resources. *Journal of Environmental and Health Science*, *3*(11), 25–32.

Ficken, K. J., Li, B., Swain, D. L., & Eglinton, G. (2000). An n-alkane proxy for the sedimentary input of submerged/floating freshwater aquatic macrophytes. *Organic Geochemistry*, *31*(7–8), 745–749.

Fitton, J. G. (1980). The Benue trough and cameroon line - A migrating rift system in West Africa. *Earth and Planetary Science Letters*, *51*(1), 132–138.

Fleet, A. J., & Scott, A. C. (1994). Coal and coal-bearing strata as oil-prone source rocks: an overview. *Geological Society, London, Special Publications*, *77*(1), 1–8.

Flores, R. M., & Sykes, R. (1996). Depositional controls on coal distribution and quality in the Eocene Brunner Coal Measures, Buller Coalfield, South Island, New Zealand. *International Journal of Coal Geology*, *29*(4), 291–336.

Formolo, M., Martini, A., & Petsch, S. (2008). Biodegradation of sedimentary organic matter associated with coalbed methane in the Powder River and San Juan Basins, U.S.A. *International Journal of Coal Geology*, *76*(1–2), 86–97.

Friederich, M. C., Moore, T. A., & Flores, R. M. (2016). A regional review and new insights into SE Asian Cenozoic coal-bearing sediments: Why does Indonesia have such extensive coal deposits? *International Journal of Coal Geology*, *166*, 2–35.

Fulton, I. M. (1987). Genesis of the Warwickshire Thick Coal: A group of long-residence histosols. *Geological Society Special Publication*, *32*, 201–218.

Galarraga, F., Reategui, K., Martïnez, A., Martínez, M., Llamas, J. F., & Márquez, G. (2008). V/Ni ratio as a parameter in palaeoenvironmental characterisation of nonmature medium-crude oils from several Latin American basins. *Journal of Petroleum Science and Engineering*, *61*(1), 9–14.

Ganz, H. H., & Kalkreuth, W. (1991). IR classification of kerogen type, thermal maturation, hydrocarbon potential and lithological characteristics. *Journal of Southeast Asian Earth Sciences*, *5*(1–4), 19–28.

Ganz, H., & Kalkreuth, W. (1987). Application of infrared spectroscopy to the classification of kerogentypes and the evaluation of source rock and oil shale potentials. *Fuel*, *66*(5), 708–711.

Gayer, R. A., Rose, M., Dehmer, J., & Shao, L. Y. (1999). Impact of sulfur and trace element geochemistry on the utilization of a marine-influenced coal-case study from the South Wales Variscan foreland basin. *International Journal of Coal Geology*, *40*(2–3), 151–174.

Geng, W., Nakajima, T., Takanashi, H., & Ohki, A. (2009). Analysis of carboxyl group in coal and coal aromaticity by Fourier transform infrared (FT-IR) spectrometry. *Fuel*, *88*(1), 139–144.

Genik, G. J. (1993). Petroleum geology of Cretaceous-Tertiary rift basins in Niger, Chad, and Central African Republic. *AAPG Bulletin*, *77*(8), 1405–1434.

Goodarzi, F., & Swaine, D. J. (1993). Chalcophile elements in western Canadian coals. *International Journal of Coal Geology*, *24*(1–4), 281–292.

Goodarzi, F., & Swaine, D. J. (1994). The influence of geological factors on the concentration of boron in Australian and Canadian coals. *Chemical Geology*, *118*(1–4), 301–318

Goossens, H., Due, A., de Leeuw, J. W., van de Graaf, B., & Schenck, P. A. (1988). The Pristane Formation Index, a new molecular maturity parameter. A simple method to assess maturity by pyrolysis/evaporation-gas chromatography of unextracted samples. *Geochimica et Cosmochimica Acta*, *52*(5), 1189–1193.

Grice, K., Nabbefeld, B., & Maslen, E. (2007). Source and significance of selected polycyclic aromatic hydrocarbons in sediments (Hovea-3 well, Perth Basin, Western Australia) spanning the Permian-Triassic boundary. *Organic Geochemistry*, *38*(11), 1795–1803.

Grice, K., Riding, J. B., Foster, C. B., Naeher, S., & Greenwood, P. F. (2015). Vascular plant biomarker distributions and stable carbon isotopic signatures from the Middle and Upper Jurassic (Callovian-Kimmeridgian) strata of Staffin Bay, Isle of Skye, northwest Scotland. *Palaeogeography, Palaeoclimatology, Palaeoecology*, *440*, 307–315.

Gürdal, G., & Bozcu, M. (2011). Petrographic characteristics and depositional environment of Miocene Çan coals, Çanakkale-Turkey. *International Journal of Coal Geology*, *85*(1), 143–160.

Haberer, R. M., Mangelsdorf, K., Wilkes, H., & Horsfield, B. (2006). Occurrence and palaeoenvironmental significance of aromatic hydrocarbon biomarkers in Oligocene

sediments from the Mallik 5L-38 Gas Hydrate Production Research Well (Canada). *Organic Geochemistry*, *37*(5), 519–538.

Hageman, H. (1987). Palaeobathymetrical changes in NW Sarawak during the Oligocene to Pliocene. *Bulletin of the Geological Society of Malaysia*, *21*, 91–102.

Hakimi, M. H., Abdullah, W. H., Sia, S.-G., & Makeen, Y. M. (2013). Organic geochemical and petrographic characteristics of Tertiary coals in the northwest Sarawak, Malaysia: implications for palaeoenvironmental conditions and hydrocarbon generation potential. *Marine and Petroleum Geology*, *48*, 31–46.

Han, S., Zhang, Y., Huang, J., Rui, Y., & Tang, Z. (2020). Elemental geochemical characterization of sedimentary conditions and organic matter enrichment for lower cambrian shale formations in northern guizhou, south china. *Minerals*, *10*(9), 793.

Hanisch, S., Ariztegui, D., & Püttmann, W. (2003). The biomarker record of Lake Albano, central Italy - Implications for Holocene aquatic system response to environmental change. *Organic Geochemistry*, *34*(9), 1223–1235.

Haszeldine, R. S. (1989). Coal reviewed: Depositional controls, modern analogues and ancient climates. *Geological Society Special Publication*, *41*, 289–308.

Hautevelle, Y., Michels, R., Malartre, F., & Trouiller, A. (2006). Vascular plant biomarkers as proxies for palaeoflora and palaeoclimatic changes at the Dogger/Malm transition of the Paris Basin (France). *Organic Geochemistry*, *37*(5), 610–625.

Hay, W. W., & Floegel, S. (2012). New thoughts about the Cretaceous climate and oceans. *Earth-Science Reviews*, *115*(4), 262–272.

Hayashi, K. I., Fujisawa, H., Holland, H. D., & Ohmoto, H. (1997). Geochemistry of ~1.9 Ga sedimentary rocks from northeastern Labrador, Canada. *Geochimica et Cosmochimica Acta*, *61*(19), 4115–4137.

He, D., Huang, H., & Arismendi, G. G. (2019). n-Alkane distribution in ombrotrophic peatlands from the northeastern Alberta, Canada, and its paleoclimatic implications. *Palaeogeography, Palaeoclimatology, Palaeoecology*, *528*, 247–257.

He, Y., Buch, A., Szopa, C., Williams, A. J., Millan, M., Guzman, M., … Mahaffy, P. R. (2020). The search for organic compounds with TMAH thermochemolysis: From Earth analyses to space exploration experiments. *TrAC - Trends in Analytical Chemistry*, *127*, 115896.

Hennig-Breitfeld, J., Breitfeld, H. T., Hall, R., & BouDagher-Fadel, M. (2020). Reply to Discussion: Hennig-Breitfeld, J., H.T. Breitfeld, R. Hall, M. BouDagher-Fadel, and M. Thirlwall. 2019. A new upper Paleogene to Neogene stratigraphy for Sarawak and Labuan in northwestern Borneo: Paleogeography of the eastern Sundaland margin. Ea. *Earth-Science Reviews*, *202*, 103066.

Hennig-Breitfeld, J., Breitfeld, H. T., Hall, R., BouDagher-Fadel, M., & Thirlwall, M. (2019). A new upper Paleogene to Neogene stratigraphy for Sarawak and Labuan in northwestern Borneo: Paleogeography of the eastern Sundaland margin. *Earth-Science Reviews*, *190*, 1–32.

Ho, K. F. (1978). Stratigraphic framework for oil exploration in Sarawak. *Bulletin of the Geological Society of Malaysia*, *10*, 1–13.

Hobday, D. K. (1987). Gondwana coal basins of Australia and South Africa: Tectonic setting, depositional systems and resources. *Geological Society Special Publication*, *32*, 219–233.

Hoffmann, B., Kahmen, A., Cernusak, L. A., Arndt, S. K., & Sachse, D. (2013). Abundance and distribution of leaf wax n-alkanes in leaves of acacia and eucalyptus trees along a strong humidity gradient in Northern Australia. *Organic Geochemistry*, *62*, 62–67.

Holbourn, A., Kuhnt, W., Lyle, M., Schneider, L., Romero, O., & Andersen, N. (2014). Middle Miocene climate cooling linked to intensification of eastern equatorial Pacific upwelling. *Geology*, *42*(1), 19–22.

Horsfield, B. (1989). Practical criteria for classifying kerogens: some observations from pyrolysis-gas chromatography. *Geochimica et Cosmochimica Acta*, *53*(4), 891–901.

Hou, J., D'Andrea, W. J., MacDonald, D., & Huang, Y. (2007). Hydrogen isotopic variability in leaf waxes among terrestrial and aquatic plants around Blood Pond, Massachusetts (USA). *Organic Geochemistry*, *38*(6), 977–984.

Hower, J. C., Ruppert, L. F., & Eble, C. F. (2007). Lateral variation in geochemistry, petrology, and palynology in the Elswick coal bed, Pike County, Kentucky. *International Journal of Coal Geology*, *69*(3), 165–178.

Huang, H., Zhang, S., & Su, J. (2015). Pyrolytically Derived Polycyclic Aromatic Hydrocarbons in Marine Oils from the Tarim Basin, NW China. *Energy and Fuels*, *29*(9), 5578–5586.

Huang, X., Meyers, P. A., Xue, J., Gong, L., Wang, X., & Xie, S. (2015). Environmental factors affecting the low temperature isomerization of homohopanes in acidic peat deposits, central China. *Geochimica et Cosmochimica Acta*, *154*, 212–228.

Huang, X., Xie, S., Zhang, C. L., Jiao, D., Huang, J., Yu, J., … Gu, Y. (2008). Distribution of aliphatic des-A-triterpenoids in the Dajiuhu peat deposit, southern China. *Organic Geochemistry*, *39*(12), 1765–1771.

Hughes, W B. (1984). Use of thiophenic organosulfur compounds in characterizing crude oil derived from carbonate versus siliciclastic sources. In *Petroleum Geochemistry and Source Rock Potential of Carbonate Rocks* (pp. 181–196).

Hughes, William B., Holba, A. G., & Dzou, L. I. P. (1995). The ratios of dibenzothiophene to phenanthrene and pristane to phytane as indicators of depositional environment and lithology of petroleum source rocks. *Geochimica et Cosmochimica Acta*, *59*(17), 3581–3598.

Hunt, J. M. (1991). Generation of gas and oil from coal and other terrestrial organic matter. *Organic Geochemistry*, *17*(6), 673–680.

Hutchinson, C. S. (2005). *Geology of North-West Borneo: Sarawak, Brunei and Sabah* (1st ed., Vol. 52). Elsevier Science.

ICCP, I. (2001). New inertinite classification (ICCP System 1994). *Fuel*, *80*(4), 459–471.

Inan, S., Yalçin, M. N., & Mann, U. (1998). Expulsion of oil from petroleum source rocks: inferences from pyrolysis of samples of unconventional grain size. *Organic Geochemistry*, *29*(1–3), 45–61.

Inglis, G. N., Naafs, B. D. A., Zheng, Y., McClymont, E. L., Evershed, R. P., & Pancost, R. D. (2018). Distributions of geohopanoids in peat: Implications for the use of hopanoid-based proxies in natural archives. *Geochimica et Cosmochimica Acta*, *224*, 249–261.

Isaksen, G. H., Curry, D. J., Yeakel, J. D., & Jenssen, A. I. (1998). Controls on the oil and gas potential of humic coals. *Organic Geochemistry*, *29*(1), 23–44.

Jablonski, N. G. (2005). Primate homeland: Forests and the evolution of primates during the Tertiary and Quaternary in Asia. *Anthropological Science*, *113*(1), 117–122.

Jacob, J., Disnar, J. R., Boussafir, M., Spadano Albuquerque, A. L., Sifeddine, A., & Turcq, B. (2007). Contrasted distributions of triterpene derivatives in the sediments of Lake Caçó reflect paleoenvironmental changes during the last 20,000 yrs in NE Brazil. *Organic Geochemistry*, *38*(2), 180–197.

Jauro, A., Obaje, N. G., Agho, M. O., Abubakar, M. B., & Tukur, A. (2007). Organic geochemistry of Cretaceous Lamza and Chikila coals, upper Benue trough, Nigeria. *Fuel*, *86*(4), 520–532.

Jiang, C., Alexander, R., Kagi, R. I., & Murray, A. P. (1998). Polycyclic aromatic hydrocarbons in ancient sediments and their relationships to palaeoclimate. *Organic Geochemistry*, *29*(5–7), 1721–1735.

Jiang, L., Ding, W., & George, S. C. (2020). Late Cretaceous–Paleogene palaeoclimate reconstruction of the Gippsland Basin, SE Australia. *Palaeogeography, Palaeoclimatology, Palaeoecology*, *556*, 109885.

Jiang, L., & George, S. C. (2018). Biomarker signatures of Upper Cretaceous Latrobe Group hydrocarbon source rocks, Gippsland Basin, Australia: Distribution and palaeoenvironment significance of aliphatic hydrocarbons. *International Journal of Coal Geology*, *196*, 29–42.

Jiang, L., & George, S. C. (2019). Biomarker signatures of Upper Cretaceous Latrobe Group petroleum source rocks, Gippsland Basin, Australia: Distribution and geological significance of aromatic hydrocarbons. *Organic Geochemistry*, *138*, 103905.

Jimoh, A. Y., & Ojo, O. J. (2016). Rock-Eval pyrolysis and organic petrographic analysis of the Maastrichtian coals and shales at Gombe, Gongola Basin, Northeastern Nigeria. *Arabian Journal of Geosciences*, *9*(6), 1–13.

Johari, D., Kiat, L. K., Pei, C. S., Wan Akil, W. Z., Tan, V., & Jau, J. J. (1994). *Economic Geology Bulletin 4: Evaluation of the Coal Resources of the Tebulan Block Merit-Pila Coalfield, Sarawak*. Sarawak.

Jones, B., & Manning, D. A. C. (1994). Comparison of geochemical indices used for the interpretation of palaeoredox conditions in ancient mudstones. *Chemical Geology*, *111*(1–4), 111–129.

Kaal, J., Abdullah, W. H., Makeen, Y., Mustapha, K. A., Asiwaju, L., Sia, S. G., & Almendros, G. (2017). Effects of maturity on the pyrolytic fingerprint of coals from North Borneo. *International Journal of Coal Geology*, *182*, 1–13.

Ketris, M. P., & Yudovich, Y. E. (2009). Estimations of Clarkes for Carbonaceous biolithes: World averages for trace element contents in black shales and coals. *International Journal of Coal Geology*, *78*(2), 135–148.

Kiat, L. K., Pei, C. S., Johari, D., Tan, V., & Jau, J. J. (1987). *Economic Geology Bulletin 3: Evaluation of the coal resources of the Merit Block Merit Pila Coal Field, Sarawak.* Sarawak.

Kiipli, T., Hints, R., Kallaste, T., Verš, E., & Voolma, M. (2017). Immobile and mobile elements during the transition of volcanic ash to bentonite – An example from the early Palaeozoic sedimentary section of the Baltic Basin. *Sedimentary Geology*, *347*, 148–159.

Killops, S. D., Funnell, R. H., Suggate, R. P., Sykes, R., Peters, K. E., Walters, C., … Boudou, J. P. (1998). Predicting generation and expulsion of paraffinic oil from vitrinite-rich coals. *Organic Geochemistry*, *29*(1-3–3 pt 1), 1–21.

Killops, S. D., Raine, J. I., Woolhouse, A. D., & Weston, R. J. (1995). Chemostratigraphic evidence of higher-plant evolution in the Taranaki Basin, New Zealand. *Organic Geochemistry*, *23*(5), 429–445.

Killops, S., & Killops, V. (2013). Chemical Composition of Organic Matter. In *Introduction to Organic Geochemistry* (Second, pp. 30–70).

Killops, Steve D., Woolhouse, A. D., Weston, R. J., & Cook, R. A. (1994). A geochemical appraisal of oil generation in the Taranaki Basin, New Zealand. *American Association of Petroleum Geologists Bulletin*, *78*(10), 1560–1584.

Kombrink, H., van Os, B. J. H., van der Zwan, C. J., & Wong, T. E. (2008). Geochemistry of marine and lacustrine bands in the Upper Carboniferous of the Netherlands. *Geologie En Mijnbouw/Netherlands Journal of Geosciences*, *87*(4), 309–322.

Kramer, L., Arouri, K., & McKirdy, D. (2001). Petroleum expulsion from Permian coal seams in the Patchawarra Formation, Cooper Basin, South Australia. In *PESA Eastern Australasian Basins Symposium* (pp. 329–340). Melbourne: The Australasian Institute of Mining and Metallurgy.

Krzeszowska, E. (2019). Geochemistry of the Lublin Formation from the Lublin Coal Basin: Implications for weathering intensity, palaeoclimate and provenance. *International Journal of Coal Geology*, *216,* 103306.

Ladant, J. B., Poulsen, C. J., Fluteau, F., Tabor, C. R., Macleod, K. G., Martin, E. E., … Rostami, M. A. (2020). Paleogeographic controls on the evolution of Late Cretaceous ocean circulation. *Climate of the Past*, *16*(3), 973–1006.

Lane, C. S. (2017). Modern n-alkane abundances and isotopic composition of vegetation in a gymnosperm-dominated ecosystem of the southeastern U.S. coastal plain. *Organic Geochemistry*, *105*, 33–36.

Langford, F. F., & Blanc-Valleron, M. M. (1990). Interpreting Rock-Eval pyrolysis data using graphs of pyrolizable hydrocarbons vs. total organic carbon. *American Association of Petroleum Geologists Bulletin*, *74*(6), 799–804.

Larter, S. R. (1984). Application of Analytical Pyrolysis Techniques To Kerogen Characterization and Fossil Fuel Exploration/Exploitation. In *Analytical pyrolysis* (pp. 212–275). Butterworth-Heinemann.

Larter, S. R., & Douglas, A. G. (1980). A pyrolysis-gas chromatographic method for kerogen typing. *Physics and Chemistry of the Earth*, *12*(C), 579–583.

Li, B., Zhuang, X., Querol, X., Moreno, N., Córdoba, P., Li, J., … Shangguan, Y. (2019). The mode of occurrence and origin of minerals in the Early Permian high-rank coals of the Jimunai depression, Xinjiang Uygur Autonomous Region, NW China. *International Journal of Coal Geology*, *205*, 58–74.

Li, M., Wang, T., Zhong, N., Zhang, W., Sadik, A., & Li, H. (2013). Ternary diagram of fluorenes, dibenzothiophenes and dibenzofurans: Indicating depositional environment of crude oil source rocks. *Energy Exploration and Exploitation*, *31*(4), 569–588.

Li, Y., Shao, L., Fielding, C. R., Wang, D., Mu, G., & Luo, H. (2020). Sequence stratigraphic analysis of thick coal seams in paralic environments – A case study from the Early Permian Shanxi Formation in the Anhe coalfield, Henan Province, North China. *International Journal of Coal Geology*, *222*, 103451.

Liechti, P., Roe, F. W., & Haile, N. S. (1960). *The geology of Sarawak, Brunei and western part of north Borneo* (Vol. 3). Geological Survey Department, British Territories in Borneo.

Linnert, C., Robinson, S. A., Lees, J. A., Bown, P. R., Pérez-Rodríguez, I., Petrizzo, M. R., … Russell, E. E. (2014). Evidence for global cooling in the Late Cretaceous. *Nature Communications*, *5*, 1–7.

Linnert, C., Robinson, S. A., Lees, J. A., Pérez-Rodríguez, I., Jenkyns, H. C., Jenkyns, H. C., … Falzoni, F. (2018). Did Late Cretaceous cooling trigger the Campanian–Maastrichtian Boundary Event? *Newsletters on Stratigraphy*, *51*(2), 145–166.

Liu, J., Dai, S., Song, H., Nechaev, V. P., French, D., Spiro, B. F., … Zhao, J. (2021). Geological factors controlling variations in the mineralogical and elemental compositions of Late Permian coals from the Zhijin-Nayong Coalfield, western Guizhou, China. *International Journal of Coal Geology*, *247*, 103855.

López-Días, V., Urbanczyk, J., Blanco, C. G., & Borrego, A. G. (2013). Biomarkers as paleoclimate proxies in peatlands in coastal high plains in Asturias, N Spain. *International Journal of Coal Geology*, *116–117*, 270–280.

Lowe, L. E., & Bustin, R. M. (1985). Distribution of sulfur forms in six facies of peats of the Fraser River Delta. *Canadian Journal of Soil Science*, *65*(3), 531–541.

Lücke, A., Helle, G., Schleser, G. H., Figueiral, I., Mosbrugger, V., Jones, T. P., & Rowe, N. P. (1999). Environmental history of the German Lower Rhine Embayment during the Middle Miocene as reflected by carbon isotopes in brown coal. *Palaeogeography, Palaeoclimatology, Palaeoecology*, *154*(4), 339–352.

Lunt, P. (2020). Discussion on: A new upper Paleogene to Neogene stratigraphy for Sarawak and Labuan in northwestern Borneo: Paleogeography of the eastern Sundaland margin. *Earth-Science Reviews*, *202*, 102980.

Lunt, P., & Madon, M. (2017). A review of the Sarawak Cycles: History and modern application. *Bulletin of the Geological Society of Malaysia*, *63*, 77–101.

Lv, D., Li, Z., Wang, D., Li, Y., Liu, H., Liu, Y., & Wang, P. (2019). Sedimentary model of coal and shale in the Paleogene Lijiaya Formation of the Huangxian Basin: Insight from petrological and geochemical characteristics of coal and shale. *Energy and Fuels*, *33*(11), 10442–10456.

Macgregor, D. S. (1994). Coal-bearing strata as source rocks — a global overview. *Geological Society, London, Special Publications*, *77*(1), 107–116.

Madon, M. (1999a). Basin Types, Tectono-Stratigraphic Provinces, and Structural Styles. In *The Petroleum Geology and Resources of Malaysia* (pp. 77–90).

Madon, M. (1999b). Geological setting of Sarawak. In *The Petroleum Geology and Resources of Malaysia* (pp. 273–290).

Madon, M., & Abolins, P. (1999). Balingian Province. In *The Petroleum Geology and Resources of Malaysia* (pp. 345–367).

Madon, M., Kim, C. L., & Wong, R. (2013). The structure and stratigraphy of deepwater Sarawak, Malaysia: Implications for tectonic evolution. *Journal of Asian Earth Sciences*, *76*, 312–333.

Makeen, Y. M., Abdullah, W. H., Ayinla, H. A., Shan, X., Liang, Y., Su, S., … Asiwaju, L. (2019). Organic geochemical characteristics and depositional setting of Paleogene oil shale, mudstone and sandstone from onshore Penyu Basin, Chenor, Pahang, Malaysia. *International Journal of Coal Geology*, *207*, 52–72.

Marshall, C., Large, D. J., Meredith, W., Snape, C. E., Uguna, C., Spiro, B. F., … Friis, B. (2015). Geochemistry and petrology of Palaeocene coals from Spitsbergen - Part 1: Oil potential and depositional environment. *International Journal of Coal Geology*, *143*, 22–33.

Marynowski, L., Smolarek, J., Bechtel, A., Philippe, M., Kurkiewicz, S., & Simoneit, B. R. T. (2013). Perylene as an indicator of conifer fossil wood degradation by wood-degrading fungi. *Organic Geochemistry*, *59*, 143–151.

Marynowski, L., Smolarek, J., & Hautevelle, Y. (2015). Perylene degradation during gradual onset of organic matter maturation. *International Journal of Coal Geology*, *139*(1), 17–25.

Marzi, R., Torkelson, B. E., & Olson, R. K. (1993). A revised carbon preference index. *Organic Geochemistry*, *20*(8), 1303–1306.

Mastalerz, M., Hower, J. C., & Taulbee, D. N. (2013). Variations in chemistry of macerals as reflected by micro-scale analysis of a Spanish coal. *Geologica Acta*, *11*(4), 483–493.

Mat-Zin, I. C., & Swarbrick, R. E. (1997). The tectonic evolution and associated sedimentation history of Sarawak Basin, eastern Malaysia: a guide for future hydrocarbon exploration. *Geological Society, London, Special Publications*, *126*(1), 237–245.

McCabe, P. J. (1984). Depositional Environments of Coal and Coal-Bearing Strata. In R. A. Rhamani & R. M. Flores (Eds.), *Sedimentology of Coal and Coal-Bearing Sequences* (pp. 13–42).

McCabe, P. J. (1987). Facies studies of coal and coal-bearing strata. *Geological Society Special Publication*, *32*, 51–66.

McLennan, S. M., Hemming, S., McDaniel, D. K., & Hanson, G. N. (1993). Geochemical approaches to sedimentation, provenance, and tectonics. In *Special Paper of the Geological Society of America* (Vol. 284, pp. 21–40).

Meyers, P. A. (1994). Preservation of elemental and isotopic source identification of sedimentary organic matter. *Chemical Geology*, *114*(3–4), 289–302.

Meyers, P. A. (1997). Organic geochemical proxies of paleoceanographic, paleolimnologic, and paleoclimatic processes. *Organic Geochemistry*, *27*(5–6), 213–250.

Meyers, P. A. (2003). Applications of organic geochemistry to paleolimnological reconstructions: A summary of examples from the Laurentian Great Lakes. In *Organic Geochemistry* (Vol. 34, pp. 261–289).

Miles, J. A. (1994). *Illustrated glossary of petroleum geochemistry*. *Illustrated glossary of petroleum geochemistry* (illustrate). Oxford, United Kingdom: Oxford University Press.

Misra, S., Varma, A. K., Das, S. K., Mani, D., & Biswas, S. (2018). Thermal controls of lamprophyre sill on hydrocarbon generation outlook of shale beds in Raniganj basin, India. *Journal of Natural Gas Science and Engineering*, *56*, 536–548.

Moore, P. D. (1987). Ecological and hydrological aspects of peat formation. *Geological Society, London, Special Publications*, *32*(1), 7–15.

Moore, T. A., & Shearer, J. C. (2003). Peat/coal type and depositional environment - Are they related? *International Journal of Coal Geology*, *56*(3–4), 233–252.

Moore, T. A., Li, Z., Nelson, C. M., B., F., & Rob, B. (2005). Concentration of Trace Elements in Coal Beds. In *Metal Contaminants in New Zealand* (pp. 81–113).

Morley, R. J. (1998). Palynological evidence for Tertiary plant dispersals in the SE Asian region in relation to plate tectonics and climate. *Biogeography and Geological Evolution of SE Asia*, (June), 211–234.

Morley, R. J. (2012). A review of the Cenozoic palaeoclimate history of Southeast Asia. In *Biotic Evolution and Environmental Change in Southeast Asia* (pp. 79–114).

Morley, R. J. (2013). Cenozoic ecological history of South East Asian peat mires based on the comparison of coals with present day and late quaternary peats. *Journal of Limnology*, *72*(S2), 36–59.

Morley, R. J., & Morley, H. P. (2013). Mid Cenozoic freshwater wetlands of the Sunda region. *Journal of Limnology*, *72*(s2), 18–35.

Mukhopadhyay, P. K. (1994). Vitrinite Reflectance as Maturity Parameter. In P. K. Mukhopadhyay & W. G. Dow (Eds.), *Vitrinite reflectance as a maturity parameter: Applications and Limitations* (Vol. 570, pp. 1–24). American Chemical Society.

Mukhopadhyay, P. K., Hatcher, P. G., & Calder, J. H. (1991). Hydrocarbon generation from deltaic and intermontane fluviodeltaic coal and coaly shale from the Tertiary of Texas and Carboniferous of Nova Scotia. *Organic Geochemistry*, *17*(6), 765–783.

Murchison, D. G. (1987). Recent advances in organic petrology and organic geochemistry: an overview with some reference to “oil from coal”. *Coal and Coal-Bearing Strata: Recent Advances*, *32*(1), 257–302.

Murray, A. P., Sosrowidjojo, I. B., Alexander, R., Kagi, R. I., Norgate, C. M., & Summons, R. E. (1997). Oleananes in oils and sediments: Evidence of marine influence during early diagenesis? *Geochimica et Cosmochimica Acta*, *61*(6), 1261–1276.

Murtaza, M., Rahman, A. H. A., Sum, C. W., & Konjing, Z. (2018). Facies associations, depositional environments and stratigraphic framework of the Early Miocene-Pleistocene successions of the Mukah-Balingian Area, Sarawak, Malaysia. *Journal of Asian Earth Sciences*, *152*, 23–38.

Naafs, B. D. A., Inglis, G. N., Blewett, J., McClymont, E. L., Lauretano, V., Xie, S., … Pancost, R. D. (2019). The potential of biomarker proxies to trace climate, vegetation, and biogeochemical processes in peat: A review. *Global and Planetary Change*.

Naeher, S., Hollis, C. J., Clowes, C. D., Ventura, G. T., Shepherd, C. L., Crouch, E. M., … Sykes, R. (2019). Depositional and organofacies influences on the petroleum potential of an unusual marine source rock: Waipawa Formation (Paleocene) in southern East Coast Basin, New Zealand. *Marine and Petroleum Geology*, *104*, 468–488.

Nakamura, H., Sawada, K., & Takahashi, M. (2010). Aliphatic and aromatic terpenoid biomarkers in Cretaceous and Paleogene angiosperm fossils from Japan. *Organic Geochemistry*, *41*(9), 975–980.

Nichols, J. E., Booth, R. K., Jackson, S. T., Pendall, E. G., & Huang, Y. (2006). Paleohydrologic reconstruction based on n-alkane distributions in ombrotrophic peat. *Organic Geochemistry*, *37*(11), 1505–1513.

Noble, R. A., Alexander, R., & Kagi, R. I. (1987). Configurational isomerization in sedimentary bicyclic alkanes. *Organic Geochemistry*, *11*(3), 151–156.

Noble, R. A., Alexander, R., Kagi, R. I., & Knox, J. (1985). Tetracyclic diterpenoid hydrocarbons in some Australian coals, sediments and crude oils. *Geochimica et Cosmochimica Acta*, *49*(10), 2141–2147.

Noble, R. A., Alexander, R., Kagi, R. I., & Nox, J. K. (1986). Identification of some diterpenoid hydrocarbons in petroleum. *Organic Geochemistry*, *10*(4–6), 825–829.

Nott, C. J., Xie, S., Avsejs, L. A., Maddy, D., Chambers, F. M., & Evershed, R. P. (2000). n-Alkane distributions in ombrotrophic mires as indicators of vegetation change related to climatic variation. *Organic Geochemistry*, *31*(2–3), 231–235.

Nwachukwu, J. I. (1985). Petroleum prospects of Benue trough, Nigeria. *AAPG Bulletin*, *69*(4), 601–609.

Nytoft, H. P., Samuel, O. J., Kildahl-Andersen, G., Johansen, J. E., & Jones, M. (2009). Novel C15 sesquiterpanes in Niger Delta oils: Structural identification and potential application as new markers of angiosperm input in light oils. *Organic Geochemistry*, *40*(5), 595–603.

O'Keefe, J. M. K., Bechtel, A., Christanis, K., Dai, S., DiMichele, W. A., Eble, C. F., … Hower, J. C. (2013). On the fundamental difference between coal rank and coal type. *International Journal of Coal Geology*, *118*, 58–87.

Obaje, N. G., Ligouis, B., & Abaa, S. I. (1994). Petrographic composition and depositional environments of Cretaceous coals and coal measures in the Middle Benue Trough of Nigeria. *International Journal of Coal Geology*, *26*(3–4), 233–260.

Obaje, N. G., Wehner, H., Abubakar, M. B., & Isah, M. T. (2004a). Nasara-I Well, Gongola Basin (Upper Benue Trough, Nigeria): Source-rock evaluation. *Journal of Petroleum Geology*, *27*(2), 191–206.

Obaje, N. G., Wehner, H., Scheeder, G., Abubakar, M. B., & Jauro, A. (2004b). Hydrocarbon prospectivity of Nigeria's inland basins: From the viewpoint of organic geochemistry and organic petrology. *American Association of Petroleum Geologists Bulletin*, *88*(3), 325–353.

Ofoegbu, C. O. (1985). A review of the geology of the Benue Trough, Nigeria. *Journal of African Earth Sciences*, *3*(3), 283–291.

Ogala, J. E., Ola-Buraimo, A. O., & Akaegbobi, I. M. (2009). Palynological and Palaeoenvironmental Study of the Middle-Upper Maastrichtian Mamu Coal Facies in Anambra Basin , Nigeria. *Applied Sciences*, *7*(12), 1566–1575.

Olade, M. A. (1975). Evolution of Nigeria's Benue Trough (Aulacogen): A tectonic model. *Geological Magazine*, *112*(6), 575–583.

Orem, W. H., & Finkelman, R. B. (2003). Coal Formation and Geochemistry. In *Treatise on Geochemistry* (Vol. 7–9, pp. 191–222).

Ortiz, J. E., Moreno, L., Torres, T., Vegas, J., Ruiz-Zapata, B., García-Cortés, Á., … Pérez-González, A. (2013). A 220 ka palaeoenvironmental reconstruction of the Fuentillejo maar lake record (Central Spain) using biomarker analysis. *Organic Geochemistry*, *55*, 85–97.

Oskay, R. G., Christanis, K., Inaner, H., Salman, M., & Taka, M. (2016). Palaeoenvironmental reconstruction of the eastern part of the Karapınar-Ayrancı coal deposit (Central Turkey). *International Journal of Coal Geology*, *163*, 100–111.

Otto, A., Walther, H., & Püttmann, W. (1997). Sesqui- and diterpenoid biomarkers preserved in Taxodium-rich oligocene oxbow lake clays, Weisselster basin, Germany. *Organic Geochemistry*, *26*(1–2), 105–115.

Otto, A., & Wilde, V. (2001). Sesqui-, di-, and triterpenoids as chemosystematic markers in extant conifers - A review. *Botanical Review*, *67*(2), 141–238.

Otto, Angelika, Simoneit, B. R. T., Wilde, V., Kunzmann, L., & Püttmann, W. (2002a). Terpenoid composition of three fossil resins from Cretaceous and Tertiary conifers. *Review of Palaeobotany and Palynology*, *120*(3–4), 203–215.

Otto, Angelika, White, J. D., & Simoneit, B. R. T. (2002b). Natural product terpenoids in Eocene and Miocene conifer fossils. *Science*, *297*(5586), 1543–1545.

Pancost, R. D., Baas, M., Van Geel, B., & Sinninghe Damsté, J. S. (2002). Biomarkers as proxies for plant inputs to peats: An example from a sub-boreal ombrotrophic bog. *Organic Geochemistry*, *33*(7), 675–690.

Parrish, J. T., Demko, T. M., & Tanck, G. S. (1993). Sedimentary palaeoclimatic indicators: what they are and what they tell us. *Philosophical Transactions - Royal Society of London, A*, *344*(1670), 21–25.

Patricia, G. R. O., Blandón, A., Perea, C., & Mastalerz, M. (2020). Petrographic characterization, variations in chemistry, and paleoenvironmental interpretation of Colombian coals. *International Journal of Coal Geology*, *227*, 103516.

Pearson, M. J., & Obaje, N. G. (1999). Onocerane and other triterpenoids in Late Cretaceous sediments from the Upper Benue Trough, Nigeria: Tectonic and palaeoenvironmental implications. *Organic Geochemistry*, *30*(7), 583–592.

Pepper, A. S., & Corvi, P. J. (1995a). Simple kinetic models of petroleum formation. Part I: oil and gas generation from kerogen. *Marine and Petroleum Geology*, *12*(3), 291–319. https://doi.org/10.1016/0264-8172(95)98381-E

Pepper, A. S., & Corvi, P. J. (1995b). Simple kinetic models of petroleum formation. Part III: Modelling an open system. *Marine and Petroleum Geology*, *12*(4), 417–452. https://doi.org/10.1016/0264-8172(95)96904-5

Peters, K. E., & Cassa, M. R. (1994). Applied source rock geochemistry. *The Petroleum System - from Source to Trap*, 93–120.

Peters, K. E., Walters, C. C., & Moldowan, J. M. (2005). *The Biomarker Guide Volume 2* (2nd ed.). Cambridge: Cambridge University Press.

Peters, K E. (1986). Guidelines for evaluating petroleum source rock using programmed pyrolysis. *AAPG Bulletin*, *70*(3), 318–329.

Peters, Ken E., Fraser, T. H., Amris, W., Rustanto, B., & Hermanto, E. (1999). Geochemistry of crude oils from eastern indonesia1. *AAPG Bulletin*, *83*(12), 1927–1942.

Petersen, H. I. (2006). The petroleum generation potential and effective oil window of humic coals related to coal composition and age. *International Journal of Coal Geology*, *67*(4), 221–248.

Petersen, H. I., Andsbjerg, J., Bojesen-Koefoed, J. A., & Nytoft, H. P. (2000). Coal-generated oil: source rock evaluation and petroleum geochemistry of the Lulita oilfield, Danish North Sea. *Journal of Petroleum Geology*, *23*(1), 55–90.

Petersen, H. I., & Nielsen, L. H. (1995). Controls on peat accumulation and depositional environments of a coal-bearing coastal plain succession of a pull-apart basin; a petrographic, geochemical and sedimentological study, Lower Jurassic, Denmark. *International Journal of Coal Geology*, *27*(2–4), 99–129.

Petersen, H. I., & Nytoft, H. P. (2006). Oil generation capacity of coals as a function of coal age and aliphatic structure. *Organic Geochemistry*, *37*(5), 558–583.

Petters, S. W., & Ekweozor, C. M. (1982). Petroleum Geology of Benue Trough and Southeastern Chad Basin, Nigeria: GEOLOGIC NOTES. *AAPG Bulletin*, *66*(8), 1141–1149.

Philp, R. P. t, & Gilbert, T. D. (1986). Biomarker distributions in Australian oils predominantly derived from terrigenous source material. *Organic Geochemistry*, *10*(1), 73–84.

Pickel, W., Kus, J., Flores, D., Kalaitzidis, S., Christanis, K., Cardott, B. J., … Wagner, N. (2017). Classification of liptinite – ICCP System 1994. *International Journal of Coal Geology*, *169*, 40–61.

Powell, T. G., & Boreham, C. J. (1994). Terrestrially sourced oils: where do they exist and what are our limits of knowledge? - A geochemical perspective. *Geological Society Special Publication*, *77*, 11–29.

Poynter, J., & Eglinton, G. (1990). *Molecular composition of three sediments from hole 717C: the Bengal Fan. Proc., scientific results, ODP, Leg 116, distal Bengal Fan*.

Pu, F., Philip, R. P., Zhenxi, L., & Guangguo, Y. (1990). Geochemical characteristics of aromatic hydrocarbons of crude oils and source rocks from different sedimentary environments. *Organic Geochemistry*, *16*(1–3), 427–435.

Radhwani, M., Bechtel, A., Singh, V. P., Singh, B. D., & Mannaï-Tayech, B. (2018). Petrographic, palynofacies and geochemical characteristics of organic matter in the Saouef Formation (NE Tunisia): Origin, paleoenvironment, and economic significance. *International Journal of Coal Geology*, *187*, 114–130.

Radke, M., Vriend, S. P., & Ramanampisoa, L. R. (2000). Alkyldibenzofurans in terrestrial rocks: Influence of organic facies and maturation. *Geochimica et Cosmochimica Acta*, *64*(2), 275–286.

Radke, M., & Welte, D. H. (1983). The methylphenanthrene index (MPI): a maturity parameter based on aromatic hydrocarbons. In M. Bjoroy (Ed.), *Advances in Organic Geochemistry 1981* (pp. 504–512). Wiley.

Radke, M., Welte, D. H., & Willsch, H. (1986). Maturity parameters based on aromatic hydrocarbons: Influence of the organic matter type. *Organic Geochemistry*, *10*(1–3), 51–63.

Radke, Matthias, Leythaeuser, D., & Teichmüller, M. (1984). Relationship between rank and composition of aromatic hydrocarbons for coals of different origins. *Organic Geochemistry*, *6*(C), 423–430.

Randlett, M. E., Bechtel, A., van der Meer, M. T. J., Peterse, F., Litt, T., Pickarski, N., … Schubert, C. J. (2017). Biomarkers in Lake Van sediments reveal dry conditions in eastern Anatolia during 110.000–10.000 years B.P. *Geochemistry, Geophysics, Geosystems*, *18*(2), 571–583.

Ramkumar, M., Santosh, M., Nagarajan, R., Li, S. S., Mathew, M., Menier, D., … Prasad, V. (2018). Late Middle Miocene volcanism in Northwest Borneo, Southeast Asia: Implications for tectonics, paleoclimate and stratigraphic marker. *Palaeogeography, Palaeoclimatology, Palaeoecology*, *490*, 141–162.

Rimmer, S. M. (2004). Geochemical paleoredox indicators in Devonian-Mississippian black shales, Central Appalachian Basin (USA). *Chemical Geology*, *206*(3–4), 373–391.

Romero-Sarmiento, M. F., Riboulleau, A., Vecoli, M., Laggoun-Défarge, F., & Versteegh, G. J. M. (2011). Aliphatic and aromatic biomarkers from Carboniferous coal deposits at Dunbar (East Lothian, Scotland): Palaeobotanical and palaeoenvironmental significance. *Palaeogeography, Palaeoclimatology, Palaeoecology*, *309*(3–4), 309–326.

Rommerskirchen, F., Plader, A., Eglinton, G., Chikaraishi, Y., & Rullkötter, J. (2006). Chemotaxonomic significance of distribution and stable carbon isotopic composition of long-chain alkanes and alkan-1-ols in C4 grass waxes. *Organic Geochemistry*, *37*(10), 1303–1332.

Roy, D. K., & Roser, B. P. (2013). Climatic control on the composition of Carboniferous-Permian Gondwana sediments, Khalaspir basin, Bangladesh. *Gondwana Research*, *23*(3), 1163–1171.

Sachse, D., Billault, I., Bowen, G. J., Chikaraishi, Y., Dawson, T. E., Feakins, S. J., … Kahmen, A. (2012). Molecular paleohydrology: Interpreting the hydrogen-isotopic composition of lipid biomarkers from photosynthesizing organisms. *Annual Review of Earth and Planetary Sciences*, *40*, 221–249.

Sachse, D., Radke, J., & Gleixner, G. (2006). δD values of individual n-alkanes from terrestrial plants along a climatic gradient - Implications for the sedimentary biomarker record. *Organic Geochemistry*, *37*(4), 469–483.

Samad, S. K., Mishra, D. K., Mathews, R. P., Ghosh, S., Mendhe, V. A., & Varma, A. K. (2020). Geochemical attributes for source rock and palaeoclimatic reconstruction of the Auranga Basin, India. *Journal of Petroleum Science and Engineering*, *185*, 106665.

Sarki Yandoka, B. M., Abdullah, W. H., Abubakar, M. B., Hakimi, M. H., & Adegoke, A. K. (2015a). Geochemical characterisation of Early Cretaceous lacustrine sediments of Bima Formation, Yola Sub-basin, Northern Benue Trough, NE Nigeria: Organic matter input, preservation, paleoenvironment and palaeoclimatic conditions. *Marine and Petroleum Geology*, *61*, 82–94.

Sarki Yandoka, B. M., Abdullah, W. H., Abubakar, M. B., Hakimi, M. H., Mustapha, K. A., & Adegoke, A. K. (2015b). Organic geochemical characteristics of Cretaceous Lamja Formation from Yola Sub-basin, Northern Benue Trough, NE Nigeria: implication for hydrocarbon-generating potential and paleodepositional setting. *Arabian Journal of Geosciences*, *8*(9), 7371–7386.

Scalan, E. S., & Smith, J. E. (1970). An improved measure of the odd-even predominance in the normal alkanes of sediment extracts and petroleum. *Geochimica et Cosmochimica Acta*, *34*(5), 611–620.

Schefuß, E., Ratmeyer, V., Stuut, J. B. W., Jansen, J. H. F., & Sinninghe Damsté, J. S. (2003). Carbon isotope analyses of n-alkanes in dust from the lower atmosphere over the central eastern Atlantic. *Geochimica et Cosmochimica Acta*, *67*(10), 1757–1767.

Schefuß, E., Schouten, S., & Schneider, R. R. (2005). Climatic controls on central African hydrology during the past 20,000 years. *Nature*, *437*(7061), 1003–1006.

Schimmelmann, A., Sessions, A. L., Boreham, C. J., Edwards, D. S., Logan, G. A., & Summons, R. E. (2004). D/H ratios in terrestrially sourced petroleum systems. *Organic Geochemistry*, *35*(10), 1169–1195.

Schlanser, K. M., Diefendorf, A. F., West, C. K., Greenwood, D. R., Basinger, J. F., Meyer, H. W., … Naake, H. H. (2020). Conifers are a major source of sedimentary leaf wax n-alkanes when dominant in the landscape: Case studies from the Paleogene. *Organic Geochemistry*, *147*, 1–17.

Schou, L., & Myhr, M. B. (1988). Sulfur aromatic compounds as maturity parameters. *Organic Geochemistry In Petroleum Exploration*, 61–66.

Schwark, L., Zink, K., & Lechterbeck, J. (2002). Reconstruction of postglacial to early Holocene vegetation history in terrestrial Central Europe via cuticular lipid biomarkers and pollen records from lake sediments. *Geology*, *30*(5), 463–466.

Scott, A. C. (2002). Coal petrology and the origin of coal macerals: a way ahead? *International Journal of Coal Geology*, *50*(1), 119–134.

Scott, A. C., & Glasspool, I. J. (2007). Observations and experiments on the origin and formation of inertinite group macerals. *International Journal of Coal Geology*, *70*(1-3 SPEC. ISS.), 53–66.

Seifert, W. K., & Moldowan, J. M. (1980). The effect of thermal stress on source-rock quality as measured by hopane stereochemistry. *Physics and Chemistry of the Earth*, *12*(C), 229–237.

Sen, S. (2016). Review on coal petrographic indices and models and their applicability in paleoenvironmental interpretation. *Geosciences Journal*, *20*(5), 719–729.

Shanmugam, G. (1985). Significance of coniferous rain forests and related organic matter in generating commercial quantities of oil, Gippsland Basin, Australia. *American Association of Petroleum Geologists Bulletin*, *69*(8), 1241–1254.

Shibaoka, M., & Saxby, J. D. (1978). Hydrocarbon Generation in Gippsland Basin, Australia - Comparison With Cooper Basin, Australia. *AAPG Bulletin (American Association of Petroleum Geologists)*, *62*(7), 1151–1158.

Shotyk, W. (1988). Review of the inorganic geochemistry of peats and peatland waters. *Earth Science Reviews*, *25*(2), 95–176.

Sia, S.-G., Abdullah, W. H., Konjing, Z., & Koraini, A. M. (2014). The age, palaeoclimate, palaeovegetation, coal seam architecture/mire types, paleodepositional environments and thermal maturity of syn-collision paralic coal from Mukah, Sarawak, Malaysia. *Journal of Asian Earth Sciences*, *81*, 1–19.

Sia, S. G., & Abdullah, W. H. (2012). Geochemical and petrographical characteristics of low-rank Balingian coal from Sarawak, Malaysia: Its implications on depositional conditions and thermal maturity. *International Journal of Coal Geology*, *96–97*, 22–38.

Sia, S. G., Abdullah, W. H., Konjing, Z., & John, J. (2019). Floristic and climatic changes at the Balingian Province of the Sarawak Basin, Malaysia, in response to Neogene global cooling, aridification and grassland expansion. *Catena*, *173*, 445–455.

Silva, T. R., Lopes, S. R. P., Spörl, G., Knoppers, B. A., & Azevedo, D. A. (2012). Source characterization using molecular distribution and stable carbon isotopic composition of n-alkanes in sediment cores from the tropical Mundaú-Manguaba estuarine-lagoon system, Brazil. *Organic Geochemistry*, *53*, 25–33.

Sinninghe Damste, J. S., & De Leeuw, J. W. (1990). Analysis, structure and geochemical significance of organically-bound sulfur in the geosphere: State of the art and future research. *Organic Geochemistry*, *16*(4–6), 1077–1101.

Sinninghe Damsté, J. S., Van Duin, A. C. T., Hollander, D., Kohnen, M. E. L., & De Leeuw, J. W. (1995). Early diagenesis of bacteriohopanepolyol derivatives: Formation of fossil homohopanoids. *Geochimica et Cosmochimica Acta*, *59*(24), 5141–5157.

Smith, B. N., & Epstein, S. (1971). Two categories of c/c ratios for higher plants. *Plant Physiology*, *47*(3), 380–384.

Solli, H., Bjorøy, M., Leplat, P., & Hall, K. (1984). Analysis of organic matter in small rock samples using combined thermal extraction and pyrolysis-gas chromatography. *Journal of Analytical and Applied Pyrolysis*, *7*(1–2), 101–119.

Spackman, W. (1958). Section of geology and mineralogy: the maceral concept and the study of modern environments as a means of understanding the nature of coal. *Transactions of the New York Academy of Sciences*, *20*(5 Series II), 411–423.

Spears, D. A., & Tewalt, S. J. (2009). The geochemistry of environmentally important trace elements in UK coals, with special reference to the Parkgate coal in the Yorkshire-Nottinghamshire Coalfield, UK. *International Journal of Coal Geology*, *80*(3–4), 157–166.

Spears, D. A. (2017). The role of seawater on the trace element geochemistry of some UK coals and a tribute to goldschmidt. *Minerals*, *7*(8), 148.

Stefanova, M., Kortenski, J., Zdravkov, A., & Marinov, S. (2013). Paleoenvironmental settings of the Sofia lignite basin: Insights from coal petrography and molecular indicators. *International Journal of Coal Geology*, *107*, 45–61.

Stein, R. (1991). *Accumulation of Organic Carbon in Marine Sediments*. *Accumulation of Organic Carbon in Marine Sediments: results from the Deep Sea Drilling Project/Ocean Drilling Program (DSDP/ODP)*. Berlin: Springer-Verlag.

Stojanović, K., & Životić, D. (2013). Comparative study of Serbian Miocene coals - Insights from biomarker composition. *International Journal of Coal Geology*, *107*, 3–23.

Strachan, M. G., Alexander, R., & Kagi, R. I. (1988). Trimethylnaphthalenes in crude oils and sediments: Effects of source and maturity. *Geochimica et Cosmochimica Acta*, *52*(5), 1255–1264.

Stüben, D., Kramar, U., Berner, Z. A., Meudt, M., Keller, G., Abramovich, S., … Stinnesbeck, W. (2003). Late Maastrichtian paleoclimatic and paleoceanographic changes inferred from Sr/Ca ratio and stable isotopes. *Palaeogeography, Palaeoclimatology, Palaeoecology*, *199*(1–2), 107–127.

Suggate, R. P. (1959). *New Zealand coals, their geological setting and its influence on their properties*. *New Zealand Department of Scientific and Industrial Research Bulletin 134*.

Suggate, R. P. (2000). The Rank (Sr) scale: its basis and its applicability as a maturity index for all coals. *New Zealand Journal of Geology and Geophysics*, *43*(4), 521–553.

Sykes, R. (2004). Peat biomass and early diagenetic controls on the paraffinic oil potential of humic coals, Canterbury Basin, New Zealand. *Petroleum Geoscience*, *10*(4), 283–303.

Sykes, R., & Snowdon, L. R. (2002). Guidelines for assessing the petroleum potential of coaly source rocks using Rock-Eval pyrolysis. *Organic Geochemistry*, *33*(12), 1441–1455.

Sykes, R., Volk, H., George, S. C., Ahmed, M., Higgs, K. E., Johansen, P. E., & Snowdon, L. R. (2014). Marine influence helps preserve the oil potential of coaly source rocks: Eocene Mangahewa Formation, Taranaki Basin, New Zealand. *Organic Geochemistry*, *66*, 140–163.

Sykes, R. (1994). Coal seams and peat-forming environments. In S. W. Edbrooke, R. Sykes, & D. T. Pocknall (Eds.), *Geology of the Waikato Coal Measures, Waikato Coal Region, New Zealand.* (pp. 102–175).

Sykes, Richard. (2001). Depositional and rank controls on the petroleum potential of coaly source rocks. *Eastern Australasian Basins Symposium*, (November 2001), 591–601.

Sýkorová, I., Pickel, W., Christanis, K., Wolf, M., Taylor, G. H., & Flores, D. (2005). Classification of huminite - ICCP System 1994. *International Journal of Coal Geology*, *62*(1-2 SPEC. ISS.), 85–106.

Tao, S., Xu, Y., Tang, D., Xu, H., Li, S., Chen, S., … Gou, M. (2017). Geochemistry of the Shitoumei oil shale in the Santanghu Basin, Northwest China: Implications for paleoclimate conditions, weathering, provenance and tectonic setting. *International Journal of Coal Geology*, *184*, 42–56.

Taylor, S. ., & McLennan, S. M. (1985). *The continental crust: its composition and evolution*. Oxford: Blackwell Scientific.

Thompson, S., Cooper, B. S., & Barnard, P. C. (1994). Some examples and possible explanations for oil generation from coals and coaly sequences. *Geological Society Special Publication*, *77*, 119–137.

Tribovillard, N., Algeo, T. J., Lyons, T., & Riboulleau, A. (2006). Trace metals as paleoredox and paleoproductivity proxies: An update. *Chemical Geology*, *232*(1–2), 12–32.

Uguna, J. O., Carr, A. D., Marshall, C., Large, D. J., Meredith, W., Jochmann, M., … Olaussen, S. (2017). Improving spatial predictability of petroleum resources within the Central Tertiary Basin, Spitsbergen: A geochemical and petrographic study of coals from the eastern and western coalfields. *International Journal of Coal Geology*, *179*, 278–294.

van Aarssen, B. G. K., Alexander, R., & Kagi, R. I. (2000). Higher plant biomarkers reflect palaeovegetation changes during Jurassic times. *Geochimica et Cosmochimica Acta*, *64*(8), 1417–1424.

van Aarssen, B. G. K., Bastow, T. P., Alexander, R., & Kagi, R. I. (1999). Distributions of methylated naphthalenes in crude oils: Indicators of maturity, biodegradation and mixing. *Organic Geochemistry*, *30*(10), 1213–1227.

van Dongen, B. E., Rowland, H. A. L., Gault, A. G., Polya, D. A., Bryant, C., & Pancost, R. D. (2008). Hopane, sterane and n-alkane distributions in shallow sediments hosting high arsenic groundwaters in Cambodia. *Applied Geochemistry*, *23*(11), 3047–3058.

van Dongen, B. E., Talbot, H. M., Schouten, S., Pearson, P. N., & Pancost, R. D. (2006). Well preserved Palaeogene and Cretaceous biomarkers from the Kilwa area, Tanzania. *Organic Geochemistry*, *37*(5), 539–557.

Vejahati, F., Xu, Z., & Gupta, R. (2010). Trace elements in coal: Associations with coal and minerals and their behavior during coal utilization - A review. *Fuel*, *89*(4), 904–911.

Venkatesan, M. I., Ruth, E., & Kaplan, I. R. (1986). Terpenoid hydrocarbons in Hula peat: Structure and origins. *Geochimica et Cosmochimica Acta*, *50*(6), 1133–1139.

Vosoughi Moradi, A., Sarı, A., & Akkaya, P. (2016). Geochemistry of the Miocene oil shale (Hançili Formation) in the Çankırı-Çorum Basin, Central Turkey: Implications for Paleoclimate conditions, source–area weathering, provenance and tectonic setting. *Sedimentary Geology*, *341*, 289–303.

Waldo, G. S., Carlson, R. M. K., Moldowan, J. M., Peters, K. E., & Penner-hahn, J. E. (1991). Sulfur speciation in heavy petroleums: Information from X-ray absorption near-edge structure. *Geochimica et Cosmochimica Acta*, *55*(3), 801–814.

Wan Hasiah, A. (1999). Oil-generating potential of tertiary coals and other organic-rich sediments of the Nyalau Formation, onshore Sarawak. *Journal of Asian Earth Sciences*, *17*(1–2), 255–267.

Wang, S., Tang, Y., Schobert, H. H., Guo, Y., Gao, W., & Lu, X. (2013). FTIR and simultaneous TG/MS/FTIR study of Late Permian coals from Southern China. *Journal of Analytical and Applied Pyrolysis*, *100*, 75–80.

Weiss, H. M., Wilhelms, A., Mills, N., Scotchmer, J., Hall, P. B., Lind, K., & Brekke, T. (2000). *NIGOGA - The Norwegian Industry Guide to Organic Geochemical Analyses [online]. Edition 4.0.* https://www.npd.no/globalassets/1-npd/regelverk/rapportering/bronner/eng/guide-organic-geochemical-analyses.pdf (accessed 16 November 2021).

Wen, Z., Ruiyong, W., Radke, M., Qingyu, W., Guoying, S., & Zhili, L. (2000). Retene in pyrolysates of algal and bacterial organic matter. *Organic Geochemistry*, *31*(7–8), 757–762.

Weston, R. J., Philp, R. P., Sheppard, C. M., & Woolhouse, A. D. (1989). Sesquiterpanes, diterpanes and other higher terpanes in oils from the Taranaki basin of New Zealand. *Organic Geochemistry*, *14*(4), 405–421.

Widodo, S., Bechtel, A., Anggayana, K., & Püttmann, W. (2009). Reconstruction of floral changes during deposition of the Miocene Embalut coal from Kutai Basin, Mahakam Delta, East Kalimantan, Indonesia by use of aromatic hydrocarbon composition and stable carbon isotope ratios of organic matter. *Organic Geochemistry*, *40*(2), 206–218.

Widodo, S., Oschmann, W., Bechtel, A., Sachsenhofer, R. F., Anggayana, K., & Puettmann, W. (2010). Distribution of sulfur and pyrite in coal seams from Kutai Basin (East Kalimantan, Indonesia): Implications for paleoenvironmental conditions. *International Journal of Coal Geology*, *81*(3), 151–162.

Wilkins, R. W. T., & George, S. C. (2002). Coal as a source rock for oil: A review. *International Journal of Coal Geology*, *50*(1–4), 317–361.

Wolfenden, E. B. (1960). *The geology and mineral resources of the lower Rajang Valley and adjoining areas, Sarawak. British Territories Borneo Region Geological Survey Department, Memoir* (Vol. 11).

Xu, H., George, S. C., & Hou, D. (2019). Algal-derived polycyclic aromatic hydrocarbons in Paleogene lacustrine sediments from the Dongying Depression, Bohai Bay Basin, China. *Marine and Petroleum Geology*, *102*, 402–425.

Yan, G., Xu, Y. H., Liu, Y., Tang, P. H., & Liu, W. Bin. (2019). Evolution and organic geochemical significance of bicyclic sesquiterpanes in pyrolysis simulation experiments on immature organic-rich mudstone. *Petroleum Science*, *16*(3), 502–512.

Yin, M., Huang, H., Brown, M., Lucach, S. O., Caminero, L. G., Chavez, S. M., & Oldenburg, T. B. P. (2020). A novel biodegradation parameter derived from bicyclic sesquiterpanes for assessing moderate levels of petroleum biodegradation. *Organic Geochemistry*, *147*, 104049.

Young, D. J. (1967). Oil-bearing paparoa coal measures near Rewanui, Greymouth coalfield. *New Zealand Journal of Geology and Geophysics*, *10*(3), 666–674.

Yunker, M. B., Macdonald, R. W., Vingarzan, R., Mitchell, R. H., Goyette, D., & Sylvestre, S. (2002). PAHs in the Fraser River basin: A critical appraisal of PAH ratios as indicators of PAH source and composition. *Organic Geochemistry*, *33*(4), 489–515.

Zachos, J., Pagani, H., Sloan, L., Thomas, E., & Billups, K. (2001). Trends, rhythms, and aberrations in global climate 65 Ma to present. *Science*, *292*(5517), 686–693.

Zainal Abidin, N. S., Mustapha, K. A., Abdullah, W. H., & Konjing, Z. (2022). Paleoenvironment reconstruction and peat-forming conditions of Neogene paralic coal sequences from Mukah, Sarawak, Malaysia. *Scientific Reports*, *12*(1), 8870.

Zakir Hossain, H. M., Sampei, Y., & Roser, B. P. (2013). Polycyclic aromatic hydrocarbons (PAHs) in late Eocene to early Pleistocene mudstones of the Sylhet succession, NE Bengal Basin, Bangladesh: Implications for source and paleoclimate conditions during Himalayan uplift. *Organic Geochemistry*, *56*, 25–39.

Zakrzewski, A., Kosakowski, P., Waliczek, M., & Kowalski, A. (2020). Polycyclic aromatic hydrocarbons in Middle Jurassic sediments of the Polish Basin provide evidence for high-temperature palaeo-wildfires. *Organic Geochemistry*, *145*, 1–14.

Zhao, B., Zhang, Y., Huang, X., Qiu, R., Zhang, Z., & Meyers, P. A. (2018). Comparison of n-alkane molecular, carbon and hydrogen isotope compositions of different types of plants in the Dajiuhu peatland, central China. *Organic Geochemistry*, *124*, 1–11.

Zhao, H. J., Zhang, M., & Wang, Z. Y. (2009). Oil and gas potential assessment for coal measure source rocks on absolute concentration of n-alkanes and aromatic hydrocarbons. *Science in China, Series D: Earth Sciences*, *52*(SUPPL. 1), 51–58.

Zheng, Y., Zhou, W., Meyers, P. A., & Xie, S. (2007). Lipid biomarkers in the Zoigê-Hongyuan peat deposit: Indicators of Holocene climate changes in West China. *Organic Geochemistry*, *38*(11), 1927–1940.

Zhou, M., Zhao, L., Wang, X., Nechaev, V. P., French, D., Spiro, B. F., … Dai, S. (2021). Mineralogy and geochemistry of the Late Triassic coal from the Caotang mine, northeastern Sichuan Basin, China, with emphasis on the enrichment of the critical element lithium. *Ore Geology Reviews*, 104582.